Universidade de Aveiro Departamento de Engenharia Mecânica
2017

Diogo Antunes Gonçalves

Energy Management Systems based on adaptive surrogate modelling

Metamodelos e otimização em Sistemas de Gestão de Energia

Diogo Antunes Gonçalves

Energy Management Systems based on adaptive surrogate modelling

Metamodelos e otimização em Sistemas de Gestão de Energia

Tese apresentada à Universidade de Aveiro para cumprimento dos requisitos necessários à obtenção do grau de Doutor em Sistemas Energéticos e Alterações Climáticas, realizada sob orientação científica do Doutor Nelson Amadeu Dias Martins e da Doutora Mónica Sandra Abrantes de Oliveira Correia, Professores Auxiliares do Departamento de Engenharia Mecânica da Universidade de Aveiro.

"Sanity is not statistical."
George Orwell, 1984

O júri / The jury

Presidente / President

Doutor Rui Luís Andrade Aguiar
Professor Catedrático da Universidade de Aveiro

Doutor Carlos Henggeler Antunes
Professor Catedrático da Faculdade de Ciências e Tecnologia, Universidade de Coimbra

Doutor Carlos Augusto Santos Silva
Professor Auxiliar do Instituto Superior Técnico, Universidade de Lisboa

Doutor Jorge Augusto Fernandes Ferreira
Professor Auxiliar da Universidade de Aveiro

Doutor Nelson Amadeu Dias Martins
Professor Auxiliar da Universidade de Aveiro (orientador)

Doutor Bruno Cardoso Lamas
Engenheiro de Exploração e Produção, Galp Energia, S.A.

Agradecimentos

A todos os que me ajudaram nesta viagem e desafio, muito obrigado! Obrigado pai, mãe, família, amigos e em especial, à minha companheira de viagem, Lúcia – Obrigado por tornares tudo mais simples e me fazeres feliz todos os dias.
Agradeço aos meus orientadores, Nelson e Mónica, por serem uma equipa de mentores positivos, inteligentes e inspiradores. Vocês são os maiores!
Agradeço a toda a comunidade open-source por esse Mundo fora que tornam trabalhos como este possíveis.
À GALP SA, pelo suporte financeiro e pelos desafios dados.

Acknowledgements

To everyone who supported me during this journey. Thank you! Thank you parents and family, friends and, especially, my journey companion, Lúcia – Thank you for making things easier and making me happy everyday.
To my supervisors Nelson and Mónica, for being those positive, intelligent and inspiring team of professionals and mentors. You are great!
To all the open-source community around the World, for making this work possible.
To GALP SA, for the financial support, and all the challenges.

Palavras-chave Sistemas de Gestão Inteligente de Energia; Aprendizagem Computacional; Modelação; Otimização; Controlo Preditivo.

Resumo

Estima-se que o sector dos edifícios seja responsável por cerca de 40% da totalidade de energia consumida na União Europeia e Estados Unidos da América. 50% dessa energia está alocada a sistemas de aquecimento, ventilação e ar-condicionado (AVAC), dos quais 20% estimam-se ser desperdiçados devido a ineficiência na gestão de energia. Considera-se pertinente focar-se no melhoramento da eficiência energética do edificado, reduzindo o desperdício de forma a evitar a escassez de recursos fósseis, bem como para mitigar os problemas ambientais e as alterações climáticas causadas pelo consumo e produção de energia.

A tese propõe abordagens e metodologias que permitem tomar o controlo preditivo de supervisão dos sistemas de climatização enquanto medida de reabilitação energética na requalificação de edifícios. A principal contribuição deste trabalho prende-se com a implementação e desenvolvimento de metamodelos adaptativos baseados em aprendizagem computacional que assistam o processo de otimização multi-objetivo inerente ao controlo supervisor da gestão de energia em edifícios de serviços. Esta metodologia deverá ainda permitir a sua implementação de forma agnóstica à natureza dos sistemas AVAC existentes no edíficio.

A metodologia apresentada propõe uma abordagem convergente com o estado da arte no desenvolvimento científico na área da inteligência artificial. O esforço mínimo requerido para a implementação deste tipo de sistema de gestão inteligente é avaliado, concluindo-se que o seu potencial de aplicação é significativo. Para este fim, foi desenvolvida uma aplicação informática capaz de conduzir toda a metodologia em regime de simulação computacional de modo a averiguar a utilidade das soluções propostas pelo sistema de controlo supervisor desenvolvido.

Os resultados obtidos apresentam soluções compatíveis com o melhoramento do paradigma energético-ambiental corrente, contribuíndo desse modo para uma maior sustentabilidade do edificado obsoleto em termos energéticos. Os custos com energia alocada a sistemas AVAC podem alcançar uma redução de 27% dos custos base, acompanhando uma melhoria ao nível do conforto dos ocupantes. Mesmo em casos em que a requalificação da envolvente do edifício e do sistema de climatização seja anterior à implementação de um sistema de gestão inteligente, ou que a envolvente seja já competente em termos de eficiência energética (como o caso de estudo apresentado), a poupança energética é, ainda assim, assegurada devido à natureza flexível e autodidata do sistema de supervisão proposto. Portanto, recomenda-se que a reabilitação energética de edifícios tome como prioridade a requalificação do sistema de controlo AVAC por sistemas avançados e supervisores de controlo de forma a potenciarem a inércia dos edifícios, bem como toda a informação disponível na atual era digital.

Keywords Intelligent Energy Management Systems; Energy retrofitting; Machine Learning; Modelling; Optimization; Supervisory Predictive Control.

Abstract

Buildings account for almost 40% of the total energy consumption in the European Union and the United States combined. From that fraction, 50% is allocated to the heating, ventilation and air-conditioning systems (HVAC), from which 20% is wasted due to system's inefficiency. Considering that most of this energy is obtained from scarce fossil reserves and its consumption has an adverse impact on the climate change problem, it is of utmost importance to reduce energy wastes, namely by improving the overall energy efficiency of buildings.

This thesis postulates the implementation of intelligent supervisory control systems for new or existing HVAC equipment as an energy retrofitting measure concurrent with conventional architectural and systems retrofitting. The proposed methodology is characterized by a flexible, yet robust predictive control algorithm, capable of supervising generic HVAC systems in real-time by suggesting high-level controls, resulting in an optimized compromise between occupants' comfort requirements and energy consumption (and/or cost), taking advantage of the building constructive characteristics and information availability.

The proposed solution integrates the flexibility of machine learning techniques with the robustness of surrogate models to deliver data-driven predictive models capable of assisting the multi-objective optimization problem of minimizing energy consumption and cost while improving occupants comfort. The proposed modelling and optimization strategies are presented as a novelty capable of answering the quest for a robust yet flexible supervisory predictive control for generic HVAC systems. A software package capable of delivering advanced and generic supervisory predictive controls, especially focusing on the scope of building energy retrofitting was developed and used as the delivery method for the results presented in this thesis.

The obtained results suggest that office buildings, characterized by a contemporary construction and HVAC system, can be improved regarding overall energy efficiency and occupants comfort by retrofitting the control solution adding a supervisory predictive control level, external to the existing HVAC system. The expected energy saving by considering the proposed control are in line with the requirements imposed by the present energy and climate change framework, with up to 27% savings of energy related costs due to autonomous demand shifting. Moreover, it is recommended that building energy retrofits should consider as a priority the update of the energy control strategies by adding supervisory solutions capable of capitalizing the use of the building thermal inertia as well as the available data in this current information era (occupancy schedules, weather, etc.).

Contents

List of Tables

List of Figures

Chapter 1

Introduction

1.1 Context

World's population is dramatically rising. In the edge of the last century the world's population accounted for 6 billion, and 12 years later, in 2011, the numbers have reached the 7 billion mark with prospects of being 8 billion by the spring of 2024 [1]. More than half of that population is living in urban areas, and by 2030, that number is expected to have risen to 70%. This societal evolution pattern creates the conditions to the rise of air-conditioning systems importance for guaranteeing the adequate thermal comfort and indoor air quality levels to the growing number of building occupants. Collateral effects such as the heat-island effect, which is especially observed in the cities, leads the average temperatures measured in the cities to rise, and consequently, to the increase the need of smart HVAC systems and a consequent buildings energy consumption [2].

Figure 1.1 shows that 83% of the total anthropogenic emissions of CO_2 (which is a relevant greenhouse gas) from Annex I[1] countries are related to the use of energy (production and consumption). Worldwide estimates consider that 65% of all CO_2 emissions are also related to the same issue[4]. Accordingly, the energy consumption associated with buildings (construction and operation) takes a significant portion of the world's total energy consumption and related greenhouse gases emissions. Studies show that buildings in the European Union (EU) and the United States(US) are accountable for more than 40% of the total energy consumption of those regions [5, 6]. Moreover, about 50% of the whole energy consumed in buildings is used by HVAC systems, from which up to 20% is estimated to be wasted due to control faults [7, 8].

The EU Climate & Energy have set as a target the reduction of 20% of the Greenhouse gases and 20% energy savings by 2020 to take action against this carbon-intensive framework [9, 10]. Acting towards the energy efficiency of the built environment is also acting towards the saving of resources and climate change mitigation, which has become a mandatory responsibility to achieve a more sustainable Society and the prosperity of

[1] Annex I countries of the United Nations Framework Convention on Climate Change [3].

the future generations.

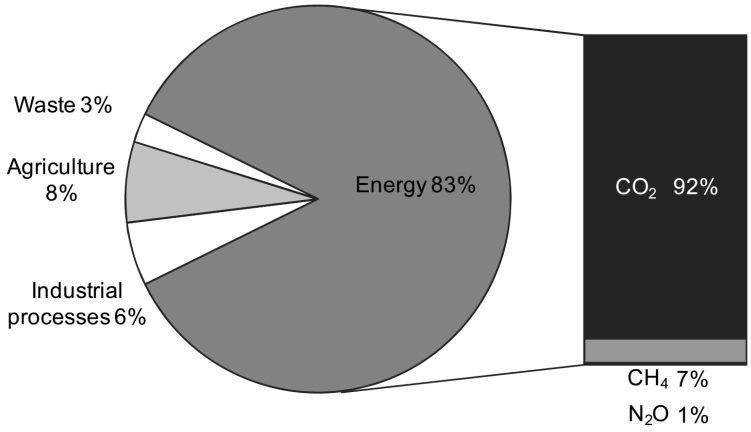

Figure 1.1: Shares of anthropogenic GHG emissions in Annex I countries, 2010 [3].

The reader of this thesis has a high probability of being inside a building constructed before 1990. In fact, only around 20% of the residential buildings in central Europe were constructed after the 90's [11]. Moreover, in the US, more than half of the commercial buildings were built before 1970. Therefore, considering that the lifespan of a building is long, the respective energy retrofitting is a cornerstone to the challenge of cutting on the energy waste associated with buildings, adjusting them to current and future energy frameworks. Shaikh et al. [12], highlighted in a review work the prospects of energy consumption savings potential by building energy retrofitting, including the reduction of greenhouse gases emission related to buildings. The authors concluded that the saving potential ranges from 5 to 30% globally. In Europe, it ranges from 27% to 30%, and the US suggest a 20% savings mark.

The approaches to accomplish such energy saving potentials are vast and with concordant concepts which could be working as symbiosis, namely the retrofitting of the envelope or architecture, replacing or improving HVAC systems, or implementing advanced and intelligent controls. The dissemination of such advanced building controls has been hindered because the majority of buildings do not have a network of sensors, nor energy meters, building data is still sparse, and systems and buildings need retrofit [13]. Such requirements have been diverting advanced control solutions from being considered as appropriate energy retrofitting options when planning building renovations [8, 14].

The literature reviewed reinforces that the most common retrofitting strategies are passive and quite similar in their nature, with the most frequent applications related to the insulation of the envelope, replacement of windows, HVAC systems, appliances and lighting [15]. However, most of the energy saving components are often selected without considering alternatives, demonstrating that the decision to select a specific measure is

still highly intuitive [7]. Moreover, the optimal set of measures regarding architectural retrofitting is embedded in uncertainty, compromising the actual utility of such actions and the expected saving potential. Hence, decision-making processes must take into account the different techno-economic scenarios, especially when the costs regarding such investments are significant, and the technical impact is not straightforward. As a result, Academia and Industry are engaged in establishing more efficient buildings and improving the demand side energy management and decision-making, via modelling and optimization procedures (See Fig. 1.2). Hence, successful retrofits should embrace modelling and multi-criteria optimization approaches to help to find the optimal set of measures capable of fulfilling building operators' expectations [16, 17, 18].

Modelling and optimization routines are becoming commonplace in the literature reviewed, mainly due to ever decreasing costs of computational power, data availability and storage, as well as the advent and dissemination of cloud computing. In buildings research, the most frequent applications are related to the modelling and optimization of energy management systems, optimization of building designs in early project phases, and assisting the decision-making process on the retrofitting of building elements and systems [19].

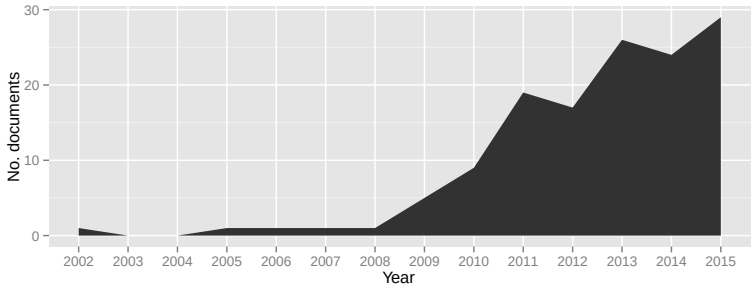

Figure 1.2: Trend of published articles using Scopus data. Query: Abstract, Title and Keywords containing simultaneously "Building", "Energy", "Optimization".

As pointed out in the review from Pombo et al. [20], many authors have been addressing the issue of finding the best retrofitting solution via multi-criteria optimization problem, with expected savings from envelope retrofit of around 20%. However, a problem facing these optimization problems, especially in the case of large service buildings, is incorporating uncertainty into retrofit decision-making because modelling the uncertainty regarding climate and economic scenarios, energy prices, government tariffs and subsidies is a very complex task [13]. The uncertainty towards climate and economy calls for flexible retrofitting solutions which are capable of accommodating different working conditions, climates, operational conditions, and economic and tariff scenarios, particularly at the verge of the smart-grids advent, self-production of energy, and an ever increasing availability of renewable and intermittent sources of energy.

The interest in sophisticated and advanced control has grown increasingly on all levels of the grid with the aim of achieving efficient use of energy in industrial, commercial, and residential buildings [21]. Building energy management calls for flexibility due to the addition of complexity and non-linearity to the nature of their energy systems by the coupling of heterogeneous devices in buildings such as appliances, HVAC, energy production and storage systems, as well as electric vehicles and renewable sources of energy. Advanced controls enable adaptive energy management strategies, changing the way energy is consumed and produced while improving building energy performance and occupants' comfort [22]. Moreover, well-designed control systems can increase building efficiency up to 30% without the need to upgrade existing appliances [23, 24].

The most popular advanced building control solution among the scientific community is the Model Predictive Control (MPC) [12]. MPC combines measurement, building modelling, disturbances forecasting and optimization formulations to simulate, select and set the controllable variables that will maximize building energy performance [25]. In contrast with conventional control techniques (rule-based, or scheduled), MPC includes endogenous and exogenous instabilities in the optimization process directly, leading to more energy savings and better occupants comfort.

HVAC controls can be divided into two big groups: the local control, and the supervisory control. Local control is the control on the machine level, i.e. the control of the HVAC system at the lowest level, namely the pumps, motors, and boilers. Whereas, the supervisory control is the control at the highest level of abstraction, namely the control accessible to the occupants: the temperature set-points of a thermostat, the temperature level of a radiator, the position of a blind, and so on [26]. Model predictive controllers at the local level are known for their robustness, and capability of improving the energy efficiency by the reduction of energy consumption and an overall increase of systems performance. However, the studies found regarding this type of solution often neglect building occupants comfort, focusing on achieving the best performance for a given group of set-points of a group of systems [26, 27]. Model predictive controllers on the supervisory level are designed to find energy or cost-efficient control settings for all local controllers, taking into account the system level or subsystem level characteristics and interactions, as well as performing information fusion from external sources (internet, web services, IoT). These energy or cost-efficient control settings are optimized in order to minimize the overall system energy input or operating cost without violating the operating constraints of each component and without sacrificing the indoor environment quality provided [26, 28]. Moreover, with the dissemination of artificial intelligence and machine learning algorithms, especially those of supervised learning, the supervisory model predictive controls are presented as versatile and holistic solutions capable of offering energy and cost-efficient control schemes while considering the thermal occupants comfort [29].

In sum, the current energy framework demands for building retrofitting to reduce the energy waste in buildings while guaranteeing or improving the well-being of their occupants. However, the solutions proposed do require to be more flexible and adaptive

to capitalize the energy savings potential. The retrofitting of buildings' systems and architecture, and the retrofitting of the control solutions should be combined to accumulate the expected savings from both the advanced control and building architectural and systems retrofitting.

The present thesis will focus on the research for a generic, flexible and robust solution, based on the state-of-the art of modelling and optimization techniques, to be capable of assisting the building's holistic energy retrofitting.

1.2 General objectives

The fundamental goal of this thesis is to improve the energy efficiency of buildings by finding an alternative to the current solutions presented, aiming at finding a solution capable of integrating the two branches of building energy retrofitting apparently disconnected, namely the improvement of the building architecture and system, and the optimization of building control.

This thesis proposes to explore the architectural, systems, and advanced control solutions as possible retrofit measures and investigate the techno-economic and environmental impact of such solutions. The initial part of the research is focused primarily on reviewing the solutions proposed in the literature to tackle the building retrofitting problem, especially those concerning advanced techniques capable of extracting the most information out of the available data and information society.

The following literature review gathers solutions to the problem of building energy efficiency improvement via modelling and optimization approaches. First, the modelling and optimization of architecture and systems retrofitting is presented, followed by the review on building control optimization state-of-the-art.

1.3 Literature Review

In the present section, a literature survey focused on buildings energy retrofitting approaches is made. Its objective is devoted to demonstrating the need and relevance of modelling and optimization solutions aiming at improving buildings energy efficiency and occupants comfort. The reviews on specific topics relevant to the developed research programme will be made in the respective chapters

The range of applications in building energy modelling and optimization is vast, and great effort has been made reviewing the different approaches to such applications. Figure 1.3 summarizes the main applications of building modelling and optimization found in the literature, and proposes a classification depending on the scope of the works encountered following the surveys from Anderson et al. [30], Perez-Lombard et al. [31] and Hong et al. [16].

There are two main groups dividing the literature. One is concerned with the optimization of new buildings. These, focus mainly in the optimization of the life-cycle of the

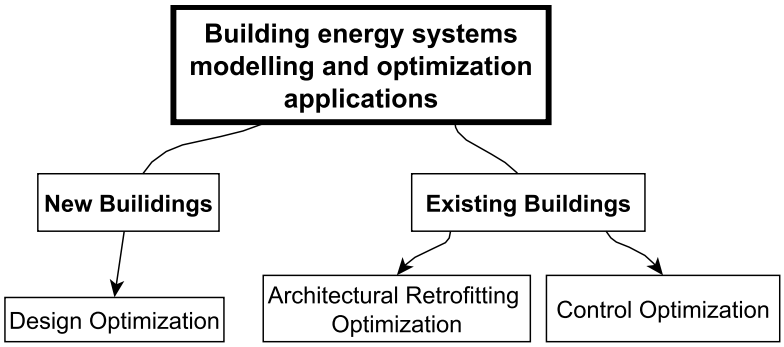

Figure 1.3: Building energy systems modelling and optimization applications.

building, focusing on minimizing the environmental and techno-economic impacts due to the expected energy consumption throughout the building lifespan. The other group tackles issues concerning existing buildings. These applications tend to be broader, both in what concerns the approach and scope, and focus essentially on the optimization of the energy usage and comfort improvement.

Despite the different objectives, constraints, and variables, the generic process of optimization is similar. The problems reported may include the enhancement of energy efficiency, or cost savings, the search for the option which guarantees the minimum payback time in architectural retrofit proposals, or optimizing new buildings designs. The problems can also focus on assisting energy managers in setting up priorities, and decision making for the systems under their supervision, or even problems concerned with optimizing HVAC control set-points at a local of supervisory level, adapting decisions to current and future conditions, guaranteeing the desired comfort for the lowest possible costs.

These applications require primarily the development of a building energy model capable of forecasting the building dynamics and response to the variables under investigation (candidates), as well as environmental conditions, occupancy profiles, architecture, energy sources, and so on. Secondly, these applications require the definition of an optimization problem, requiring the development of an objective function, which has to represent the absolute utility of choosing one candidate over another, among all possible candidates [32]. Finally, finding that *optimal* solution it requires an optimization algorithm capable of searching for feasible candidates, among all possible choices, and in an computationally efficient fashion.
The following list summarizes the requirements for implementing a modelling and optimization process, especially focusing on building energy systems applications:

- Development of a building energy model;
- Formulation of the optimization model (decision variables; constraints; objective function(s));

- Application of an optimization method;

The subsequent sections focus on reviewing mainly works from the *existing buildings* class, since it is the motivation of this thesis to investigate the relevance of *optimized control* solutions and *architectural retrofitting optimization* as energy retrofitting measures. Nevertheless, some building design optimization works will be also referenced, because architectural retrofitting optimization and building design optimization are similar approaches subjected to different constraints and decision variables limitations, namely in the degrees of freedom on the optimization of designs.

1.3.1 Architecture and systems retrofitting

Architectural retrofitting analysis are peculiarly complex and difficult to solve, since besides dealing with building energy systems response, they should fulfil the expectations of numerous and heterogeneous criteria, concerning energy efficiency, human comfort, environmental regulations, political directives, and, at last, but often the most intransigent, the economic performance. Moreover, the irreversibility inherent to the implementation of a retrofitting project adds additional risk to the decision makers and stakeholders, and complexity to the assessment.

Idealistically, stakeholders would expect to implement a set of building retrofits capable of saving energy consumption, while diminishing greenhouse gases emissions, saving natural resources, increasing human living comfort, with the shortest financial payback time. However, since real-world problems are everything but idealistic, building retrofitting optimization is required to solve the complex problem of choosing appropriate combinations of energy efficiency architectural and systems retrofits, finding the most suitable compromises by means of modelling and optimization strategies. Figure 1.4 highlights the generic process of building retrofitting optimization.

Asadi et al. [33] implemented a multi-objective optimization problem envisioning the minimization of the energy consumption after the retrofit of a Portuguese residential building, while guaranteeing the minimum investment possible. The building energy performance model was based on the static formulation proposed by the Portuguese directives and the building's energy rating prior to retrofit was C class. Through an iterative Pareto assessment of both objectives they presented the best solutions and compromises, bringing the potentiality of each investment into focus, and highlighting two optimal solutions which with a slight increment in the investment (95€) would improve the energy classification of the building by one level, from B- to B, as depicted in Fig. 1.5. They've implemented a Mixed-Integer Linear Programming (MILP) to search for the best combinations of walls and roof insulation, type of glassing and size of PV Panel.

Later, and following the work form Magnier et al. [34], the same research group has reformulated the retrofitting problem to include the replacement of the HVAC system as the optimization candidate, and added the objective of maximizing occupants

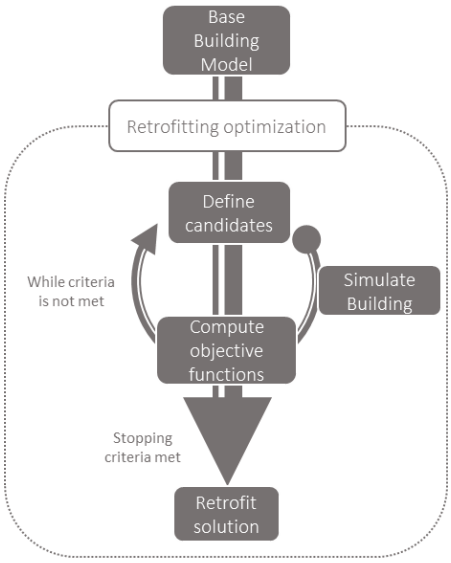

Figure 1.4: Building retrofitting optimization iterative process.

comfort, while optimizing the architecture and systems of a school building [18]. The building energy model was updated to a TRNSYS implementation of the building capable of delivering the occupants comfort indicator, augmenting the complexity of the optimization problem to a tri-objective, as well as the associated computational burden. Therefore, they've implemented a surrogate model of this building simulator, which was then optimized via a genetic algorithm named NSGA-II (Non-dominated Sorting Genetic Algorithm II) which is specifically designed for solving multi-objective and discrete optimization problems [35]. The development of the surrogate model was carried out by a Neural Network algorithm, trained and validated from a set of 950 samples (TRNSYS simulations) that were selected by the Latin Hypercube Sampling method (LHS). Despite presenting various combinations of Pareto curves, no assessment was found concluding the energy saving potentials of each solution.

Magnier et al. [34] implemented the same methodology (TRNSYS + NN + Genetic Algorithm), but for the problem of optimizing building design variables and seasonal HVAC set-points. In this case, the authors pointed out the advantages of using surrogates for saving computational time. The construction of the database specified by LHS and simulated by TRNSYS took 3 weeks to complete. Afterwards, each optimization took 7 minutes to complete, while if using the simulator directly, they've estimated it would take 10 years each. A relevant work in building design optimization is the one conducted by Eisenhower et al. [36], where they've used a quasi-Monte Carlo sampling approach to create the database from Energy Plus simulations for surrogate model implementation

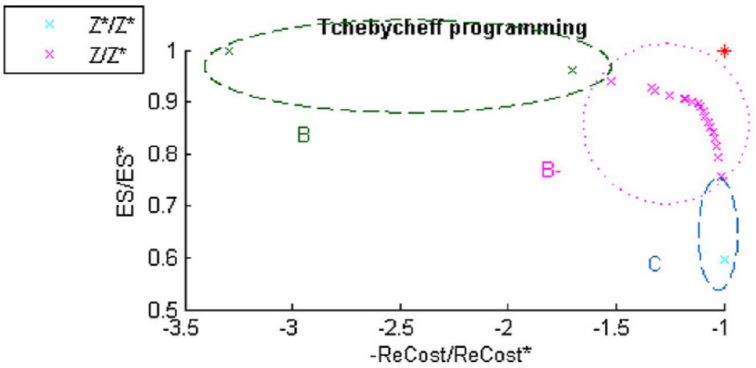

Figure 1.5: Normalized multi objective solutions for the building retrofit strategies [33].

via Support Vector Regression [2].The optimization routine was conducted by the Interior Point method which is gradient based, and the objectives were formulated by a meta-objective function combining both comfort (PMV) and energy consumption indicators.

In contrast, Chantrelle et al. [37] developed a tool called MultiOpt for multi-objective optimization of building retrofitting, based on TRNSYS and NSGA-II. As optimization candidates it considers building envelope (roof, wall, windows), HVAC systems, and control strategies (blind control threshold), while the selected objectives were the environmental impact (GHG emissions), the energy consumption, the thermal comfort (PPD $< 15\%$[3]), and the retrofit investment. In their case-study, they also presented various combinations of Pareto curves, but no remarks were drawn on the energy saving potentials of each solution.

Two other works from Ascione et al. [39, 40] have also followed a methodology without considering a surrogate model. In both works simulations were carried by EnergyPlus, and the optimization routines computed by NSGA-II algorithm were limited to 750 iterations. Their first work [39] focused on the retrofitting of a residential building of apartments in Italy. The objectives were concerned with minimizing the energy consumption while improving of occupants comfort (PPD $< 20\%$), and were limited by the investment budget. The retrofitting options focused on installing external insulation for envelope improvement, windows replacement, installing a free cooling system, upgrading the HVAC system and optimizing its seasonal heating and cooling set-points. The calculated potential savings for the highest possible budget would reach 78%. Their latest work [40] described the implementation of a two-phase optimization of the building

[2]urlhttp://www.support-vector-machines.org/

[3]PPD – Predicted Percentage of Dissatisfied, ranging from 5% to 100%, mirroring the percentage of the occupants which would be uncomfortable for a given thermal environment, according to Fanger [38]. The PMV, which is used for calculation of PPD, varies from -3 to 3, representing environments too cold and too warm, respectively. The best PMV is 0, yielding 5% of PPD.

retrofitting. The first optimization aimed at minimizing both the heating and cooling energy demand from choosing the best combination of energy efficiency measures similar to the previous work, although including renewable energy sources. The second optimization phase searched for the best compromise between primary energy consumption and the total investment cost. The energy consumption was calculated following the EPBD Recast European Directive, since the computational burden of Energy Plus to assess the 596,700 iterations would have been prohibitive. They've concluded that in the presence of a limitless economic availability, the retrofits would yield 12% of energy consumption reduction from primary sources, and a related 24.5% cut in the global cost. This study neglected the occupants comfort as optimization objective, so no information can be drawn on the effects of such retrofit in the indoor climate quality.

Penna et al. [41] have implemented a TRNSYS model based on the Italian directives and coupled it with NSGA-II. Their research investigates the relationship between the initial characteristics of residential buildings and the definition of optimal retrofit solutions in terms of either maximum economic performance (Net Present Value method – NPV), or energy consumption minimization towards net-Zero Energy Buildings, while maximizing occupants thermal comfort according to the Italian directive. They concluded that conventional Energy Efficiency Measures manage to reach the net-zero energy target, while satisfying the economical convenience, but aggravating comfort.

Malatji et al. [42] have presented an econometric optimization of the retrofitting optimization of HVAC system and lighting equipment, and the implementation of an energy management system. The multi-objective formulation competed between the ratio of the initial investment cost by the cost savings through the NPV formulation, and the total annual energy savings, which were limited by the initial investment budget, a defined payback, and a minimum energy savings target. The considered energy saving potentials were the nominal difference between equipment, neglecting externalities due to buildings' dynamics. The authors defined both objectives to be equal to each other and implemented a genetic algorithm to search for the best compromise between objectives. The results presented a maximum of 23,4% savings in the energy cost, with a payback period of around 20 months (NPV's discount rate of 9%).

Another econometric retrofitting optimization is presented by Wang et al. [43] and the objective formulation is similar to the work of Malatji et al. [42]. Moreover, Wang et al. have included a Life Cycle Cost Analysis (LCCA) term to the NPV function, as representation of the maintenance cost, or systems wearing. The candidates were lighting and HVAC improvements and the chosen optimization algorithm was Differential Evolution (DE – see Section 2.3). The authors based their case study on the work of Malatji et al. [42], and for the best scenario, the retrofit solution would save 24.76% of energy related costs, and would have a payback period of 34 months, which is significantly higher compared to the work of Malatji et al.

The literature review reveals the formulation of objective functions as an often cumbersome task and prone to the adoption of assumptions and uncertainty sources, making this field of study highly multi-disciplinary, and populating it with perspectives from

both econometric and engineering stand points. The list bellow presents the most common objective functions in retrofitting optimizations, and is corroborated by the review articles from De Boeck et al. [44], and [45]:

- Energy objectives, namely whole and primary energy consumption savings;
- Environmental objectives, namely GHG emissions from energy consumption, as well as environmental impact from materials and energy, usually derived from Life Cycle Assessments;
- Economical objectives, namely budget limitations, maximizing government incentives, and minimizing payback periods by NPV calculations and Life Cycle Costs.

The extensive literature review from Pombo et al. [20] listed as the most common energy efficiency measures:

- Improving building's envelope through insulation of ceiling, walls and foundations.
- Replacement of windows, and glassed envelope;
- Replacement and/or optimizing season set-points of HVAC Systems;
- Heat recovery systems;
- Replacing lighting equipment;
- Implementation of Renewable Energy Sources, mostly PV panels;

Regarding building energy performance models, the most common are physics based simulation conducted by TRNSYS and EnergyPlus™. Some authors had implemented surrogates based on NNs, and they've highlighted the benefits in terms of the computational burden of such decision. Finally, other authors have conducted their analysis on static load models based on their countries directives, simplifying the optimization process, but inducing uncertainties to their solutions due to the limitation of building dynamics. Nevertheless, this solution may be sufficient if the purpose is solely to improve energy classification as the case of Asadi et al. [33], because the optimization process will be more focused on the problem to solve.

The most popular optimization algorithm encountered in this review, it is beyond doubt the NSGA-II, with a review article considering Differential Evolution, and another considering interior point method. This observation is to be expected since architectural and systems retrofitting problems are often multi-objective and combinatorial problems for which NSGA-II is particularly suitable.

The works reviewed pointed that further work should focus on the development of methodologies capable of assessing retrofitting strategies from the environmental and economic life cycle approach, including climate change and societal change models in

their approaches [18, 44, 15]. There is still room for the improvement of building energy models, namely in what concerns the accuracy, resolution time-step, and computational effort [33, 46].

Architectural features and systems retrofit proves to be a very complex task, populated with uncertainty regarding the real effects of a specific measure on the environmental, economical, and societal impacts. Life cycle assessments and sensitivity analysis have been conducted to reduce uncertainties. However, the variability encountered on the economy, climate, energy framework, and society only propagate higher uncertainty to the decision making process of renovating a building [13].

The subsequent section will review relevant articles presenting applications of building control optimization, where more emphasis is given to the Model Predictive Control, both from local and supervisory layers.

1.3.2 Building advanced control retrofitting

Building energy management systems, also termed building automation systems, or building control systems, are generally centralized, integrated, hardware and software networks populated with sensors and actuators with the goal of monitoring and controlling the indoor climatic conditions in building facilities. The current trend for building control schemes among the scientific community is the Model Predictive Control (MPC), with 'sensorized' buildings, called Smart Energy Buildings (SEBs), as the natural candidates for these control systems [12]. One usual objective encountered in building energy management systems is focused on the ambiguous concept of comfort requirements, either thermal, visual and air quality, adding the occupant's preferences and behaviours. The other one is the competing energy and cost savings maximization strategies. Naturally, this problem characteristics call for the formulation of a multi-objective optimization formulation.

A typical a MPC implementation, based on the review works from Afram et al. [25], Shaikh et al. [12], Lazos et al. [47] and Hilliard et al. [48] can be depicted as the flowchart in Figure 1.6.

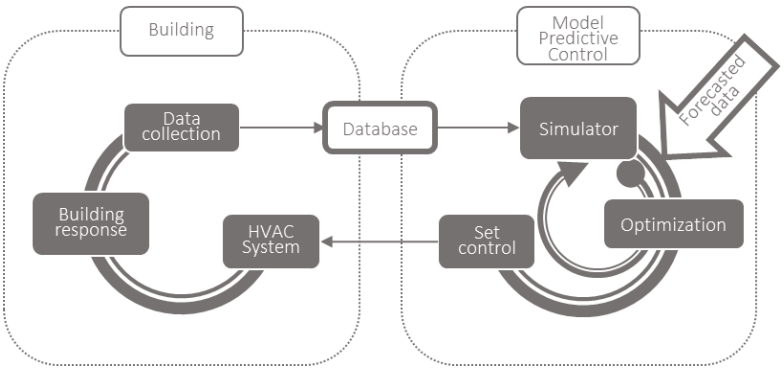

Figure 1.6: Model Predictive Control iterative process.

Generally, a continuously updated database feeds a Building Energy Simulator, or model, along with forecast variables, which influence the building response, such as internal and external loads, as well as energy production and storage data if existing. The prediction of the required minimum energy consumption to face internal and external loads, and to respond towards a desired comfort level is calculated by the simulator, whereas the optimal control set-points are solved by the optimization process, limited by the forecast window uncertainty.

This group of optimized control set-points are then sent to the building HVAC control system, inducing a building response. In the end of the cycle, the relevant variables are measured and stored in the database, and the entire process is then recursively repeated [25].

Model predictive control (MPC) is a type of building dynamic control solution applied in whole buildings, zones, or even independent systems operation. It can also be seen as a Building Energy Management System, since, generally, it couples measurement, forecasting, optimization and control theory to perform the tasks of simulation, selection and actuate the controllable variables that will maximize building energy performance [25].

Since this control optimization method is dynamic and adaptive to the current and predicted building dynamics and behaviours, it differs from works where the seasonal static HVAC set-points for heating and cooling were optimized [34, 36, 37].

As it can be depicted from Fig. 1.7, the intrinsic principle of the MPC is to optimize the set of controls denoted by $U = \{u(t), ..., u(t+k)\}$ for the available forecast window of k time steps, taking into account the predicted outcomes $Y = \{y(t+1), ..., u(t+k)\}$ of such controlling decision (top graphic). Then, the first step of decision, $u(t)$, which is the optimal set-points at step t, are communicated to the Building. However, as new data is gathered by the building response measurement at each time step, it leads the group of optimized set-points calculated at the precedent time step to be unadjusted, urging the optimization algorithm to seek for new optimal controls for the forecast window (bottom graphic) [27, 49].

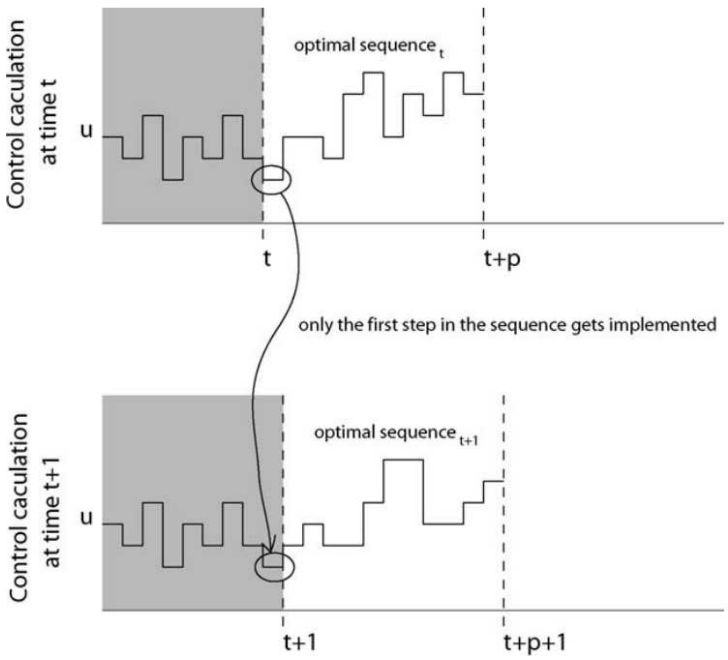

Figure 1.7: Illustration of the receding horizon control approach: at each time step, t, the optimal control input, u, is generated over the control horizon, but only the first value u(t) is applied. The procedure is repeated at the next time step t + 1, which will become time step t [49].

Bengea et al. [27], have implemented a Model Predictive Control at a supervisory level, as depicted in Fig. 1.8, after the retrofitting of the HVAC system from pneumatic to direct digital control at a mid-size commercial building. The objective of the MPC dealt with the minimization of the energy consumption of the HVAC system for a 3h horizon, through the adjusting of mass supply flow rate, mixed-air temperature, hot and cold deck discharge air temperatures, and supply temperatures for each zone, while guaranteeing a 0.56^oC band around the occupant-adjusted zone thermostat setting. The predictive model of the energy consumption included weather forecast real data, and was obtained through a Resistance-Capacitance network for each space, and the optimization was solved by the interior-point non-linear programming solver IPOPT. This strategy yield energy savings of 70% on average during heating season.

Garnier et al. [29] studied the influence of a Model Predictive Control, implementing a surrogate model of seasonal EnergyPlus simulations (November to December and June to September), based on an array of Neural Networks for each zone, capable of predicting the energy consumption, the air temperature, and the radiant temperature for each zone. Temperature predictions were used for computing the Predicted Mean Vote (Fanger). Predictions mean relative error comparing to two months of EnergyPlus simulations,

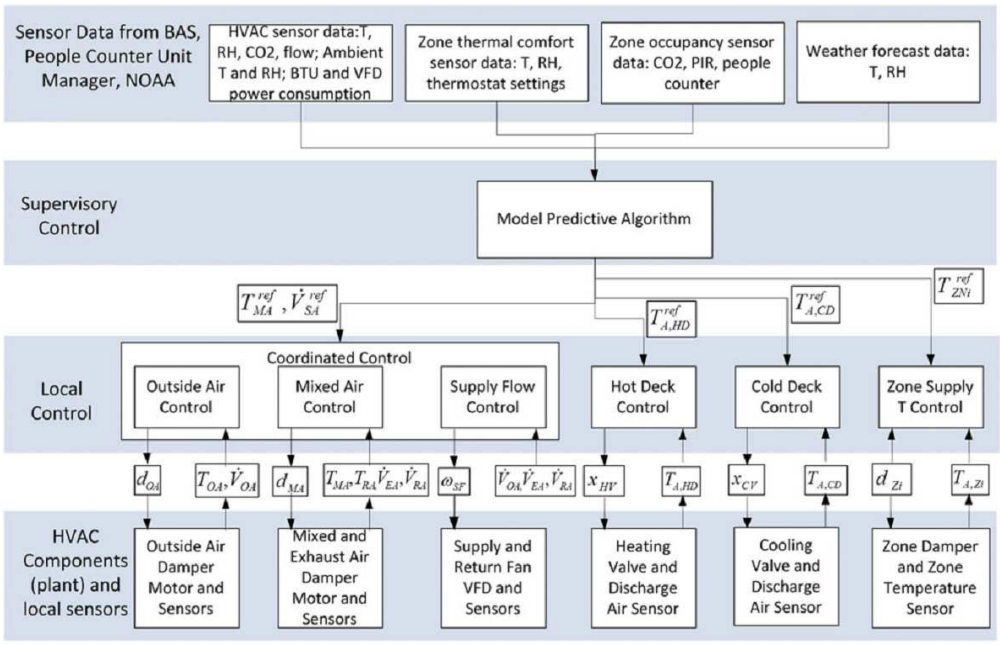

Figure 1.8: Illustration of the Hierarchical control architecture diagram with MPC algorithm at supervisory level and HVAC actuator control at low level [27].

and averaged to all three zones were 3% and 3.5% for winter and summer Zone Air Temperatures, respectively. Radiative temperatures converged to 3.7% and 4% for winter and summer, respectively. The energy consumption prediction errors were 2.9% for winter and 4.1% for summer. These results show the increasing degree of difficulty in predicting building dynamics in cooling season conditions. Occupancy was known in advance, the weather forecast was predicted by using the previous day measurements corrected by current values. They chose a Genetic Algorithm implementation from MATLAB®toolbox to solve the optimization problem and compare results with five case scenarios. The model predictive control improves the comfort comparing to all cases and improves the energy consumption compared with the current control mode, which turns on two hours prior occupation time and turns off two hours after. However, regarding energy consumption during heating, early switch off technique (2h prior to no occupation) proves to be the most economic, saving 21.45% of energy consumption ($Wh/day \cdot m^2$) comparing to MPC, but yielding an increase of 12.1% of uncomfortable hours during occupation to 18.5%. During the cooling periods, this technique may save 16.8% of energy consumption when compared to MPC, but inflating the uncomfortable percentage of hours from 0.1% to 13.4%. It is evident the struggle from the optimized controller to meet comfort criteria, dictating an aggravation in the energy consumption. It could be interesting to perform a Pareto curve, comparing different comfort thresholds in order to assess if the compromise between energy consumption and comfort could

be improved i.e. to save energy without extremely compromising the comfort index. Another way would be to survey the occupants to assess how dissatisfied they are with the thermal comfort and plan the optimization targets accordingly.

An example of the superiority of MPC over PID controllers is presented by Morosan et al [24], where they conducted simulations of zone temperature regulation using decentralized, centralized, and distributed MPC. The authors claimed an overall reduction of the energy consumption of 18,9% and an improvement of thermal comfort of 36,7% by a centralized MPC system, which considered the interaction between different building zones, whereas PI controllers could not consider such coupling effects. The modelling and optimization approach was employed by SIMBAD toolbox, a building simulation toolbox for MATLAB/Simulink®.

Prívara et al. [50] and Široký et al. [51], from the same research group, compared an MPC for zone temperature control of the heating system in a large university building with a weather-compensated controller, and the heating curve control method, respectively. Experimental results show the benefits of the MPC system based on subspace identification methods connected to a Kalman filter. The MPC application registered a reduction of up to 29% less energy (normalized by Heating Degrees Day method) while maintaining the same thermal comfort level in both applications. Nevertheless, no account was made to occupancy differences between case-studies. As it turns out, the building showed a time delay of 12 h in its temperature response, leading the weather-compensated controller to supply hot water to the radiant ceiling heating system at a higher temperature compared with that of the MPC controller, resulting in higher energy consumption. Comparatively, the heating curve method heated the building mass during the night, turning off the heating system in the morning, while the MPC also preheated the building during the evening, however, not switching it off during the day, resulting in a significant peak energy reduction.

A survey from Afram and Janabi-Sharifi identifies MPC's main advantages the capability of conducting anticipatory control rather than corrective control strategies, and the guarantee of achieving desired objectives by employing advanced optimization algorithms [25]. The authors also point out that predictive control of slow-moving processes with considerable time delays, namely energy storage systems, or thermal storage in the building mass, enable demand response strategies, such as peak load shifting, and allocating pre-heating, or pre-cooling tasks, to off-peak periods with lower energy tariffs. This latter application does not always result in lower energy consumption, but may result in lower operating costs, and lower environmental footprint if coupled with renewable energy production systems. Moreover, MPC applied in HVAC systems has shown to outperform most control techniques, providing superior performance in terms of achieving lower energy consumption, better transient response, robustness to disturbances, and consistent performance under varying conditions.

Despite the significant improvements showed in the literature by MPC applications, direct comparison of the savings observed in the literature is not particularly meaningful, since it depends on the eligible room for optimization in each particular case, as referred

in the review work from Lazos et al. [47]. It also reflects the difficulty in establishing an absolute superiority of a specific group of techniques for this purpose [47]. Instead, there are distinct advantages and disadvantages depending on the available resources, complexity and magnitude of each case where a forecasting algorithm is used to assist energy management. As the authors point out, the major finding from the literature review is that the consideration of local weather variable forecasting is mandatory, since it always produces enhanced accuracy compared to the approaches with non-weather data. Later, the same author proposes an enhanced short-term weather forecast model (outside temperature and humidity) to assist building energy management, however, no results are presented regarding the enhancement of energy management [52].

A recent review from Hilliard et al [48] summarized the key building characteristics which are advantageous for MPC success:

- High thermal storage capacity (Building mass and active storage systems);
- Large predictable loads (occupancy, weather, etc.);
- Broad thermal comfort and indoor air quality (IAQ) ranges;
- Slow HVAC systems;
- Low infiltration;
- High insulation.

The reviewed studies indicate that the slower the building response, the better the MPC may perform in comparison to feedback response control systems, since MPC's strategy takes into account future information of the building loads, whereas feedback strategies don't.

Some works that did not use the Model Predictive Control taxonomy are presented ahead. These works are still relevant to the building control optimization section and to the scope of this thesis. The latter included the works from He et al. [53] and Kusiak et al. [54] which were based on Soft Computing and had highlighted saving potentials in HVAC systems of a service building. Both developed a model with Neural Networks and have incorporated it into an optimization strategy based on Swarm Optimization. Kusiak et al. [54] have implemented four energy models (chiller, fan, pump and heat exchanger) with less than 7.5 % of error (MAPE). It is claimed that optimization results by the PSO algorithms over a baseline have reduced total energy consumption by over 7% of the HVAC. Later, the same group focused on optimizing a HVAC system performance along with room comfort. The introduction of room temperature ramp control to the objective function was beneficial for smoothing the control settings of the set points and achieving better room thermal comfort.

Shaikh et al. [55] developed an HVAC control system considering both energy efficiency and occupants comfort. Fuzzy logic was applied to determine the relationship

between energy consumption and temperature target set-points. A Multi Objective Genetic Algorithm was responsible to simultaneously minimize two competitive objective functions. On the one hand, there was the power demand. On the other hand, there was occupants' discomfort level (Discomfort = 1 - Comfort). The control system based on GA (Genetic Algorithm) optimization is claimed to be effective on the improvement of energy consumption and comfort. In fact, by analysing the results, average comfort is clearly improved by this method, while the same cannot be depicted when comparing the optimized power consumption with the proposed baseline. Since the problem involves two competitive objectives, energy consumption and overall comfort, it may be required to increase the power consumption in order to achieve a better occupant's comfort index.

Yang and Wang [56] employed a particle swarm optimizer (PSO) in a supervisory Building Energy Management System (BEMS) to determine the energy distribution of a multi-zone building served by renewable-energy resources and batteries. The algorithm aims at maximizing the building occupants' comfort based on temperature, illumination and CO_2 concentration data. Even in power-supply shortage periods, the intelligent controller has proven to be able to distribute the energy appropriately maintaining high overall comfort levels. This result reflects an oversized initial power-demand because the necessary energy to achieve highly acceptable comfort levels is lower than the estimated one. Furthermore, the proposed future work addresses the need to implement energy-savings in consumption in the optimization target.

Kusiak et al. [57] compared eight Data-mining algorithms in order to build four models of energy consumption by an HVAC system (Chiller, Fan, Pump and Reheat). The most reliable algorithm, with 3.77% of MAPE, was the Multilayer Perceptron (MLP) ensemble, an NN widely applied in classification problems. The A single-objective optimization model was solved via a particle swarm optimization (PSO) algorithm to minimize the total energy consumption. PSO algorithm was used to search the near-optimal solution of the system control set-points. Each operating-hour received simulated input sets in response to different patterns of the internal load and other uncontrollable parameters. The optimization results are presented and claimed to be responsible for approximately 7% savings of the total of energy consumption.

Though the advances in the computational power have allowed the implementation of MPC and building optimized control in general, there are still current limitations regarding the computational efficiency and model detail trade-off of the used predictive models in these applications. For example, most optimization methods, but especially the state-of-the-art methods, such as Evolutionary Computing algorithms, often require a high number of model evaluations, leading to a prohibitive assessment time, preventing real-time implementations. Moreover, Linear Programming optimization methods usually are not suitable because of the non-linearity and combinatorial nature of these problems. With that in mind, Hilliard et al. [48] also point the room for improvement in this area:

- Building response model;

- Simulation time-step and forecast horizon;
- Forecast resolution;
- Optimization algorithm.

Similarly to building architecture and systems retrofitting optimization, building control optimization also focuses on the reduction of the energy consumption, and comfort enhancement,especially the case of supervisory Model Predictive Controls. However, through the reviewed cases focused on optimizing both objectives, it seems that the baseline on the thermal comfort before applying the optimization strategies is low, leading to an increase of the energy consumption to achieve desired comfort levels. It could be beneficial to address the energy saving potential by minimizing the energy objective function, while maintaining the previous levels of comfort via restriction methods. Therefore, the room for energy savings would be extended and the comfort would remain similar to before, leading to a reduction of the energy objective.

Comparing the retrofitting solutions regarding the optimization of comfort via supervisory predictive control with the local predictive control, it should be highlighted the flexibility with which a supervisory model predictive control can be adapted to different working conditions, different climates and operational conditions, different tariffs and economic scenarios. On the case of retrofitting services buildings which contemplate HVAC systems, the implementation of a supervisory model predictive control capable of actuating above the HVAC system level, using the available set-points could provide a beneficial, non intrusive, and less risky retrofitting solution.

For accomplishing that purpose, advanced methods for developing the predictive models are required. However, the unaffordable computational cost, the lack of robustness of the predictive models, and suitable optimization algorithms are hindering the dissemination of such advanced model based HVAC supervisory control systems [48]. Therefore, an opportunity is presented to investigate a methodology capable of improving the flexibility and robustness of supervisory model predictive controllers.

1.3.3 Remarks from literature review

The retrofitting of building architecture and systems has shown promising results regarding the energy efficiency improvement. However, it seems to be pertinent to give higher emphasis to the advanced control systems in the retrofitting assessments, since there is evidence that optimized control is capable of improving the building energy performance post-retrofit implementations. For example, the experimental case of an HVAC system retrofit from pneumatic to direct digital control at a mid-size commercial building has yield energy savings of 70% on average during heating season by changing the control solution to MPC [27]. Moreover, the environmental and cost effectiveness of the implementation of an advanced supervisory predictive control is expected to be higher while presenting lower risks than building architecture renovation, especially if

presented as a flexible solution. For example, while with a supervisory predictive control it might be straightforward to update the software governing the control and improve it throughout its lifetime, the update of an architectural feature would be more cumbersome, involving civil work and its externalities.

No studies were found combining both approaches as retrofitting measure, namely assessing the effectiveness of combining a supervisory model predictive control in the architectural and systems retrofitting. This fact seems particularly relevant since architectural features are influencing the response of advanced controls positively [48]. Probably, the high computational costs related to building energy simulation and optimization algorithms are preventing this confluence, as well as the integration of endogenous and exogenous disturbances predictions for the desired control horizon with the optimization routines [48].

The reviewed works regarding model predictive control have shown a lack of flexibility in their approach, preventing the employment on the assessment of different buildings, or types of HVAC systems.

The literature reviews of both themes have pointed the necessity of improving the predictive models employed in their optimization routines. To overtake the issue of high computational costs of optimization routines, the integration of surrogate models based on machine learning algorithms is the current state-of-the-art measure [58]. Surrogate models are also known as response surface models, meta-models, proxy models or emulators, and they are intended to mimic the complex behaviour of the underlying simulation model. The purpose behind the surrogate model approach is to avoid the temptation to invest the computational budget in answering the question at hand, but instead, invest it in developing fast-response mathematical approximations to the simulators. Given these approximations, many case-studies could be explored, and many hypotheses could be tested at a fraction of the expected computational cost [36, 59].

1.4 Specific objectives and research questions

The main goal of this Ph.D. is to deliver a methodology implemented in software, capable of assisting practitioners in the area of building energy management.

Moreover, it is anticipated the answering of the following research questions:

- How to design a HVAC supervisory advanced control system independent of the HVAC itself?
- How does a HVAC supervisory predictive control solution compare with architecture and systems retrofitting approaches?
- How to implement a real-time supervision system for a large commercial and services building, capable to establishing optimal operating conditions within an acceptable computational cost?

The cornerstones should be robustness and flexibility, to enable the inclusion of advanced control solutions as a feasible and straightforward solution to building retrofitting by the community of researchers and energy management practitioners.

The expected challenges are the high computational costs related to building energy simulation and optimization algorithms, and the integration of forecast variables (or forecast simulation) in the model predictive control implementation. To overtake the former issue, the integration of surrogate models based on machine learning algorithms is the current state-of-the-art measure. However, this leads to the simulation of different case-scenarios and the drawing of a Design of Experiments for guaranteeing the statistical representativeness of the domain of such models. At last, to overtake the latter problem, the integration of a noise simulator to disturb the exogenous and endogenous uncontrollable variables, such as weather, occupancy, and tariffs, may be a sufficient solution for preliminary implementations.

1.5 Expected original contribution

The main goal of this PhD is to deliver a methodology implemented in software, capable of assisting practitioners in the area of building energy management. This method should integrate the supervisory model predictive control strategy for building energy performance simulators, hence providing the means to deliver appropriate assistance in the investigation of building designs, and new solutions to advanced controls. Therefore, the flexible, general and robust supervisory model predictive control system developed must be agnostic to the equipment being supervised, which may vary substantially. It can be different boilers, chillers, AHU units, all of them together, or even buildings characterised by different materials and designs.

This methodology should enable the open integration of a supervisory model predictive control strategy with building energy performance simulators, such as EnergyPlus™, hence providing the means to deliver appropriate assistance to the investigation of building designs, and new solutions to advanced controls. Moreover, it must be capable of running much faster than the real clock to anticipate the future response of the building and suggest optimal operating conditions for a real world implementation. The hardware requisites should comprise only a standard personal computer (desktop or laptop PC) for assisting in the dissemination of the contribution.

1.6 Thesis organization

Chapter 1 presented the objectives and contribution of the thesis to the society. Additionally, and supporting the latter, a literature review synthesized the state-of-the-art approaches to the building energy retrofitting problem, namely the optimization of architecture and systems retrofitting, and the building control optimization.

Chapter 2 serves as a support chapter to the methodology conducted further. This chapter intention is to provide the fundamental tools and techniques to solve the problem at hands which is the development of a supervisory predictive model.

Chapter 3 proposes the methodology to implement a generic supervisory predictive control solution in a co-simulation environment. It presents the *eppyco* module which is a software package to assist the development of data-driven models of buildings, while performing on-line optimization of building settings and enabling co-simulation with building energy simulators.

Chapter 4 presents the results of implementing a supervisory predictive control in an office building reference case-study via co-simulation. The robustness of the method is investigated and the conclusions are drawn regarding the performance benchmark of the advanced control solution proposed.

Finally, Chapter 5 summarizes the major results obtained and draws the recommendations and questions to be answered in future research.

Chapter 2

Fundamentals

This chapter intends to provide an insight on the fundamental tools and techniques most commonly used and that best assist the development of an adequate methodology for building supervisory control.

The first section tackles building energy dynamics fundamentals. It summarizes the building thermodynamic as an attempt to understand which role does a supervisory predictive control play in the building energy system. Furthermore, the method for defining building occupants' thermal comfort is addressed.

The second section addresses modelling and optimization techniques applied in building energy optimization problems, where a set of techniques and methods are defined to allow for the development of a supervisory predictive control capable of providing robust answers with an acceptable computational burden.

2.1 Building Energy Dynamics

The objective of this section is to introduce the fundamentals of building energy dynamics, namely the thermodynamics governing a building energy system, as well as the characterization of occupants' thermal comfort for a given set of interior environment.

2.1.1 Building Thermodynamics

Buildings are complex and transient thermodynamic systems. They can be described as heat and mass transfer balances with boundaries at the exterior envelope of the air-conditioned areas. Following the first law of thermodynamics, the sum of all loads present in a building should equal to zero. These loads, according to Hunn et al. [60], comprehend the four types listed below, and depicted from Fig. 2.1:

- Climate-driven envelope loads;
- Internal gains;

- Storage or release of energy;
- HVAC system loads.

A fine tuning of building envelope during design stages is necessary to take most advantage out of the uncontrollable and climate related loads. The desired objectives in this envelope selection can be often competitive, focusing either in leading a building to absorb desirable loads, or letting it be transparent for undesirable loads. For instance, solar gains are advantageous during the heating season, whereas they are undesirable during the cooling season. Building envelope may also influence its mass and its capability of energy passive-storage.

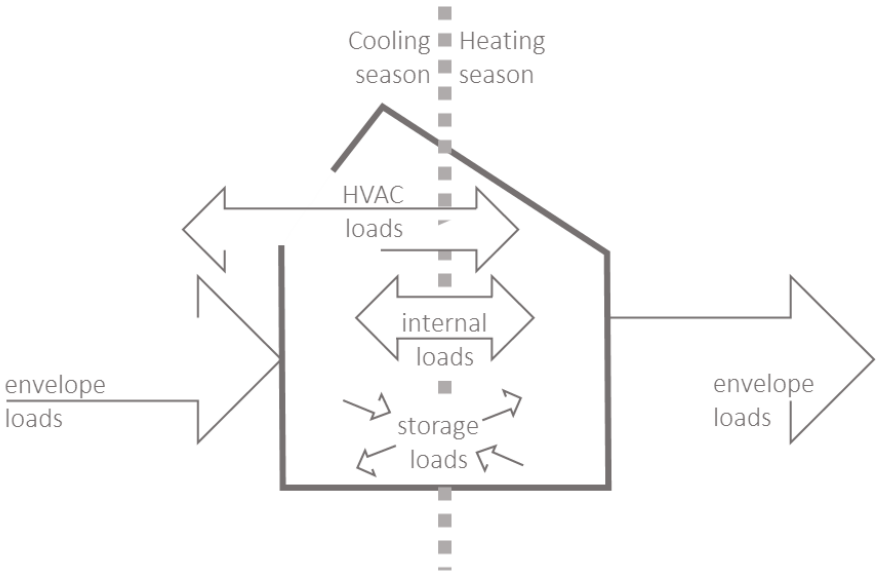

Figure 2.1: Building loads balance.

Internal gains are induced by interior equipment and lighting inefficiencies, and intensity of occupants' activity. They relate to the utilization purpose of buildings and occupancy profile types. These loads are the ones that always contribute to the thermal energy rise inside buildings.

Finally, HVAC system loads exist to lead internal environment conditions to comply with the comfort requisites for occupants. The addition of heating or cooling loads to air-conditioned areas alters the thermodynamic system state, which needs to attain equilibrium by reaching a new temperature set-point. Heating and cooling loads imposed by HVAC systems result from external climatic factors, internal occupancy characteristics, and the building design, allowing occupants to live in a different, and more comfortable environment than the one on the outside [60]. These loads usually require energy conversion from a wide variety of sources, and account for around 50 % of the total energy employed in buildings [7].

Building energy management systems, especially HVAC control systems, struggle with the minimization of this amount of energy while maintaining, or increasing, occupants' comfort standards. HVAC control schedule schemes focus on defining HVAC systems set-points that imply minimum loads capable of achieving required standards [60, 52].

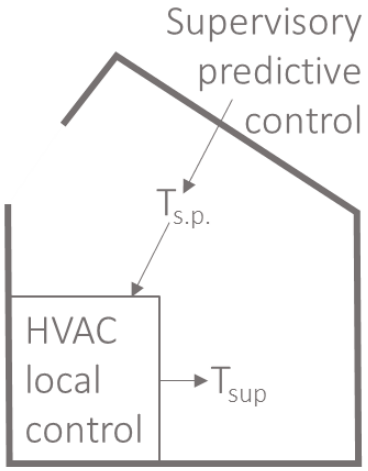

Figure 2.2: Supervisory and local HVAC control example.

HVAC controlling strategies may be divided into two well defined groups: in the bottom layer there lies the HVAC local controls which deal with the setting of all related equipment set-points to achieve a desired objective at an upper level. For instance, as it can be depicted from 2.2, the set-points of hot water supplying the radiators at a specific temperature (T_{sup}), that are heating up a group of zones to a certain temperature set-point defined by occupants ($T_{s.p}$), or a supervisory control system [60, 27, 52].

The scientific community has been dedicating a considerable amount of effort to this thematic. Haniff et al. [61], reviewed several HVAC systems scheduling techniques and highlighted the conventional "early switch-off" (ESO); "pre-heating (or pre-cooling) for demand reduction" (DR); "alternate switch-on/off" (ASOO); and other more advanced techniques, such as Agent-based control, and Model Predictive Control. Garnier et al [29], have also referred these techniques and have employed them as baseline to benchmark their solution against their proposed Model Predictive Control.

These advanced controlling techniques have proven its superiority against classical techniques in achieving better buildings' energy performances [27, 61, 52]. They have taken into account the prediction of disturbances to the systems and calculate appropriate set-points over a prediction horizon into the future. The confluence of these advanced controlling techniques with renewable energy sources, variable energy pricing, and smart-grids, has also proven to be of great economical advantage [52].

The work conducted in this thesis focuses on the development of such a supervisory predictive control, aiming at minimizing both energy consumption and occupants discomfort. The principle lies on the optimization of heating and cooling set-points over a prediction horizon of the loads disturbing the system. Such predictive capacity of the controller is delivered by surrogate models based on machine learning algorithms which are capable of continuous learning and adapt to dynamic conditions.

2.1.2 Occupants Thermal Comfort

Whereas the energy consumption of a building is fully described and determined by the energy balance of its loads, its occupants' thermal comfort is that condition of mind that expresses satisfaction with the thermal environment. Individuals draw conclusions on their thermal comfort and discomfort depending on direct temperature and moisture sensations from the skin, deep body temperatures, and the efforts necessary to regulate body temperatures [62]. In general, comfort occurs when body temperatures are held within narrow ranges, skin moisture is low, and the physiological effort of regulation is minimized. Furniture, interior decoration and lighting affects human thermal comfort, as well as actions taken by the occupants, leading to reducing or increasing comfort estimation, even if the only effect is psychosomatic. For example, complaining, leaving the space, changing posture or location, or changing the thermostat setting are actions dictated by one's comfort. Other examples of the latter include altering clothing, activity, or even opening a window [62].

The comfort metric developed by Fanger, namely the PMV (Predicted Mean Vote) and PPD (Predicted Percentage of Dissatisfied), have been adopted by the international standards as thermal comfort indicators [62, 63]. Fanger [38] identified the PMV (Predicted Mean Vote) index with heat balance equations and empirical studies about skin temperature to define comfort. The imbalance between heat flows leaving and entering the body induces a thermal discomfort which in this index is categorized as a seven-point scale comprised between -3 as cold sensation, and 3 as hot sensation, with zero being the ideal value, representing thermal neutrality. The thermal sensation scale developed by Fanger is adopted by the ASHRAE Standard 55 and EN-15251 and can be characterized as [38]:

+3	Hot
+2	Warm
+1	Slightly warm
0	Neutral
-1	Slightly cool
-2	Cool
-3	Cold

Fanger's PMV simplified equation to compute the above scale can be defined as

presented by equation 2.1.1 [38, 64]:

$$PMV = (0.303 \cdot e^{-0.036M} + 0.028) \cdot (H - L) \tag{2.1.1}$$

where M is the metabolic rate per unit area, H is the internal heat production rate of an occupant per unit area, and L represents all the modes of energy loss from the body. The later includes the convection and radiant heat loss from the outer surface of the clothing, the heat loss by water vapour diffusion through the skin, the heat loss by evaporation of sweat from the skin surface, the latent and dry respiration heat loss and the heat transfer from the skin to the outer surface of the clothing. Moreover, the PMV model assumes that a person is thermally at a steady state with the environment.

Such an approach to define thermal comfort seems particularly convenient because by using one index alone, a classification of a particular combination of variables is enabled. Those variables include: air temperature, mean radiant temperature, relative humidity, air speed, metabolic rate, and clothing insulation. Furthermore, the international standards for occupants comfort simplified the recommended ideal comfort as a range of PMV between -0.5 and +0.5, assuming air velocities lower than $0.2m/s$, and clothing insulation indexes equal to 0.5 and 1 clo, for Summer and Winter, respectively [63, 62].

After estimating the PMV with equation 2.1.1, the predicted percent of dissatisfied (PPD) people with a set of the given conditions can be estimated as well. Through statistical analysis, Fanger related the PPD to the PMV as established by equation 2.1.2:

$$\text{PPD} = 100 - 95 \cdot e^{-0.03353 \cdot \text{PMV}^4 - 0.2179 \cdot \text{PMV}^2} \tag{2.1.2}$$

Figure 4.29 shows the relationship between PMV and PPD. The plot also shows the acceptable limits ideally comprising a PMV equal to -0.5 and +0.5 in green, and the expanded limit in red, considering a non-steady thermal state between body and environment, hence, a PMV between -1 and +1 [65].

The PMV-PPD model is widely used and accepted for design and field assessment of comfort conditions, and literature is found where optimization problems defined such a model as the cornerstone to the thermal comfort of occupants. Ascione et al. [39] focused on minimizing the energy consumption while improving occupants comfort to PPD $< 20\%$. Chantrelle et al. [67] formulated the multi-objective problem as minimizing the environmental impact (GHG emissions) and the energy consumption while setting the thermal comfort to PPD $< 15\%$. Whereas, Garnier et al. [29] were more ambitious, setting the comfort limits to PPD $< 10\%$. None of the works found referred the upper limit of 25% as the minimum level of comfort. However, this consideration might be acceptable given the conditions of the building before retrofitting, especially when considering supervisory control towards retrofitting. That is to say, an optimized control could stretch the comfort of occupants to its limits but, maximizing the energy-saving potential.

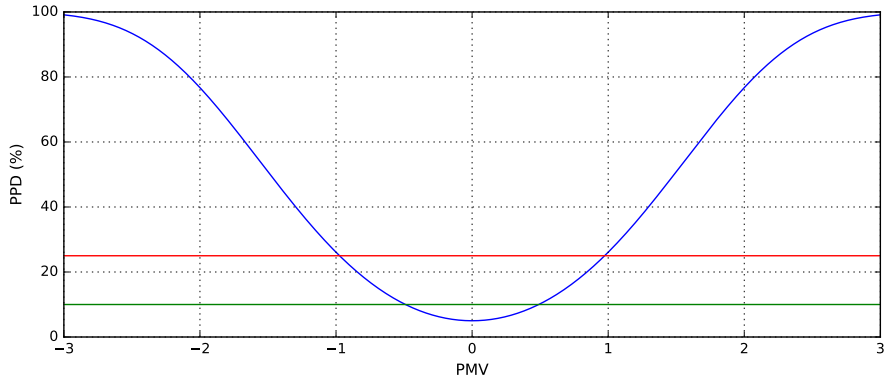

Figure 2.3: Fanger's Predicted Percentage of Dissatisfied (PPD) as a function of Predicted Mean Vote (PMV) [66]. The red line is a PPD equal to 25%, whereas the green line represents a PPD of 10%.

Given the relevance of the PPD-PMV index as a definition of thermal comfort, it seems pertinent to use Fanger's model to infer people comfort regarding the interior environment.

2.2 Modelling strategies

As referred previously, the approaches to implement modelling and optimization applications require primarily the development of a building energy model capable of forecasting the energy consumption, which depends on a set of conditions influencing it, namely the environmental conditions, the occupants behaviour, its architecture, among the most relevant ones. However, the modelling of energy consumption in buildings can be achieved by a wide range of approaches, and the scientific community has been employing great effort in its classification.

This work proposes the classification presented in Fig. 2.4, which follows Fumo's work in summarizing the different categories of building energy modelling found in the literature [68].

Throughout the Literature, three types of approaches have been consistently considered in what concerns energy modelling applications, as shown in Fig. 2.4 [68, 58, 69, 70, 52].

- Data-driven models based on Machine Learning algorithms;
- Physics-based methods, such as Building Energy Performance Simulators (EnergyPlus™);
- Hybrid methods, basically, combinations of the above.

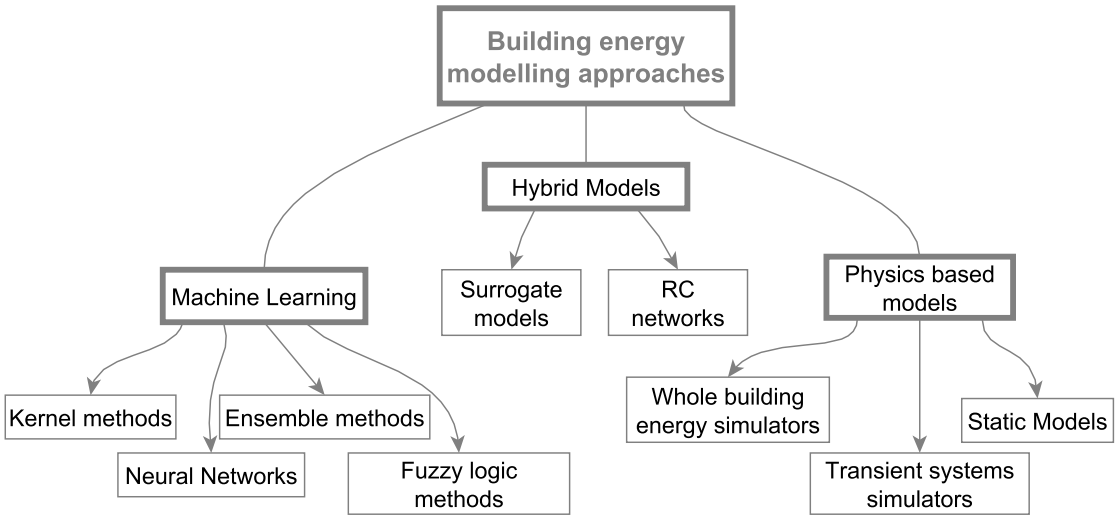

Figure 2.4: Building Energy Modelling approaches.

The subsequent sections will focus on reviewing the main approaches from each defined class of building energy modelling.

2.2.1 Machine learning models

Data dependent methods are often called Machine Learning, Soft Computing, Artificial Intelligence, statistical, or black-box methods. This is the trendiest approach due to the advent of Internet of Things, providing an almost incommensurable flux of data, and the dissemination of Data Science solutions by the reduction in computational cost, and powerful open source solutions to process data. This group deals with the modelling and forecasting of any system or process based on data patterns extracted by statistical methods, or algorithms.

As pioneer in this matter, the ASHRAE's contest "The Great Energy Predictor Shootout" unveiled the potential of Artificial Neural Networks for the building energy forecasting task, awarding the work of Mattias Ohlsson et al. [71] for their outstanding performance.

Since then, many initiatives have been created, focusing on improving the energy forecasting in buildings, namely "The Great Energy Predictor Shootout - II", and the Kaggle competition "Global Energy Forecasting Competition 2012 - Load Forecasting".

Kaggle[1] is the world's largest community of data scientists, and is focused on providing real world challenges to the community, disseminating the best open source practices in machine learning, and helping companies, and researchers, in the solving of highly dimensional and incomplete problems related with data.

[1] `https://www.kaggle.com`

Other works focused only on building energy consumption prediction are put into focus, such as the work from Subodh Paudel et al.[72] where they have used NN and orthogonal arrays to develop a pseudo-dynamic model of the heating demand in a building, with the goal to assist the energy supplier with predictive consumption to act towards efficiency. The architecture of the neural network is well detailed, and equations to determine architecture adjustments are proposed. The model inputs include climate data, occupancy profiles, operational characteristics and pseudo-dynamic transitional attributes. The latter are obtained by the orthogonal arrays to provide a smoother transition, and it allowed the creation of a more robust model.

Also, Li et al. [73] proposed a new method for forecasting the energy consumption of the air-conditioning system installed in a hotel, and claimed that hybrid genetic algorithm-hierarchical adaptive network-based fuzzy inference system (GA-HANFIS) achieved smaller coefficient of variation than an NN implementation. The hierarchical structure of the fuzzy-based model revealed to be significant as without it, the NN revealed to be more accurate. In this study an interesting manner to employ different SC algorithms was implemented, including a time-series model to predict the hotel's daily AC energy consumption [74]. One year later, this research group published a new work with the same comparison applied to the prediction of a public library energy consumption. Once again, the GA-HANFIS has higher accuracy than NN. It was also shown the ability of GA to optimize the parameters of the fuzzy-rules present in the ANFIS methodology.

An extensive review was carried out by Rajesh Kumara et al. [75] where they pointed several applications of NN, mostly for predicting building's energy consumption. Conversely, a review paper by Mohanraj et al. [76] has extensively surveyed Neural Network applications in predicting the performance of refrigeration, air conditioning and heat pump systems (RACHP). In their paper, there were found some limitations to the NN approach, such as: inability to extrapolate beyond the training data; inability to generalize by over training the network; and difficulty in selecting the optimum network architecture. The reviewed solutions suggested the creation of more relevant databases to train the NN more widely, to avoid over-fitting by fine-tuning the network's learning parameters, and finally, to improve the selection of an ideal architecture by the employment of genetic algorithm optimization. Notwithstanding, the overall conclusion was that NN can be effective in modelling and predicting the performance of RACHP systems.

Ahmad et al [77] have reviewed the performance of the most popular algorithms among researchers focused on electrical energy forecast, the Support Vector Machine (Kernel methods) and the Artificial Neural Networks. Though ANNs usually perform well in time-series forecast, and SVM rarely over-fitting the training data, the reviewed models have their own advantages and disadvantages. They acknowledge the difficulty in deciding which one is the best in forecasting. However, they conclude that the combination of models can ensure better forecasting performance. This method is called ensemble of algorithms and it is widely used in the most advanced Data Science prob-

lems, such as in Kaggle competitions [78].

Following this trend of the approach, Fan et al. [79] have implemented an ensemble of algorithms for the prediction of next-day building energy consumption and peak power demand. Their methodology for developing ensemble model applications can be depicted in Fig. 2.5. They have trained individually a Multi Layer Perceptron (a type of ANN), a Boosting tree (Tree-based method), a Random forest (Ensemble method), a Support Vector Machine (SVM, kernel method), a k-nearest neighbour (kernel method), and linear regression combinations in order to predict the same outputs.

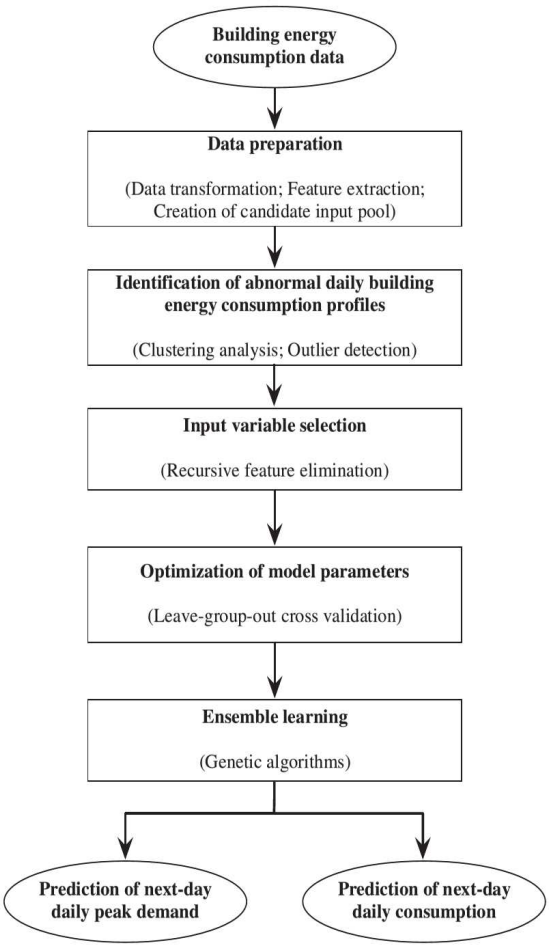

Figure 2.5: Schematic outline of Ensemble method implementation [79].

Finally, the ensemble model is developed by combining all models through a weighted sum, from which the weights associated with each predictive models were optimized using a genetic algorithm (GA) with the objective of minimizing the error. The case-study was the tallest building in Hong Kong, and the prediction accuracies of the ensemble

models measured by mean absolute percentage error (MAPE) were 2.32% and 2.85% for the next-day energy consumption and peak power demand, respectively. Whereas the best performing algorithm alone was the SVM with MAPE of 3.11% and 3.34% for the same predictions. The authors highlight the importance of feature elimination since it derived more accurate models while reducing the computational burden. Moreover, the superiority of ensemble ensemble models is evident since the accuracy of the combination of models was higher than the best model independently.

The available open-source machine learning libraries integrated to great diversity of programming languages has never been wider. Consequently, the number of algorithms is also overwhelming. Fernández-Delgado et al [80] have conducted an extensive review and tested 179 algorithms on 121 publicly available data sets, arriving to the conclusion that the most robust type of algorithm was the random forests, followed by support vector machines. They also concluded that while Support Vector Machines can be the most accurate in smaller problems (lower number of input), Random Forests easily beat the other options when the complexity of the problem and the number of inputs gets higher.

It seem relevant to also explore the capabilities of Random Forests, besides Artificial Neural Networks and Support Vector Machines. Artificial intelligence techniques are usually employed to solve classification and regression problems. Classification problems include discrete data, and the goal is to divide the set of data in several categories, whose characteristics are given by the user. A running example is predicting whether tomorrow it is going to rain or not.

A regression analysis deals with function approximation, where data is continuous and the goal of the algorithm is to approximate a continuous function as good as possible to whole possible outputs. Since the nature of energy consumption data is continuous and there is the need to approximate a data-driven models to a physics-based model (surrogate model), this review will only focus on the regression versions of the machine learning algorithms proposed subsequently.

Artificial Neural Networks – NN

Artificial Neural Networks development was triggered by the attempt of mimicking the human brain ability of learning from experiences, enabling it to predict possible consequences of new actions. Human neural networks consist on a large group of neurons connected by synapses. These connections have the capacity to adjust their synaptic weight and store the information extracted during learning activities, regarded as a general synaptic modification, first stated by Hebb [81]. Supervised Artificial Neural Networks also learn from experiences, by means of a learning algorithm, enabling it to develop heuristic relationships between experiences, presented as a form of input and output pairs of samples in a database.

The selection of which learning algorithms are more suitable for mimicking the human brain has been the subject of several researchers, and it still remains a struggling one to

be delivered fully. Nevertheless, Artificial Intelligence and Soft Computing are delivering breakthroughs in Science [82, 83].

This section presents a Momentum Modification Backward Propagation Neural Network Algorithm, for which the book of Hagan et al [84] served as a helpful support. Fig. 2.6 shows an example of the architecture of an artificial Neural Network that comprises one input layer with four inputs; one hidden layer with five neurons, and one output layer with one unit.

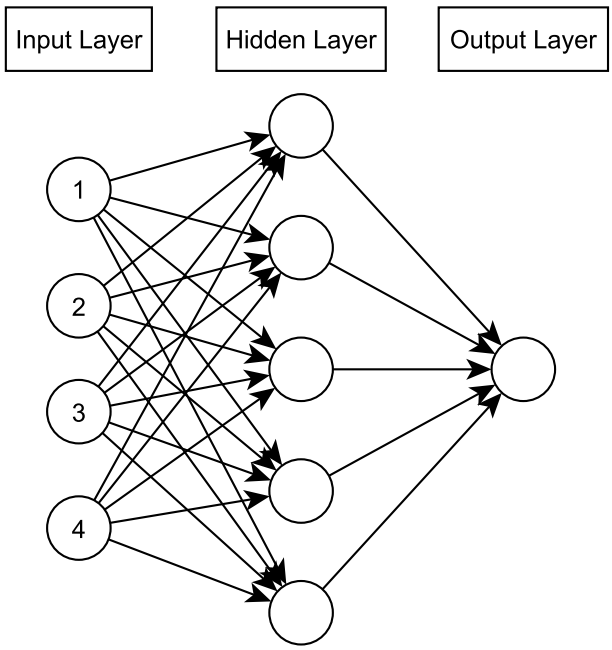

Figure 2.6: Scheme of a Feed Forward Neural Network.

The architecture of an artificial neuron includes an activation, or transfer function, synaptic weights on connections between other units, and a bias term. The mathematical model of a neuron is described as follows:

$$a = f(wp + b) \tag{2.2.1}$$

where a is the output signal (activation) of the transfer function f in order to the synaptic weight w times the input p plus a bias value b. Note that w and b are the scalars adjusted by the learning process, and where the learned information will be stored. Function f depends on the problem to solve, however, logistic sigmoid and hyperbolic tangent are the most popular, and convenient to apply.

A commonly used Neural Network for regression problems is the multilayer feed forward with three layers, similar to the one shown on Fig. 2.6 [85, 86]. A multilayer

feed forward Neural Network sequentially computes the signals from inputs towards outputs. The output of each layer is the input of the subsequent, and the model of a layer is the conversion of neuron's model to matrix form. It is written as follows (equations 2.2.1 and 2.2.2):

$$a^{m+1} = f^{m+1}(n^{m+1}) \tag{2.2.2}$$

where network n is

$$n^{m+1} = W^{m+1}a^m + b^{m+1} \tag{2.2.3}$$

for $m = 0, 1, ..., M-1$.

The upper-script, m, represents the layer number. The vector of inputs p is the first activation (a^0), and the hypothesis of the Neural Network is defined as a^M, where M is the total number of layers. The transfer function f applied in this particular work is the logistic sigmoid, and it is defined in equation 2.2.4.

$$f(x) = \frac{1}{1 - e^{-x}} \tag{2.2.4}$$

The learning process is here regarded as an optimization problem, where weights and biases are adjusted aiming at minimizing the error of Neural Network's predictions. Therefore, a performance function and an optimization algorithm are required for this purpose. A commonly and effective performance estimator is the summed square error (SSE), which allows for the evaluation of discrepancy between hypotheses' vector $a^M_{W,b}(p)$ and targets' vector t for input p. Therefore, the approximation of the SSE is defined as in equation 2.2.5.

$$\widehat{P}(W, b; p, t) = \big(t - a^M_{W,b}(p)\big)^T \big(t - a^M_{W,b}(p)\big) \tag{2.2.5}$$

Note that the performance estimation requires the evaluation of all n samples presented on the data-set. In this particular work, the choice of learning algorithm is the batch momentum modification back propagation, which tends to converge faster, with lower computational cost, and with the ability to avoid minor local minima, when compared with its predecessor – steepest descent algorithm. These are gradient-based optimization algorithms. Thus, they are expected to converge due to the quadratic nature of the presented fitness function, Eq.2.2.5, and due to the smoothness of the transfer function Eq. 2.2.4. The momentum modification to back propagation update rule of the weights and biases of network's layer m at iteration $k+1$, is defined in equations 2.2.6 and 2.2.7.

$$W^m(k+1) = \gamma W^m(k) - (1-\gamma)\alpha \left[\frac{1}{n}\nabla_{W^m}\widehat{P}(W, b; p, t)\right] \tag{2.2.6}$$

$$b^m(k+1) = \gamma b^m(k) - (1-\gamma)\alpha \left[\frac{1}{n}\nabla_{b^m}\widehat{P}(W, b; p, t)\right] \tag{2.2.7}$$

where γ is the momentum weight, α is the learning rate, and $\nabla_{W^m}\widehat{P}(W,b;p,t)$ and $\nabla_{b^m}\widehat{P}(W,b;p,t)$ are the gradients of performance function at layer m in order to the weights and biases, respectively. The addition of a momentum coefficient allows for the use of a larger learning rate, while improving algorithm stability, and consequently, accelerating convergence at the end of training (where gradient descent tends to slow down). The gradient terms are the core to this learning algorithm, since they deliver valuable information about the topology of the performance function. The gradient of the last layer can be calculated by deriving the performance function, while the same cannot be applied at the hidden layers, where there is no performance function. Consequently, the solution is to apply the back propagation algorithm, which propagates the error terms to the inner layers. This error term δ^m, also known as sensitivities, provides the algorithm with a measure of the influence of each hidden neuron on the hypotheses. Hence, applying the chain rule of derivatives, sensitivities at the last layer M are computed as presented in equation 2.2.8 and 2.2.9.

$$\begin{aligned}\delta^M &= \frac{\partial}{\partial n^M}\widehat{P}(W,b;p,t) \\ &= -2(t-a^M)\circ f'\left(W^M a^{M-1}+b^M\right)\end{aligned} \tag{2.2.8}$$

For layers $m = M-1,...,2,1$, it is set as

$$\delta^m = \left(W^{m+1}\right)^T \delta^{m+1}\circ f'\left(W^m a^{m-1}+b^m\right) \tag{2.2.9}$$

Where $\circ$ represents the element-wise multiplication of matrices, and f' represents the first order derivative of the transfer function.

A derivative term could increase significantly the complexity of training a Neural Network. However, the derivative of logistic sigmoid transfer function is considered *mathematically convenient* and it is described in Eq. 2.2.10,

$$f'\left(n^m\right) = \left(1-a^m\right)a^m \tag{2.2.10}$$

The computational and mathematical convenience of this derivative is indubitable, since it only depends on terms already calculated during forward computation, i.e. on itself. With sensitivities computed on every layer, the gradients of performance function in order to the weights and biases can be written as described in 2.2.11, respectively, as

$$\begin{aligned}\nabla_{W^m}\widehat{P}(W,b;p,t) &= \delta^m\left(a^{m-1}\right)^T \\ \nabla_{b^m}\widehat{P}(W,b;p,t) &= \delta^m\end{aligned} \tag{2.2.11}$$

Hereafter, equations 2.2.6 and 2.2.7 can be updated for each k^{th} iteration until performance function reaches stopping criteria. Once the learning process is complete, their

weight matrices ,W^m, and biases vectors,b^m, for each layer, m, are obtained. Then, validation assessment and error estimation must be performed on a test dataset (hidden from training) in order to assess over-fitting and generalization error, by applying feed forward propagation on the NN, equations 2.2.2 and 2.2.3, to predict new hypotheses $a(p_{new})$ to the new inputs, p_{new}. for a two layer NN, it can be rewritten as:

$$a(p_{new}) = f(W^2 f(W^1 p_{new} + b^1) + b^2) \tag{2.2.12}$$

The major limitations of this algorithm are the whole architecture and training features requiring fine tuning, and influencing performance considerably. Furthermore, without sufficient data, obtaining reasonable accuracy becomes unattainable. For the specific application in Building Energy Modelling, neural networks have the advantage of modelling non-linearity and complex patterns with more accuracy than other regression methods and physically based models. The disadvantage is to have no control over the physical-related behaviour of the outputs because of to the complexity of the networks, since the approximation to reality is based on high-dimensional weight matrices, proving little information on what input features the algorithm employs in the search for lower prediction errors.

Nevertheless, Neural Networks are undoubtedly very powerful techniques to model complex systems and help on building dynamics forecasting tasks.

Support Vector Machines – SVM

Support Vector Machines have been introduced in 1995 by Vapnik and Cortes [87] as an answer to solve the handwritten character recognition problems in a more robust way compared to Artificial Neural Networks (classification problem). The following explanation is based on the works from Scholkopf et al. [88], and the review from Foucquier et al. [58].

The principle of the SVM for regression is to find the optimal generalization of the model, in order to promote sparsity. Therefore, the quest for a generalized solution is in its nature. They rely on the definition of a performance function (soft margin loss function) which ignores errors located within a defined boundary - ε epsilon.

Figure 2.7 shows an example of one-dimensional linear approximation by this type of approach. During the optimization process of the model learning, the performance of the model in any point inside the boundary band have *zero* error.

Suppose that the represented training data $\{(x_1, y_1), ..., (x_n, y_n)\}$, x_i with input data $x \subset \mathbf{R}^n$ and output data $y \subset R$ is provided.

To create a model of a non-linear space, the basic idea is to overcome the non-linearity by mapping variables x to $\Phi(x)$, converting the new inputs to a linear map such as the one presented.

The goal of the learning process is to find a function $f(x)$ with a small test error, that means to have no more than ε deviation from the measured outputs y_i present in the training data.

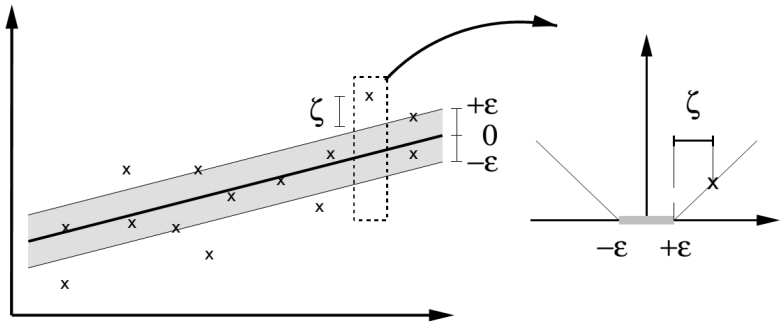

Figure 2.7: The soft margin loss setting for a linear SVM [89].

$$f(x) = \langle \omega, \Phi(x) \rangle + b \tag{2.2.13}$$

where $\langle , \rangle$ denominates a dot product, $\Phi(.)$ is the non-linear function to map the inputs to a higher dimensional feature space, and ω and b are the parameters to be estimated via optimization problem 2.2.14 focused on minimizing the training error.

$$\min_{\omega,b,e} \quad \frac{1}{2}\|\omega\|^2 + \frac{\gamma}{2}\sum_{i=1}^{l} e_i \tag{2.2.14}$$

$$\text{subjected to} \quad y_i = \langle \omega, \Phi(x_i) \rangle + b + e_i \tag{2.2.15}$$

where γ is a predefined regularization constant, and e_i is the penalization to the performance function $(\zeta_i + \zeta_i^*)$, representing the error above the threshold ε. However, to be able to find the extreme of a constrained function such as 2.2.14, it's necessary to use a Lagrangian multiplier α applied to the constraint 2.2.15, which represents the support vectors.

$$\mathcal{L}(\omega, b, e, \alpha) = \frac{1}{2}\|\omega\|^2 + \frac{\gamma}{2}\sum_{i=1}^{l} e_i - \sum_{i=1}^{l} \alpha_i(\langle \omega, \Phi(x) \rangle + b + e_i - y_i) \tag{2.2.16}$$

Then, the solution to the optimization problem is encountered by finding the first order derivatives for each variable of the Lagrangian. From $\frac{\partial \mathcal{L}}{\omega} = 0$, the values of ω take the form of

$$\omega = \sum_{i=1}^{l} \alpha_i \Phi(x_i) \tag{2.2.17}$$

and from $\frac{\partial \mathcal{L}}{\alpha} = 0$ and $\frac{\partial \mathcal{L}}{b} = 0$ we obtain Equations 2.2.21 and 2.2.22, respectively.

$$y_i = \langle \omega, \Phi(x) \rangle + b + e_i \tag{2.2.18}$$

$$\sum_{i=1}^{l} \alpha_i = 0 \tag{2.2.19}$$

Substituting 2.2.17, into 2.2.13 the regression model is rewritten as follows

$$y_i = \sum_{i=1}^{l} \alpha_i k(x_i, x_j) + b \tag{2.2.20}$$

from where the parameters α and b can be obtained by regressing the equation to the training data. $k(x_i, x_j)$ is the kernel function responsible for mapping the variables to the higher dimension, substituting the dot product $\langle \Phi(x_i), \Phi(x_j) \rangle$. This kernel can take many forms to adapt to the nature of data. The most common and reliable kernel function is the radius basis function, or Gaussian function and it is expressed as

$$\langle \Phi(x_i), \Phi(x_j) \rangle = k(x_i, x_j) = e^{\frac{\|x_i - x_j\|^2}{\sigma^2}} \tag{2.2.21}$$

Finally, the Support Vector Regression model can estimate new hypotheses for a given input from the equation 2.2.22 if considering a Gaussian function kernel:

$$y_i = \sum_{i=1}^{l} \alpha_i e^{\frac{\|x_i - x_j\|^2}{\sigma^2}} + b \tag{2.2.22}$$

Only leaving for architecture parameters definition, the choice of γ which will compromise between over-fitting if too small and high variance if too high i.e. regularization term, as well as the ϵ value for the error-free band.

For a rather more detailed mathematical validation of the steps conducted above, the work from Smola and Schölkopf [89] provide sufficient information.

Vapnik's theory is helpful in preventing model over-fitting, since it employs an estimator of the complexity of the model vs its accuracy, the so called Structural Risk Minimization, the optimization problem in 2.2.14, which prevents the SVM architecture of becoming too complex. Another advantage of this algorithm, especially comparing to Neural Networks is its implementation robustness, since there are no architectural parameters to be defined other those of the kernel function. However, the main drawback of this approach is its computational burden due to the quadratic optimization problem derived from the Lagrangian approximation.

Nevertheless, if the problem doesn't have too many dimensions and the database is not very large ($<$ 100k samples), this algorithm is definitely a choice to retain.

Again, the proposed algorithm is sufficient and able to be implemented as learning algorithm. However, for performance purposes the open-source packages from Python™

libSVM[2] and scikit-learn[3] may provide more stable implementations, as well as R package e1071.

Random Forests – RF

Random forests algorithm, the most recent modelling strategy of the ones reviewed, belongs to the ensemble learning methods from machine learning, and they are mainly employed in classification and regression tasks. Ensemble methods for regression problems are learning algorithms that construct a set of many individual learners (base learners) and combine them to predict new data by taking a weighted vote of each individual learner. It is now established that ensemble methods are often more accurate than the individuals composing that ensemble [90].

Random forests have proven to give generalization error rates (over-fitting prevention) that compare favourably to the best statistical and machine learning methods, such as SVM and NN. In fact, random forests are among the most accurate general-purpose classifiers available [78, 80].

In 2001, Breiman [91] introduces the term Random Forests algorithm as a general ensemble of decision trees, which depend on independent sets of data with the same distribution. The results provided from the whole group are combined through averaging, yielding a global hypothesis for a determined input vector.

Classification and Regression Trees (CART) are a type of decision trees capable of solving classification and regression problems. In a regression model such as those of energy consumption prediction, a CART slips the inputs' subspace in a predefined number of splits, and location, with the goal of minimizing the variance of the output depending on the inputs presented in each partitions. Once the tree is trained and a new input is given, the predicted result will be the average of the outputs comprehended within the region assigned to each combination of inputs. The 2001's book from Berk [92] provides comprehensive dissemination material not only on CART algorithm, but also on Random Forests.

The following description of the flow of the algorithm is adapted from the work original work of Breiman [91], and the work from Abdulsalam et al. [93], its reading is advised for further information on the subject.

1. A database contains N pairs of samples, $\mathbf{S} = \{(x_1, y_1), ..., (x_N, y_N)\}$, each x_i with D attributes as $x_i = (x_i1, ..., x_iD)$, and each output y_i with $\mathbf{O}$ targets as $y_i = (y_i1, ..., y_iO)$.

2. For B number of trees, T_i, assign a random subset of the $\mathbf{S}$ database records, by sampling with replacement method[4], and get $S_i = \{S_1, ..., S_B\}$.

[2] `https://www.csie.ntu.edu.tw/~cjlin/libsvm/` which is available for a breadth programming languages, including C++, Java, and R.

[3] `http://scikit-learn.org/stable/modules/svm.html`

[4] Sampling with replacement method is also known as bootstrap bagging, i.e. the same sample can be

3. For each tree T_i and dataset S_i, select a m number of attributes from x_i, with $m < D$, and train each tree to predict y_i, simply an average of each area associated with each leaf.

4. For a new input u, predict $\hat{y}$ as an average of the individual hypothesis proposed by each tree:

$$\hat{y} = \frac{1}{B} \sum_{i=1}^{B} T_i(u) \tag{2.2.23}$$

The step number four is the essence of an ensemble model which can accommodate other forms of decision methods, such as majority vote rule, or weighted sums depending on the individual models performance.

According to Abdulsalam et al. [93], the Random Forest algorithm error depends mostly on two things:

- The correlation among the trees: the smaller the correlation among the trees the more variance cancelling takes place as the trees vote, and therefore the smaller the error rate.

- The strength of each individual tree: the more accurate each tree is, the better its individual vote, and therefore the smaller the error rate.

In conclusion, and according to the referred authors, it seems that the main advantage of random forests is providing superior accuracy, when comparing to other algorithms. Moreover, this algorithm rarely over-fits (if the data has representativeness) and does not require test set validation since circa 33% of data is always hidden from each tree during the training phase because of the bootstrap sampling, allowing for as well the *out-of-bag* score can be computed internally during training. However, if the computational budget is not an issue, other methods should be considered for cross-validation, such as k-fold.

As additional information, due to the random permutations of the available input variables that each tree uses for prediction, it is possible to get the importance of each variable computing the reduction of variance on the predictions when a certain input is provided – Step two of the process depicted previously. In the same fashion, it can provide information on what group of samples are more important for training.

When comparing Random Forests with Support Vector Machines and Neural Networks, it can be said they provide models with the same accuracy. However, Random

selected every time. Therefore, the training dataset for each tree contains multiple copies of the original database. This type of random selection with replacement ensures that about 1/3 of all data is not included in the training set which are called out-of-bag (OOB) samples. Computing trees' performance on OOB samples provide a embedded evaluation of the test error, saving considerable computational time against other machine learning methods [91, 93].

Forests are more interpretable (*less* black-box), are faster to train, handle incomplete data, and do not require cross-validation.

It seems important to assess the viability of using Random Forests as heuristic modelling approach to building energy modelling applications.

2.2.2 Physics-based models

On the other spectrum of approaches, there are the physics-based modelling, engineering approach, or also called white-box methods. This type remains the benchmark and the most reliable approach since it provides the robustness of the laws of physics, finite element methods, and several years of research investment. The methods can be validated either by calibration with real measured data, or by consistent bottom-up validation of the physical laws involved in each subsystem. Simulations using dynamic tools such as TRNSYS or EnergyPlus, are most robust and widely implemented as observed previously, namely due to their ability to capture the salient physical and transient interactions between most of the elements present in a building energy system. Crawley et al. [94] have dedicated a whole article reviewing these and other important building energy simulation software, highlighting the capabilities and limitations of each software.

EnergyPlus is an open-source software especially dedicated to building performance simulation. It is capable of performing simulations with a variable time step, predicting energy and water consumption in buildings, and calculating heating and cooling transient loads. This software has proven to be able to deliver models of heating, cooling, lighting, ventilation, and other energy flows, allowing for the integration of external weather data files. Its robustness has been verified by the ANSI/ASHRAE Standard 140-2001 (BESTEST) [95]. EnergyPlus™ includes an Energy Management System capability which has been proven to be useful for the assessment of co-simulation problems such as testing model predictive control strategies by the integration with external control simulation software such as MATLAB/Simulink®, and BCVTB (Building Controls Virtual Test Bed) [96, 97].

EnergyPlus™is made accessible through a range of both free and commercial graphical user interfaces (GUIs), most notably the DesginBuilder GUI. Moreover, it is the most widely used of all available building performance simulation tools. Crawley et al. [94] have dedicated a whole article reviewing this and other important building energy simulation software, highlighting the capabilities and limitations of each one.

Overall, this type of approach involves thermal, solar and air flow modelling and concerns the geometry, materials, control and systems of the building, occupation and activity schedules. While this is accessible for buildings under design phase, the same information can be cumbersome to obtain in existing buildings, since the access for physical properties to implement such models is limited. Frequently, this inherent degree of complexity leads to the adoption of assumptions on the materials properties and systems behaviour, compromising the robustness, and applicability of such approach [68, 58]. Nevertheless, these are the most robust solutions regarding building energy simulation

and its utility is unquestionable, either during development, or energy management tasks of existing buildings.

2.2.3 Hybrid models

In between both methods there lay the hybrid approaches, also known as grey-box methods, which its principle is to couple both classes described previously.

As any hybrid element, those methods are also the combination of two, or more elements, and in the light of the building energy system it combines a physical building model to represent the structure or physical configuration of a building, a zone, or the HVAC system, for then to simplify by statistically identifying the important parameters which are representative of the key physical parameters and characteristics under investigation [68, 58].

One way to implement such combinatorial approach consists in using machine learning algorithms for physical parameters search. In this approach, practitioners usually couple a building representative nodal model (Resistance-Capacitance networks) with an optimization algorithms, such as Genetic Algorithm, simplex method, and so on.

Another way is implementing a Physics-based model to represent the structure, or physical configuration of the whole building, or HVAC equipment, being later simplified by the implementation of a data-driven model based on the response of the simulator to a limited, but sufficient, number of chosen data points and parameters. These samples have to be representative of the physical building's characteristics [68, 58].

For the purpose of modelling and optimization applications, the state-of-the-art approach seems to be the use of high-fidelity surrogate (or meta-) models of dynamic building energy simulations to rapidly evaluate the technology decision space, according to Foucquier et al. [58].

Models of this sort can undertake optimization of dynamic building operations, but at a fraction of the overall computational cost, since, after validation, a surrogate model has the capability of delivering simulation responses promptly. Surrogate models characteristics are especially suited for the optimization problems solved by meta-heuristic and population-based optimization algorithms, as they can undertake the required extensive objective function evaluations, but at a fraction of the overall computational cost.

Although after validating surrogate models they are capable of promptly deliver simulation responses, the process of generating a dataset, defined by a Design of Experiments (DOE), to regress a meta-model can be time consuming, and for simpler analysis, it can be even prohibitive when compared with regular building simulations, as pointed out by Eisenhower et al. [36]. On the other hand, many researchers have proven the superiority of this approach in building design optimization, especially in retrofitting optimization, but also in Building Control Optimization, as presented earlier.

Since surrogate modelling approach seems to be pertinent for conducting this thesis, more emphasis will be placed in the following section, reviewing the methodology behind the approach to hybrid building modelling.

Surrogate modelling methodology

The simulation of case-scenarios, or even optimization routines, such as those reviewed in sections 1.3.1 and 1.3.2, are often conducted as depicted in Fig. 2.8.

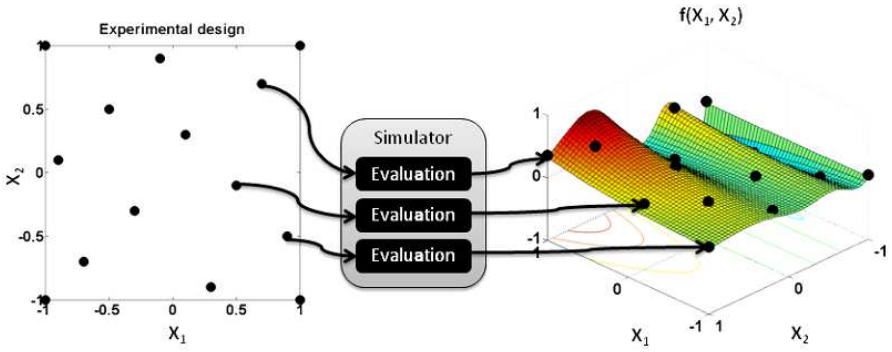

Figure 2.8: General approach to simulation based experiments [98].

A set of variables X_1 and X_2 (left side) is defined, either by a design of experiment, or by an optimization iteration, then sent to a simulator to compute the corresponding result, or objective function value (right side). The results may be evaluated by the researcher, or the optimization algorithm, leading to simulate another set of variables while results are not satisfactory enough. Frequently, this method leads to the simulation of not so relevant case-scenarios, compromising the available time for experiments, and in the number of optimization attempts, as referred in section 1.3.1 [59]. Where this may be feasible for simpler problems, or analysis, the same may be limiting in high complexity scenarios.

Surrogate models, also known as response surface models (RSM), meta-models, proxy models or emulators, are intended to mimic the complex behaviour of the underlying simulation model [98]. The basic idea in the surrogate model approach is to avoid the temptation to invest the whole computational budget in answering the question at hand and, but instead, invest it in developing fast-response mathematical approximations to the physics-based simulators with acceptable accuracy. Given these approximations, many case-studies may be explored, and many hypotheses tested at a fraction of the expected computational cost.

Once a group of satisfactory hypotheses, or optimizations, are found, it is possible to return to the main simulator to test such ideas and, if necessary, update the surrogate model and repeat the process [59].

The generic steps of the surrogate modelling process remain essentially the same throughout a wide range of applications, and such steps are illustrated in the flowchart in Fig. 2.9, which follows the principles stated by Forrester et al [59], and adapts the building energy modelling scenario.

First, a set of inputs is obtained, typically by sampling the decision domain and

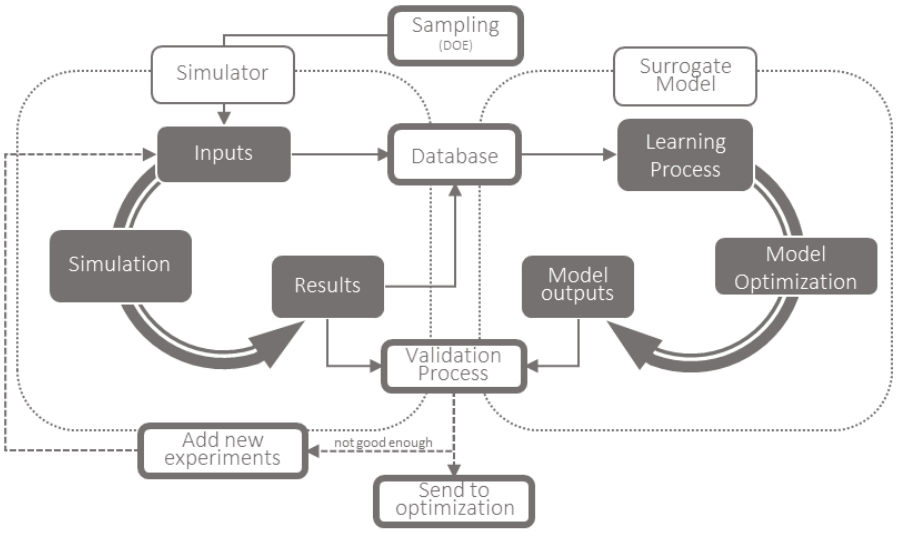

Figure 2.9: Classification of building energy modelling approaches.

the range of the uncontrollable variables. In other words, a number of possible events are generated and sent to the simulator as inputs. Then the simulations take place, generating the results and updating the database with the corresponding result for each event, reflecting the building's transient response to systems set points and uncontrollable variables.

Once this database is created, a Machine Learning algorithm, for example Neural Networks, learns the patterns from the provided data, delivering a simplified model of the building response. This model's architecture is then optimized in terms of the intrinsic model parameters, and model outputs are provided. With data saved for validation, the results are compared with the surrogate outputs, providing data for error analysis and model validation. While the yielded model is not sufficiently satisfactory, other experiments are drawn, sent to the simulator, repeating the whole process.

Having constructed a suitably accurate model, it is then finally embedded in the computation of the fitness function subject to optimization.

The following list summarizes the three steps required for the implementation of the surrogate model, envisioning subsequent optimization, according to Forrester et al [59]:

Sampling case-scenarios: Sampling methods are designed to overcome the *curse of dimensionality* problem stated in the Fig. 2.10. In this case a cube represents the full factorial combinations of 3 variables, x_1 with three distinct value, x_2 with four and x_3 with 5, totalling 60 possibilities $(3 \cdot 4 \cdot 5)$.

Taguchi demonstrated that the number of runs can be significantly reduced based on a degrees-of-freedom approach as given below in equation 2.2.24:

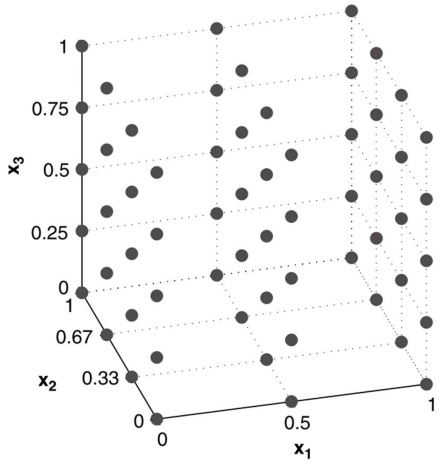

Figure 2.10: Example of a 3 variables full factorial sampling plan [59].

$$N = 1 + \sum_{i=1}^{NV} (L_i - 1) \tag{2.2.24}$$

where N is total number of experiments required, NV is number of independent variables, and L is number of bound levels. Taguchi's method involved a new adaptation of the conventional DOE method, and is capable of greatly reducing the number of required samples to uniformly populate the design space. In the case of building energy modelling, Yi et al [99] evaluated the consequences of early design decisions with the implementation of a meta-model sampled by Taguchi's method. They considered 8 design variables with 3 distinct values [-1:1], what would have led to 6561 possible combinations (3^8). However, a Taguchi L_{18} orthogonal array has been adopted instead, reducing to 18 runs the required DOE to cover the search space. Still in building design optimization, the same methodology was implemented by Gong et al [100], and Filfli and Marchio [101], both reducing a 2^{31} combinatorial design (over 2 billion combinations) to 32 experiments in a L_{32} Taguchi array.

Another sampling method employed in building design optimization [100, 101, 102], and in retrofitting calibration [103] is the Latin Hypercube Sampling, a particular case of stratified sampling. The range of each input factor is divided into l ($l > 2$) intervals of equal marginal probability, and within each interval one observation is made randomly. This sampling method has the advantage of representing all portions of a variable distribution by a statistical technique which involves dividing each dimension of the design space into equal sections, randomly selecting a section from each, and then eliminating those sections until all others have been used [104].

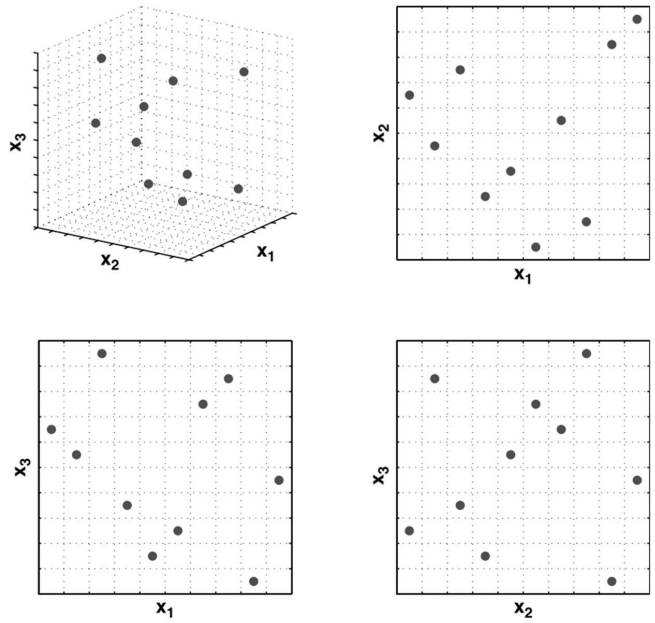

Figure 2.11: Example of a 10 samples Latin Hypercube Sampling of a 3 variable problem [59].

Nevertheless, both methods present interesting features and they should be accessed in this research. Once completed the sampling part, it is time for updating the database and define the samples in the simulation process.

Samples simulation: In this step, a white-box model is required, as referred previously in Section 2.2.2. This white-box model can be a whole building energy simulator, or any other transient systems simulator which calculates the influence of external and internal loads in the comfort conditions inside living spaces and the energy consumption associated with the control of the HVAC system, lighting, and equipment.

The available approaches to building energy simulators are vast, but especial interest is given to TRNSYS, and EnergyPlus, due to their proven capability of delivering robust building energy models.

Heuristic model development: The accumulation of the previously sampled and relevant data in a database should be fulfilled by previous simulations. The collected data should represent the effects of each decision variable (candidate) in the desired objective function, such as comfort index, energy consumption, and so on.

There exists several methods to assess feature's sensitivity, ranging from variable ranking methods based on variable correlations, or to the reviewed Neural Net-

works' sensitivity assessments, or to Random Forests embed feature ranking.

From the created database is expected an implementation of an heuristic model, based on machine learning, such as the ones reviewed in Section 2.2.1, or other regression techniques.

According to reviewed works in Section 2.2.1, Machine learning approaches seem suited, and the actual scientific trend.

Each highlighted step has its contribution to the limitations of the surrogate approach. A key limitation that may arise in building energy modelling, because this type of problems have to deal with multiple dimensions (variables), is the exponential increase of the number of points needed to give reasonably uniform coverage of the domain of building's operation - the so-called *curse of dimensionality*. That is to say, given a straightforward full-factorial sampling scenario, if n variables are sampled in k distinct values, the number of required simulations is k^n. Basically, the complexity of the problem at hand may limit the implementation of surrogate models. For example, another complexity-related limitation may occur in the modelling algorithm step. If the problem is highly stochastic, or a high number of variables, the learning algorithm may simply be unable to extract the patterns from data, converging in an inaccurate model, representing an improper surrogate.

2.2.4 Remarks on building energy modelling strategies

Considering the reviewed approaches to the modelling problem, hybrid models seem the natural choice to take into account for the development of a supervisory predictive control, with a particular focus on surrogate models.

Firstly, this work is conducted under a simulation environment, so, a purely black-box approach would not be feasible since there is no real data available. Furthermore, in a real-world scenario, available data is rarely fully available. For example, a building architecture and energy systems might be well described technically, but sensor data is unavailable, incomplete, or too repetitive, or a building might be equipped with sensors, but its technical description is poor, or unreliable. Alternatively worse, both scenarios can be combined, hindering the implementation of a reliable predictive control. Hence, in a real world application, there will always be something missing, calling for flexible solutions capable of adapting to different sources of data, and capable of maximizing the available data via data fusion approaches.

The development of grey-box approaches follows the trend in the scientific community since they are considered the state-of-the-art and a promising field in the near future to the building energy modelling [58]. Moreover, surrogate models are known for delivering results at a fraction of the computational cost of deterministic and dynamic models, and since optimization processes are highly iterative, they are expected to help in providing results with an acceptable computational cost.

This thesis will, therefore, focus on exploiting the capabilities of surrogate models based on data-driven algorithms, Machine Learning, or Soft Computing algorithms to address the complex task of building retrofitting optimization, giving more emphasis in the review of modelling algorithms of this sort.

EnergyPlus™ is the physics-based simulator selected for supporting the development of the hybrid models for the fact that it is one of the most relevant energy performance simulators [95, 94, 58]. Moreover, it enables the integration of a co-simulation environment via BCVTB communication protocol which allows for the validation and assessment of control strategies [97, 105].

2.3 Optimization strategies

Optimization problems focus on the search for one or more solutions which improve the objective, or objectives desired to be improved. One of the most challenging tasks in optimization is to understand what needs to be improved, and how two solutions are comparable regarding its utility in improving what is needed. That is called objective function and determines what is required to be minimized (or maximized). The process of finding the set of conditions which promote that minimization is held by an optimization algorithm which searches for those conditions as fast and as accurate as possible.

This section focuses on reviewing a set of approaches and techniques relevant to defining and solving the multi-optimization problem inherent to the supervisory predictive control.

2.3.1 Optimization problem formulation

Similarly to any optimization problem, building retrofitting optimization and building optimized control are based on the same mathematical foundations [32]:

$$\begin{array}{ll} \text{minimize} & f_0(x) \\ \text{subject to} & p_i(x) \leq b_i, i = 1, ..., m. \\ & g_j(x) = 0 \end{array} \tag{2.3.1}$$

Where the vector $x = (x_1, ..., x_n)$ is the optimization variable of the problem, the function $f_0 : \mathbf{R}^n \to \mathbf{R}$ is the objective function, the functions $p_i : \mathbf{R}^n \to \mathbf{R}$, $i = 1, ..., m$, are the inequality constraint functions, and the constants $b_1, ..., b_m$ are the limits, or bounds, for those constraints. The functions $g_j : \mathbf{R}^k \to \mathbf{R}$, $j = 1, ..., k$, are the equality constraint functions. A vector x^* is called optimal, or a solution to the problem 2.3.1, if and only if it has the smallest objective value among all vectors that satisfy the constraints: for any z constrained by $p_i(z) \leq b_i, ..., f_m(z) \leq b_m$, and $g_j(z) = 0$, such that $f_0(z) \geq f_0(x^*)$ is verified.

The optimized solution, set-point, or decision is the candidate which will have the absolute better adequacy, fitness, or cost over any possible candidate while satisfying

the imposed constraints.

As such, every building energy optimization problem has an objective function f_0, or several (in the case of multi-objective optimization), representing the utility of choosing different energy efficiency measures. Correspondingly, the optimized control has an objective function as well, depicting the utility of choosing any set-point for a specific period. This utility function can take a breadth variety of forms, namely energy consumption, or the costs related to it, the comfort of occupants, indoor air quality, the environmental impacts, and so on. Ultimately, it would be preferable to minimize (or maximize) every possible objective, but that is impracticable (Utopia point in Fig. 2.12), since most objectives are conflicting with each other, requiring the implementation of a multi-objective approach.

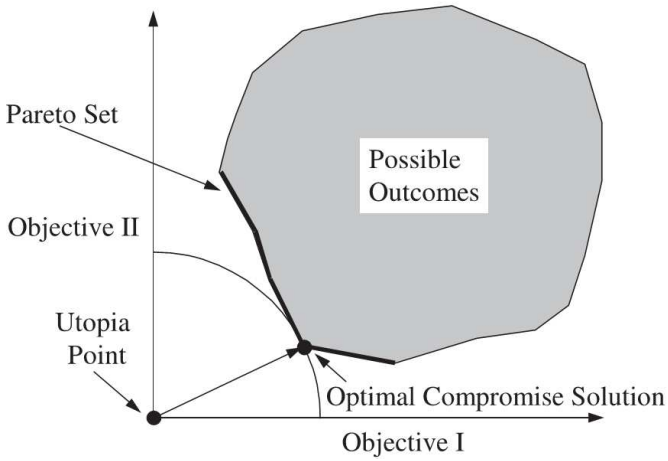

Figure 2.12: Optimal compromise solution.

Multi-objective optimization is commonplace, and there are two popular ways of addressing this issue:

- The first is by the formulation of a meta-objective, also called *linear scalarization*, which combines the various objectives through a weighted sum, transforming it in a single objective, which then formulates an optimization problem such as the one depicted in equation 2.3.1. This approach requires expert knowledge regarding the relative weight of the handled objective and is depicted as:

$$\text{minimize} \qquad \sum_{i=1}^{k} \omega_i f_i(x), \tag{2.3.2}$$

  where ω_i is the weight given to each objective f_i.

- Alternatively, by the implementation of a Pareto rank, which consists in considering all the possible combination of objective functions, converges in a Pareto

front. This Pareto front, depicted in Fig. 2.12, represents all the possible solutions which are optimal in the wider sense (for each defined compromise), leaving the decision of a trade-off between solutions for a post-process. Therefore, the optimal compromise point is the member of the Pareto set which lies geometrically closest to the utopia point by calculating the vector distance in the performance space by metrics such as Manhattan, Euclidean, or Chebyshev [106]. In this way it's possible to explore the *entire* Pareto front without prior knowledge about the problem [107].

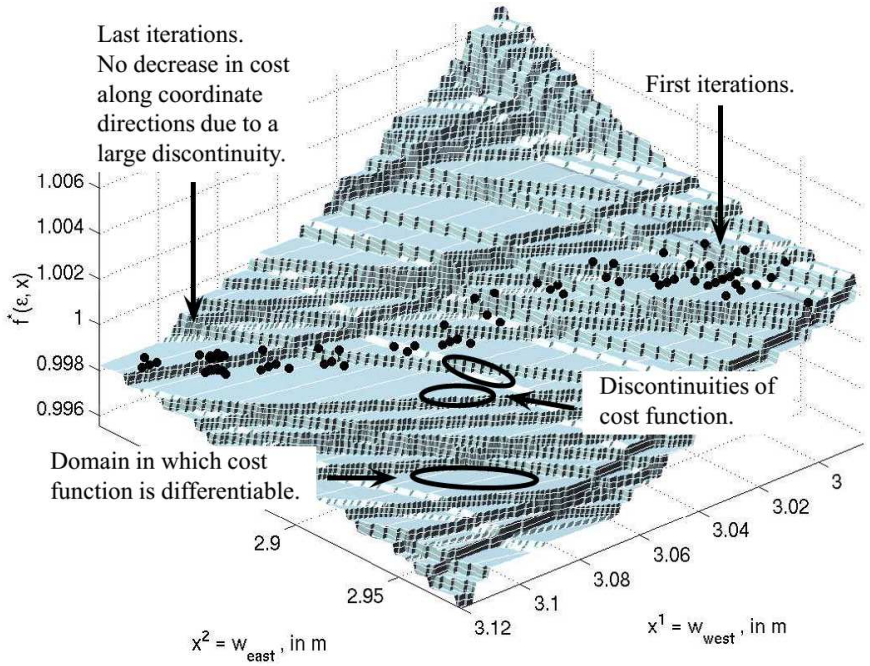

Figure 2.13: Parametric plot of the normalized source energy consumption for cooling and lighting as a function of the width of the west and east facing window. [108].

2.3.2 Optimization algorithms

Once a robust optimization problem is formulated it's possible to implement an optimization algorithm to search for the optimal solution. However, as it turn out, in most of the real-world applications there is no guarantee of finding the absolute best candidate because problems are too non-linear, or have discontinuities, leading to the convergence to solutions which are local optima, such as depicted in Fig. 2.13 [108].

This gap leads scientists to competing for the absolute best optimization method, and works proposing better optimization algorithms populate the literature for building

energy applications. A comparison between several optimization algorithms for the optimization of energy consumption in the design phase of buildings has been performed in a work from Wetter and Polak [109].

The overview of the current trend of optimization algorithms for building energy modelling optimization is presented subsequently.

Particle Swarm Optimization - PSO

Swarm intelligence is the collective behaviour of decentralized, self-organized groups, natural or artificial. The inspiration of Swarm intelligence often comes from nature, especially biological systems, such as, ant colonies, bird flocking, animal herding, bacterial growth, and fish schooling. The agents follow very simple rules intrinsically specified, developing isolated and social interactions inside population, leading to the emergence of a holistic intelligent behaviour, which is unknown to the individual. The Introduction of this theory to the field of Artificial Intelligence in 1989 triggered the development of several global optimization algorithms [110].

Particle Swarm Optimization (PSO) was proposed by James Kennedy and Russell Eberhart as a simulator of social behaviour, assuming every individual would be simultaneously the teacher and the learner, relating it to Artificial Life, Evolutionary Computing, and therefore, Soft Computing [111]. PSO has been proved to be an efficient method for many global optimization problems, and in some cases it does not suffer the difficulties encountered by other optimization techniques, such as local minima convergence, and the limitation to continuous and smooth fitness functions. Moreover, it does not require gradient estimation, and uses an elementary mathematical approach.

In contrast with different adaptive stochastic search algorithms, population-based Evolutionary Computation techniques simultaneously exploit a group of potential solutions, detecting the optimal solution through communication, cooperation, or competition among the individuals of a population [112]. The PSO algorithm has a straightforward implementation and often provide superior results when comparing to specific genetic algorithm implementations and optimization problems, such as presented by Blum and Li [113].

To understand the physics behind this optimization algorithm is often helpful to consider a particle as a bird, and visualizing a flock of birds flying over a landscape, with the objective of finding the deepest valley. In PSO, a population of potential solutions (birds) is employed to fly over a search space domain (optimization boundaries), and each bird has a position, and velocity, defining its movement. Each bird has also the memory to remember its best position (the deepest valley in a minimization problem) so far visited. In addition, all birds can share their position to the swarm, guaranteeing, that at any time, each bird knows where it is located flock's current best position. Thus, each bird movement is continuously adapted, accelerating towards the personal best and the best solution of the population simultaneously. In this collective search, all the swarm may fly over a significant part of the search space domain, and probably find

a satisfactory solution to the problem. Fig. 2.14 shows the diagram of each particle position updating-rule.

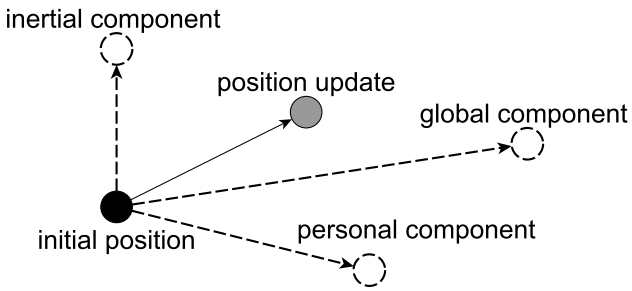

Figure 2.14: Particle Swarm Optimization position update rule diagram.

The following explanation of the mathematical intuition behind the Particle Swarm Optimization algorithm applied in this work is mostly based on three well documented articles, all based on the work of Kennedy and Eberhart, documented and studied by Blum and Li [113], Parsopoulos and Vrahatis [112], and Poli et al [114]. Further comprehension on the subject may include the reading of the cited articles.

Suppose that the search space is **N**-dimensional (dimension of the candidates vector), then the position of the i^{th} bird of the swarm can be represented by a **N**-dimensional vector, $x_i = (x_{i1}, ..., x_{iN})$. The velocity of this bird, can be represented by another **N**-dimensional vector, $v_i = (v_i 1, ..., v_{iN})$. The best previously visited position of the i^{th} bird is denoted as $p_i^{best} = (p_{i1}, ..., p_{iN})$. Defining g^{best} as the best bird in the swarm (i.e., g is the current optimization solution). The superscripts k refers the iteration number, and the swarm movement is updated according to the equations 2.3.3 and 2.3.4, while stopping criteria are not met.

$$v_i^k = \omega^k v_i^{k-1} + c_1 r_1^k \circ \left(p_i^{\text{best}} - x_i^{k-1}\right) + c_2 r_2^k \circ \left(g^{\text{best}} - x_i^{k-1}\right) \tag{2.3.3}$$

$$x_i^k = x_i^{k-1} + v_i^t, \tag{2.3.4}$$

where the operator $\circ$ denotes element-wise multiplication; $i = 1, ..., B$, for B birds; ω is the inertial weight factor; c_1 and c_2 are, respectively, the cognitive (individual) and the social (group) accelerating parameter that provide the relative importance that each particle gives to its own information and to its neighbours information when performing the next step; finally, $r \in \mathbf{R}^B \subset [0, 1]$ is a vector with randomly generated numbers.

Cognitive and social parameters, c_1 and c_2 of Equation 2.3.3, are not considered to be critical for PSO's convergence. However, proper fine-tuning may result in faster convergence and, more importantly, improvement of non-convergence to a local minima. As default values, $c_1 = c_2 = 2$ are proposed by Kennedy [115], but, on the literature, no agreement exists for the right magnitude of these parameters besides the argument

$c_1 + c_2 \leq 4$ [116]. Since these parameters are the weights of the weighted sum of both components of velocity, one may interpret them as the quality of giving emphasis either to the personal opinion of each element, or to the opinion of the group.

The updated velocity of a bird is equal to the previous velocity and a certain degree of inertia, adding the meta-heuristic terms based on personal and social learning. The inertia weight is proved to be crucial for the convergence of the algorithm, since it represents a compromise between local and global search. On one hand, the large weight of a heavy bird detains inverting its velocity's direction, forcing it to fly in a widely search space. On the other hand, a light bird is more agile, allowing it to change its position constantly in a relatively small space. This behaviour is also recognized by the algorithm, and so, Blum and Li suggested in [113] to decrease bird's inertia weight gradually through the optimization routine, from 0.9 to 0.2, forcing it to become lighter and diminish the probability of any bird flying over a minimum without detecting it. Therefore, the inertia weight should follow a linear function of k, Equation 2.3.5.

$$\omega(k) = \frac{\omega_{min}}{\omega_{max}}(k-1) + \omega_{max} \tag{2.3.5}$$

where subscripts min and max refer to the minimum and maximum referred values of inertia weight. The choice of positive inertia weights ranging $0 < \omega < 1$ prevents the velocity update to reverberate in a positive-feedback loop and generate high-velocity values that might compromise the desired convergence, and force birds to fly to outside the search space each epoch. This approach is expected to be sufficient for limiting undesirable magnitudes of velocity without controlling, like in the original version of PSO, each component of v_i to be confined within the range of $[-V_{max}, +V_{max}]$ [111].

A pseudo-code describing the implementation of a basic variant of PSO is provided in Algorithm 1. The implementation of this algorithm in Python™can be accessed in the author's public code repository [5].

[5] `https://github.com/diogoncalves/pyswarm_control`

Algorithm 1 Pseudo-code for Particle Swarm Optimization

```
Initialize each particle randomly, satisfying all the search space domain constraints;
k = 1
while stopping criteria is not met do
    for each particle i do
        Find current particle velocity, v_i, by Eq. 2.3.3
        Find current particle position, x_i, by Eq. 2.3.4
        Update particle historical best:
        if f(x_i^k) < f(p_i^best) then
            p_i^best ← x_i^k
        end if
        Update current global best of the swarm:
        if f(p_i^best) < f(g^best) then
            g^best ← p_i^best
        end if
        Update bird's inertial weight, ω(k), by Eq. 2.3.5
    end for
    k = k + 1;
end while
return best particle, g^best.
```

Differential Evolution - DE

The term differential evolution was coined by R. Storn and K. Price, borrowing the idea from Nelder & Mead optimization algorithm and Simulated Annealing [117]. The method of differential evolution's functioning is similar to genetic algorithm's approach and is summarized in the Pseudo-code – Algorithm 2. Differential Evolution like Genetic Algorithms allows for each population of solutions to evolve. However, DE is mostly suited for real valued optimization variables, in the contrast to the binary nature of genetic algorithms. The idea behind the method of differential evolution is that the difference between two vectors yields a vector which can be used with a scaling factor to traverse the search space.

According to R. Storn and K. Price [118], in DE algorithm, the individuals (candidate solutions) are carried around the search-space through simple mathematical formulæ which combine positions between the existing individuals in the population, to propose new position to them. If this proposal represents an improvement to the objective function of the individual, the new step will use the combinations of inputs found, otherwise this proposal is rejected.

A population, $\mathbf{X}$ of N individuals is set to solve the optimization problem.

$$\mathbf{X}^k = [x_i^k, ..., x_N^k], \qquad i = 1, 2, ..., N \tag{2.3.6}$$

where k is the generation number and N is the population size.

The set of decision variables for each individual, x_i^k, can be represented by a **D**-dimensional vector, $x_i^k = (x_{i1}^k, ..., x_{i\mathbf{D}}^k)$. Which for first generation is randomly initiated within decision variables boundaries $x_{ij}^{\min} \leq x_{ij} \leq x_{ij}^{\max}$, where $x_{ij}^{\min}$ and $x_{ij}^{\max}$ are, respectively, the lower and upper bounds for the j variable.

Consecutively, the DE algorithm creates a mutant solution m_i^k for each candidate x_i^k, by adding to a random candidate x_{r1}^k a weighted difference between two other candidates randomly chosen from the population, and different than x_i^k, according to Storn and Price [117]:

$$m_i^{k+1} = x_{r1}^k + F \cdot (x_{r2}^k - x_{r3}^k) \tag{2.3.7}$$

where F is a weight coefficient responsible for the severity of the mutation, r_1, r_2 and r_3 are random integers from $1, ..., N$, but different from i. Depending on the mutation strategy, r_1 can either be a random integer or the best member of the population. The weight F is usually considered as a random number for improving the robustness of the algorithm and is the weight allocated to the mutation of the *individual* x_i. Usually, it is advisable to use the dither technique which improves convergence especially for noisy objective functions. Thus F takes any random real $\mathcal{U}_{[0.5,1]}$. Values lower than 0.5 reduce the effect of the differential mutation, whereas, values greater than 1 usually hinder the converging process by potentiating the exploratory nature of the algorithm [117, 119, 118].

Figure 2.15 represents a scheme of this mutation process, Eq. 2.3.7.

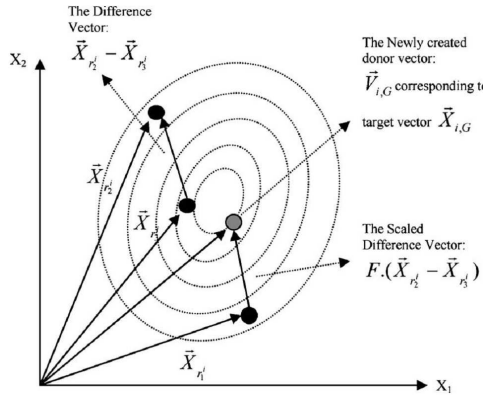

Figure 2.15: Illustrating a simple DE mutation scheme in 2-D parametric space [120].

After applying the mutation operator, the crossover (mating) operation is performed, allowing for the incorporation of successful candidates from previous generation. A new candidate u_i^{k+1} is generated, from either the genes ofx_i^k, or the genes of its correspondent mutation m_i^{k+1}, depending on a random real number compared with a defined crossover probability (CR), according to Eq. 2.3.8.

for each $i = 1, ..., N$,

$$u_{ij}^{k+1} = \begin{cases} x_{ij}^{k} & \text{if } \text{rand}_j[0,1] \leq \text{CR or } j = \text{I}_{\text{rand}} \in \{1, ..., \mathbf{D}\} \\ m_{ij}^{k+1} & \text{if } \text{rand}_j[0,1] > \text{CR and } j \neq \text{I}_{\text{rand}} \in \{1, ..., \mathbf{D}\}, \end{cases} \tag{2.3.8}$$

where I_{rand} is a random integer picked from $1, ..., \mathbf{D}$. The crossover probability, can take values in the range of $[0, 1]$. This crossover process is similar in nature to the Genetic Algorithm crossover.

Finally, the new candidate u_i^{k+1} is compared with the current position x_i^k for the following selection process:

$$x_i^{k+1} = \begin{cases} u_i^{k+1} & \text{if } f_1(u_i^{k+1}) \leq f_1(x_i^k) \\ x_i^k & \text{otherwise,} \end{cases} \qquad \text{with} \qquad i = 1, ..., N. \tag{2.3.9}$$

If u_i^{k+1} has a better objective value than its current position x_i^k, then x_i changes position to $u_i^k + 1$ generation. Otherwise, *status quo* is maintained. These whole process is repeated until a stopping criteria is met.

Implementations of this algorithm for all main programming languages are freely disseminated by UC Berkeley's International Computer Science Institute Differential Evolution algorithm's repository[6].

Algorithm 2 Pseudo-code for Differential Evolution

1: Initialise all N individuals with random positions throughout the feasible search-space. $k = 0$.
2: **while** stopping criteria is not met **do**
3: **for** Each individual x_i^k in $i = 1, ..., N$ **do**
4: Randomly pick three candidate solutions and perform mutation through Eq. 2.3.7, and get m_i^{k+1};
5: Change random variables from x_i^k with the mutation vector m_i^{k+1}, through Eq. 2.3.8, and get candidate proposal, u_i^{G+1}.
6: Evaluate the objective function, f_1, select best candidate through Eq. 2.3.9, and get new candidate's position x_i^{k+1};
7: **end for**
8: $k = k + 1$;
9: **end while**
10: **return** Best solution.

2.3.3 Remarks on Optimization

Building modelling optimization problems, as reviewed previously, are mostly multi-objective optimization tasks because they consider several conflicting objectives simulta-

[6] `www1.icsi.berkeley.edu/~storn/code.html`

neously. Therefore, there is rarely a single optimal solution, but rather multiple alternatives with different trade-offs between objectives. The definition of what a good trade-off means, usually requires the intervention of a decision maker. However, in a supervisory predictive control implemented in a simulation environment it seems impracticable to halt the simulation process and conduct a decision making process for every time an optimization problem is required, i.e. every simulation time step. Moreover, the trade-offs should be investigated during the implementation of the optimization process of the supervisory predictive control to find the one most suitable for the task.

This section reviewed the general approaches used for implementing multi-objective problems on building energy performance enhancement. Although the algorithms reviewed being similar in nature, each one has its own idiosyncrasies, which can play a crucial difference in the reduction of the computational cost allocated for optimization, as well as their capability of finding global solutions. Nevertheless, the Nelder-Mead Simplex, and the Conjugate Gradient Descent will be tested along as reference benchmark.

Chapter 3

Methodology

The methodology for implementing a supervisory predictive control based on surrogate modelling and real-time optimization is presented in this chapter. Its principal objective is to design a generic process for delivering supervisory predictive controllers which can operate at the level of control accessible to the supervisor of the HVAC system, i.e. at the high level. Hence the control solution should be capable of delivering robust, energy efficient and cost-effective decisions, while the methodology should be agnostic to the type of HVAC system being operated and building.

The quest for independence to the HVAC system can be justified by the variability encountered in the built environment regarding the presence of HVAC systems which can be boilers, chillers, variable refrigerant flow AC, and so on. Thus, a versatile supervisory control might be straightforwardly disseminated potentiating the energy and cost saving capabilities of supervisory predictive control as a retrofit measure.

First, an overview of the proposed supervisory predictive control solution is presented. The requirements for accomplishing its implementation are drawn, and the overall process is described. Afterwards, the Python™ module *eppyco* is introduced, exposing the manner in which it enables the co-simulation process, and integrates the whole entities required in the development process of supervisory predictive controls. The surrogate modelling strategy based on data-driven models development is delineated, highlighting the proposal for re-sampling techniques for improving models' predictive capabilities. At last, the optimization problem inherent to the supervisory predictive control is formulated, defining the multi-objective optimization problem, its targets and constraints.

3.1 Supervisory Predictive Control – Overview

A supervisory predictive control may be seen as a centralized Model Predictive Control (MPC) configuration which focuses on controlling building energy systems from a supervisory layer [24, 12]. To accomplish the latter, during this work it is followed

the approach suggested by Lamoudi et al. [121], that it encompasses a co-simulation environment, which implies the development of:

a. A building computational model;

b. A Surrogate-model to account to predict building response to specific controls and disturbances;

c. An optimization algorithm capable of solving the underlying control problems.

d. A communication server to connect and transfer data between entities.

Figure 3.1 provides a comprehensive flowchart of the whole process of the proposed predictive control and how required developments listed previously should integrate it. The goal of the supervisory predictive control is to deliver the most suitable group of set-points for the following time-step, given a building thermodynamic state, and expected disturbances forecast. The flowchart exemplifies the recursive process of building energy simulation, for each t from zero to the end of simulation T_{sim}. Where, k denotes the maximum timeframe window to the past building states, and N denotes the maximum forecast window in time-step units.

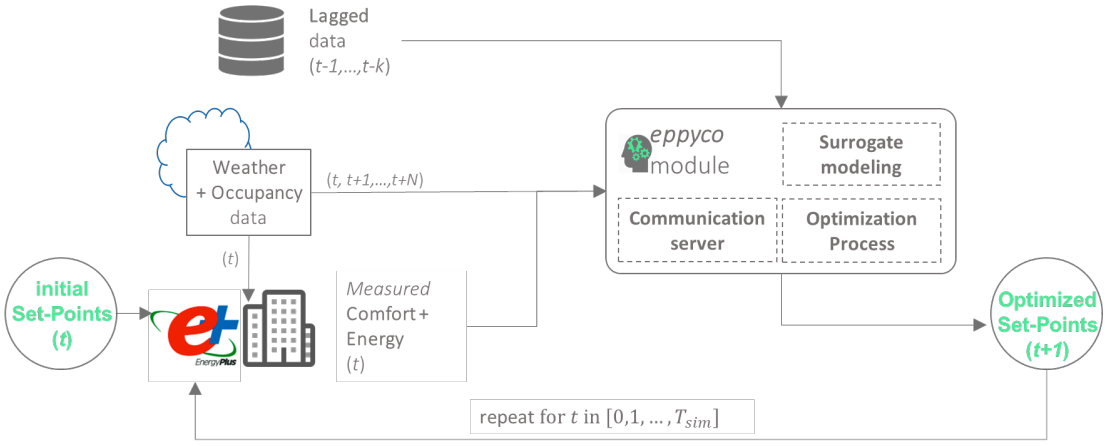

Figure 3.1: Overview of supervisory predictive control process.

The building computational model serves two purposes in this work. First, since the implementation is to be carried in a simulation environment, the deterministic model plays the part of a real building via a co-simulation implementation explained in Section 3.4. Moreover, it is the data provider to the whole process. On the one hand, it gathers the data required for the training of the predictive models throughout the various stages of the co-simulation. On the other hand, it provides the baseline data to benchmark against the supervisory predictive control proposed by this methodology. The baseline

data comprises the results from the simulation of conventional strategies of HVAC supervisory control, namely control solutions with scheduled set-points (heating, cooling, and set-back). In a real-world implementation of the proposed methodology, the inclusion of a building computational model may not be neglected, since data-fusion techniques might enable the maximization of data usage by providing data-driven models with both real data from sensors, and information-rich data from simulations. Section 3.2.2 explains the data gathering process thoroughly, pointing out which conventional control strategies are to be used as baseline data.

The surrogate modelling is the process of delivering accurate and fast approximation models to the response of the building energy simulator used in the co-simulation process. Section 3.2 delivers the methodology for developing such surrogate models. The predictions carried out by these models to the given set of data streams are used during the optimization process which is highly iterative, Fig. 3.1. The data streams required for a supervisory predictive control are the forecast of weather and occupancy data, the measured data from the current time-step, the lagged data from previous time steps related to the endogenous and exogenous variables, such as weather, occupancy and control variables, as well as output variables such as energy consumption, comfort and inner environmental conditions.

For each time-step of the co-simulation process, a new set-point is required to be delivered to the simulator for computing the following time-step. The optimization process searches for a group of set-points which should lead to an acceptable compromise between the energy consumption and the thermal comfort requirements over the forecast horizon selected. Section 3.3 explains further the development of the optimization formulation of the supervisory predictive control. Once the set-points are founded by the optimization algorithm, the communication server sends them to the building energy simulator, EnergyPlus™, and the process is repeated until the end of the period of the co-simulation.

The co-simulation process regarded as the building simulation process using the supervisory predictive control is enabled only via a communication server which manages the data flows presented in Fig. 3.1. This communication server allows for the EnergyPlus™ to send the results of each time-step to a database, and halts the EnergyPlus™ simulation process while the supervisory predictive control optimization process finds the most suitable set-points for the following time-step. Once the optimization process has converged in one solution, the same communication server sends the set-points for the following time-step.

The whole co-simulation process is included in the Python™ module developed for this thesis which is called *eppyco*. The name *eppyco* stands for EnergyPlus™ and Python™ CO-simulation, and its main goal is to enable the supervisory predictive control development from scratch to deployment. This module integrates the surrogate modelling process, the optimization process, the communication server, and all the functions required for conducting a co-simulation process of a supervisory predictive control using EnergyPlus™. The co-simulation process development, as well as the summary of *eppyco*

functionalities is thoroughly exposed in the Section 3.4.

3.2 Surrogate modelling strategy

Machine learning modelling based on supervised learning algorithms rely upon the heuristic nature of learning processes which can be simplified as comparisons between inputs and outputs, or between actions and its consequences [122, 123]. Data-driven modelling of energy intensive processes requires a representative database which accommodates concise examples of output responses to various inputs variations [124]. As reviewed earlier, machine learning algorithms are capable of delivering energy models on gathered data from process operation [29, 54].

Shmueli [122] summarizes the steps for data-driven modelling as follows:

1. Define goal;
2. Collect data;
3. Prepare data;
4. Exploratory Data Analysis;
5. Choose variables;
6. Choose methods;
7. Evaluate, Validate & Model Selection;
8. Use model.

During this work the above listed methodology will be followed to serve as guide during the description of the Surrogate Modelling carried out. The intended goal during surrogate modelling was the development of a fast and accurate data-driven model capable of predicting the energy performance of the building, so the resulting data could serve the optimization routines within the supervisory predictive control.

The development of surrogate models shares the same methodology of developing data-driven models through machine learning, or soft computing algorithms. The most valuable asset, in both cases, lies in the available database of the systems behaviour. It should be mentioned, however, that in the case of surrogates development, all data is acquired through simulations of complex and physics-based simulators, rather than with real-world systems' sensoring data, as it is common practice in a regular data-driven model development. As referred to earlier, EnergyPlus is the simulator selected for conducting this thesis, the reason for this selection lies in the fact that it is one of the most relevant energy performance simulators and its robustness and reliability has been continuously exposed in the open literature [95, 94, 58]. Furthermore, it enabled the integration of a co-simulation environment via BCVTB communication protocol, a fact

considered detrimental having into account the nature of the work under development [97, 105].

3.2.1 Goal definition

The goal regarding surrogate modelling lies in the development of accurate models of the building thermal response to the endogenous and exogenous disturbances to enable the integration of an on-line optimization process present which is part of the supervisory predictive control strategy.

All data used in this work is provided by a computational model of the building under investigation. Therefore, a model is developed, describing the architecture, type construction, location conditions, HVAC systems, equipment, zone utilization types and occupancy profiles. This computational model (physics-based simulator) is considered as the *ground truth* of the building under investigation because the models are solely based on simulated data. In machine learning, and specifically in supervised learning, the term *ground truth* stands for the measurements of the outputs which the models should approximate.

The simulations of the building energy performance result in time-series data with each sample representing the response of the building for the period a simulated time step. The proposed methodology divides resulting database in three categories of time-dependent variables:

- Disturbance variables, x_t, containing the information regarding system disturbances which are uncontrollable, namely weather data, occupation, equipment utilization, and so on;
- Control variables, u_t, which accommodate all variables allowing for manipulation, such as high level HVAC control;
- Output variables, y_t, reflecting building's energy system response to the exogenous and endogenous disturbances. Usually, these outputs are energy consumption, occupants' comfort, interior air quality, environmental impact, and so on.

Given a database of inputs and its dependent results, the objective of surrogate modelling is to find approximation functions, S, capable of predicting a building response, $\hat{y}_t$ at a given time step t, as a function of the combination of effects imposed by supervisory level HVAC controls u_t, and disturbance variables x_t. The accent $\hat{}$ over the variables such as in $\hat{y}_t$, and $\hat{x}_t$ denotes that the variable has been estimated by a model rather than presented by the database. The surrogate model is a response of the energy system behaviour, and its predictions can be generally represented as

$$\hat{y}_t = S(u_t, u_L, \hat{x}_t, x_L, y_L), \tag{3.2.1}$$

where the subscript L denotes the lagged versions of variables at play, which are past values from previous time-steps to account for the inertia and the slow response of buildings towards disturbances. The right variables are defined in an exploratory data analysis based on auto-correlation explained further in Section 3.2.3. The aggregation of these lagged variables is commonplace in the development of time-series regression models of non-random data[1].

3.2.2 Data collection

Sampling techniques to conduct design of experiments have been proposed in the literature as referred in Section 2.2.3. However, such techniques may still lead to computationally prohibitive costs, and often tend to lack robustness when tackling issues concerning the development of surrogate models for building design, as identified by Eisenhower et al. [36]. Consequently, further sampling is often required, and or simulations, for filling the poorly populated data domains, leading to additional computational efforts [36, 59]. This thesis proposes an adaptive data gathering methodology, which is especially relevant for the development of supervisory predictive controls based on surrogate models.

Benchmark data collection

Performance assessments of model predictive control can be accomplished by comparing building's energy performance results using a proposed technique against the performance obtained by simulations of conventional demand reduction techniques for the same building [29].

Building energy simulations of three HVAC techniques for non-predictive control are here considered as the reference case-studies. These simulations will constitute the baseline database which will be used to create the first surrogate models (base-models). The techniques used for HVAC modelling non-predictive control can be listed as it follows:

TC is based on a timer controller. The system is turned off after occupants leaving the building and it is turned on 2h before expected people's arrival. At an office case-study the systems would be activated at 07:00, and deactivated at 18:00. Conversely, at a residential building it would be turned on at 17:00 and turned off at 7:00. This technique is commonly used in office and services building nowadays [29].

[1] Data exhibiting autocorrelation is called non-random, i.e. there is time dependence in the data [123]. Buildings are known for being stable energy systems with slow dynamics, especially those of high inertia [125, 51]. This characteristic makes building data naturally non-random, and time-dependent. Non-randomness assessment will be held in this thesis through data exploratory analysis of the auto-correlation effects, especially useful for assisting the choice of the number of time delays to use in the predictive model [79].

EO is the "early switch-off". This technique is also based on a timer controller. This particular case accounts for the building thermal inertia and turns off the HVAC System prior to the occupants departure. EO switch-off the system 2 hours before non-occupancy, therefore the system schedule implies a switch off at 16:00 at an office building.

DR is demand reduction by pre-heating, or pre-cooling. Basically, it is intended to turn Systems off during peak hours. According to Garnier et al. [29], in a non-residential building it means switching on between 05:00 and 07:00, then from 08:00 to 12:00 the system is deactivated, and finally, reactivated from 13:00 to 18:00. The system is left deactivated during the remaining hours

The learning stage of the first surrogate models (base-model) will only use data from the baseline database. The predictions carried out by these models integrated in the supervisory predictive control will populate a new database called adaptive database Control anomalies should be investigated in this database to decide whether or not is necessary to update the surrogate model to new data.

Adaptive data collection

The training process of data-driven models on data streams, such as the predictive models included in a supervisory predictive control, should not be considered as a fixed and one-time-only event because of the problem regarded as *concept drift*. The *concept drift* is the evidence that the output variable is deviating from the measured values, leading a previous valid model to perform poorly due to incorrect predictions [126]. The problem of concept drift can be observed as well in the surrogate modelling for conveying time dependent optimization problems, because the data initially gathered (via deterministic simulations) for training the predictive models may not provide statistical relevance to the domain where the optimization algorithms converge, leading to abnormal results due to model mismatches. Usually, a batch of simulations, defined by a sampling technique, or randomly, has to be conducted to construct such a database. This task often proves to be computationally demanding, and not sufficiently robust, leading to the simulation of more samples to fill poorly populated domains [36, 59]. The objective of this adaptive sampling is to limit the Design of Experiments to the minimum required samples, but instead of being the sampling technique to establish the number of samples, it is the attainment of the convergence criteria of both the optimization and predictive models that define the important samples to retain. Overall, both computational effort and database size are expected to decrease considerably if compared to classical sampling techniques.

This adaptive data collection strategy relies on the nature of the machine learning algorithms that are capable of learning through experience, and the acknowledged *concept drift* problem. This learning principle can be compared with the capability of an intelligent individual of learning from its own mistakes. In this thesis, surrogate models are

expected to learn from undesirable experiences. The latter being absurd HVAC controls in terms of energy consumption, with which the surrogate models are expected to learn and avoid such set of controls in order to attain a better energy building performance in future optimization problems.

The first surrogate models are trained solely using the initial existing data, i.e. the baseline data gathered via the simulation of the conventional control techniques as presented in the Section 3.2.2. Although being possible to deliver accurate models for the domain of that data, these models may lack from knowledge diversity since they were trained using very repetitive data. Thus, base-models may render unreliable results for unconventional, or poorly populated domains of operation, expecting optimization convergences to building control anomalies. However, such control anomalies due to models mismatches are to be expected during preliminary runs, and their occurrence is quite useful in this methodology since they present rich information about the region of interest of the optimization problems.

The implementation of a supervisory predictive control should accommodate a batch of preliminary simulations for the available computational budget with the objective of including enough representative data for the surrogate model to reach a satisfactory predictive control for the proposed controller.

De Coninck et al. [28] have pointed out the necessity of having reliable models for the implementation of a model predictive control. In fact, they have stated that the model mismatch between expected and observed values could be the cause for some unsatisfactory results they were facing on their implementation of model predictive control in a services building.

The identification of a control anomaly can be conducted through the comparison of optimization's multi-objective scores employed using data resulting from control implementation with the scores computed using predicted data provided by surrogate models. Assuming that the optimization process is well defined and capable of convergence to *optimal* solution, the error assessment of the predictions held by the surrogate models and the results provided by the EnergyPlus™ after computing the building's response using the set-point provided by the supervisory predictive control may serve as an indication of the model mismatch, the *concept drift*, and surrogate models overfitting. Thus, the model mismatch may be computed as the predictive error, as presented in Eq. 3.2.2, which is an adaptation of the Normalized Mean Error.

$$NME_{mismatch} = \frac{\sum_{t=0}^{N} |y(t) - \hat{y}(t)|}{\mu_y} \tag{3.2.2}$$

where $y(t)$ is the observed building response to the output y at time step t, $\hat{y}(t)$ is the correspondent prediction held by the surrogate model for the same time step, and N is the total number time steps simulated so far. μ_y is the whole database's mean value of the target output, y. This metric might be computed on-line during the co-simulation process, or performed after the process to investigate the models mismatches and infer

the necessity for re-training the surrogate models.

If models mismatch proves to be significantly higher than the error expected by the surrogate models through validation process, then the models should be retrained.

This adaptive data gathering approach can be related to sequential sampling techniques employed in surrogate-based engineering design optimization [127, 128]. Sasena et al. [127], compared several sampling criteria for surrogate model sampling optimization. Sequential sampling for design optimization emphasizes finding the global optimum by balancing a search for the optimal performance of a surrogate model and a search for unexplored regions to avoid missing promising areas due to the inaccuracy of the surrogate model [128]. However, the methods founded are mostly based on the Krigging modelling technique [2] and parameters related to it. A fact that prevents a straightforward implementation with the machine learning algorithms selected in this thesis because the hyperparameters of the models used in Kriging influence are used in the surrogate models directly.

The purpose of the sampling technique here proposed lies on the improvement of the supervisory predictive control approach, by minimizing the required simulated data and the control anomalies, applicable to general data-driven surrogate models employed in predictive control applications. Moreover, it is expected that the surrogate models after being re-trained with the new sampled data show an improvement in the optimization problems being investigated [28, 36].

3.2.3 Data preparation and Exploratory Data Analysis

Data preparation and exploratory data analysis (EDA) are key initial steps in predictive modelling. In fact, previous studies have shown that data preparation might take 80% of the total time of data mining projects [130]. It consists of summarizing the data numerically and graphically, reducing its dimension, and preparing it for the more formal training step. EDA can be employed either to capture relationships between variables which might be unknown, or to sustain theoretically specified causal relationships [122].

Time dependence investigation

Buildings are known to be slow transient, and time dependent systems. It is, therefore, expected for a buildings thermal inertia to play an important part on its energy performance. It is also a fact the most data-driven algorithms' learning process focuses on improving model prediction capability for each presented sample. When time series modelling is concerned, it is common to employ delayed inputs and outputs to account for their influence on each sample, i.e. influence of past disturbances in current time and the dependency of past results in the present.

[2] Kriging is a geo-statistical technique which interpolates the value of a random field at an unobserved location from observations of its value at a nearby location. The main difference from other regression techniques lies in the assumption that the uncertainty of the surrogate model at known points is zero. This method has been extensively used in surrogate model engineering design optimization [129, 59].

To investigate this lagged influence and to create a pool of possible inputs, an exploratory analysis is conducted using the autocorrelation function (ACF) and the partial autocorrelation function (PACF), following the suggestions from Montgomery et al. [123] and work conducted by Fan et al [79]. Both assessments are commonly used for time series data analysis to identify non-randomness of variables, helping in the selection of possible inputs for regression modelling.

ACF is the linear dependence of a variable with itself at two points in time. PACF is the autocorrelation between two points in time without considering the linear dependence of observations between these two time points [123, 79].

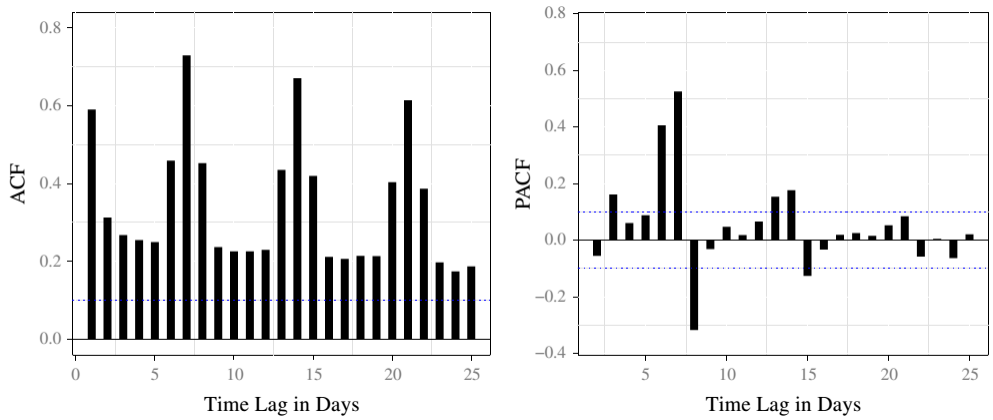

Figure 3.2: ACF and PACF of daily energy consumption of a commercial building in Hong Kong [131].

From Fig. 3.2 it can be depicted the autocorrelation (left) and the partial autocorrelation (right) for the daily energy consumption at a commercial building in Hong Kong. The dotted lines represent the 5-95% confidence interval. As it can be depicted in the ACF plot, there is higher correlation between today's energy consumption (lag $t-0$) and the energy consumption every past 7 days (lag $t-7i$ for $i = 1, ..., 3$). Moreover, a pattern that repeats itself for a seven day period can be observed, highlighting non-randomness of data. However, partial autocorrelation presents no significance of time lags superior than 15 days. Hence, the authors have only considered as possible inputs for developing the data-driven model lagged values of energy consumption up to 15 days prior ($t-15$). In this study, all the variables with a time lag superior to the confidence interval cut-off will be considered to the input variables pool, according to the suggestions from Fan et al [79], and Montgomery et al [123]. Afterwards, feature selection process will determine which variables should be preserved for conducting the final learning process.

Data Normalization

The successful implementation of some predictive algorithms, especially SVR and ANN, imply the use of variables detaining commensurate scales [132, 79].

Feature normalization is required to avoid to model bias to larger valued variables, and with sparser distributions. Moreover, if the problem has two or more output variables and the error function is scale-sensitive, like the least squares error function, then the variability of each target relative to the others can affect how well the algorithm learns each target. If one target has a range of 0 to 1, while another target has a range of 0 to 1,000,000, the training process will expend most of its effort learning the second target.

Despite the fact that Random Forests are frequently claimed to have no sensitivity towards incommensurable inputs [3], Breiman et al [91] also applied normalization of variables when linear combinations of variables were required. Furthermore, since in regression Random Forests models the split criterion is the reduction of residuals squares, the normalization of the outputs may influence the algorithm training.

According to Iglewicz, normalization that sets to zero the mean, or median, or other measure of central tendency, is likely to deliver more robust models, and often perform better for input variables with extreme outliers (Iglewicz, 1983). Normalization is achieved by subtracting the means and dividing by the standard deviations which are determined from the training set.

The most common approach to normalize variables is by applying Eq. 4.3.1.

$$\upsilon_i' = \frac{\upsilon_i - \mu_{\upsilon_i}}{\sigma_{\upsilon_i}} \tag{3.2.3}$$

where υ_i is the sample value of the i^{th} variable, μ_{υ_i} is variable's mean, σ_{υ_i} is the standard deviation, and υ_i' the normalized variable value.

This method is widely used in many machine learning algorithms (support vector machines, logistic regression, and neural networks), and data mining, when close-to-Gaussian distributions of variables are assumed. Therefore, this thesis employs normalization to all variables considered, input and output ones.

3.2.4 Feature selection

Any individual capable of learning from experience must discriminate between the relevant and irrelevant parts of its experience [133]. Although this selective ability may lead to single-minded humans, it also leads to information specialists, who are knowledgeable individuals within a particular domain of their interest [134]. Data-driven models are expected to be specialists within the system under modelling, requiring as well a selective capability from the available experience.

[3] Random Forests are ensembles of CART models. The training of a CART is invariant to monotonic transformations of individual features, because each node split decision is input independent [91].

The objective of feature selection is to comprise the delivery of a subspace of minimal dimension containing the whole relevant information about the output, while preserving the original features. It allows for the development of more interpretable models of reduced dimension, while improving performance, and computational time related to the learning process. A good selection of inputs leads to better performing models, and to a better understanding of the underlying structure of the data representing the system.

Guyon Elisseeff [132], introduces variable and feature selection pointing out its different approaches, revealing the non-existence of an absolute best method. Along with several authors, it is stated that employing such strategies does not imply sacrificing prediction performance. On the contrary, it appears alleviate the problem of overfitting, delivering more general and robust models [135, 136, 137].

When developing a surrogate model of a building energy performance simulator, the variables available for selection are extensive. A direct approach would be to choose all possible variables, employing them later in data-driven model training. However, that usually leads to models of high variance and with higher risk of *overfitting* due to the "curse of dimensionality". This phenomenon implies a prohibitive number of samples for describing the influences of all variables in the output. Furthermore, since each input represents a dimension of the problem, high computational cost related to training process and predicting tasks are to be expected [138]. This work reviews some of the most important approaches to Feature Selection.

The first approach pointed out by Guyon [132], and Liu and Motoda [138], relies on practitioners expertise to select the important variables of the system under investigation, often called *expert-domain*, or knowledge-based selection techniques. For example, a building energy system is composed by a balance of loads as described earlier, variables related to measurements of the sources of these loads should be relevant for constructing a robust model. The combination of thermodynamics on building energy systems with domain knowledge from energy management operations should highlight a set of important features. Table 3.1 summarizes the variables which might be relevant for delivering a data-driven building energy model, identified as expert-domain from the literature review [54, 29, 68, 79]. It accommodates weather related variables, building's occupation, control set-points, comfort standards, and energy consumption.

However, expert-domain may be biased by practitioners' experience which can lead to either select irrelevant and redundant inputs, or to eliminate important but imperceptible variables. Moreover, no information is available regarding each variable's importance to the model predictive ability, preventing an earlier interpretation of the underlying variables' interactions. Thus, combining domain knowledge with feature selection algorithms may deliver more reliable models [138, 132].

Table 3.1: Description of generic Inputs/Outputs and exogenous variables related to one zone of the building.

Group	Description
Control	Heating Set-point
Control	Cooling Set-point
Input	Outdoor Air Drybulb Temperature
Input	Horizontal Infrared Radiation Rate per Area
Input	Outdoor Air Relative Humidity
Input	Zone People Occupant Count
Output	Zone Mean Air Temperature
Output	Zone Mean Air Humidity Ratio
Output	HVAC Electric Energy Consumption
Output	Boiler Energy Consumption
Output	Zone Thermal Comfort Fanger Model PPD or PMV

Feature Selection algorithms

The scientific community has been dedicating significant research efforts to the delivery of feature selection methods to help choosing smaller subsets of features. Feature selection algorithms can be broadly classified as *filter*, or *wrapper* methods, depending on whether it is treated as a pre-process or intertwined with the learning task [139, 138, 132]:

- ***Wrapper*** methods select the subset of features based on variables influence on the predictive performance of the selected machine learning model. The criterion can be error rate, inconsistency rate, information measure, distance measure, or dependence measure.

- ***Filters*** examine each input variable individually to determine the strength of the relationship between itself and the outputs. The criterion employed is usually a correlation score, information measure, or a distance measure.

Wrapper methods require a search algorithm in order to converge in a final subset of features. Greedy search algorithms seem to be computationally advantageous comparing to brute-force, offering two possible searching directions: forward selection and backward elimination. The most disseminated of these algorithms is the recursive features elimination algorithm (RFE). Its principle uses a backward selection technique which often leads to better prediction performances than other methods [140, 138, 141]. A flowchart of RFE can be depicted from Fig. 3.3.

Firstly, a model is trained considering all variables of a predefined group. Then, a ranking criterion, which evaluates each variable importance, is computed for all variables. Those which result in the smallest ranking are removed, and the model is trained again.

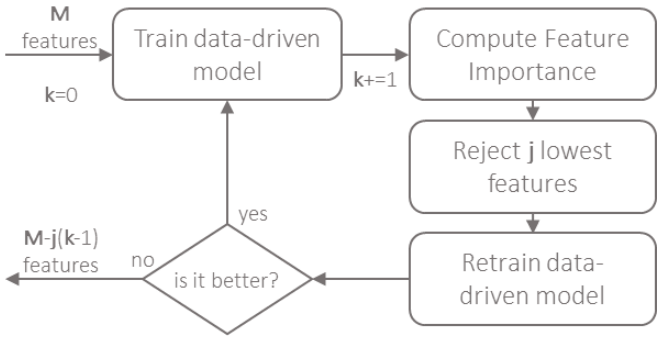

Figure 3.3: The Recursive Feature Selection algorithm.

The whole process is recursively repeated until a decrease of models' accuracy occurs. The latter subset of input variables is selected as the inputs for developing the final model.

As pointed out, this greedy search algorithm invokes the computation of a variable importance ranking to assess which variables should be discarded first at each iteration. Computing such ranking variable importance often relies upon the sensitivity analysis of each input in the output error of the trained model, i.e. its importance in the prediction task. This index is to be distinguished from filter methods, since it requires extensive use of the machine learning algorithm responsible for modelling. Variable importance ranking is further discussed ahead.

Although intuitive and of straightforward interpretation, this method encounters three evident drawbacks:

1. It requires a ranking variable method.

2. It can be very computationally demanding, since many prediction models with different feature subsets have to be built.

3. The results of the wrapper strategy lack generality, since it depends on the selected machine learning model.

Filter methods attempt in answering these limitations by providing a preprocessing approach to feature selection. They are consistently much faster and general than most wrappers, since they are independent of any data-driven model, allowing for its employment in any regression problem.

However, the most notorious disadvantages lie on the redundancy of the subset selected due to its univariate approach comparing to wrappers, and its incapability of highlighting redundant variables [132].

Filters provide a *relevance criterion* which represents a degree of relationship between input variables and outputs subjected to modelling, therefore, they can be related and

employed as model independent *Feature Ranking*. The most popular criteria found in literature are Pearson correlation, Spearman correlation, and the Mutual Information score [136, 135, 132, 142].

The Pearson correlation evaluates the linear relationship between two continuous variables. A relationship is linear when a change in one variable is associated with a proportional change in another variable [142]. For feature X with values x and classes Y with values y treated as random variables it is defined as:

$$\rho_{X,Y} = \frac{cov(X,Y)}{\sigma(X)\sigma(Y)} = \frac{\sum_i^N (x_i - \bar{x})(y_i - \bar{y})}{\sqrt{\sum_i^N (x_i - \bar{x})^2 \sum_i^N (y_i - \bar{y})^2}} \tag{3.2.4}$$

The Spearman correlation evaluates the monotonic relationship between two variables. In a monotonic relationship, the variables tend to change together, but not necessarily at a constant rate[135]. The Spearmans correlation is a commonly used nonparametric statistical measure of similarity (or correlation) between paired rankings. The null hypothesis of the test is that no correlation exists between two rankings. Spearmans correlation coefficient, r_s, is calculated by

$$r_s = \frac{cov(rg_X, rg_Y)}{\sigma_{rg_X}\sigma_{rg_Y}} \tag{3.2.5}$$

Both Pearson and Spearman correlations range in value from -1 to 1, and they equal on the event of a perfect linear correlation between two variables. Although Pearson correlation fails to measure non-linear relationships, Spearman correlation coefficients depict non-linear and monotonic relationships. For example, an exponential relationship between two variables ($y = e^x$) yields a Spearman correlation of 1, and a Pearson of about 0.25. Hence, a comparative analysis of both correlations is much advised to infer variables' relationships, and define a threshold for variable discarding.

Another filter method which accounts for the linear dependency between inputs and outputs is the one-way ANOVA (ANalysis Of VAriance) F-test statistic. This method uses the analysis of variance between each input variables individually and the investigated output. The importance of each feature is given by the calculated p-values of the test statistic as (1-p). This parametric method is especially relevant for continuous variables [143, 142]. Performing a one-way ANOVA F-test regarding continuous variables for testing whether or not a variable x is relevant for predicting y, can be defined as a two steps computation. First the cross-correlation between output each i input is calculated as Eq. 3.2.6.

$$\rho_{x_i,y} = \frac{(x_i - \mu_{x_i}) \cdot (y - \mu_y)}{\sigma_{x_i} \cdot \sigma_y} \tag{3.2.6}$$

where μ is the mean, σ is the standard deviation and x and y denote input and output, respectively.

Then, the F-score is computed as Eq. 3.2.7.

$$F = \frac{\rho^2_{x_i,y}}{1-\rho^2_{x_i,y}} \cdot \texttt{dof} \tag{3.2.7}$$

where dof are the degrees-of-freedom which equals $(N-1)$ where N is the number of samples in data. From the F-score, the p-value can be computed from Student's t statistic, considering $t^2 = \text{F}$. The feature importance is given by $(1-p\text{-value})$.

Mutual information is another popular relevance criteria introduced by information theory [136]. Mutual information coefficient, which is related to an information gain IG, measures the dependency between two variables, and is defined as

$$IG(X;Y) = H(Y) - H(Y|X) \tag{3.2.8}$$

where $H(Y)$ and $H(Y|X)$ are the entropy and conditional entropy, respectively.

In information theory, the information contained in a variable distribution is equal to the negative of entropy. The mutual information is the reduction of entropy (gain of information) of the output Y once variable X is presented. As a feature selection criterion, a feature subset having a high mutual information with the output is likely to reduce the uncertainty on the output prediction [136, 144, 142].

However, since $H(Y)$ is fixed and does not depend on the choice of features, selecting features X which maximize $IG(X;Y)$ can be achieved by focusing on minimizing $H(Y|X)$ which is computed as

$$H(Y|X) = -\sum_{i}^{K} \int \mathcal{P}(y_i, x) \log_2(\mathcal{P}(y_i, x)) dx \tag{3.2.9}$$

where $\mathcal{P}(y_i, x), j = 1...K$ is the joint density function of y knowing x [142].

Feature Importance ranking

This work presents three common model dependent techniques for variable importance ranking:

- **Mean decrease impurity** is a novel feature ranking method which is inherent to the Random Forest algorithm. Random Forests consist of ensembles of decision trees named CART (Classification and Regression Trees). The nature of this machine learning algorithm, provides a ranking score for the inputs based on how much each input decreased the variance of each tree. Each node in the decision tree represents a condition to a specific feature. The training algorithm is greedy and designed to converge to a node condition which splits the dataset in two, aiming for clustering similar responses (lower variances) together in the new partitions. The measure based on which the (locally) optimal condition is chosen is called impurity. For regression problems as the ones encountered in this work, impurity

is represented by the variance of the output variable in each partition. Thus when training a tree, or a forest, it can be computed how much each feature decreased the impurity in each tree. For a forest, the impurity decrease from each feature and can be averaged to all trees and weighted to the number of data allocated to each one, so that the features importance's can be ranked accordingly.

- **Random Permutation Feature Importance** was proposed by Breiman [91] in his preliminary work on Random Forest algorithm. The variable importance of a feature is computed as the average decrease in model performance on the out-of-bag samples when the values of the respective feature are randomly permuted. However, this approach can be generalized to other machine learning algorithms [145, 92, 144].

  Suppose there are M input variables describing a system. After the training process is completed, and the baseline error estimation is calculated, the values of the m_{th} variable in the validation dataset are randomly permuted, predictions are computed on this data, and a new error estimation is calculated. The process is repeated for $m = 1, 2, ..., M$, and once completed, feature importance's can be ranked according to the comparison of their influence on models' performance [91]. Variables with permutations that induced higher error estimations are considered more important than those yielding lower errors.

- **Clamping Technique** relates to Random Permutation, since it also relies on the observation of performance's degradation of a data-driven model when the information content of a particular feature is removed. Ranking features' importances by this approach consists of testing a trained model to obtain the baseline predictive performance, computing the same validation error for each feature and, then, fixing its value to the observed mean of that feature in the whole database. Finally, by comparing model's predictive performance for each clamped variable with that of the baseline performance should highlight which variables induced higher errors. Again, the lowest performance decrease indicates the least important feature to the model's purpose. This technique seems to be particularly suitable to neural networks models, as proposed by Wang et al. [135, 146].

3.2.5 Validation and Model Selection

Understanding if a particular data-driven model is a good model has been the quest of several statisticians, and the conclusions are abundant [123, 147, 92, 122]. However, the goodness of a model usually is evaluated through the estimation of the errors it will produce to a given situation. Hence, the error estimation of a model is the discrepancy between measured reality and model hypotheses.

Many metrics exist for the estimation of the predictive error of a model [123, 147, 92, 122]. Four metrics are referred and applied in this thesis due to their popularity in the reviewed literature:

★ Root Mean Squared Error (RMSE), Eq. 3.2.10,

$$RMSE = \sqrt{\frac{\sum_{k=1}^{n} \left(t(k) - a(k)\right)^2}{n}} \tag{3.2.10}$$

★ Mean Absolute Error (MAE), Eq. 3.2.11,

$$MAE = \frac{1}{n} \sum_{k=1}^{n} |y(k) - \hat{y}(k)| \tag{3.2.11}$$

★ Mean Absolute Percentage Error (MAPE), Eq. 3.2.12,

$$MAPE = \frac{100}{n} \sum_{k=1}^{n} \frac{|y(k) - \hat{y}(k)|}{y(k)} \tag{3.2.12}$$

★ Normalized Mean Error (NME), Eq. 3.2.13,

$$NME = 100 \times \frac{\sum_{k=1}^{n} |y(k) - \hat{y}(k)|}{\mu_y} \tag{3.2.13}$$

where $y(k)$ is the k^{th} target output present in the data-set, $\hat{y}(k)$ is the correspondent hypothesis predicted by the machine learning model, and n is the number of samples present in the data-set. μ_y is the database's mean value of the target output, y.

The machine learning algorithms employed in this thesis (and most of all regression models available in literature) employ a least squares rule, which is the minimization of the mean square error (MSE) estimation during the learning process of fitting the model to the data presented. This MSE is related to the presented RMSE, and it is an obvious estimate of the model's predictive error, and it is known as training error.

Unfortunately, training error is often too optimistic, and it is not a good estimate of a true error estimation. On the other hand, a test error, which is calculated in the same fashion, is more indicative of the performance of the model, since it is calculated on a data-set which was hidden during the training stage, hence containing samples unknown to the model.

According to Hastie et al [147], the training error is incapable of providing information on model's performance, as it does not properly account for model complexity, as it can be seen from Figure 3.4.

As depicted in Fig. 3.4, the training error tends to decrease whenever model complexity is increased, leading to an eventual zero error estimation if all data points are met by the model. Increasing model's complexity is often a tempting approach when developing data-driven models because models do fit the data more thoroughly. However, a model with zero training error is overfit to the training data and will typically generalize poorly [147].

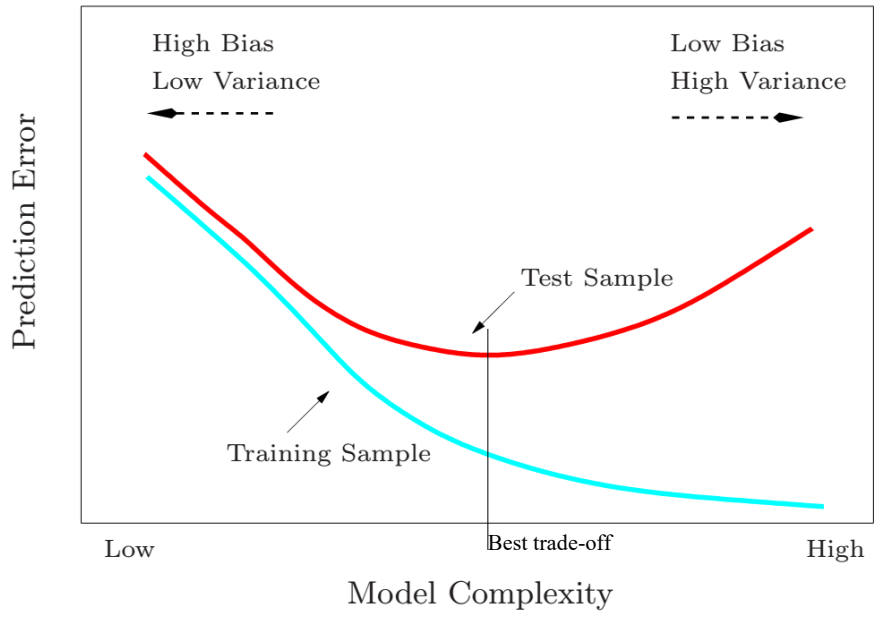

Figure 3.4: Test and training error as a function of model complexity. (Adapted from Hastie et al. [147])

This impossibility to generalize is called overfitting. That is, with excessive fitting (high variance), the model adapts itself too closely to the training data, and will not predict well similar data presented by the test data set. In contrast, if the model is not complex enough, it will underfit the training set and may have large bias, again resulting in poor generalization.

Although some algorithms tend to suffer more from overfitting, such as neural networks, the bias-variance trade-off is applicable for all of data-driven algorithms presented in this thesis. For further enlightening on the subject the work of Hastie et al. [147], and Berk et al. [92] are advised. These authors point different statistical learning procedures to address the bias-variance trade-off in different ways. Nevertheless, they also pointed out that in practical terms, the best bias-variance trade-off for a problem, given an abundant database, can be encountered by the minimization of the test error while fine-tuning the algorithms architecture.

Although such test error is calculated using data which was hidden from the learning process, the data-driven model do often exhibit a certain bias to this test data-set [147]. To avoid a poor validation, a third data-set is required for cross-validation of the model's architecture, and should be solely employed for that purpose. Hence, the test data-set should be kept hidden throughout the whole process, and only employed on the selecting of distinct data-driven models [123, 147].

Data-sets division, and cross-validation

No golden rule seems to exist in what concerns the database division proportions for training, validation and test data-sets.

For example, according to Hastie et al. [147] a typical division might be 50% for training, and 25% each for validation and testing. The authors stress the difficulty to give a general rule on how to choose the number of observations in each of the three parts, as this depends on the signal-to-noise ratio in the data and the training sample size. Whereas, Montgomery et al. [123] points out that a good rule of thumb is to leave 20 or 25 observations for the test data-set.

A popular alternative to data division of training and validation sets is employing cross-validation, especially when databases are small and modelling algorithms are computationally inexpensive [122]. N-fold cross-validation is a popular example in statistical modelling [92, 147], and widely employed in building energy predictive modelling [70, 148, 79].

In N-fold cross-validation, the database reserved for training and validation is randomly partitioned into N equal sized data-sets. Of the N data-sets, a single one is retained as the validation data-set, and the remaining $N1$ data-sets are used as training data. The cross-validation process is then repeated N times, computing the validation error for each of those N folds, as it can be seen in Fig. 3.5. The N resulting error assessments from the iterative process can then be averaged (or maximized) to produce a single estimation.

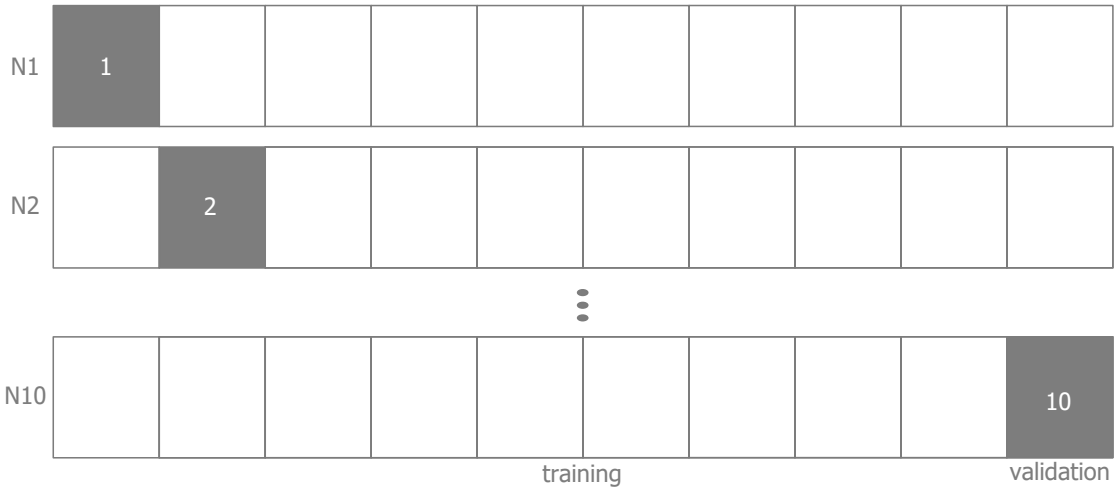

Figure 3.5: 10-folds cross-validation.

The advantage of this method over re-sampling methods like bootstrap sampling is the employment of all data available, and observation validated exactly once. 10-fold cross-validation is commonly used in literature, but again there is no general rule

regarding this parameter, and the higher the number of folds the higher the tendency for overfitting [147, 92].

This thesis approach follows the N-fold cross-validation approach, and the partitioning proposed by Hastie et al [147]. That is 25% of data is reserved for test error assessment and the remainder 75% are employed in 10-fold cross-validation for model selection, and for fine-tuning the complexity of the data-driven algorithms, by changing their architecture features.

Architecture selection

Any machine learning has architecture features which should be carefully tuned depending on the problems at hand, and the characteristics of its data. The following list summarizes the parameters which should be selected for each of the data-driven algorithms referred in this thesis, while assessing cross-validation error estimation:

- **Artificial Neural Networks** have several tuning parameters, depending on the type of architecture selected, or the type of problem. However, this thesis choice falls on the Feed Forward with Back Propagation Neural Network, having one hidden layer, and sigmoid as transfer function, leaving as remaining tuning parameters the **number of neurons**, the **momentum weight**, and the **learning rate**.

- **Support Vector Machines** used in this thesis are especially designed for regression problems. The employed kernel in the Gaussian function, leaving the **standard deviation**, and the **regularization constant** as tunable parameters.

- **Random Forests** main sensitive features are the **number of trees** present in the forest, and the **maximum depth** allowed for each tree to grow, representing how many times the algorithm partitions each variable's domain.

Once each algorithm is fine-tuned through a grid-search approach, the one having the best performance error will be taken for the supervisory predictive control task.

3.2.6 Remarks on surrogate modelling

This section exposed a comprehensive methodology for developing machine learning models applied to building energy problems, especially those regarded with the development of supervisory predictive controls. Since the techniques proposed are generic to the development of statistical models, its employment in building energy modelling based on sensor data is expected to present no major limitations. Moreover, a novel methodology for conducting re-sampling for the update of surrogate models employed in supervisory predictive control has been proposed as well via the adaptive data collection method.

3.3 Supervisory Predictive Control optimization strategy

As discussed in the previous section, the surrogate model is responsible for predicting the building states for a forecast horizon. This section presents the approach to the problem of minimizing energy consumption of a building and its energy related costs, while maximizing the comfort conditions within a range accepted to take into account the occupants opinion.

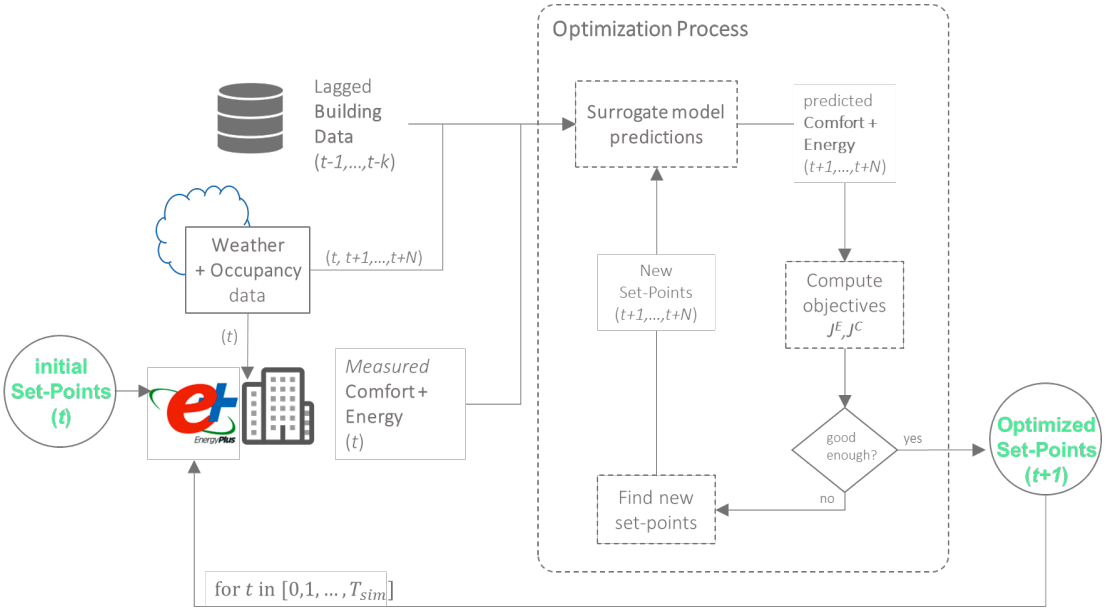

Figure 3.6: Flowchart close-up depicting supervisory predictive control optimization process.

From Fig. 3.6, it can be depicted the main events occurring during the proposed supervisory predictive control, especially focusing on the optimization process. In general, the optimization algorithm invests a computational effort to decide which control set-point it should deliver to the building energy simulator for computing the subsequent time-step. To accomplish that, it needs the surrogate model to provide the predictions of relevant objectives, concerning the disturbance variables forecast, the lagged variables, the current building state and algorithm's hypotheses for control set-points for the given forecast window. Once the surrogate model delivers a satisfactory result to a set of controls, the optimization routine is finished and the controls for next time-step are sent to EnergyPlus™which performs the required computation. Its results are observed by the supervisory predictive control and the process is repeated recursively till the end of the simulation process.

The Literature has deployed a profusion of efforts on Model Predictive Control strategies for Building Energy Management Systems (BEMS) [29, 24, 121, 48]. The proposal

of this thesis differs from its resembling works not only from the approach to system identification, which is surrogate-model driven through adaptive data gathering, but also the optimization problem formulation which is presented in this section. Nevertheless, the works from Moroşan et al. [24], Lamoudi et al. [121], and more recently from Garnier et al. [29], served as great inspiration for this methodology, and its reading is much advised for an interested reader.

3.3.1 Objective function development

The remainder of this section formulates the optimization problem inherent to the supervisory predictive control problem. First, it should be recalled the generic multi-objective optimization problem from Section 2.3.1, and then it should be adapted to the case of energy consumption and discomfort minimization:

$$\underset{U}{\text{minimize}} \qquad \left\{J^E, J^C\right\} \tag{3.3.1}$$

where J^E, and J^C are respectively the objective functions related to energy consumption and occupants comfort, and U is the control set-points matrix to be found by the optimization algorithm.

Energy consumption objective function

The objective function for energy consumption, J^E, is defined as

$$J^E = \frac{1}{N_E + N_a} \sum_{e=1}^{N_E} \sum_{i=1}^{N_a} \left(\Gamma \odot \hat{Y}^E\right) \mathbf{n}_{\gamma y} \tag{3.3.2}$$

where $\odot$ is the element-wise multiplication of matrices, Γ is the time-dependent tariff matrix for all energy sources available, and $\hat{Y}^E$ is the energy consumption for all energy sources,N_E, predicted by the surrogate model over the required forecast horizon, N_a. The variable tariffs matrix, Γ, is defined as

$$\Gamma = \begin{bmatrix} \gamma_t^{(1)} & \cdots & \gamma_t^{(N_E)} \\ \vdots & \gamma_{t+i}^{(e)} & \vdots \\ \gamma_{t+N_a}^{(1)} & \cdots & \gamma_{t+N_a}^{(N_E)} \end{bmatrix} \tag{3.3.3}$$

where N_E is the number of energy sources available, and N_a is the total number of time-steps considered for the forecast window.

Conveniently, considering Γ as a unit matrix[4], the minimization of the costs related to energy is converted to the minimization of energy intensity. Moreover, Γ can accommodate the carbon intensities of each of the energy sources, converting the optimization problem in a carbon-footprint minimization problem.

[4] Integer matrix consisting of all *ones*.

$\mathbf{n}_{\gamma y}$ is a normalizing vector for the *energy cost*, $\Gamma \odot \hat{Y}^E$.

$$\mathbf{n}_{\gamma y} = \left[\frac{100}{\gamma_{\max}^{(e)} \cdot \mathbf{y}_{\max}^{(e)}}, \quad \cdots, \quad \frac{100}{\gamma_{\max}^{(N_E)} \cdot \mathbf{y}_{\max}^{(N_e)}} \right]^T, \qquad \text{for } e = 1, ..., N_E, \tag{3.3.4}$$

where $\mathbf{y}_{\max}^{(e)}$ is the maximum energy consumption, $y^{(e)}$, for the energy source e, observed in the database for surrogate modelling; whereas $\gamma_{\max}^{(e)}$ is the maximum tariff, $\gamma^{(e)}$, for source, e, which is user specified.

$\hat{Y}^E$ is the matrix conveying energy consumption for all energy sources, N_E, over a prediction horizon, N_a, defined as

$$\hat{Y}^E = \begin{bmatrix} \hat{y}_t^{(1)} & \cdots & \hat{y}_t^{(N_E)} \\ \vdots & \hat{y}_{t+i}^{(e)} & \vdots \\ \hat{y}_{t+N_a}^{(1)} & \cdots & \hat{y}_{t+N_a}^{(N_E)} \end{bmatrix}, \tag{3.3.5}$$

Note that the matrix of predicted energy consumption also included current time-step predictions, $\hat{y}_t^{(1)}, ..., \hat{y}_t^{(N_E)}$. Since time is considered discrete, each variable is averaged to the correspondent time-step duration. Thus, the average of the variable for the current time-step is unknown until the duration of the time-step is finished, i.e. the measured energy consumption of current time-step (t) requires to be estimated.

$\hat{Y}^E$ matrix is computed by the surrogate model, $\mathcal{S}$, as

$$\hat{Y}^E = \mathcal{S}\Big(U, U_L, \hat{X}^E, X_L^E, Y_L\Big), \tag{3.3.6}$$

where:

- U, and U_L, are the matrices of controllable inputs (set-points) for the forecast window, and from past time-steps (lags), respectively;
- $\hat{X}^E$, and X_L^E, are the matrices of the forecasted disturbances relevant for energy consumption predictions (weather and occupation related), and the lags of past disturbances, respectively;
- Y_L is matrix of lagged outputs which are important to the surrogate-driven energy prediction.

Controllable inputs U, and U_L, are defined respectively as

$$U = \begin{bmatrix} u_t^{(1)} & \cdots & u_t^{(N_{s.p.})} \\ \vdots & u_{t+i}^{(j)} & \vdots \\ u_{t+N_a}^{(1)} & \cdots & u_{t+N_a}^{(N_{s.p.})} \end{bmatrix}; \qquad U_L = \begin{bmatrix} u_{t-1}^{(1)} & \cdots & u_{t-1}^{(N_{s.p.})} \\ \vdots & u_{t-k}^{(j)} & \vdots \\ u_{t-N_l}^{(1)} & \cdots & u_{t-N_l}^{(N_{s.p.})} \end{bmatrix} \tag{3.3.7}$$

where $N_{s.p.}$ is the total number of controllable set-points; N_a is the number of time-steps ahead for the forecast horizon; N_l is the total number of lagged time-steps considered in the surrogate modelling.

The optimization algorithm should find the controllable inputs matrix, U, which minimizes both objectives, J^E, and J^C. Note that the objective function for energy consumption only sums the time-steps concerning the forecast window, i.e. for $i = 1, ..., N_a$. Thus, only the control set-points, u^j_{t+i}, from rows $t+1$ to $t+N_a$ are subjected to optimization, whereas the first row of controls, $u^{(1)}_t$ to $u^{(N_{s.p.})}_t$, remains unaltered, since it is the result of previous optimization time-step, and its effect is currently being measured.

Accordingly, disturbances X^E_L, and $\hat{X}^E$, are defined respectively as

$$\hat{X}^E = \begin{bmatrix} \hat{x}^{(1)}_t & \dots & \hat{x}^{(N_d)}_t \\ \vdots & \hat{x}^{(d)}_{t+i} & \vdots \\ \hat{x}^{(1)}_{t+N_a} & \dots & \hat{x}^{(N_d)}_{t+N_a} \end{bmatrix}; \qquad X_L = \begin{bmatrix} x^{(1)}_{t-1} & \dots & x^{(N_d)}_{t-1} \\ \vdots & x^{(d)}_{t-k} & \vdots \\ x^{(1)}_{t-N_l} & \dots & x^{(N_d)}_{t-N_l} \end{bmatrix} \tag{3.3.8}$$

where N_d is the total number of disturbances inputs selected during surrogate modelling. The disturbances forecast, $\hat{X}^E$, differ from the predictions made by the surrogate models because they are independent to the building thermodynamic system. Thus, they should be provided via an external service, or approximated via the injection of uncertainty to the known data to propagate the forecast error to the supervisory predictive control co-simulation.

Finally, the lagged outputs matrix, Y_L, is defined respectively as

$$Y_L = \begin{bmatrix} y^{(1)}_{t-1} & \dots & y^{(N_y)}_{t-1} \\ \vdots & y^{(e)}_{t-k} & \vdots \\ y^{(1)}_{t-N_l} & \dots & y^{(N_y)}_{t-N_l} \end{bmatrix} \tag{3.3.9}$$

where N_E is the total number of energy sources predicted, N_y is the number of outputs which are considered as relevant variables for the energy prediction. N_a is the time-steps ahead considered in the forecast window, and N_l is number of lagged outputs.

Note that occupants comfort related variables may be taken into account. For example, it is expected that the thermal states of a building in previous time-steps, $t-k$, influence the energy required to change from state y_{t-1} to current time-step state y_t.

Occupants comfort objective function

The objective function for occupants comfort, J^C, is defined as

$$J^C = \begin{cases} \frac{1}{N_z+N_a} \sum_{z=1}^{N_z} \sum_{i=1}^{N_a} \left(\omega_{t+i}^{(z)} \cdot \left(\hat{y}_{t+i}^{(z)} - C^* \right) \right), & \text{if } C^* < \hat{y}_{t+i}^{(c)} < C^{pen} \\ \max_{z=1}^{N_z} \left[\max_{i=1}^{N_a} \left[\omega_{t+i}^{(z)} \cdot \left(\hat{y}_{t+i}^{(z)} \cdot \frac{y_{max}^C - \psi C^{pen}}{y_{max}^C} + \psi C^{pen} \right) \right] \right], & \text{if } \hat{y}_{t+i}^{(c)} \geq C^{pen} \\ 0, & \text{otherwise} \end{cases}, \tag{3.3.10}$$

where N_z is the number of zones considered for the optimization, and N_a is the total number of time-steps considered for the forecast window. $\omega_{t+i}^{(z)}$ are the elements of matrix Ω of the occupation forecast related filter, $\hat{y}_{t+i}^{(z)}$ are the elements of matrix $\hat{Y}^C$ of the discomfort indexes predicted by the surrogate model over the required forecast horizon. C^* is the comfort objective target, C^{pen} is the comfort constraint added as a penalty term to the comfort objectives via multiplication with a penalty term ψ. Note that the penalization terms are normalized to the maximum discomfort y_{max}^C to maintain the objective function commensurate.

In multi-objective optimization may be not possible to satisfy all constraints imposed, so penalty functions are applied. This is accomplished by penalty of the objective function if the desirable conditions on those objectives, or variables, are not satisfied [149]. The choice of a penalty method for handling the constraints for comfort is twofold. First, it is impractical to consider occupants thermal comfort as a hard constraint for most buildings, as it is not directly measurable, and it is presented as an abstract concept independent to individuals [150]. Moreover, it is commonplace to employ such a method when considering evolutionary algorithms for solving multi-objective optimization problems which is the case of the work conducted in this thesis [119].

The objective function, J^C, is designed for maximizing the expected comfort up to a desired value, C^*. Its behaviour is a positive linear function from C^* to C^{pen}, being zero for values lower than C^* to allow for the optimization algorithm to focus on minimizing the energy cost solely when the comfort levels are expected to be met. Moreover, to avoid the comfort levels to reach undesired values, $y^C > C^{pen}$, due to the attempt of the algorithm in saving energy, the penalty term of the type L1 is activated which is comprehended between the maximum allowed value for discomfort (1-comfort) and the constraint C^{pen}. Thus, these two comfort targets may be viewed as soft and hard targets for comfort, C^* and C^{pen}, respectively.

The occupation filter forecast matrix, Ω, is represented as

$$\Omega = \begin{bmatrix} \omega_t^{(1)} & \dots & \omega_t^{(N_z)} \\ \vdots & \omega_{t+i}^{(z)} & \vdots \\ \omega_{t+N_a}^{(1)} & \dots & \omega_{t+N_a}^{(N_z)} \end{bmatrix}, \tag{3.3.11}$$

where N_z is the number of air-conditioned zones, and N_a is the total number of time-steps considered for the forecast window. ω is a filter given to the comfort objective

function, removing the interest of reaching the comfort objective if the zone is not occupied. The conditional filter, ω, is formulated as

$$\omega = \begin{cases} 1, & \text{if } \hat{x}^{Occ} > 1 \\ 0, & \text{otherwise} \end{cases}, \tag{3.3.12}$$

$\hat{Y}^C$ is the matrix of the predictions of occupants comfort index for all air-conditioned zones, N_z, by the surrogate model, $\mathcal{S}$, over a prediction horizon, N_a, and is defined as

$$\hat{Y}^C = \begin{bmatrix} \hat{y}_t^{(1)} & \dots & \hat{y}_t^{(N_z)} \\ \vdots & \hat{y}_{t+i}^{(z)} & \vdots \\ \hat{y}_{t+N_a}^{(1)} & \dots & \hat{y}_{t+N_a}^{(N_z)} \end{bmatrix}; \tag{3.3.13}$$

which is obtained through predictions from the surrogate model described as

$$\hat{Y}^C = \mathcal{S}\Big(U, U_L, \hat{X}^C, X_L^C, Y_L\Big), \tag{3.3.14}$$

where U is the matrix of controllable inputs (set-points), U_L is its lagged version, $\hat{X}^C$ is forecast matrix of the disturbances relevant for comfort index predictions, X_L^C is the lagged matrix of those disturbances, and Y_L is matrix of lagged outputs which are relevant to predictions. Controllable inputs are considered the same as for energy minimization and for comfort maximization. Thus, control matrices U, and U_L, for this case should be the same defined in 3.3.7.

Disturbances matrices for related to comfort are, $\hat{X}^C$, for disturbances forecast, and X_L^C, for lagged disturbances. They are are characterized respectively as

$$\hat{X}^C = \begin{bmatrix} \hat{x}_t^{(1)} & \dots & \hat{x}_t^{(N_d)} \\ \vdots & \hat{x}_{t+i}^{(d)} & \vdots \\ \hat{x}_{t+N_a}^{(1)} & \dots & \hat{x}_{t+N_a}^{(N_d)} \end{bmatrix}; \qquad X_L = \begin{bmatrix} x_{t-1}^{(1)} & \dots & x_{t-1}^{(N_d)} \\ \vdots & x_{t-k}^{(d)} & \vdots \\ x_{t-N_l}^{(1)} & \dots & x_{t-N_l}^{(N_d)} \end{bmatrix} \tag{3.3.15}$$

where N_d is the total number of uncontrollable inputs, or disturbances, selected during surrogate modelling. Note that the forecast matrix of input disturbances includes the current time-step, t. Since time is considered discrete, each variable is averaged for the correspondent time-step duration. Thus, the average of the variable for the current time-step is unknown until the duration of the time-step is finished, i.e. the average of the variable for current time-step has to be approximated.

Finally, lagged outputs matrix, Y_L^C, relevant for predicting the comfort indexes by the surrogate model is defined as

$$Y_L = \begin{bmatrix} y_{t-1}^{(1)} & \dots & y_{t-1}^{(N_y)} \\ \vdots & y_{t-k}^{(c)} & \vdots \\ y_{t-N_l}^{(1)} & \dots & y_{t-N_l}^{(N_y)} \end{bmatrix} \tag{3.3.16}$$

where N_y is the number of outputs which are considered as relevant variables to comfort index predictions, and N_l is number of lagged outputs. Being buildings slow dynamic thermodynamic systems it is expected that the effects on occupants comfort for the energy employed in the current hour to be delayed a certain amount of time.

3.3.2 Meta-objective optimization formulation

The minimization of occupants comfort is often synonym of consuming more energy, making both objective functions competing with each other. Therefore, a meta-objective, **J**, is required to allow for an optimization algorithm to solve the optimization problem, which usually means a weighted sum of objectives functions:

$$\mathbf{J}(U, U_L, X, X_L, Y_L) = \sum_{p=\{E,C\}} \alpha^{(p)} \cdot J^{(p)}\Big(U^{(p)}, U_L^{(p)}, X^{(p)}, X_L^{(p)}, Y_L\Big) \tag{3.3.17}$$

where $\alpha^{(p)}$ is the weight associated with the objective, $J^{(p)}$ which should be investigated through analysis of Pareto front of the optimization results delivered by changing such a parameter. Hence, the initial multi-objective optimization problem 3.3.17, is rewritten in the form of

$$\underset{U^E, U^C}{\text{minimize}} \qquad \mathbf{J}(U, U_L, X, X_L, Y_L) \tag{3.3.18}$$

Subject to:

$$\begin{aligned} \underset{U^E, U^C}{\text{minimize}} \quad & \mathbf{J}(U, U_L, X, X_L, Y_L) \\ \text{subject to} \quad & u_{\max}^{(j)} - u^{(j)} \geq 0, \qquad \text{for } j = 1, ..., N_{setpoints} \\ & u^{(j)} - u_{\min}^{(j)} \geq 0, \qquad \text{for } j = 1, ..., N_{setpoints} \end{aligned} \tag{3.3.19}$$

where $u_{\max}^{(j)}$, and $u_{\min}^{(j)}$ are respectively the maximum, and minimum, limits allowed for the control set-point $u^{(j)}$, and where (j) is the index of the specified controllable variable.

3.3.3 Remarks on optimization strategy

This section exposed the formulation of the objective functions required to be minimized by the optimization algorithm every time-step to provide the supervisory predictive control with the decision capability of which set-points should be considered for the following time-step. The objective functions developed are focused both on the comfort and energy consumption. The latter has the particularity of being adaptive to which objective is to be considered, namely the minimization of the energy consumption, or costs related to it. This capability can play a major role in the utility of the supervisory

predictive control is shifting the energy consumption to times of lower tariffs, or better environmental performance.

The formulation of the optimization problem finalizes the supervisory predictive control description. However, the integration of such predictive control approach with a building energy simulator poses some challenges which are addressed subsequently.

3.4 Co-simulation implementation

While the simulation software such as EnergyPlus™ can accurately simulate the thermal behaviour of a building, its energy performance, and occupants comfort, its capabilities for advanced control design and optimization are inadequate.

The main argument seems to be the lack of multidisciplinary modelling and simulation groups. Moreover, there seems to be a general limited interaction among building modelling and simulation experts, the control systems engineers community, civil engineers, and architects. Consequently, as multidisciplinary emerges, it rises the need for versatile software tools for end-to-end design of energy-efficient buildings [96, 97].

Holistic assessments require high interactivity between all elements to investigate how architectural designs affect the operational efficiency of building automation systems, and, conversely, how high-performance control systems should affect the decision making in design and retrofitting.

The research community has been developing efforts to deliver practical tools to answer this necessity. BCVTB[5] is a software environment for coupling different simulation programs for distributed simulation. It is based on the Ptolemy II software environment and is developed at the Lawrence Berkeley National Laboratory, being the same research group of EnergyPlus™. Naturally, the external communication protocol allowing for EnergyPlus™to conduct co-simulation tasks was originally developed for BCVTB implementations. Moreover, BCVTB allows the coupling between EnergyPlus™and other programming languages such as MATLAB®and Python™. However, the full functionality of these *external* programs is limited since they are either called by BCVTB as a standalone program, or are implemented through coding the program in a BCVTB environment. For example, interactive execution and debugging allowed in Python™or MATLAB®coding is not possible via BCVTB, preventing a straightforward finding and fixing of code errors. Furthermore, BCVTB's scripting interface for Python™limits importing of all available packages, inhibiting the development of more complex data products. Nevertheless, since BCVTB and EnergyPlus™are open-source, the same applies to their communication protocol, allowing for any program capable of communications via web-socket to conduct co-simulation with EnergyPlus™.

MLE+ is an example of such programs, combining MATLAB®and EnergyPlus™via BCVTB communication protocol [97]. The authors have focused on developing a co-simulation tool capable of utilizing the simulation potentialities of EnergyPlus™ while

[5]Building Control Virtual Test Bed

taking full advantage of the MATLAB® environment for control design and virtual test [97].

MATLAB® is an accountable tool for assisting control engineers and researchers, but its limitations are imposed by being a commercial software, preventing a straightforward prototyping of new tools. Moreover, its capability for developing automated data analysis tools is limited when comparing to open-source programming languages such as Python™and **R**. Therefore, this thesis proposes a Python™package to allow for co-simulation between EnergyPlus™and Python™via BCVTB communications protocol.

Having said that, the *eppyco* module developed in this thesis is developed as a Python package to allow for co-simulation between EnergyPlus™and Python™via BCVTB communications protocol.

The development of ***eppyco*** is greatly inspired by the MLE+ toolbox [97]. The proposed package is presented as a Python3 package which couples any python program with the EnergyPlus [6]. It is designed for engineers, developers, and researchers who are familiar with Python™programming and want to use it for developing building control systems, simulations data analysis automation, and simulation-driven optimization.

The existing Python™ package ***eppy***[7] allows for changing EnergyPlus™IDF files, and output files through Python™programming. Moreover, it allows for navigate, search, and modify EnergyPlus IDF files in a systematic manner. Therefore, it is used for the development of the *eppyco* package from this thesis.

One of the main tasks conducted by ***eppyco*** is to implement a *Quasi-dynamic coupling* co-simulation architecture between the distributed simulators (Python™program and EnergyPlus™), so that simulators run in sequence, performing its computations locally and using the known outputs values from the coupled simulator. Both simulators exchange outputs only at a given synchronization time-step, and although each simulator waits for the other's response, there is no iteration between them outside the specified time-step.

Fig 3.7 presents the flowchart of the co-simulation process, focusing on the aspects of interactions between entities. From the building computational model, developed by any building modelling software such as DesignBuilder, or OpenStudio, it is required to export an IDF file describing building's architecture, construction, HVAC systems, and simulation features.

This IDF needs to be to be instrumented to allow for importing and exporting variables from and to external programs, configuring which variable outputs feed the surrogate model for conducting predictions, and which control inputs need to be read for continuing to the next step of the simulation task. Accordingly, a configuration XML file needs to be constructed to inform EnergyPlus™which variables it should consider when decoding the data packets proceeding from an external program – Supervisory Predictive Control. The BCVTB manual[96] and the External Interface manual of EnergyPlus[151]

[6] Implementation was carried using Python version 3.4, and EnergyPlus version 8.5.

[7] Documentation and package available at `http://pythonhosted.org//eppy/`

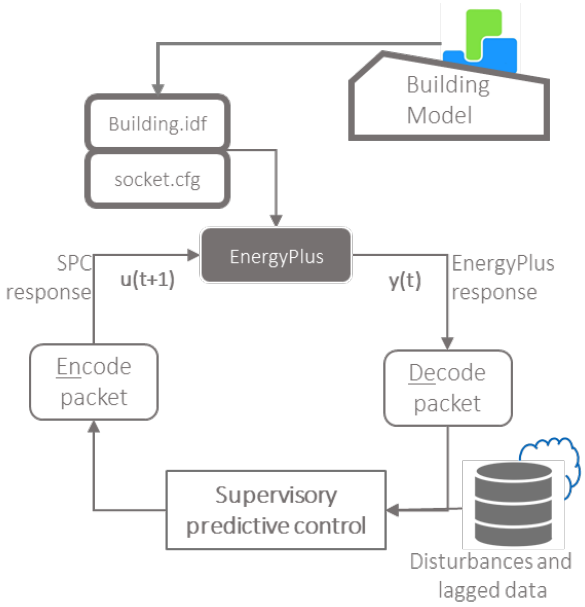

Figure 3.7: Flowchart close-up depicting co-simulation flowchart.

provide detailed information on how to configure such files.

Once both files are prepared, supervisory predictive control connects to EnergyPlus™and calls the start of co-simulation. Data is exchanged between both actors by data packets via a web socket. The task for ***eppyco*** is to decode all data coming from the EnergyPlus™and encode the control variables once the optimization routine of supervisory predictive control is completed.

3.4.1 Communication protocol

BCVTB protocol is used to exchange data during co-simulation processes via websockets [96]. Each simulators sends and receives data through packets, which are a text list containing a sequence of numbers of the following format:

$$\text{packet} := \begin{bmatrix} v & f & n_r & n_i & n_b & t & r_1 & r_2 & \dots \end{bmatrix} \tag{3.4.1}$$

where:

- v is the version number of BCVTB.
- f is a flag: 0 if simulation is flawless, 1 if simulation stopped, negative if error occurred.
- n_r, n_i, n_b are the quantity of real variables, integer variables, and Boolean variables respectively intended to send, or received. Currently, EnergyPlus requires that $n_i = 0$ and $n_b = 0$.

- t is the current simulation time in seconds.
- $r_1, r_2, ...$ are the values of the variables, starting with real ones, then integer ones, and finally Boolean ones.

3.4.2 *eppyco* functionalities summary

This package includes four classes of functions intended to:

- Machine Learning models development class:
  - Configure EnergyPlus™ IDF file via ***eppy*** package and simulate different clock-based control scenarios;
  - Report exploratory data analysis, suggesting relevant inputs for the predictive models;
  - Train a variety of Machine Learning models;
  - Report a comparative goodness-of-fit analysis to help in the decision making process of model selection;
  - Deploy predictive models to include the co-simulation process;
- Prepare co-simulation class:
  - Configure a XML file for EnergyPlus™ interpretation of interface variables, i.e. set which variables are to be sent and received by EnergyPlus™via the Energy Management System functionality;
  - Instrument the IDF file to include the variables and properties for conducting co-simulation, through ***eppy*** package;
  - Configure system to include relevant files, such as BCVTB files, weather files, and EnergyPlus dictionary of input and outputs;
  - Configure optimization process, namely optimization algorithms hyperparameters and optimization targets.
- Run co-simulation class:
  - Establish connection between Python™and EnergyPlus™via a web service connected to BCVTB;
  - Handle all data sources, namely lagged data and disturbances forecast data to feed the surrogate models and optimization process;
  - Encode and decode data packets during simulation runs;
  - Send and receive data packets to and from EnergyPlus.
- Results visualization class:

- Report EnergyPlus™ co-simulation results, namely building energy performance, and simulation logs;
- Report optimization process results;

3.5 Remarks on the implementation of a supervisory predictive control

The exposition on the implementation of an adaptive and surrogate-driven building supervisory predictive control is now complete. This chapter delivered the modelling approach suitable for developing generic building data-driven models, being especially relevant for surrogate modelling to assist the supervisory predictive control. Moreover, the optimization problem was formulated and should play crucial role on the quest for the most suitable set-points to supervise the HVAC system.

The required implementation technicalities were presented, namely those regarding the connection between the simulation software EnergyPlus™and the proposal for the supervisory predictive control. Furthermore, this chapter presented the module developed in this thesis called *eppyco* which enables the co-simulation process and the development of the supervisory predictive control.

The subsequent chapter delivers the results regarding the implementation of the methodology presented.

Chapter 4

Results

4.1 Results overview

The methodology for implementing a supervisory predictive control based on surrogate modelling and optimization of HVAC set-points considering a certain forecast window was proposed and described previously. Hence, this chapter intends to present the results obtained by implementing such a methodology. Fig. 4.26, highlights how the implementation process will be exposed. Moreover, the results obtained from the implementation of the supervisory control system developed will be presented and discussed according to the five steps identified in Fig. 4.26, and may be described as it follows:

The results regarding the development of the supervisory predictive control will follow five major steps depicted in Figure 4.26:

1. A computational model of the building case-study is developed for simulating the building energy dynamics. This task comprises the building design process, including its architecture, location, occupation, equipment, lighting,materials selection, HVAC system design, as well as activity, lighting, equipment, occupation, and HVAC system scheduling. The building dynamic simulation of the selected case-study was carried out using DesignBuilder software.

2. A database is created for implementing any data-driven modelling strategy, and it plays a central role in this thesis methodology. The thermal behaviour of the building under study populates the database by simulating three conventional HVAC control strategies using EnergyPlus™. It may be said that the latter acts as the physics-based model. As a sub-product of this task, the resulting energy performance assessment is later used as references controlling strategies on the benchmarking of the proposed controlling method.

3. Surrogate models of the behaviour of the physics-based simulator are implemented and validated in this step. The results regarding the surrogate modelling based

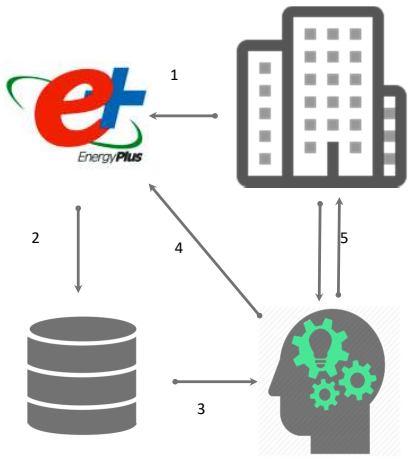

Figure 4.1: Implementation process flowchart of the proposed methodology for supervisory predictive control.

on the machine learning methods will be presented, the modelling method and relevant features will be selected, and the models delivered will be validated.

4. The on-line optimization of the HVAC set points during EnergyPlus simulations is fine-tuned in this step. The performance of optimization algorithms is investigated, selecting the most suitable for this task. The parameters required for the optimization formulation are determined and the preliminary results of the optimization process assessed. The data collection aspect of this task deserves, however, some clarification.In surrogate modelling, optimal data distribution is not known up front and populating an optimization domain represents a computational investment, implying quite often the need for using re-sampling procedures, as pointed by Eisenhower et al. [36]. During this task re-sampling is carried out on the optimization domain. Moreover, the latter is accomplished through the suggestions of the optimization algorithm, by converging to the pitfalls of surrogate models possibly over-fitted, to the initial database.

5. The supervisory predictive control is implemented as a control strategy of the building case-study. Since this implementation is simulation-based, the EnergyPlus™ will play the role of the building. Moreover, the implementation of this step is similar to that of step 4, using the module developed in this thesis for the co-simulation process (*eppyco*) for connecting EnergyPlus™ and Python™ environment in real-

time. This task major purpose is to address and discuss the energy performance of the building, considering the proposed control strategy, benchmarking it against conventional HVAC scheduling methods.

The following chapters follow each of these items, while discussing the results, and the reporting the major findings.

4.2 Building characterization – Office building case-study

The building under assessment in this case-study is a low-rise office building characterized by Portuguese's reference for constructive solutions. This service's building has only one floor which is above ground, having two conditioned zones, and comprising a total area of 207.76 m^2. Both zones are air-conditioned leaving no unconditioned area in the building. The building is located in the suburbs, it is fully exposed and there are no direct obstacles on the building's surroundings. This case-study considered the location to be Oliveira de Azeméis, in Portugal, laying 300 m above sea level. According to Köppen-Geiger climate classification system, Oliveira de Azeméis is included in the **Csb** category, characterizing a temperate climate with a dry and warm Summer [152], and accordingly to the Portuguese Directive it has a cooling season of type I_2 and a heating season of V_1 [153]. Weather data is provided by LNEG (Laboratório Nacional de Energia e Geologia) [154], derived for climatology for the Portuguese Building Certification scheme 2013 update from LNEG. This file is based on climatology data of average records from 1971 to 2000, and 2015-2060 climate change predictions from GHG emission scenarios RCP4.5 and RCP8.5 [154]. The measured variables comprehend a considerable number of weather related variables, and are conveniently distributed in a EPW format, which is compatible with EnergyPlus™.

From figure 4.2 it can be depicted the architecture of the above described building. The design is a square, compass oriented, conferring to the building an an equal exposure area to each of the cardinal directions. Two thermal zones have been defined, a smaller area, identified as ROOM, and a larger one, the HALL. The latter, encounters 141.93 m^2 of the total area of the building accommodating fourteen people working seated. The ROOM is defined to have 65.83 m^2 for the ROOM for accommodating six people also working in seated position. The density of occupation follows the Portuguese directive for offices which is 10 m^2/person. Thus the maximum number of people is 6 in the *Room* and 14 in the *Hall*.

The opaque thermal characterization of the building is listed in Table 4.1. For each element its reflectance, and its coefficient of transmission (U-factor) are given. The exterior walls consist of several layers. From the outside to the inside, a brick layer of 100mm, an insulation board of 79.5mm XPS, 100mm of heavy weight concrete, and a layer of 13mm of gypsum plasterboard are juxtaposed. The inner partitions are composed of two gypsum plasterboards of 25mm separated by an air gap of 100mm.

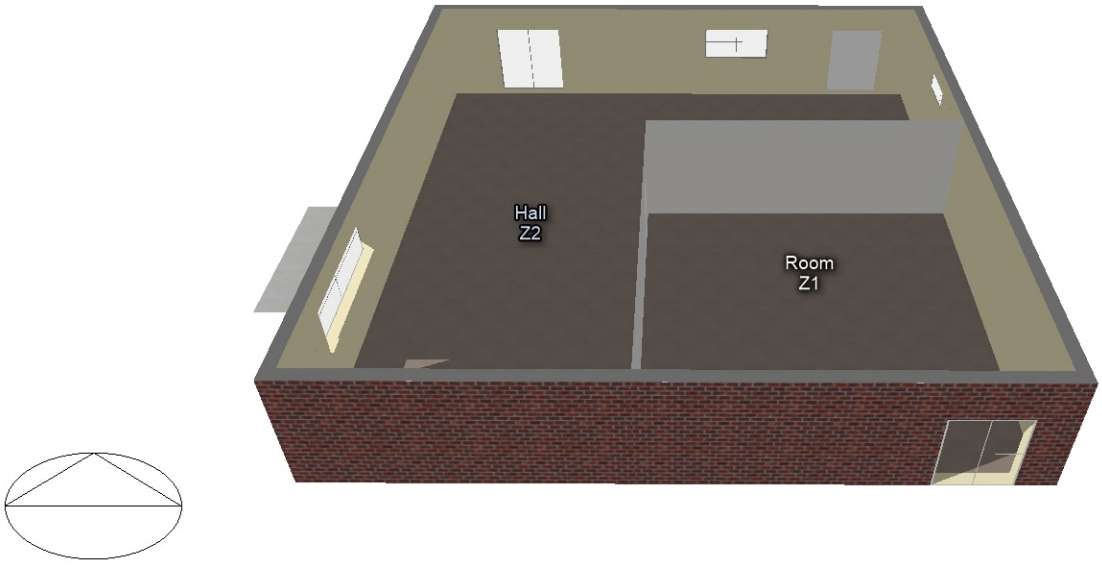

Figure 4.2: Office building reference case-study.

Table 4.1: Opaque envelope solutions' characteristics

Architectural element	**Reflectance**	**U-factor** $(W/(m^2K))$
Exterior Wall	0.30	0.372
Ground Floor	0.40	0.253
Flat Roof	0.15	0.250

There are five exterior windows of double glazing type having an air gap of 10mm. The thermal characteristics of the glazing envelope are summarized in Table 4.2. For each wall the fenestration characteristics such as: area, Solar Heat Gain Coefficient (SHGC), U-factor and shade control are also presented.

The present study focuses on managing the HVAC system serving both zones described previously, here defined as the *Hall* and the *Room*. The HVAC system is composed of a VRF (Variable-Refrigerant-Flow) system and an air-loop system responsible for zone ventilation and air renewal as depicted in Figure 4.3. The coefficient of performance of the VRF outdoor unit is 3.3 and 3.6 for cooling and for heating, respectively. According to the Portuguese Directive, such coefficients of performance represent an energy classification of B [155].

[1]SHGC – Solar Heat Gain Coefficient.

Table 4.2: Fenestration characteristics.

Cardinal direction	**Total area** (m^2)	**SHGC**[1]	**U-factor** ($W/(m^2K)$)	**Shade Control**
All	16.59	0.713	2.786	
North	6.86	0.713	2.786	No
South	3.28	0.713	2.786	Yes
East	2.06	0.713	2.786	No
West	4.38	0.713	2.786	Yes

Both zones are equipped with air temperature sensors where the temperature dual band set-points are managed by a local controller which sets the heating and cooling temperature upper and lower limits, respectively. The proposed management strategy based on a supervisory predictive controller is expected to supervise the temperature set-points and optimize each zone's dual temperature set-points for every simulated hour.

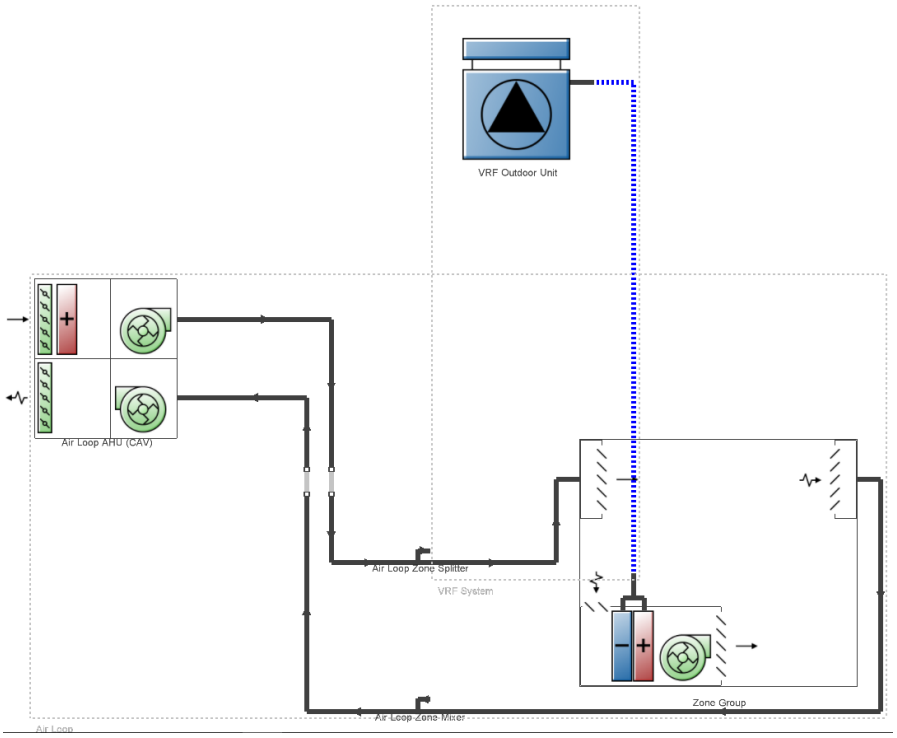

Figure 4.3: Detailed HVAC system representation of the office building case-study.

The building case-study and its HVAC system were designed in DesignBuilder software. DesignBuilder provides a user-friendly interface to EnergyPlus™ serving more than 3500 customers in 80 different countries. Their main market sectors are services engineers, building simulation experts, architects (technical), energy assessors (UK), LEED, BREEAM, Green Star assessors, university R&D and teaching [2].

4.2.1 Building energy simulation – Reference control strategies

As pointed out previously, the performance of a model predictive control can be accomplished by benchmarking a building's energy performance and comfort results using conventional controlling techniques against a proposed technique. Following the suggestions from Haniff et al [61],three non-predictive strategies have been considered

The first technique is based on a timer controller (TC). The system is turned off after occupants leave the building and is turned on 2h before the expected people's arrival. In an office building, the system would be activated at 06:00, and deactivated at 18:00 [29].

The second technique is the demand reduction by pre-heating, or pre-cooling (DR). Here, it is intended to turn off the system during peak hours of electricity consumption and pricing.

The third technique is the "early-off" (EO, This technique uses the building's thermal inertia and turns off the HVAC system before the occupants leave the building. It switches the system at 6:00, but switches it off at 16:00 - two hours before people departure. – two hours before people departure.

The following sections are reserved for the characterization of the building's energy and comfort performance of the above presented reference controlling strategies.

All simulations were performed on EnergyPlus™ software, with a detailed HVAC design and 6 time-steps per hour. The HVAC system is available 24h per day, so it turns ON every time the temperature dual-band set-point, defined for each zone, is not met. The dual temperature thresholds are the same for each zone, being 20^oC and 25^oC for heating and cooling, respectively. The setback temperatures defined were 12^oC for minimum allowed temperature and 28^oC as maximum. These limits follow the Portuguese Directive which states that the acceptable temperature range is [20, 25] for dynamic simulations on occupied zones in air-conditioned buildings such as the one in investigation [155].

Metabolic activity was considered constant throughout the year. People in offices work mostly in a sitting position and, as a result, the metabolic activity can be approximated to $70W/m^2$ (i.e. 1.2 met) according to ASHRAE. Clothing isolation is set to be dependable of the Season, being 1 *clo* for the heating season and 0.5 *clo* for cooling season.

The occupation profiles follow the Portuguese directive for office buildings. However, Gaussian noise with $0.5\sigma_{occ}$ is added to the occupation schedules as an attempt

[2] `https://designbuilder.co.uk/`

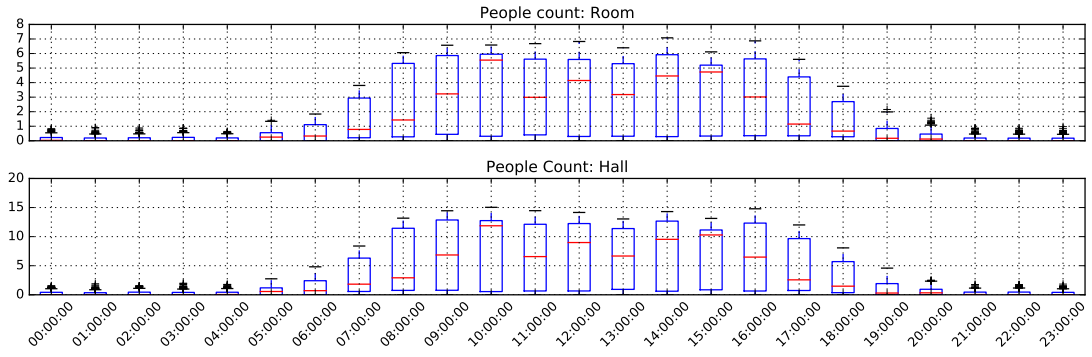

Figure 4.4: Hourly distributions of people occupant count per acclimatized zone.

to simulate the effects of occupation variability. σ_{occ} is the standard deviation of the occupation profiles. The hourly distributions of people occupant count for each zone can be depicted from Figure 4.4.

4.2.2 Timer Control strategy

The first technique to analyse is the timer controller. Fig 4.5 presents the thermal response of the building on a Winter design day (17th of January) representing the coldest day observed in the weather database provided (1.6^{o}C at 7:00). From the top, the first two graphics represent the thermal behaviour of both acclimatized air-conditioned zones: *Room* and *Hall*, respectively. The third graphic graph presents depicts the electricity demand of the VRF system both for cooling and heating loads. The bottom graph, highlights the Percentage of People Dissatisfied (PPD) for both zones, for occupations over 10% of the maximum people observed. The limits for comfort are ideally 10% and limited to 25%, and are represented as green and red lines, respectively. Such limits represent the PMV acceptable zone of approximately 0.5 (neutral) and 1 (expanded), respectively [65].

As it can be seen, the temperature inside the building takes two and a half hours to reach the set-point of 20^{o}C at the *Hall*, whereas the time to reach that same set-point in the Room is slightly above one hour. Such difference might be associated with the volumetric difference between each zone, since the HVAC system is the same for both cases. Accordingly, since temperature influences the comfort, the PPD in the Hall only reaches a satisfactory level, three hours after the set-points are altered. The Room's thermal comfort threshold is guaranteed after two hours. In both zones the PPD remains unchanged throughout the period of the day with occupation (above 10%) with a mean value of 21.5%. Overall, the mean PPD for the whole building during occupied hours is 23.79% which is lower than the defined threshold. However, the mean PPD at the Hall alone reaches 27.72%, 2.72% above the desired limit of 25%. Another comfort metric

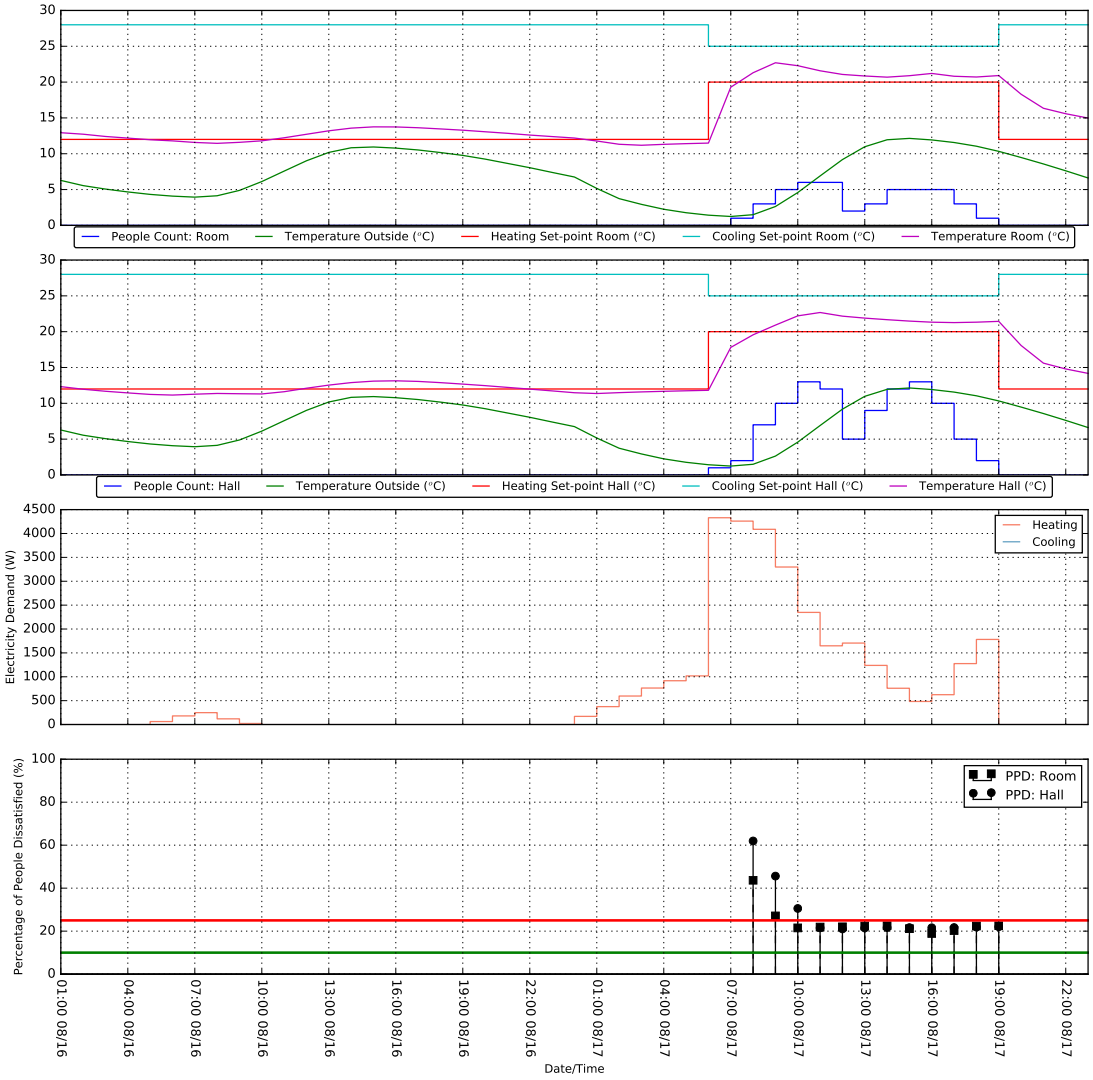

Figure 4.5: Energy performance of Timer Control (TC) strategy for Winter design day.

employed in this analysis is the accumulated people dissatisfied (APD). This metric can be viewed as a weighted PPD, calculated by multiplying the Predicted Percentage of Dissatisfied by the people present in each zone, P_{count}:

$$APD = PPD \cdot P_{count} \tag{4.2.1}$$

This value, however, has to be interpreted as a statistical metric since PPD is a statistical value itself. Nevertheless, it can be a helpful index for the magnitude of the

dissatisfaction due to air-conditioning.

The observed peak electricity demand from the VRF system due to heating was 4329.9 W at 7:00, and the total energy consumption of the represented period was 32318.2 Wh. The specific energy consumption was 152.5 Wh/m^2 for the period of 24h of the coldest day of the year. Table 4.3 summarizes the energy performance results of the reference case-study using Timer Controller for the Winter design day.

The simulation of Summer design day (22nd August) was carried out using the same control strategy as with Winter design day and it can be depicted from Fig. 4.6. Comfort is guaranteed throughout all occupied hours of the day, being the highest PPD equal to 20% and it was observed at the *Hall*. The average PPD for the whole building is 9.24%, which represents a PMV of approximately 0.45, meaning that thermal sensation is close to neutral. ASHRAE 55 standard sets 10 % as the acceptable PPD comfort limit. However, the design characteristics of limiting the temperature set-point as 20^{o}C for heating does not allow for such comfort levels. Overall, people should perceive the inner environment as more comfortable during Summer days, than during Winter.

The peak power demand observed was 4385W at 15:00, while the total energy consumption for the observed day was 24420Wh. Energy and comfort criteria for both design days and the whole year simulation are summarized in Table 4.3.

Table 4.3: Energy and comfort performance of the reference case-study using Timer Controller for the Winter design day.

Metric	**Winter day**	**Summer day**	**Year**
Accumulated people dissatisfied	50	15	9683
Percentage of PPD >25%	20.83 %	0 %	20.02 %
$\overline{PPD}$	25.788 %	9.24 %	21.34 %
$\overline{PPD}$ @ Room	23.86%	8.97%	18.80 %
$\overline{PPD}$ @ Hall	27.72 %	9.50%	23.82 %
Peak electricity demand	4330 W	4264 W	4330 W
Energy Consumption	32318 Wh	27924 Wh	2818.995 kWh
Specific energy consumption	155 Wh/m^2	134 Wh/m^2	13.80 kWh/m^2

4.2.3 Early Switch-Off strategy

The thermal behaviour of the building under the Early-Off scheduling is very similar to the one observed with the Timer Control. Nevertheless, a few differences observe mainly in what concerns the last couple of occupied hours of the day should be pointed out. As it can be observed in Fig. 4.7, the PPD limit of 25% is violated during the last hours of the working day, since the earlier temperature set-point changes to the set-back temperature of 12^oC. Thus, a rise of 16.67% of the percentage of hours outside comfort limits was observed in this case when comparing it to TC scheduling.

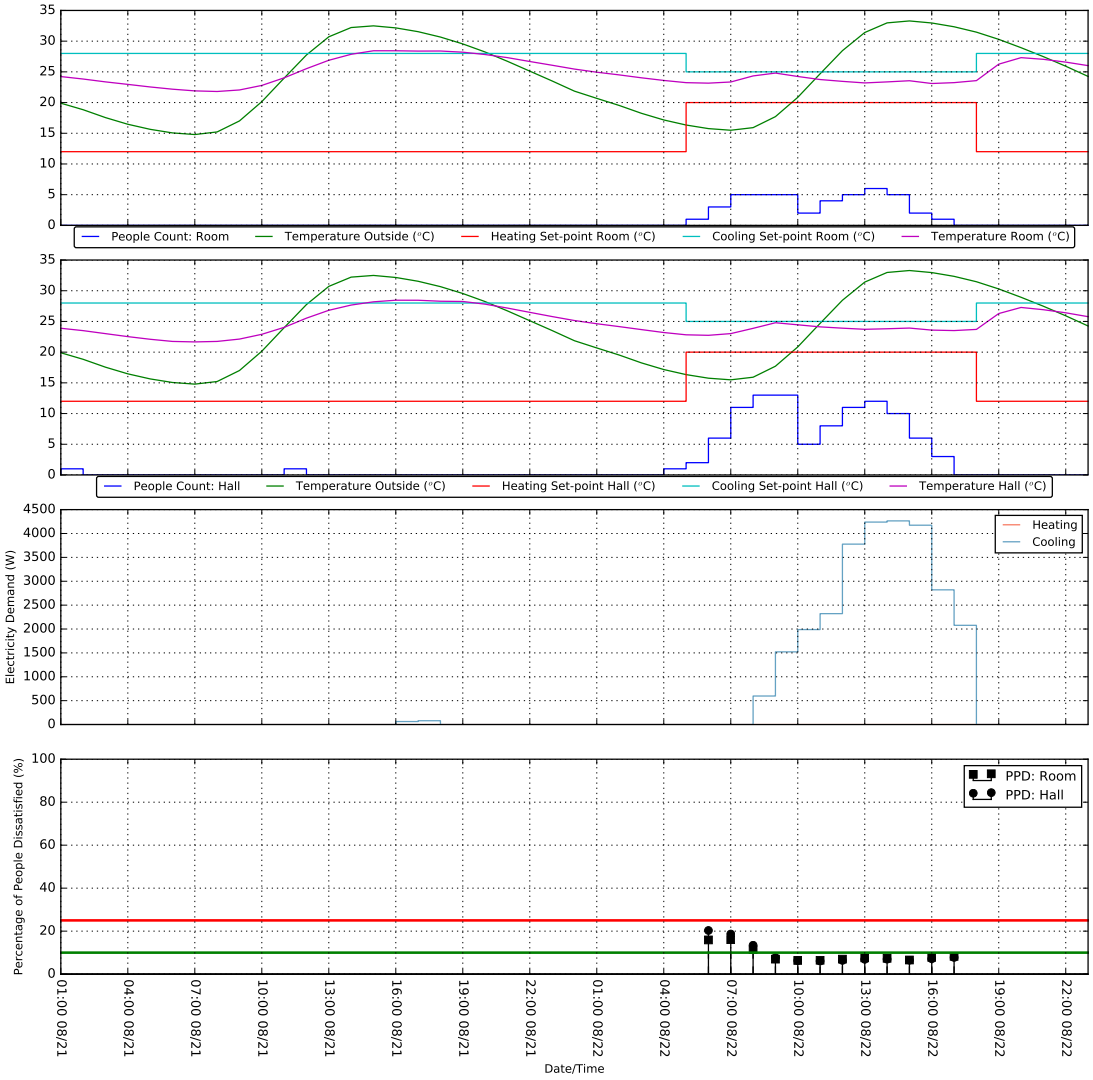

Figure 4.6: Energy performance simulation of Timer Control (TC) strategy for Summer design day.

On the other hand, it can be observed a reduction of the electricity demand and a respective reduction of the energy consumption on that last couple of hours, as it can be depicted by comparing Fig. 4.5 with 4.7. This variation accounts for a reduction of 7.96% of energy consumption of the Winter design day, summing up an energy consumption of 29747.2 Wh.

Summer design day shows strong similarity with the TC strategy in terms of comfort levels. There were no violations of the comfort limit imposed, and the overall PPD was

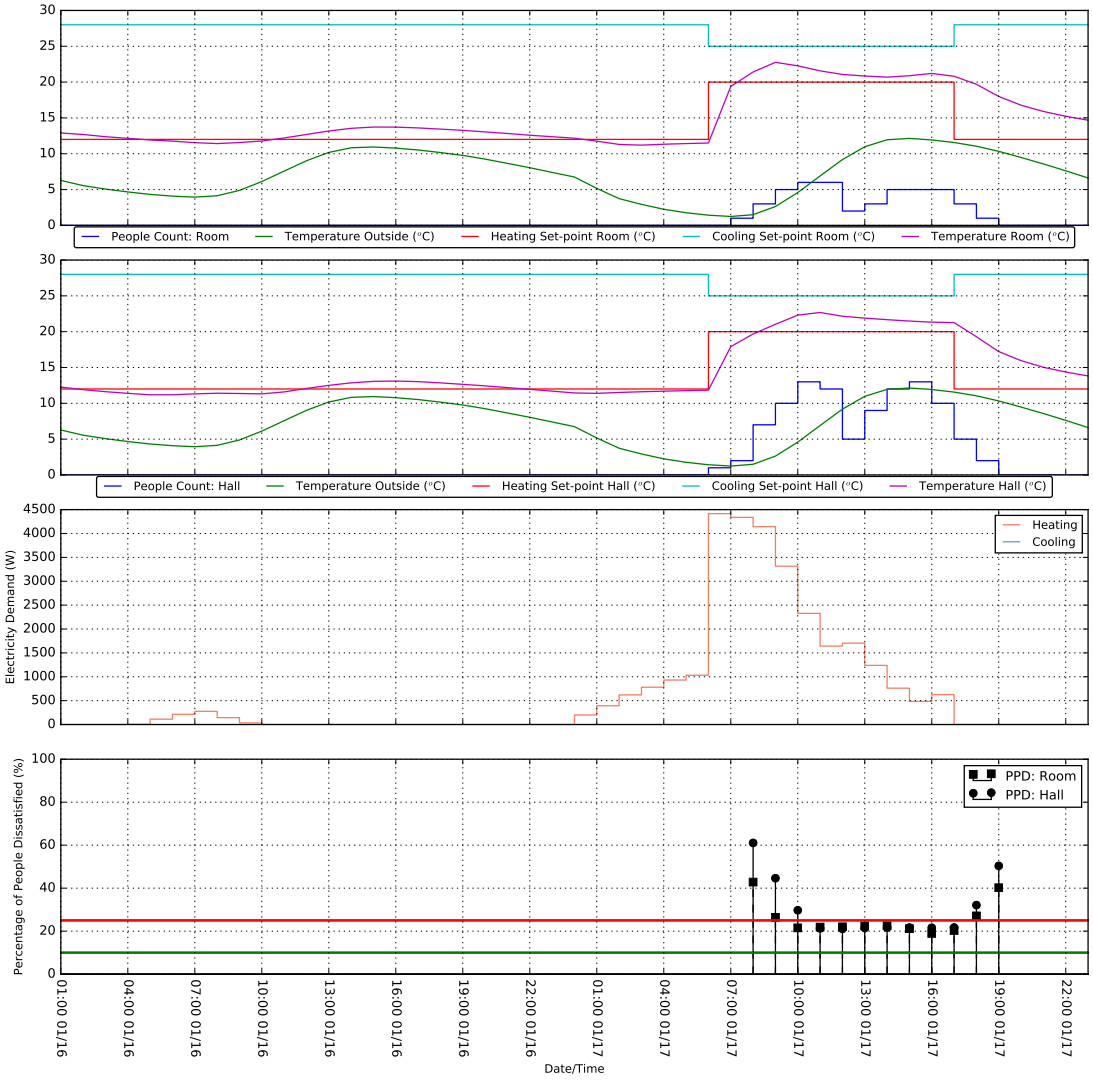

Figure 4.7: Energy performance of Early switch-Off (EO) strategy for Winter design day.

9.27%, which can be considered approximately the same as the one observed with TC. The major difference observed is the peak electricity demand, which is higher than with TC, but having an overall energy consumption lower than the first strategy studied. It seems that although a global reduction on the energy consumption is observed the peak power demands increases. The whole year, the design days energy consumption and the comfort levels are summarized on Table 4.4.

Table 4.4: Energy and comfort performance of the reference case-study using Early switch-Off strategy for the Winter design day.

Metric	**Winter day**	**Summer day**	**Year**
Accumulated people dissatisfied	51	15	9629
Percentage of PPD >25%	37.5 %	0 %	20.8 %
$\overline{PPD}$	28.1 %	9.27 %	21.25 %
$\overline{PPD}$ @ Room	25.6 %	9.06 %	18.60 %
$\overline{PPD}$ @ Hall	30.7 %	9.50 %	23.85 %
Peak electricity demand	4415.9 W	4385.4 W	4415.9 W
Energy Consumption	29747 Wh	24420 Wh	2543.297 kWh
Specific energy consumption	143 Wh/m^2	117 Wh/m^2	12.45 kWh/m^2

4.2.4 Demand Reduction strategy

The Demand Reduction strategy is the control solution implemented that presents the lower energy consumption, throughout the entire year analysed. The annual energy consumption is 18.6% lower than with the TC strategy, and less 11.6% than with the EO one. However, the peak electricity demand is 5833.9 W, a result that is higher than the ones obtained with the other strategies analysed. The energy reduction observed comes at the expense of comfort, as it can be depicted from 4.9. It was observed that with this control strategy the violations of the comfort limit increased 50% when compared with TC strategy, and more 33.3 % than the EO. The inner environment is characterized with a PPD equal to 41.5%, i.e. a PMV of approximately -1.5. All information can be seen in detail on Table 4.5.

The summer season presents similar results when the results are compared with the other controlling strategies analysed, since there were no violations of the comfort limit established for entire whole day. It could therefore be said that the other control strategies and the set-points have room for improvement during the cooling season. The thermal behaviour of the building during Summer design day is presented in Fig. 4.10. The energy consumption for this day was 24861Wh, being the lowest of all strategies. On the other hand, the peak demand of electricity for cooling is the highest for the whole year, reaching 6017 W. This strategy seems to be the least effective when comparing with the other strategies in what concerns the entire buildings dynamics. Moreover, the comfort levels reach values far from the acceptable limit. If the main purpose of a HVAC system is to provide comfort to the occupants of a building, DR has clearly failed its purpose during the heating season, presenting an average PPD of 41.5%. This comfort level represents a PMV of -1.3 which means that the occupants are likely to feel between *slightly cool* and *cold*, according to the Fanger's Predicted Mean Vote thermal sensation scale [38]. However, a combination of this strategy for the cooling season with another strategy for the heating season could represent an acceptable compromise between energy consumption and comfort.

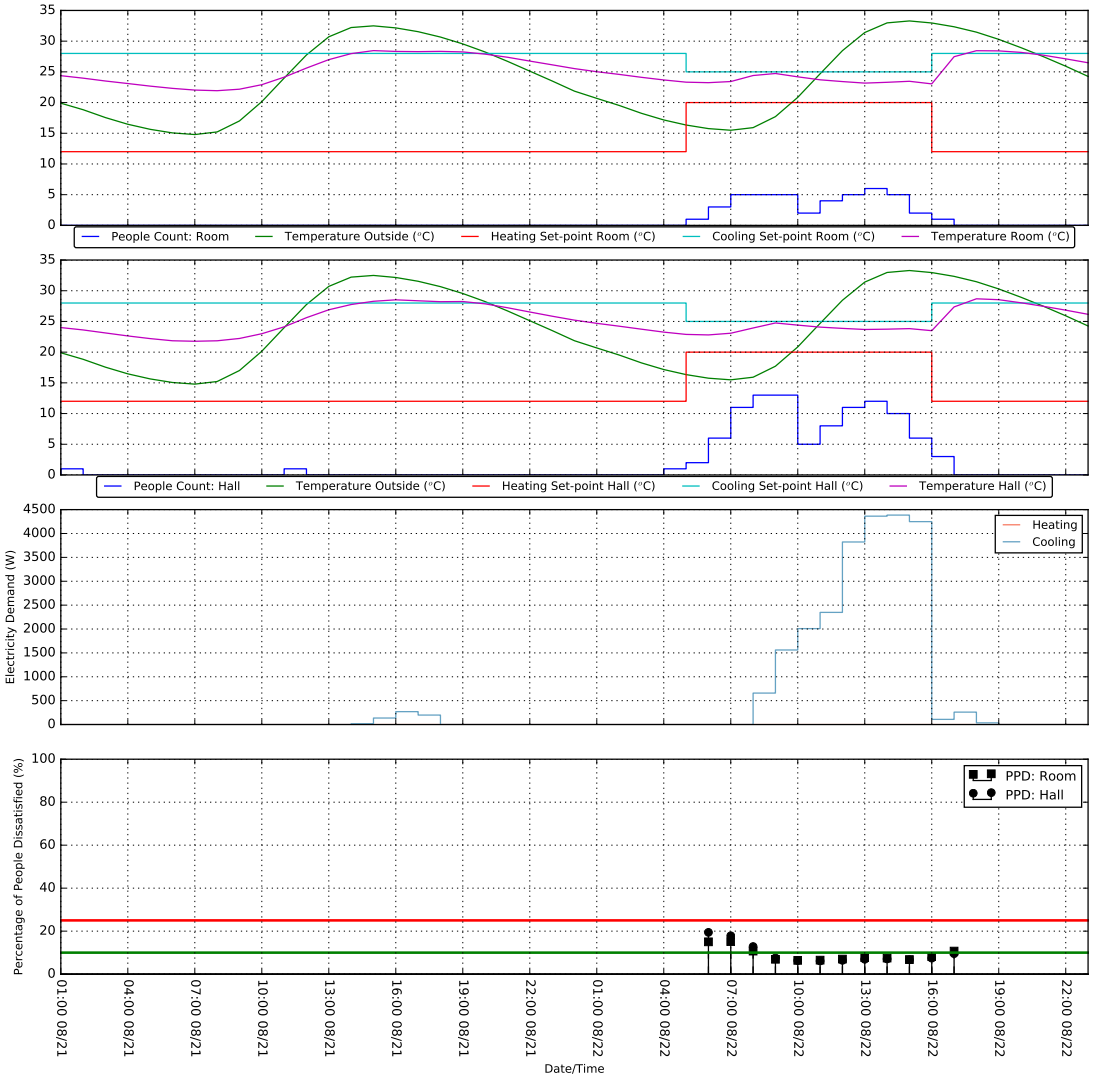

Figure 4.8: Energy performance simulation of Early switch-Off (EO) strategy for Summer design day.

Considering the whole year performance, Early switch-Off strategy seems to be a good compromise between the three controlling strategies presented, corroborating the results from Garnier et al. [29]. On the one hand, the comfort levels of this strategy are similar to the best solution regarding comfort which is the Timer Control, hence presenting higher comfort levels than the Demand Reduction controlling strategy. On another hand, the energy consumption is lower than on TC, while resulting on a higher energy demand than on DR strategy. It could therefore be said, that the Early switch-

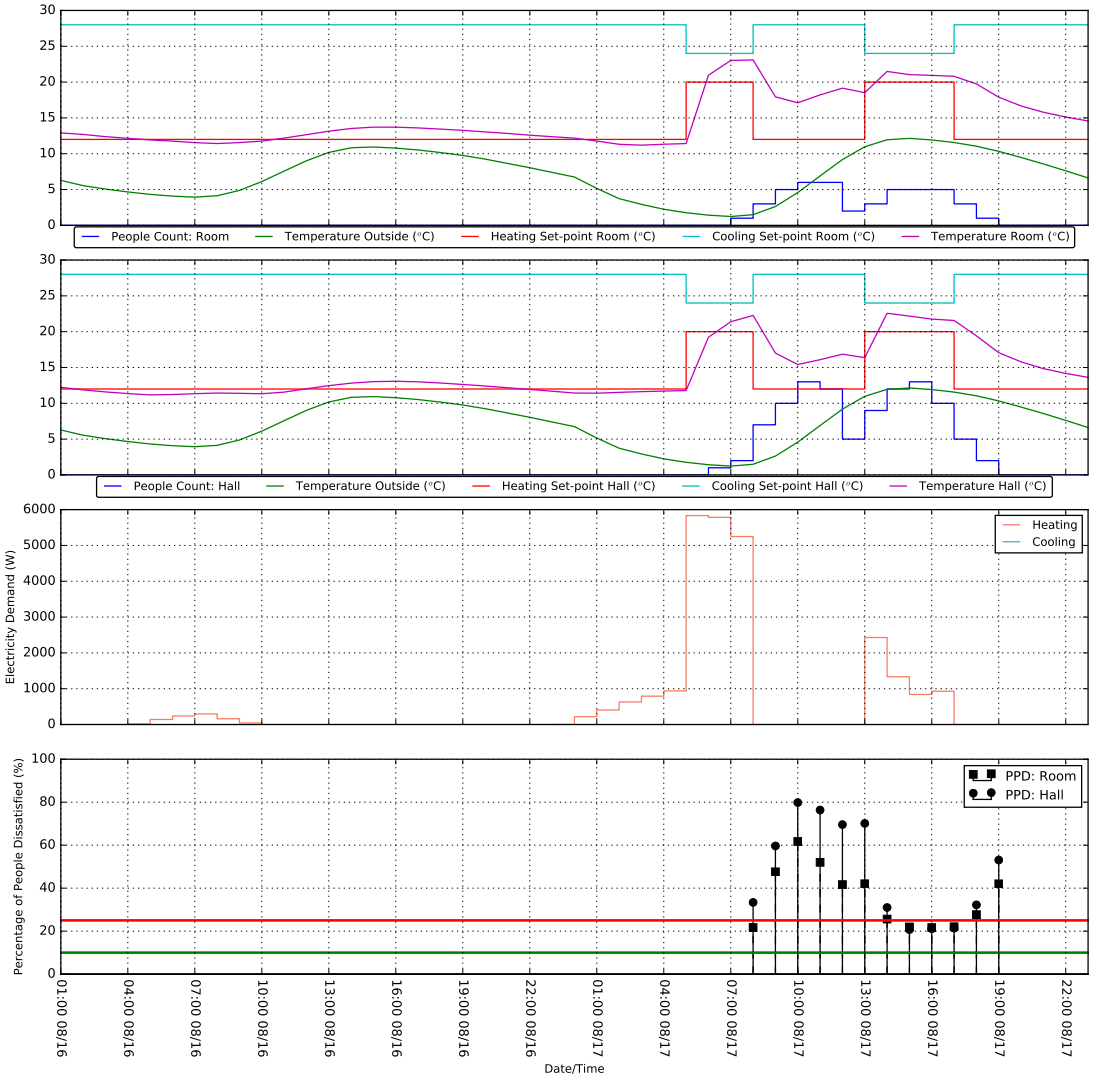

Figure 4.9: Energy performance of Demand Reduction (DR) strategy for Winter design day.

Off strategy is more relevant environmentally and economically than the Timer Control and, it what concerns the heating season, it is more useful than the Demand Reduction for providing occupants with an environment of acceptable thermal comfort levels.

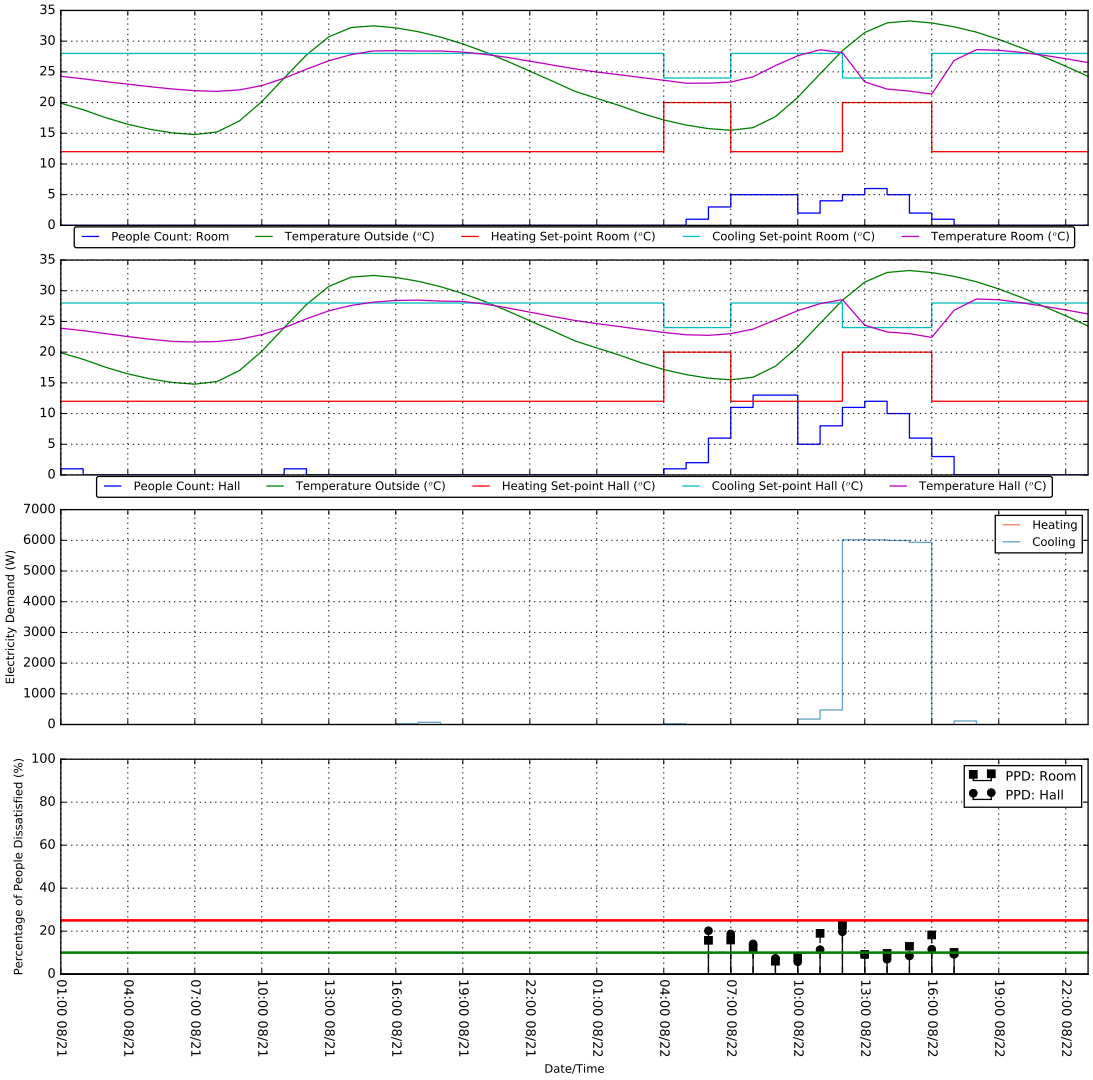

Figure 4.10: Energy performance simulation of Demand Reduction(DR) strategy for Summer design day.

4.3 Modelling strategy results

This section focuses on presenting the results of developing data-driven models which are surrogates of the responses of the deterministic simulator for the building presented as the case scenario. This section follows the methodology for developing statistical and data-driven models, presented previously, and supported by the works of Shmueli et al. [122], and Fan et al. [79].

Table 4.5: Energy and comfort performance of the reference case-study using Demand Reduction strategy for the Winter design day.

Metric	**Winter day**	**Summer day**	**Year**
Accumulated people dissatisfied	81	19	11334
Percentage of PPD >25%	70.67%	0 %	30.90 %
$\overline{PPD}$	41.5 %	12.59 % %	24.76 %
$\overline{PPD}$ @ Room	35.64 %	13.31 %	24.76 %
$\overline{PPD}$ @ Hall	47.37 %	11.87 %	28.01 %
Peak electricity demand	5833 W	6017 W	6017 W
Energy Consumption	26293 Wh	24861 Wh	2554.835 kWh
Specific energy consumption per m^2	127 Wh/m^2	120 Wh/m^2	12.5 kWh/m^2

As previously referred, the goal lies in the development of accurate models of the building thermal response to the endogenous and exogenous variables to enable the integration of an on-line optimization process which is part of the supervisory predictive control strategy.

Data has been collected by running the simulations presented previously and applying the non-predictive conventional controlling strategies. The latter provided the means to gather the initial database, that will serve the surrogate modelling presented in this section. However, this database is expected to be updated with new sample points every time a co-simulation process of EnergyPlus™and the supervisory predictive control occurs. If the new data induces unexpected model mismatching, the surrogate model is expected to be retrained to learn the new data-points.

The preparation of data for the modelling and the exploratory data analysis are combined in one section which focuses on the variables dependence with each other, and their transient dependence given the building energy system dynamics.

The choice of variables is presented via the feature selection methods and algorithms, where the importance of the available variables for modelling the building case-study is investigated.

The choice of methods has been accomplished through the literature review. The models resulting by the machine learning training are compared based on their capability to predict the building state accurately, and the best models are selected in order to include the optimization process inherent to the supervisory predictive control.

4.3.1 Data Collection

The database comprising the simulations of the HVAC controlling solutions listed in the previous section is here referred to as Reference database. The first surrogate models, here called base-models, are trained using these referred simulations alone. It is only after the first simulations of the supervisory predictive control that the database will start accumulating data resulting from the optimization routines. The investigation

of the effects of such data in the predictive performance of the data-driven surrogate models is discussed later in this section.

The Reference database summed the equivalent of three years of data, one for each control solution. Thus, a total of 35040 samples were provided by EnergyPlus, since results were delivered hourly (8760 h/year).

Simulation results are time indexed, meaning that each sample contained in the database represents the data gathered during a simulated time interval. The variables selected for the development of this database are represented on Table 4.6. Recall that variables are divided in three groups depending on their role in this methodology:

- **Control variables**, u_t, which accommodate all variables allowing for manipulation, such as HVAC temperature set-points;
- **Disturbance variables**, x_t, which contain the information regarding system disturbances which are uncontrollable, namely, weather data, and occupation;
- **Output variables**, y_t, which reflect the output response of building's energy system to the values of the previously referred variables. Usually, these outputs can include energy consumption, occupants' comfort, interior environment variables.

Table 4.6: Description of Inputs/Outputs and exogenous variables related to one zone of the building.

Group	**Description**	**Units**
u_t	Heating Temperature Set-point	^oC
u_t	Cooling Temperature Set-point	^oC
x_t	Outdoor Air Drybulb Temperature	^oC
x_t	Horizontal Infrared Radiation Rate per Area	W/m^2
x_t	Outdoor Air Relative Humidity	[%]
x_t	Zone People Occupant Count	[–]
y_t	VRF Heat Pump Cooling Electricity Demand	$[kWh]$
y_t	VRF Heat Pump Heating Electricity Demand	$[kWh]$
y_t	Zone Thermal Comfort Fanger Model PPD	[%]
y_t	Zone Air Temperature	$[^oC]$

The goal of this chapter is to deliver the most robust data-driven and predictive models of the outputs referred in Table 4.6, using as inputs the variables present in the same table. Note that two of the outputs are dependent of each zone of the building, so in total six models should be developed:

- One predictive model of electricity demand of VRF due to heating;
- One predictive model of electricity demand of VRF due to cooling;

- Two predictive models of PPD. One for each zone of the building;
- Two predictive models of temperature inside of each zone.

Data division is mandatory for helping to avoid over optimistic error assessments and consequent over-fitting of the referred models. The approach here envisaged to data division follows a combination of the 10-fold cross-validation approach, and the partitioning proposed by Hastie et al. [147]. That is to say, 25 of data is reserved for test error assessment and the remainder 75% are employed for conducting the exploratory data analysis, feature selection, and the 10-fold cross-validation for model both architecture selection, and error validation. A final error validation will be performed using the reserved 25% of data.

4.3.2 Exploratory data analysis and data preparation

Data preparation and exploratory data analysis (EDA) are key initial steps in preparing data for a predictive modelling strategy [130]. It consists of summarizing the data numerically and graphically, reducing its dimension, and preparing it for the more formal training step. EDA can be employed either to capture relationships between variables, which might be unknown, or to sustain theoretically specified causal relationships [122]. The main goal of this section is to assist in the understanding of the inherent characteristics of data and to sustain the pre-selection of input variables relevant for modelling. The discussion on lagged variables to include the transient response of buildings in the models will be held further ahead. In EDA data visualization is of utmost importance and that can accomplished from Figure 4.11, where the distribution plots of the output variables are presented. As expected, the power related variables have an exponential type of distribution, containing in its majority zero, or close to zero values. The skewness of these distributions represents a significant limitation in the development of linear regression models because the weight of zeros is considerably higher than other values and the training process would favour the reduction of the errors related to predicting zeros. Usually, feature transformations can be used to modify such behaviour. One example is to perform a log transformation of data to approximate distribution to a quasi-Gaussian. Another possibility, especially used for classification modelling, is to use sampling methods for imbalanced learning [156].

However, the latter solution still lacks robust solutions for regression models, and the former does not guarantee yielding of robust models. Moreover, the zero values shown in such distributions are likely to have considerable differences of origin, increasing greatly the task of balancing the output without compromising the other variables and the regression task itself [156]. Power demand variables can equal zero for many different configurations of input variables (Table 4.6),), depending on the precedent energy state of the building. The remainder output variables, especially the temperature inside the building zones, follow a close-to-Gaussian distribution. In what concerns this modelling task, a normalization of the variables will be carried out, since the modelling techniques

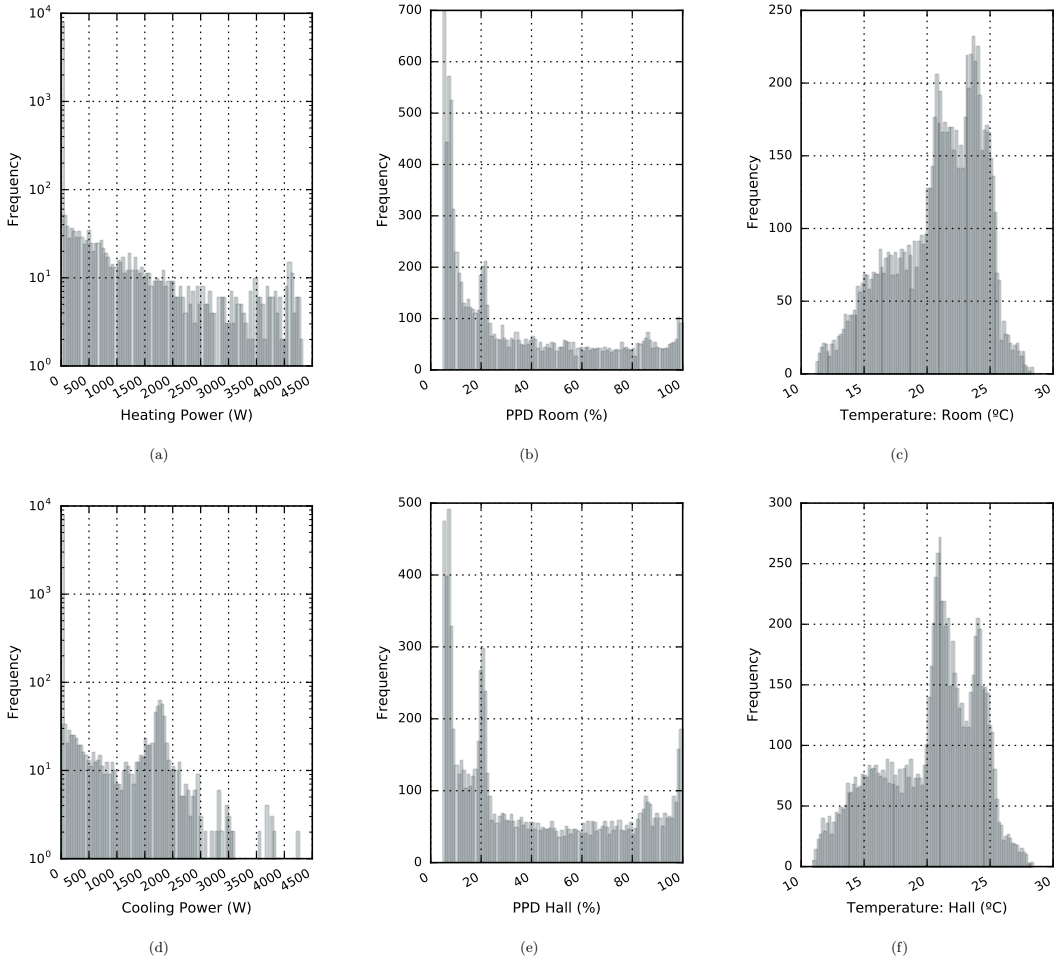

Figure 4.11: Distributions of output variables.

selected for training, especially SVR and ANN, require variables to be of commensurate scales, as previously discussed. The data provided to the Random Forest models will be also normalized. Moreover, providing the same training data to all models is expected to standardize the selection task [91].

Normalization can be computed by subtracting means and dividing by standard deviations extracted from the training set. The most common and robust approach to normalize variables is by applying Eq. 4.3.1.

$$\upsilon_i' = \frac{\upsilon_i - \mu_{\upsilon_i}}{\sigma_{\upsilon_i}} \tag{4.3.1}$$

where υ_i is the sample value of the i^{th} variable, μ_{υ_i} is variable's mean, σ_{υ_i} is the

Table 4.7: Variables statistical summary.

Variable	Mean	Std	Min	25%	50%	75%	Max
Cooling Temp. SP (^{o}C)	27.01	1.506	24	25	28	28	28
Heating Temp. SP (^{o}C)	14.45	3.690	12	12	12	20	20
Temp_out (^{o}C)	14.79	6.181	1.242	10.25	14.3	18.87	33.29
H.Radiation (W/m^2)	343.5	28.71	263	323.4	341.7	361.8	455.83
Relative Hum. out. (%)	78.42	14.78	28.58	67.75	80.17	91.17	98
People Count Room	1.563	2.154	0	0	0.2992	3.026	7.0785
People Count Hall	3.365	4.642	0	0	0.6494	6.510	15.039
Heating Power Demand (W)	173.0	663.5	0	0	0	0	5833.9
Cooling Power Demand (W)	136.9	538.12	0	0	0	0	6017.1
PPD Room (%)	34.05	29.47	5.005	9.019	21.27	54.81	99.999
PPD Hall (%)	40.54	31.47	5.001	12.79	28.79	68.99	99.999
Temperature in Room (^{o}C)	20.97	3.608	11.18	18.55	21.52	23.68	28.628
Temperature in Hall (^{o}C)	20.31	3.813	10.920	17.54	20.96	23.17	28.686

standard deviation, and v_i' the normalized variable value, for each variable present on Table 4.6.

Table 4.7 summarizes the statistical characteristics of the variables at play.

4.3.3 Input correlation analysis

The first inputs considered to develop the surrogate models are the disturbances and the control variables referred to on Table 4.6. In the development of data-driven models it is important to investigate the correlation between input variables and to remove those highly correlated. The training process of a model will enable the distribution of the correlated inputs, leading to a misinterpretation of the real importance of each variable and multicollinearity between variables [132, 142]. The problem of multicollinearity is not known for having a negative impact on the predictive reliability of a data-driven model. However, it is known for affecting the sensitivity of the model regarding individual input variables. Although the models produced may be of useful predictive capability, the influence of the control and disturbance variables on the object of prediction may not be mirrored. Figure 4.12 shows the Pearson linear correlation (ρ) between each pair of possible inputs, being 1 perfectly correlated, 0 no linear correlation, and -1 perfectly inversely correlated.

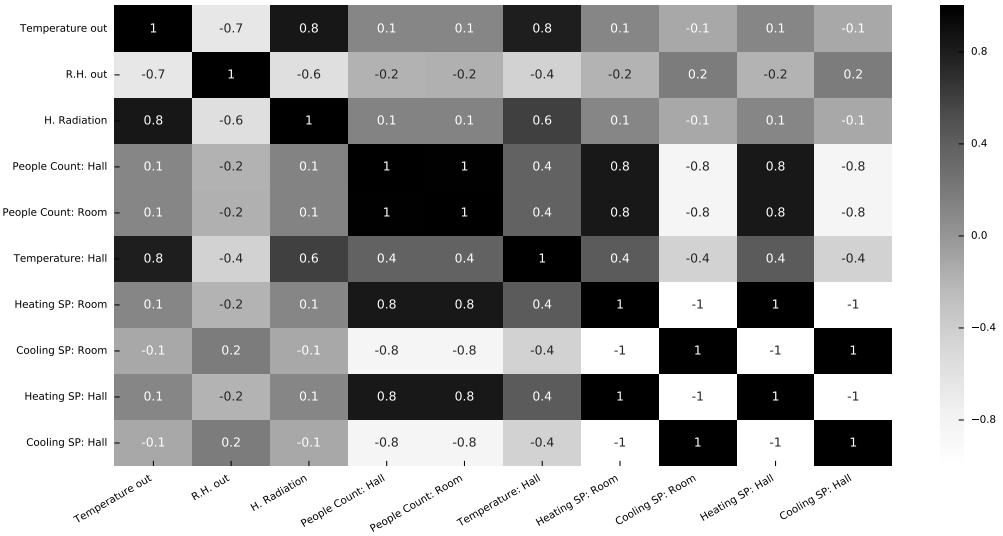

Figure 4.12: Pearson correlation of input variables (controllable and uncontrolable).

As it can be depicted, and expected, the control variables (Heating and Cooling temperature set-points) are perfectly inversely correlated on the *Reference* data. This behaviour should be expected because the upper and lower temperature set-points vary simultaneously every time there is a change in the temperature control. Moreover, temperatures set-points are correlated between zones. Other expected highly correlated inputs are the Horizontal Radiation, Outside Air Temperature, inner Air Temperature and People Occupant count of both zones. Since the correlation coefficient is 0.8, these variables are not as problematic as those from the control variables. Ideally, the input variables showing high multicollinearity would be linearly mapped into a single variable using, for example, the method of Principal Component Analysis in order to reduce the dimension and complexity of the model. However, such method would reduce the possibility of using the proposed supervisory predictive control because the singularity of each variables would be lost. This phenomenon is expected to lead the optimization algorithm to converge to control decisions which are not well mapped in the domain of operation since the influence of each control variable individually will not be mapped by the model. Thus, this re-sampling strategy using these new data points selected by the optimization algorithm is expected to decrease such multicollinearity and improve models robustness.

4.3.4 Time-dependency analysis

The employment of Auto-Correlation Function (ACF) and Partial Auto-Correlation Function (PACF) was carried out on the six output variables under study to create a pool of candidate inputs showing time-dependency. Commonly, these tools are used for

time series modelling to identify repeating patterns and select auto-regressive inputs for modelling. Whereas ACF is the linear dependence of a variable with itself at two points in time, PACF is the autocorrelation between two points in time without considering the linear dependence of observations between these same two points in time [79]. In this section, ACF and PACF functions help to study the autocorrelation of output variables and, therefore, to understand the time-dependency of each output to its precedent value. The goal is to investigate the possible usefulness of considering lagged variables as inputs to the predictive models. The ACF and PACF analysis help investigating the time-dependency of hourly electricity demand for both cooling and heating, of PPD and inside temperature for both zones. All the input variables which have significant time-lags correlations should also include the pool of candidate predictors for later investigation of relevant features. This study sets 10% of the significance level for consideration and 24h as the maximum time-lag.

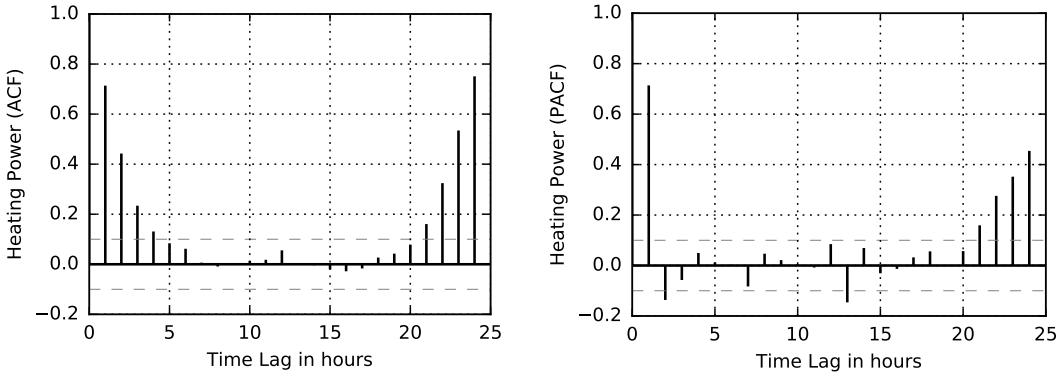

(a) ACF analysis.

(b) PACF analysis.

Figure 4.13: Auto-correlation analysis for heating electricity demand.

Figure 4.13a) shows the auto-correlation of the values of heating electricity demand. The decay of ACF in function to the time-lag suggests a somewhat local non-stationary behaviour, i.e. the past values of power demand are somewhat important to predict the current time-step [157, 123]. In a moving average model (MA), the relevant number of lagged values would be six because it is the last value before the defined cut-off of significance level represented as grey dashed lines. The partial autocorrelation analysis from Fig. 4.13 shows a less time dependency than on the ACF, proposing a time-lag limit of two lags. Hence, in this study, all the variables with a time lag of up to 2 hours (t-l...t-2) are included in the input candidate pool for modelling the heating electricity demand, from which the next task of feature selection is used to draw the most relevant inputs.

Both analyses show a strong correlation between electricity demand on time t and

Table 4.8: Pool of variables considered for variable selection task of modelling **Heating Power Demand**, and **Inside Temperature** in both zones, according to ACF and PACF analysis.

Group	**Variable**	**Lags:** $[t-k_i, ..., t-k_f]$
u_t	Heating Temp. SP (both zones)	$[t-0, ..., t-2]$
u_t	Cooling Temp. SP (both zones)	$[t-0, ..., t-2]$
x_t	Outdoor Air Drybulb Temperature	$[t-0, ..., t-2]$
x_t	Horizontal Radiation Rate	$[t-0, ..., t-2]$
x_t	Outdoor Air Relative Humidity	$[t-0, ..., t-2]$
x_t	Zone People Occupant Count (both zones)	$[t-0, ..., t-2]$
y_t	Heating Power Demand	$[t-1, t-2]$
y_t	Cooling Power Demand	$[t-1, t-2]$
y_t	Predicted Percentage of Dissatisfied (both zones)	$[t-1, t-2]$
y_t	Inside Air Drybulb Temperature (both zones)	$[t-1, t-2]$

its lagged values close to 24h. The main reason for this behaviour might be due to the repetition of daily patterns. Despite the fact that time-lags of $t-13$ and from $t-21$ to $t24$ are in the acceptable range of significance level, these variables are discarded to avoid the development of models too slow to respond to new changes imposed by the predictive control. As a result, this study gathers a pool of inputs summing up 39 variables in total, as it is presented on Table 4.8.

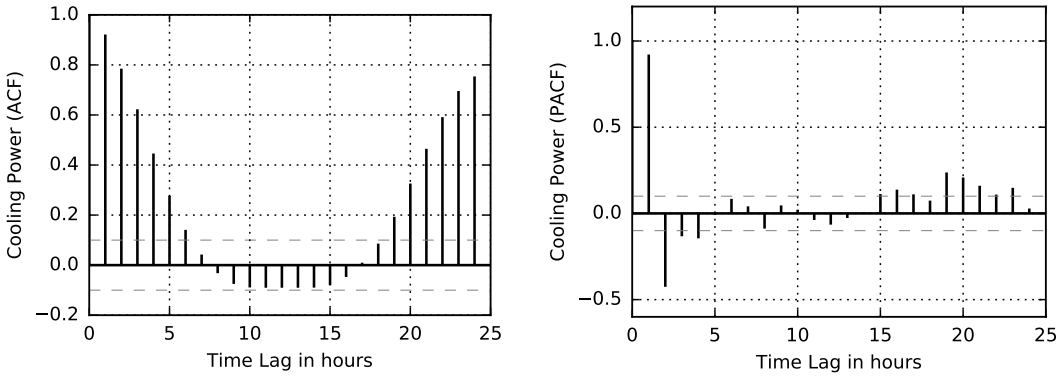

(a) ACF analysis.

(b) PACF analysis.

Figure 4.14: Auto-correlation analysis for cooling electricity demand.

Cooling electricity demand auto-correlation analysis suggests lagged variables from $t-1$ to $t-4$. Figure 4.14 (a) presents the auto-correlation of cooling electricity demand

Table 4.9: Pool of variables considered for variable selection task of modelling **Cooling Power Demand**, and **Predicted Percentage of Dissatisfied** in both zones, according to ACF and PACF analysis.

Group	**Variable**	**Lags:** $[t-k_i, ..., t-k_f]$
u_t	Heating Temp. SP (both zones)	$[t-0, ..., t-4]$
u_t	Cooling Temp. SP (both zones)	$[t-0, ..., t-4]$
x_t	Outdoor Air Drybulb Temperature	$[t-0, ..., t-4]$
x_t	Horizontal Radiation Rate	$[t-0, ..., t-4]$
x_t	Outdoor Air Relative Humidity	$[t-0, ..., t-4]$
x_t	Zone People Occupant Count (both zones)	$[t-0, ..., t-4]$
y_t	Heating Power Demand	$[t-1, t-4]$
y_t	Cooling Power Demand	$[t-1, t-4]$
y_t	Predicted Percentage of Dissatisfied (both zones)	$[t-1, t-4]$
y_t	Inside Air Drybulb Temperature (both zones)	$[t-1, t-4]$

with a slow decaying ACF suggesting a non-stationary behaviour similar to the one of heating electricity demand. Moreover, this analysis also suggests a periodic event by the rise of the correlation between values close to 24h. This pattern can be observed on all variables assessed in this time-dependency analysis. The analysis of the PACF in Figure 4.14(b) exhibits an exponential decay pattern of the partial auto-correlation values. The cut-off limit for considering lagged variables of the output in an auto-regressive model is crossed after lag four. It means that a data-driven model specialized on predicting the cooling electricity demand of the current building, should consider the lagged variables from $t-1$ to $t-4$. Therefore, the candidate input pool to consider in the following task of variable selection has 69 variables in total, summarized on Table 4.9

Figures 4.15 (b and d)exhibit a similar decay of the partial auto-correlation values for PPD values for the Room, when comparing to the other variables. There is a strong inverse partial autocorrelation in time-lag of $t-2$ which indicates an inverse proportionality of each time step with its odd pair, a common behaviour of slow systems having feedback control such as HVAC systems. The cut-off limit was crossed at the third lag, being crossed again at lag equals four, suggesting a higher non-linear relationship than with its precedent time-steps. Thus, the development of a data-driven model for predicting the PPD should consider lagged variables up to $t-4$. Table 4.9 summarizes the initial variables to consider for the development PPD predictive model of both zones. All these models have 59 variables in total along with the modelling of Cooling Power Demand.

The behaviour of ACF of PPD from Figures 4.15(a and c) show a very strong linear dependency between all the lags studied, and the same behaviour is shown as well in the ACF analyses of Inside Drybulb Temperature of both zones in Figure 4.16. ACF

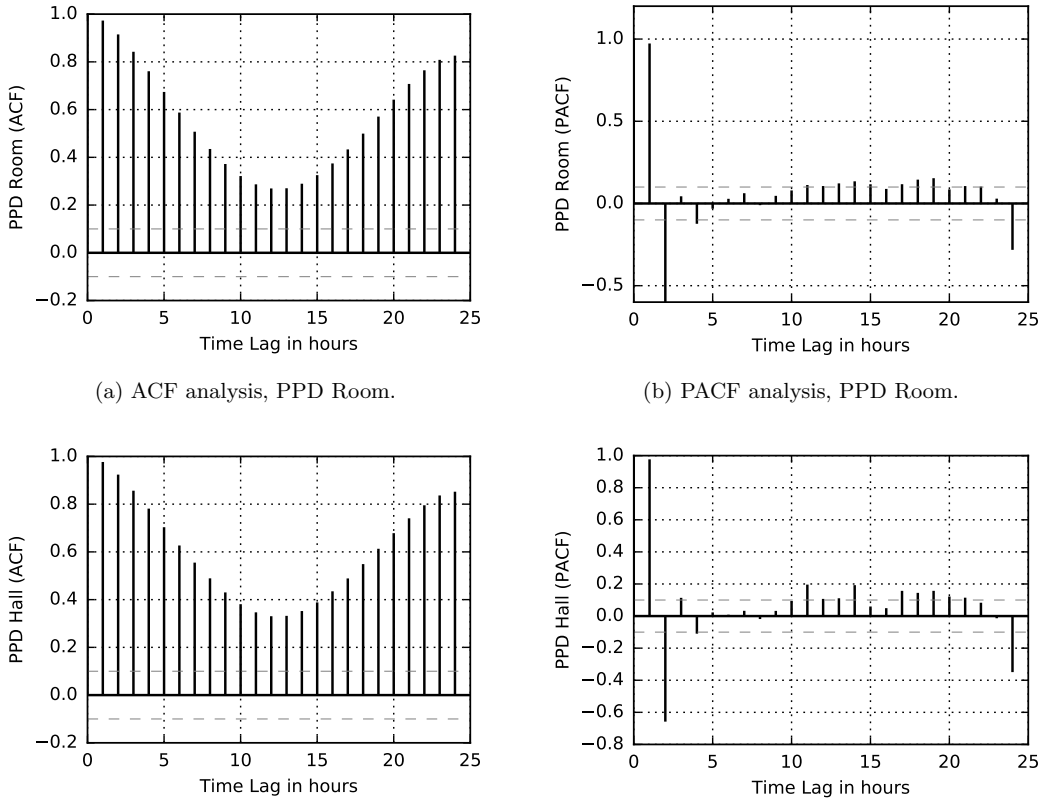

(a) ACF analysis, PPD Room.

(b) PACF analysis, PPD Room.

(c) ACF analysis, PPD Hall.

(d) PACF analysis, PPD Hall.

Figure 4.15: Auto-correlation analysis for Predicted Percentage of Dissatisfied (PPD) for *Room* and *Hall*.

values decay very slowly and autocorrelations are rather significant after long lags. This behaviour is characteristic of non-stationary time series with daily periodic events [123].

Besides the fact that inside Drybulb Temperature and PPD present very similar ACF results, the partial autocorrelation plots of Inside Drybulb Temperature show a steeper decrease than PPD for the same lags, suggesting a lag limit of $t-2$. Thus, the pool of variables selected for modelling the inside Drybulb Temperature are the same as those for the heating power demand, summarized on Table 4.8.

These analyses conclude the Exploratory Data Analysis and the pre-selection of input variables candidates for delivering the surrogate models for each of the considered outputs. Although some of these variables belong to groups that refer to controls and outputs, once they belong to the past, they can be used as information for predicting future trends; i.e. previous outputs and control variables can be used as inputs.

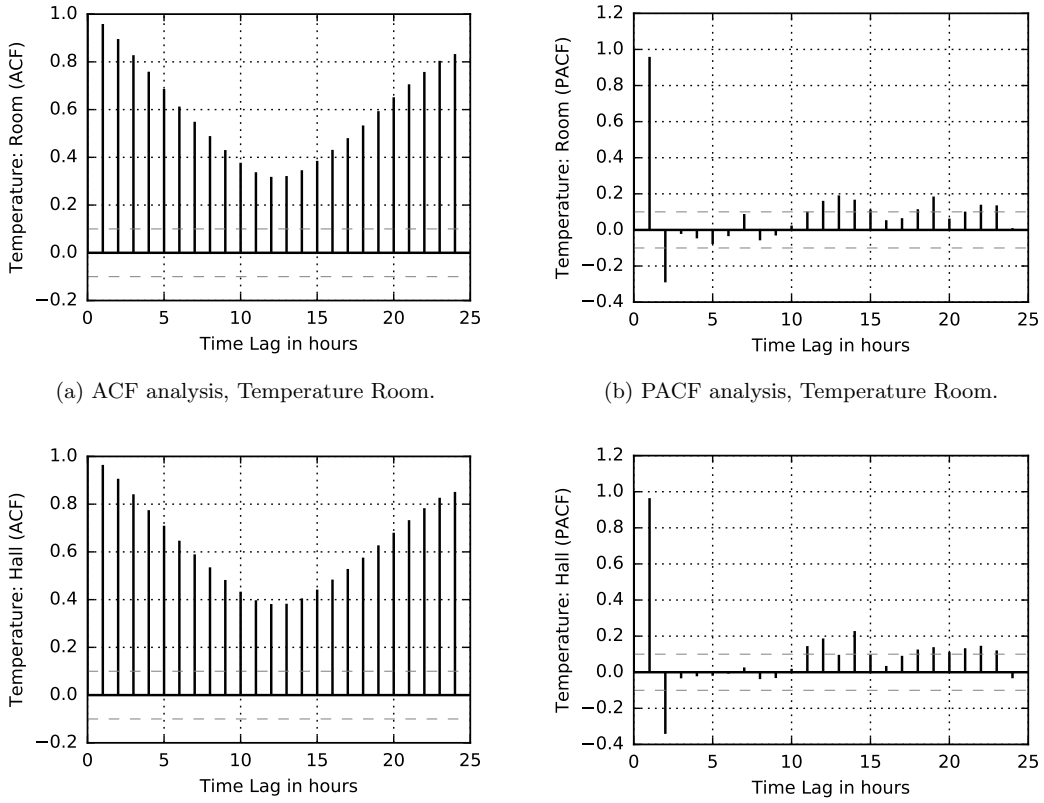

(a) ACF analysis, Temperature Room.

(b) PACF analysis, Temperature Room.

(c) ACF analysis, Temperature Hall.

(d) PACF analysis, Temperature Hall.

Figure 4.16: Auto-correlation analysis for Air Drybulb Temperature for *Room* and *Hall*.

4.3.5 Feature Selection

As referred previously, there are two main approaches to feature selection algorithms: filter methods, and wrapper methods. The input variables under investigation are the control and disturbance variables and their lagged versions, and the lagged versions of the output variables. For each output there is a different number of variables to assess, considering the results of the time dependency study, carried out previously.

The first feature selection employed in this investigation is the F-Test, which delivers the linear influence of each feature to the output. The non-linear influence of the inputs on the outputs is mapped by the mutual information score. Each input variable is ranked according to its importance to the output under investigation. The five least significant variables identified by each of the ranking methods are intersected and the resulting inputs are discarded to reduce the complexity of the initial model involved in the following and more computational intensive feature selection method – Recursive

Feature Elimination.

4.3.6 Filter methods - F-test and Mutual Information

The linear dependency of heating power demand with the proposed 33 variables from Table 4.8 can be depicted from Figure 4.17 (a), while the non-linear importance ranking through Mutual Information score is depicted in Figure 4.17 (b).

Codes Z1 and Z2 in the variable names represent zones *Room* and *Hall*, respectively; and the suffix $t0k$, where $k = 1, 2$ represents the lag $t - k$.

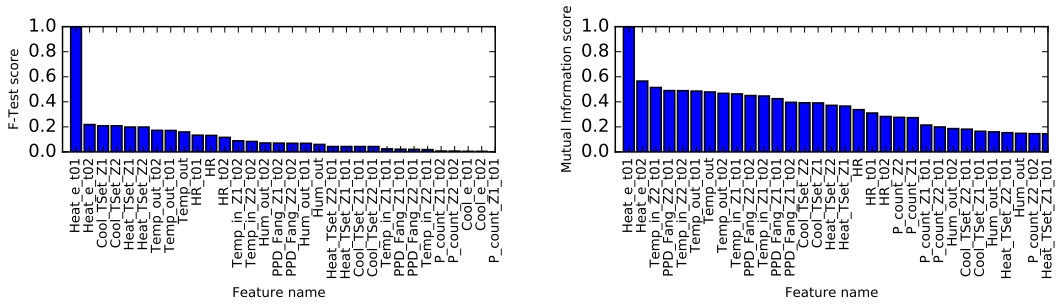

(a) F-test - Heating Power Demand.

(b) MI - Heating Power Demand.

Figure 4.17: Top 30 features for modelling Heating Power Demand according to scoring by (a) F-test and (b) Mutual Information.

As it can be depicted from the ranking of inputs importance from both methods, the two most significant variables selected are the first and second lagged versions ($t - 1$, $t - 2$) of the output variable under study (*Heat_e_t01*, *Heat_e_t02*), corroborating autocorrelation analysis results. On the other hand, the non-linear dependency mirrored by the MI method shows that the following variables in both rankings are not the concordant. F-test ranks as third and fourth *Cool_TSet_Z1* and *Cool_TSet_Z2* that represent the cooling temperature set-point for the *Room* and *Hall*, respectively. The third classification according to the MI ranks is the lagged output of inside temperature in Hall (*Temp_in_Z2_t01*), followed by PPD for the Hall. The reflection of the multicollinearity between heating and cooling temperature set-points depicted in the inputs cross-correlation analysis of previous section 3.2.3 is mirrored here by the F-test ranking, where, unexpectedly, the temperature set-point for cooling is more important to the heating power demand prediction than the temperature set-point for heating. This observation reinforces the need for combining various methods for assessing the importance of features.

Accordingly, from the initial group of 39 variables (Table 4.8), only two variables resulted from the intersection of both methods, being discarded for subsequent analysis. These variables are the cooling temperature set-points of *Room* and *Hall* for the time

lag of $t-2$.

Figure 4.18 presents the top 30 features importance ranking related to the predicting cooling power demand.

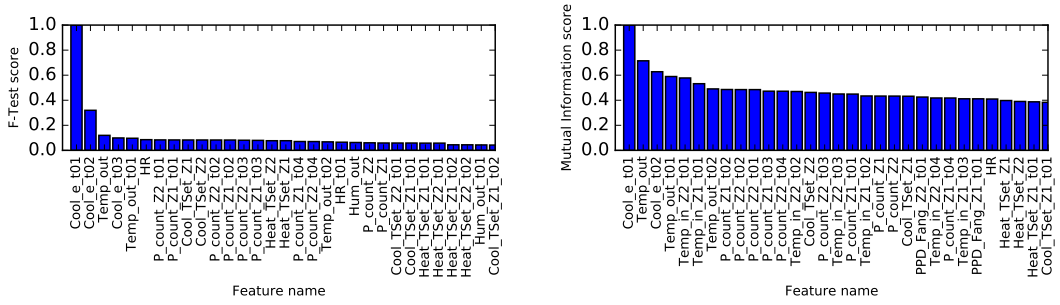

(a) F-test - Cooling Power Demand.

(b) MI - Cooling Power Demand.

Figure 4.18: Top 30 features for modelling Cooling Power Demand according to scoring by (a) F-test and (b) Mutual Information.

Similarly to heating power demand analysis, the most important variable for the modelling of the cooling power demand is its first lagged version from the previous time-step (*Cool_e_t01*), corroborating the information gathered on the auto-correlation analysis. Later, it will be seen that this behaviour is generalized to all the output variables present in this study. However, the second position in the top features differ between the F-test and Mutual Information. As it can be depicted by comparing Figures 4.18 (a) and (b) the second most important feature is the Outside Drybulb Air Temperature (*Temp_out*). Moreover, it seems that the temperature inside the building plays an important role in mapping the energy due to cooling. This phenomenon is only non-linearly supported since the F-test has not mirrored such characteristic. From the preliminary feature selection of 69 variables from Table 4.9, only 64 were selected, meaning that the intersection of the drop-out results from F-test and mutual information ranking have had a perfect match in choosing the least relevant features to include in the training.

The linear and non-linear dependencies of PPD for both zones are ranked and can be depicted from Figure 4.19. The auto-regressive dependence is again mirrored by F-Test results. Moreover, the first lagged version of the PPD of one zone is the second most important variable for predicting the PPD of the other zone, showing a strong correlation between thermal characteristics between zones. Another interesting fact is the lack of representation of variables having no time-lags in the top 30 features, showing the slow response of the building inner environment to all disturbances and controls due to its inertia.

As it can be seen by analysing PPD's F-test rankings, the Horizontal Radiation Rate (*HR*) is the first variable appearing in the ranking of PPD Room, showing that the effects of solar gains on people's comfort are reflected *instantaneously* in this zone.

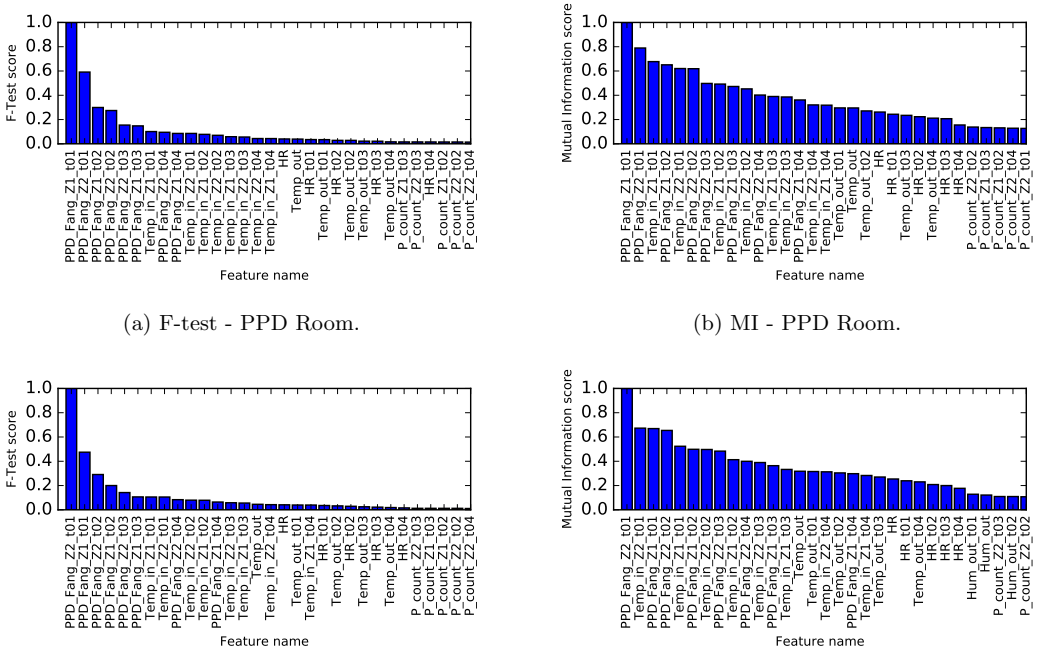

(a) F-test - PPD Room.

(b) MI - PPD Room.

(c) F-test - PPD Hall.

(d) MI - PPD Hall.

Figure 4.19: Top 30 features for modelling Predicted Percentage of Dissatisfied for the *Room* (a, b), and the *Hall*(c,d), according to scoring by F-test and Mutual Information, respectively.

Please recall building design presented in Fig. 4.2. The *Room* is the only division of the building having windows facing south. Hence, this design characteristic might be an explanation to why the positions of Horizontal Radiation Rate (*HR*) and Drybulb Outside Air Temperature (*Temp_out*) appear swapped in the *Hall* since this zone has not a significant solar exposure as the *Room*. However, this ranking behaviour is not observed in the MI score ranking, where outside temperature appears before the radiation rate. Nevertheless, both variables appear to be the most relevant climate disturbances to the prediction of PPD.

The feature selection for both outputs have dismissed the lagged heating power demand for time $t-4$. Only the filters results of PPD for the *Room* show the rejection of the lag $t-3$ of the heating power demand. Thus, the pool of inputs for conducting RFE changed from 69 to 67, and to 68, for PPD for the *Room* and for the *Hall*, respectively.

Besides the fact that the number of initial variables on the analysis of Inside Drybulb Air Temperature is considerably lower than with the case of PPD, it shows similar results, in the sense that the higher ranked variables are related to inside environmental conditions (temperature, and PPD). Moreover, the number of variables dismissed are

the same: 2 for the *Room* temperature; and 1 for *Hall* temperature. Similarly, the variables to drop-out are the heating and cooling power demand of the time-lag $t-2$ for the modelling of inside temperature in the *Room*, and the cooling power demand of the time-lag $t-2$ for inside temperature in the *Hall*.

The major difference encountered between the analysis of PPD and inside temperature is that in the latter case, the first variables are the same in both studies (F-test and MI) for each zone, showing both the autocorrelation significance as well as the slow response of the inside temperature to external or internal disturbances.

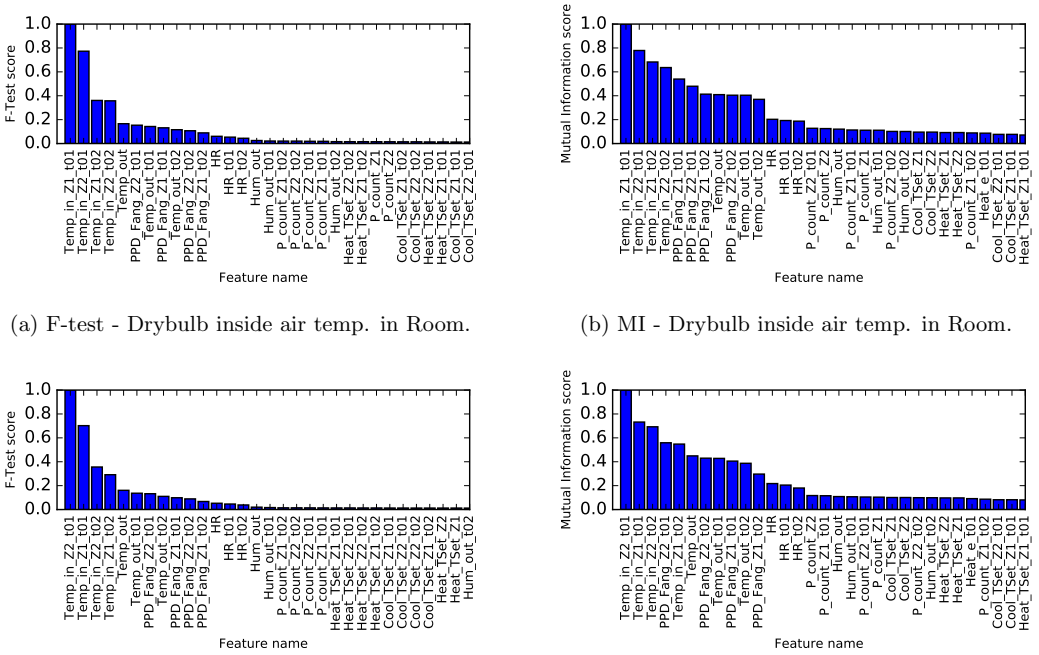

(a) F-test - Drybulb inside air temp. in Room.

(b) MI - Drybulb inside air temp. in Room.

(c) F-test - Drybulb inside air temp. in Hall.

(d) MI - Drybulb inside air temp. in Hall.

Figure 4.20: Top 30 features for modelling Predicted Percentage of Dissatisfied for the *Room* (a, b), and the *Hall*(c,d), according to scoring by F-test and Mutual Information, respectively.

Having finished the investigation of the first method of feature selection through filters importance of inputs, it may be concluded that it is advisable that combined methods are employed in such type of methodologies to avoid biased decisions. Moreover, besides the fact that it is relevant to investigate the importance of each variable to the output under investigation, this type of analyses convey no information regarding the effectiveness of models which are to be created.

The variable importance investigation conducted, yielded a smaller group of variables to be subjected to the recursive feature elimination. The latter will be presented in the

following section.

4.3.7 Wrapper method - RFE

Wrapper methods are used to select the subset of features based on the variables influence on the predictive performance of a selected model. In this thesis, the criterion used for this analysis is the coefficient of determination, R^2, which is computed by equation 4.3.2 as the ratio of the explained variance to the total variance:

$$R^2 = 1 - \frac{\sum_i (\hat{y}_i - \bar{y})^2}{\sum_i (y_i - \bar{y})^2} \tag{4.3.2}$$

The modelling algorithm selected for conducting this analysis is the Random Forests algorithm. Its mathematical convenience is evident since at the same time the model is trained, an embedded feature importance metric is provided, reducing the computational effort of this assessment [91, 79].

The wrapper method used is the recursive features elimination algorithm (RFE), combining greedy search with backward selection method. This configuration often leads to better prediction performances of the resulting models than other methods [140, 138, 141, 79].

First, the model is trained using all available input variables, computing a 10-fold cross validation error score for delivering a robust assessment of the validation error. The process can be described as it follows:

1. Sort variables according to its importance by computing the reduction of variance on the predictions for each input. The latter is carried out for each of the ten created models [91];

2. Eliminate the two least important inputs of the whole group of models;

3. Retrain the random forest;

4. Compare cross validation R^2 of the combination of the last model with the previously trained one.

5. Repeat steps 1 to 4 till the remainder number of inputs is indivisible.

The results of the process of Recursive Feature Elimination for the six models needed are presented in Figure 4.21, and summarized on Table 4.10.

As it can be depicted, all models allow for the reduction of the number of features, not only without compromising its predictive performance, but simultaneously improving their cross-validation score. Moreover, besides the case of modelling the cooling power demand, most of the models show a generalized lack of sensitivity towards the number of features selected, exhibiting a cross-validation coefficient of determination (R^2) 90%, when using at least the five most important inputs.

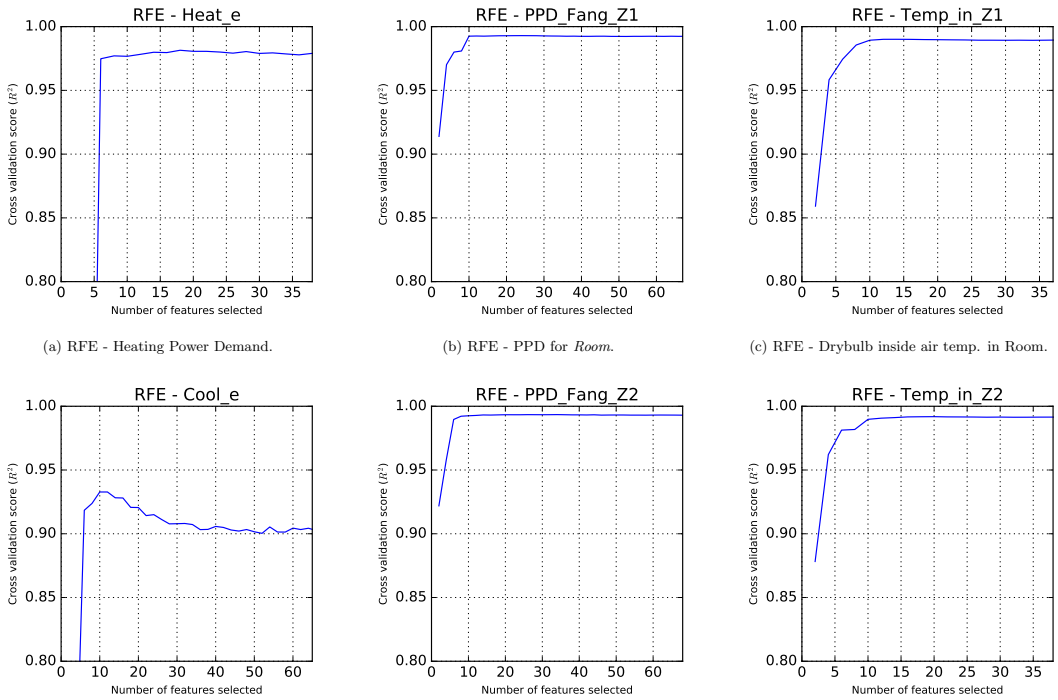

(a) RFE - Heating Power Demand.

(b) RFE - PPD for *Room*.

(c) RFE - Drybulb inside air temp. in Room.

(d) RFE - Cooling Power Demand.

(e) RFE - PPD for *Hall*.

(f) RFE - Drybulb inside air temp. in Hall.

Figure 4.21: Recursive Feature Elimination for all the output varibles subjected to modelling.

The optimal number of features gathered on the RFE process for Heating Demand Power was 16. As summarized on Table 4.10, the Halls cooling temperature set-point seems to be overrated comparing to the heating temperature set-point, which could be expected to represent a more substantial role in the determination of the energy demand, mainly concerning to heating. This behaviour might be attributed to the multicollinearity previously identified between both of these variables. A similar response, which might share the same explanation, is presented on the results of Inside Air Drybulb Temperature in the Hall. Unexpectedly, the t-2 lag of the Zone People Occupants Count for the Room is more relevant than the same variable for the Hall. In order to solve such issues, the re-sampling strategy presented previously was proposed.

Modelling the energy demand for cooling is not only the one having the lowest coefficient of determination found, but also the one showing the highest sensitivity towards a larger number of input variables. The maximum advisable number of input features is 11, being Zone People Count in the Hall and Inside Air Temperature in the Hall the only variables requiring a time-lag over t-2. Recall that during the study of the auto-correlation it was concluded that the Cooling Power Demand was exhibiting a time

dependence of t-4. Moreover, by inspecting Table 4.10 it might be said that the power demand lagged versions are the least important variables of the whole pool of input candidates.

The modelling of PPD for both zones shows a saturation of the accuracy score around ten variables, being the lowest registered R^2 above 90% with only two features. These two features are the PPD values of the Room and Hall of the previous time-step *Room* and *Hall* of the previous time-step (*PPD_Fang_Z1_t01* and *PPD_Fang_Z2_t01*), emphasizing the usefulness of the lagged variables on the modelling process. However, the best number of features is found only with 23 and 32 features for modelling the PPD for the Room, and Hall, respectively.

Table 4.10: Summary of the final features selected by the Recursive Feature Elimination method. The integers in the brackets represent the lags required for the input variable on the left. **Lags** $= K = \{k_i, ..., k_f\}$, for $(t - k_i), k_i \in [0, k_f]$.

Input variable	**Predictive Models**					
	Heat_e	**Cool_e**	**PPD_Z1**	**PPD_Z2**	**Temp_in_Z1**	**Temp_in_Z2**
Heating Temp. SP (Room)	{0}	{0}	{0}	{0}	{0}	{0}
Heating Temp. SP (Hall)	{0}	{0}	{0}	{0}	{0}	{0}
Cooling Temp. SP (Room)	{0}	{0}	{0}	{0}	{0}	{0}
Cooling Temp. SP (Hall)	{0, 1}	{0}	{0}	{0}	{0}	{0}
Outdoor Air Drybulb Temperature	{0, 1, 2}	{0}	{0}	{0, 2}	{0, 2}	{0, 1, 2}
Horizontal Radiation Rate	{0, 1}	–	–	{4}	–	–
Outdoor Air Relative Humidity	–	–	{4}	{4}	–	{2}
Zone People Occupant Count (Room)	{0}	{0}	{0}	{0, 1, 4}	{0}	{0, 1}
Zone People Occupant Count (Hall)	{0}	{0, 4}	{0, 1, 2, 3}	{0, 1, 4}	{0}	{0}
Heating Power Demand	{1}	–	–	{1, 3}	–	{1}
Cooling Power Demand	–	{1}	–	–	–	–
Predicted Percentage of Dissatisfied (Room)	–	–	{1, 2, 3, 4}	{1, 2, 3, 4}	{1}	–
Predicted Percentage of Dissatisfied (Hall)	–	–	{1}	{1, 2, 3, 4}	–	{1, 2}
Inside Air Drybulb Temperature (Room)	{1, 2}	{1, 2}	{1, 2, 3, 4}	{1, 2, 3, 4}	{1, 2}	{1, 2}
Inside Air Drybulb Temperature (Hall)	{1, 2}	{3}	{1, 2, 3, 4}	{1, 2, 3, 4}	{1, 2}	{1, 2}

The RFE results for the modelling of the Inside Air Drybulb Temperature for the Hall and the Room, present similar graphical results. However, the converging solution of both analysis show some differences worth mentioning. For instance, the number of inputs suggested for modelling differs from 13 when modelling the inside temperature in the Room, while 18 are required to model the Hall. Besides the increasing on the time-lags required, it can also be depicted that the t-2 Outdoor Air Relative Humidity and the t-1 Heating Power Demand are presented as novel inputs. This consequence might represent a higher complexity on the modelling of the inside temperature in the Room either by its architecture, or disturbances to which it is subjected.

It is a fact that during the analysis of the time-dependency, features were added, increasing the complexity of the models. Nevertheless, the feature selection methodologies, especially the Recursive Feature Elimination, have helped fine tuning the variables which are relevant for the predictive modelling process, decreasing the models' complexity and improving its accuracy. Overall, a reduction of 271 features was accomplished,

summing up a total of 113 inputs for all the models rather than the 384 input candidates previously selected. It can, therefore, be concluded that it is of the utmost importance to conduct such an approach in the development off data-driven models to reduce to complexity of models and improve their predictive capability [79].

4.3.8 Model Selection and Validation

The variables selected in the previous section were used for feeding the algorithms for the modelling task. The architecture of each model was obtained through the optimization of the hyper-parameters selected for fine tuning each algorithm. The method employed uses the Generalized Iterative Scaling (GIS), solved by the BFGS optimization algorithm, and implemented on the *skopt* API [3]. Table 4.11 summarizes the resulting architecture and error estimation for each of the models and type of the algorithms we present further.

Table 4.11: Summary of the hyper parameter selection for all the modelling algorithms under investigation.

Modelled Output variable	Modelling algorithm					
	NN		SVR		RF	
	n. neurons	learning rate	ϵ	γ	n. trees	max. depth
Heating Power Demand	39	0.008299	9788	0.09904	29	89
Cooling Power Demand	15	0.01676	15	0.01676	29	89
PPD Room	96	0.009664	1893	0.08764	212	67
PPD Hall	61	0.008108	444	0.02295	90	83
Temperature in. Room	78	0.006099	1470	0.01885	649	60
Temperature in. Hall	64	0.008214	1194	0.03246	443	63

Figure 4.22 presents the error analyses of each of the algorithms selected for modelling the Heating Power Demand:

NN: Neural Networks;

SVR: Support Vector Regression;

RF: Random Forests;

All algorithms selected have accomplished an acceptable performance in what concerns learning the Reference Database (i.e. EnergyPlus resulting data from the simulations of the reference case-studies analysed). Nevertheless, the Random Forest and SVR have produced better results than the Neural Networks.

The coefficient of determination is high for all models, with values being close to 1. RF has produced the highest score observed, showing a narrow dispersion of residuals

[3] *skopt* API is open-source and available at `https://scikit-optimize.github.io/`

around the ideal values of $y = \hat{y}$ (line in white, Fig. 4.22). Simultaneously, the mean absolute error of the Random Forests cross-validation is 4.915 %, representing the lowest of all models.

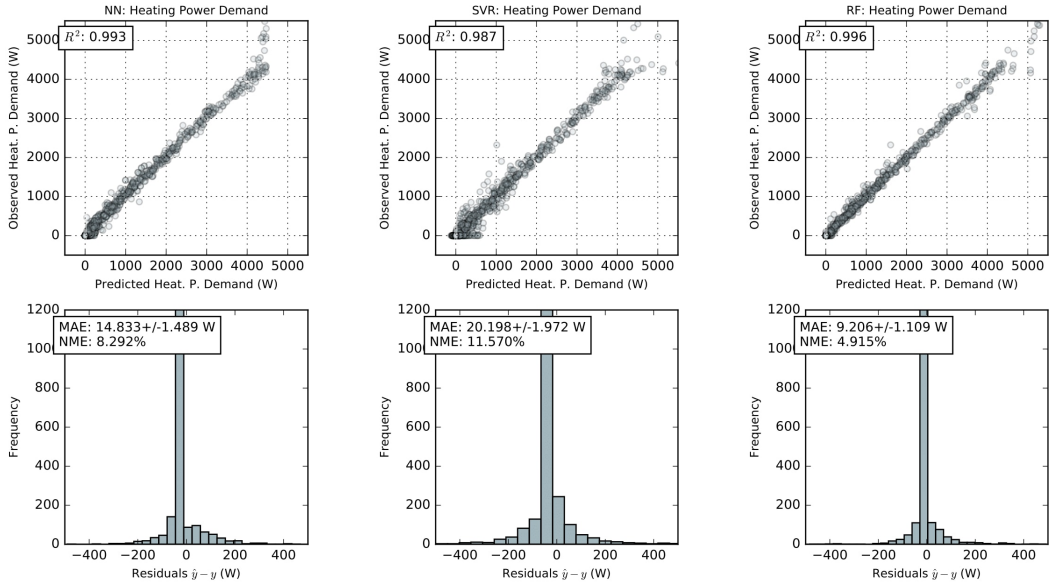

(a) Neural Network (b) Support Vector Regression (c) Random Forest

Figure 4.22: Error analysis of Heating Power Demand predictive models .

All models show a zero-centred and normal distribution of residuals. However, it seems that both SVR and NN are slightly more prone to produce negative-valued errors, whereas RF appears to be capable of avoiding such residuals, summing a higher frequency of zero valued residuals. A possible justification for this skewness might reside in the fact that the distribution of heating power demand data has, as expected, a high concentration of zeros. Data-driven models have a hard time fitting to imbalanced data because those samples that have higher representation force models to favour their error minimization in detriment of the rest of the samples. Continuous models such as NN and SVR are probably more prone to show this deviation of the mean value due to imbalanced data than ensemble models such as Random Forests. The training process of Random Forests involves a random partitioning of the features domain and assignment of different sets of data to each of the trees, mapping more evenly the whole domain of data [91].

The neural network model shows a closer coefficient of determination with the one obtained with random forests. However, R^2 does not constitute a particular measure of the accuracy of predictions (recall Eq. 4.3.2), but rather a measure of unexplained variance. Hence, Random Forests algorithm has been chosen for modelling the heating

power demand surrogate models.

The results of modelling electricity power demand for cooling are presented in Figure 4.23. As it can be depicted, when comparing these results with the analysis of the modelling of electricity power demand for heating, the overall mean absolute error for all models is higher, implying worse performances than those of the previous example.

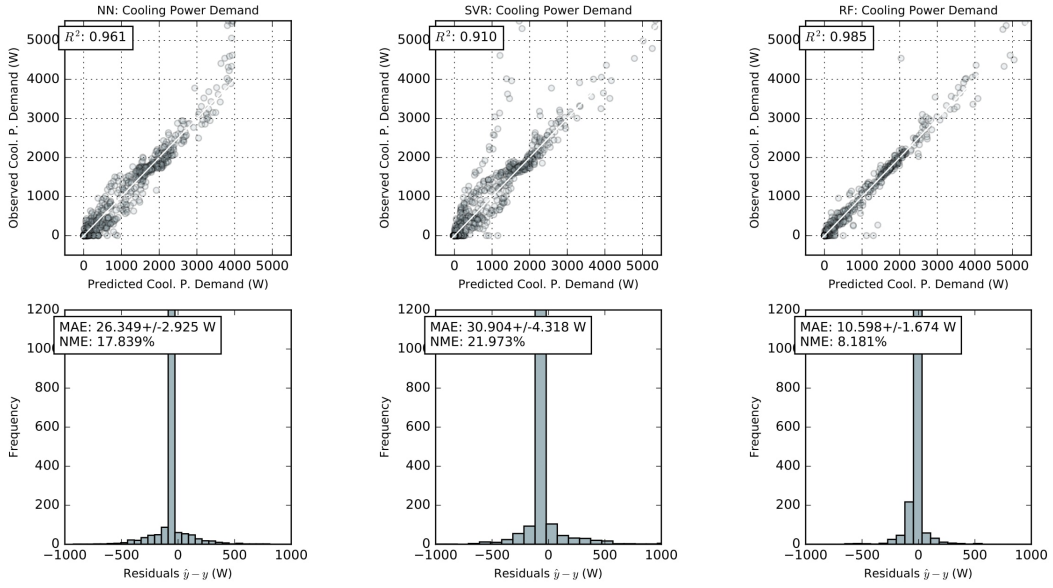

(a) Neural Network (b) Support Vector Regression (c) Random Forest

Figure 4.23: Error analysis of Cooling Power Demand predictive models .

The coefficients of determination, R^2, of all algorithms are lower than those observed on the modelling of heating power demand, meaning that models present a higher variance of residuals. Similarly, the best model regarding the coefficient of determination is the RF.

The SVR model shows the poorest performance, reflecting heteroscedasticity towards higher magnitudes of cooling power demand. The reason for such behaviour might reside in the fact that the distribution of heating power demand (Fig. 4.11) is left-skewed towards zero, making it more difficult for this model to map the higher valued cooling power.

Nevertheless, the error distributions of all models show a rather symmetric dispersion of residuals. The modelling of the cooling power demand proved to be the most cumbersome of the all six output variables presented, having the highest displayed error estimation. The algorithm performing better regarding the error estimate is the Random Forests algorithm, being the choice for cooling demand forecast during the optimization of the supervisory predictive control. The error estimation is less than 10 %, with a

mean absolute error of 10.598 +/- 1.674 W. The normalizing value used for computing the percent error (Normalized Mean Error) is 136.9W which is the average of the Cooling Power demand observed in the database and presented on Table 4.7.

The modelling processes of the Predicted Percentage of Dissatisfied and the zone inside temperature show the best results of all the outputs requiring predictive models. Figure 4.24 presents the error estimation of Rooms Predicted Percentage of Dissatisfied. The overall coefficient of determination is very high, ranging 1.

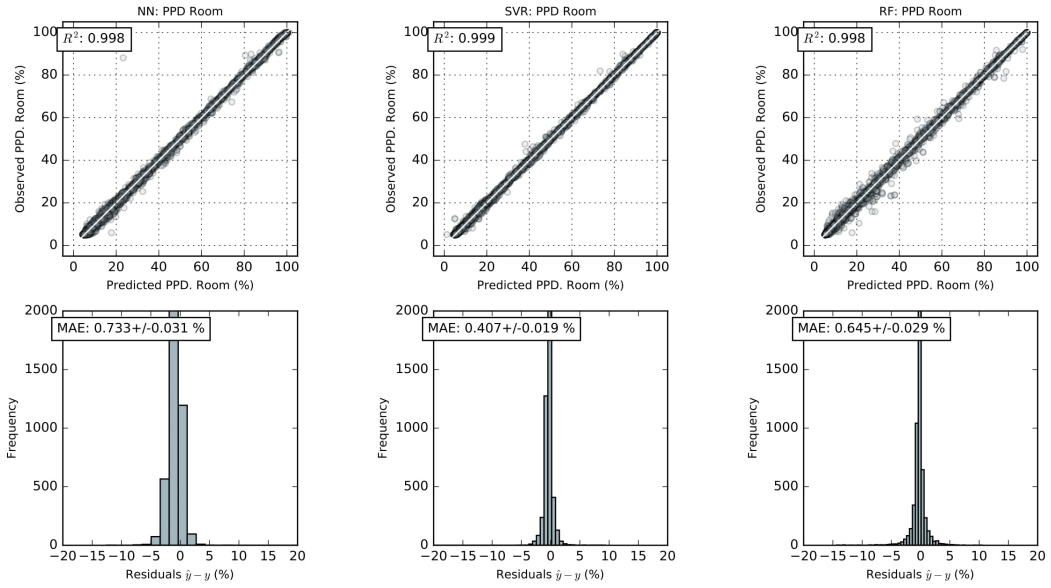

(a) Neural Network (b) Support Vector Regression (c) Random Forest

Figure 4.24: Error analysis for model selection for surrogate model of Predicted Precentage of Dissatisfied in the Room.

The most suitable model is the Support Vector Regression which exhibits a Mean Absolute Error of 0.407 +/- 0.019 %. Since this variable is presented as a percentage, there is no need to compute a relative error. The repeating pattern of left-skewed residuals distributions is further exhibited in this case, with random forests showing the most centralized distribution. Any of the presented models could have been picked for conducting the predictions during the simulation routines since all show a good performance. However, for coherence's sake, SVR is selected because it enables to reach the lowest absolute average and standard deviation of the error estimation on the test data set. The results regarding the modelling of the Predicted Percentage of Dissatisfied for the Hall show a close agreement with those from the Room. Thus, their performance summary is presented on table 4.13.

The chosen model is the Support Vector Regression in agreement with the previous

example. The nature of Support Vector Machines, proposed by Vapnik, proved to be helpful in preventing model overfitting since it employs an estimator of the complexity of the model versus its accuracy – the so-called structural risk minimization estimator [158].

The modelling of the Inside Air Drybulb Temperature for both the Room and the Hall yielded results similar to the modelling of PPD. Here, the results are presented concerning the modelling of the inside temperature in the Room in Figure 4.25, leaving Hall's error investigation as the statistical summary of Table 4.13.

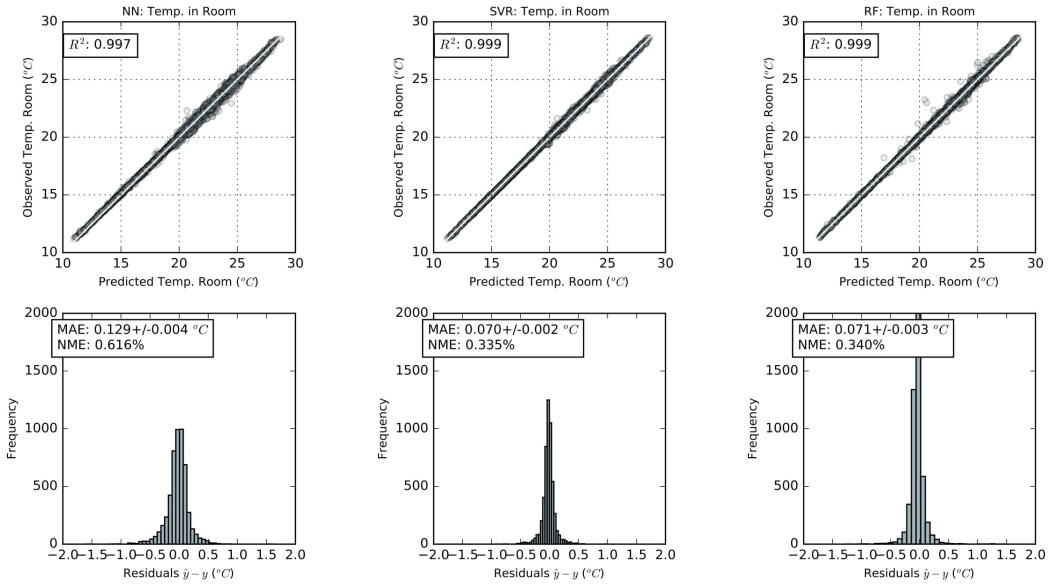

(a) Neural Network (b) Support Vector Regression (c) Random Forest

Figure 4.25: Error analysis for model selection for surrogate model of Inside Air Drybulb Temperature in the Room.

As it can be depicted the resulting error distributions share the same behaviour. The lowest R^2 R2 is 0.997, observed in the NN results, representing a good fit throughout the different algorithms. The model that best fits the results is again the SVR model, by a slight margin of 0.005% in what concerns the RF which represents a temperature difference of 0.001^oC . Thus, it can be stated that both models have about the same performance regarding error estimation. However, further investigation was conducted concerning the computational cost of prediction and SVR stands out to be the fastest of both, as presented in Table 4.12.

Predictions of 100 consecutive hours have been conducted in a closed loop of 24 hours configuration to infer the computational cost of the prediction task for each modelling algorithm presented. The fastest model both on the training and prediction tasks is

Table 4.12: Mean time to learn and time to simulate 100 hours using NN, SVR, and RF, considering a 24 hours window forecast for each simulated hour.

Algorithm	Time to learn (s)	Time to Predict (s) (24h forecast window * 100 hours)
NN	5.85	3.99
SVR	359.5	6.5
RF	126.4	21.2

the NN. However, the given error equals the double in comparison to the competitors. The slowest model in both tests is the RF, accumulating more than 21.2 seconds which represents more 200% the time required by SVR. Hence, SVR is our choice as modelling algorithm for Room's inside temperature forecast. The simulations were carried on an i7-5600U CPU@ 2.60Ghz.

Table 4.13 summarizes the modelling algorithms investigated in this chapter, highlighting the reasons supporting its selection. The criteria for choosing the most suitable models was mainly fit adequacy parameters, namely the Normalized Mean Error (NME) and the Coefficient of Determination (R^2).

The modelling algorithm performing better was the Support Vector Regression, stating its utility for conducting building energy management forecast tasks, and corroborating the results found in the literature [159, 79]. However, the Random Forest is the algorithm standing out when the problem is more complex to solve, and the Neural Networks are the algorithm to consider in rapid demanding of trained models.

Table 4.13: Summary of the model selection error analysis for all the modelling algorithms under investigation.

Modelled Output variable	Modelling algorithm					
	NN		SVR		RF	
	NME	R^2	NME	R^2	NME	R^2
Heating Power Demand	8.291%	0.993	11.570%	0.987	**4.915%**	**0.996**
Cooling Power Demand	17.839%	0.961	21.973%	0.91	**8.181%**	**0.985**
PPD Room	0.733%	0.998	**0.407%**	**0.999**	0.645%	0.998
PPD Hall	0.750%	0.998	**0.508%**	**0.999**	0.588%	**0.999**
Temperature in. Room	0.616%	0.997	**0.335%**	**0.999**	0.340%	**0.999**
Temperature in. Hall	0.451%	**0.999**	**0.316%**	**0.999**	0.337%	**0.999**

From the model selection concerning surrogate models of the reference case-study data, it can be concluded that the modelling of environmental variables such as PPD and inside temperature is less complex than modelling heating and cooling power demands, since the error analysis of the prior variables produces distributions of residuals of higher quality. The primary reason for these results might reside in the distributions of output variables which show close-to-Gaussian distributions on the PPD and inside temperature, whereas exhibiting exponential distributions on the power demand vari-

ables. The problem of modelling highly skewed outputs in regression analysis has been identified as a problem yet to be solved by the scientific community, as pointed out in the recent paper from Bartosz Krawczyk [160]. This thesis highlights the necessity for further investigation on the subject, due to its utility for the field of building energy modelling, since building occupation patterns yield sparse and imbalanced energy data. For example, there are more periods of non-occupation in a regular office than periods of occupation, leading to energy consumption to be more frequently low than high, skewing the distribution of data samples as explained in the exploratory analysis of Fig. 4.11. Nevertheless, Random Forests algorithms proved to be more robust than Neural Networks and Support Vector Regression on these more cumbersome modelling problems, showing the superiority of ensemble modelling, and allowing for the implementation of these models in a supervisory predictive control as the one here proposed.

4.4 Supervisory Predictive Control - Implementation results

4.4.1 Optimization process implementation

The optimization process is part of the supervisory predictive control system and can be depicted from Figure 4.26. The approach is based on *eppyco* – the Python™ module developed for this thesis which includes the surrogate modelling process, the on-line optimization process, and the communication server to connect all the entities in a co-simulation implementation where EnergyPlus™ plays the part of a real building. This section focuses on the optimization process required for conducting the predictive control strategy of the building reference case-study.

The goal of the optimization process is to find the most suitable set-points for time-step $t+1$ given:

1. the building conditions of the time-step t, namely the measured energy demand and comfort, and the occupancy and weather data;
2. the building past thermal behaviour of time-steps from $t-k$ to $t-1$, namely the lagged variables required by each of the surrogate models presented and summarized on Table 4.10, where k is the maximum required lag.
3. the forecasted disturbances for the time-steps from $t+1$ to $t+N$, namely the occupation and weather variables, where N is the size of the forecast window.

As presented on the results modelling strategy section 4.3, k equals 4 hours, and the size of forecast window, N, is six for the given case-study.

The initially proposed set-points along with the referred three data streams are sent via the communication server to the predictive module to infer the energy demand and the comfort for the given forecast window. The objective function computes the

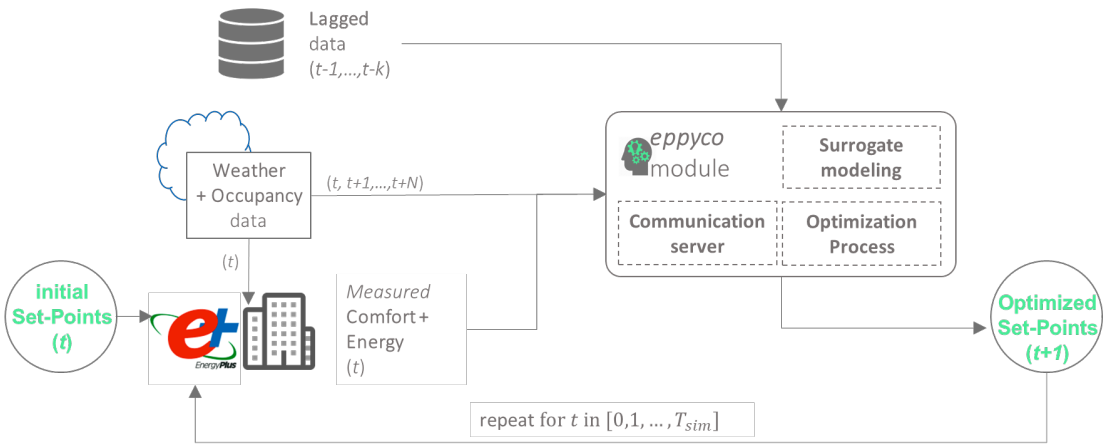

Figure 4.26: Flowchart of the optimization process in the supervisory predictive control strategy. This approach is based on *eppyco* which gathers: a surrogate model, an optimization algorithm, an objective function, and a communication server for managing all data flows during co-simulation between databases, *eppyco*, and EnergyPlus™.

fitness of such proposal, and if the results are satisfactory, these set-points are considered optimal and are sent to EnergyPlus™ and the simulation continues. Otherwise, if the computed fitness of such set-points is not suitable for the anticipated conditions of the forecast window, then an optimization process is required for searching for new set-points suitable for such conditions. The optimized set-points are sent to EnergyPlus™ via the communication server for it to continue the simulation of the time-step $t + 1$. This process is repeated for the whole simulation time, T_{sim}, defined on the EnergyPlus™ IDF model.

For the purpose of this investigation, 8640 optimization problems were tested, corresponding to a total simulation period of 360 days. Although EnergyPlus™ was set to perform simulations using six time-steps per hour, the optimization problems were defined as hourly, similar to the time-step used during the modelling of the surrogate models presented previously. These simulations serve the purpose of fine-tuning the optimization parameters while performing a re-sampling of the database considering *realistic* scenarios for later conducting surrogate models updates.

4.4.2 Data streams

The optimization process depicted previously on figure 4.26 refers the requirements for three types of data streams. This section focuses on summarizing the origins of the data used during the on-line optimization process.

Lagged data

Lagged data is the short-term historical data required by the data-driven models to use as input variables. This data is gathered during the simulation process and saved in the computer's memory so it can be promptly used by the predictive models for subsequently building energy states. Table 4.10 has summarized the variables for each surrogate model and as it can be seen, there are variables obtained by the simulator EnergyPlus™, such as comfort and energy demand for variables, as well as other variables that are disturbances to the thermodynamic system, namely climate variables, and occupation rates. This section focuses on the variables originated from the response of the building to disturbances and control.

At the beginning of any simulation using EnergyPlus™, the software sets a period of *Warming up* convergence, so when the simulation is properly initialized, it mirrors the transient state of a building thermodynamic system properly, offering reliable results and controlled inaccuracies in the loads calculation [64]. However, the data produced on those warming up periods is not meaningful to the simulation results, so it is discarded and not presented by EnergyPlus™. Moreover, no data already gathered in a database can be used to start a simulation process of the supervisory predictive control, because that data are not expected to reflect the transient state of the building, giving rise to simulation inaccuracies. Also, the lagged variables used when the *eppyco* module connects to the EnergyPlus™ are provided by the historical database, so they do not reflect the short-term past of the current building state.

To overcome those issues, every time the simulation process of the supervisory predictive control is initialized, another *Warming up* period of 24 hours is set for the co-simulation for the sake of convergence. This convergence period should guarantee that the lagged variables used by the surrogate models do reflect the transient state of the building, as well as providing meaningfulness and reliability to the results obtained from the simulation.

Disturbances Forecast

The disturbances forecast differ from the predictions made by the surrogate models because they are subjected to the building thermodynamic system external phenomena. . The forecast of weather data is from the domain of meteorology and the forecast of occupants and their behaviour also lies outside the scope of this thesis. Thus, a methodology is presented to approximate the forecast uncertainty of the disturbances required for conducting the present case-study, namely the outside drybulb air temperature, the horizontal radiation, the outside humidity, and the occupation rate of each zone.

The disturbances forecast follow an noise induction method using as reference the outside temperature short-term forecast error expectation equal to 1.27^{o}C of mean absolute error (MAE), presented in the work of Zhang et al. [161].

The forecast uncertainty induction is presented by Eq. 4.4.1.

$$\hat{X} = X + \lambda_i \cdot \sigma_X \cdot \text{rand}_n \tag{4.4.1}$$

where X is the matrix of known disturbances for subsequent time-steps, contained in the database, σ_X is the standard deviation vector of the observation for variables in X. λ_i is the weight given to the standard deviation for each time-step, for $i = 1, \ldots, N_a$. rand_n is a Gaussian randomly generated real number from the interval $[0, 1]$, (white noise).

The chosen standard deviation multiplier, λ_i, follows a linear function from 0 to 0.05, for a maximum forecast window of 24h. Figure 4.27 shows the error propagation throughout the forecast window of outside drybulb temperature.

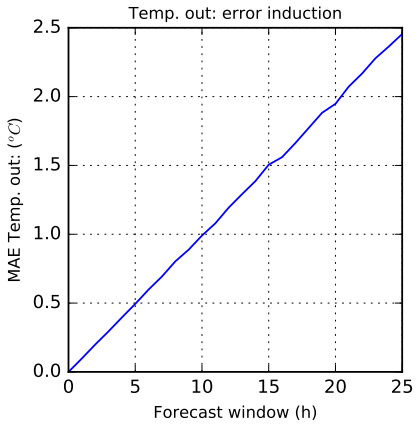

Figure 4.27: Noise induction to the disturbance variables to simulate the forecast uncertainty. The standard deviation multiplier, λ_i, ranges linearly from 0 to 0.5 for a forecast window of 24h.

The same procedure is repeated to whole disturbance variables, namely, the horizontal radiation rate, the outdoor relative humidity, and the occupation rate. Table 4.14 summarizes the mean absolute error for each of the exogenous and endogenous variable.

Table 4.14: Summary of the mean absolute error for each of the exogenous and endogenous variables.

Disturbance variable	Mean Absolute Error	
	forecast window	(t+24h)
Zone People Occupant Count (Hall)	0.690	1.329
Zone People Occupant Count (Room)	0.322	0.629
Outdoor Air Relative Humidity	2.94%	5.92 %
Horizontal Infrared Radiation Rate per Area	5.737 W/m^2	11.487 W/m^2
Outdoor Air Drybulb Temperature	1.23^{o}C	2.455 ^{o}C

The purpose of this method is to induce a realistic error in the supervisory predictive control strategy.

Measured Variables

The variables required to be *measured* during the on-line optimization process are the building thermodynamic response to the disturbances induced in the system. In this case-study, they are provided by the EnergyPlus™ at any given simulation time-step. Since the simulation time-step considered in the EnergyPlus™is six time-steps per hour and the optimization routines are carried only hourly (every 6 partial time-steps), the output variables, namely the electricity demand for heating and cooling, Predicted Percentage of Dissatisfied (PPD), and the inside drybulb temperature, are estimated by performing a weighted average of the mean value provided by EnergyPlus™ for the last five partial time-steps and the value estimated by the surrogate models for the given hour, as presented in the following equation, Eq. 4.4.2.

$$y_M^{(i)} = \frac{1}{6} \cdot y_{surrogate}^{(i)} + \frac{5}{6} \sum_{j}^{5} y_{jEnergyPlus}^{(i)} \tag{4.4.2}$$

for $i = 1, ..., N_{out}$, where N_{out} is the number of outputs.

This method expects a deviation equal to 1/6 of the expected error for each output variable from the surrogate model predictions for the given time-step. The equation 4.4.2 induces an uncertainty propagation of the surrogate model predictions to the measured variable by the proportion of the time-step allocated to the surrogate model prediction with the total duration of the time-step, and considering that the *measurement* error from EnergyPlus™ simulation is null [162]. For example, the expected *measurement* error for an output variable having 5% of predictive error translates into 0.83% or error on a simulation using six time-steps per hour.

4.4.3 Convergence analysis and optimization algorithm selection

Three algorithms were selected for conducting this investigation - the Particle Swarm Optimization, the Differential Evolution, and the Simplex, also known as the Nelder-Mead optimization algorithm. The main reason for focusing on derivative-free methods lies on the non-smoothness of the objective functions, especially by the penalty function employed on the comfort objective. Therefore, the computation of derivatives would be considered impractical. Besides being derivative free, the presented optimization algorithms are global search algorithms, providing the capacity of avoiding convergence to local minima more efficiently than the local search algorithms such as the Simplex method, and the Conjugate Gradient that were tested as well.

The population-based algorithms (PSO and DE) both have the same number of individuals: equal to number of control variables, and both are limited to 200 iterations.

Table 4.15: Hyperparameter section for Particle Swarm Optimization and Differential Evolution

Algorithm Feature	**Population size**	**Specific Hyper-parameters**	**Maximum iterations**	**Converging criteria**	**Initialization function**
PSO	N_u: 24	Cognitive parameter: 2; Social parameter:2; Maximum inertia weight: 0.9; Minimum inertia weight: 0.1;	200	tol_{rel}: 0.5 20 it. no change	LHS
DE	N_u: 24	strategy: best/1/bin; mutation: $n_r \in [0.5, 1[$; recombination: 0.9; cross-over: 1	200	tol_{rel}: 0.5 20 it. no change	LHS

The parameters setting for these algorithms are summarized on Table 4.15, following the heuristics proposed by Parsopoulos and Vrahtis [112] for the PSO algorithm, and by R. Storn and K. Price [117] for the Differential Evolution algorithm.

Besides being derivative free, PSO and DE are metaheuristic, evolutionary, and global search algorithms, providing an enhanced capacity of avoiding convergence to local minima more efficiently than the local search algorithms such as the Simplex method, and the Conjugate Gradient. While the exploratory nature of the evolutionary algorithms presented provide an enhanced capacity of identifying optimization domains of greater interest for the convergence problem, they suffer from that same exploratory capacity in the sense that closer to convergence the algorithms tend to slowdown the convergence process, leading to longer times of convergence than local search optimization algorithms [119]. Therefore, the Nelder-Mead Simplex method, and the Conjugate Gradient are tested as well.

Table 4.16 summarizes the results of optimizations conducted during the initial co-simulation process.

Table 4.16: Optimization algorithms benchmark.

Optimization algorithm	**Relative time to converge** (%)	**Winning percentage** (%)	**Relative difference of cost function to winner** (%)
Particle Swarm Opt.	**80.52**	**68.35**	–
Differential Evolution	11.12	30.38	-0.002955
Simplex Nelder-Mead	5.37	1.266	26.72
Conjugate Gradient	2.99	0	47.54

As it can be observed, the algorithm which performed better among these four examples was the Particle Swarm Optimization. However, if the time for convergence and the

difference between converging solutions are compared with the Differential Evolution results, the PSO winning is not that substantial. The time it takes PSO to converge when comparing to DE is considerable. Moreover, the time spent by the PSO for converging to a solution represents 80.52% of the total time required for optimization, taking 69.39% longer to converge than the Differential Evolution algorithm. On the other hand, the difference between solutions is negative, meaning that the solutions found by DE are in average lower than the solutions encountered by PSO. Such an in-substantial difference between these algorithms suggests that both are either converging to the global minimum of the optimization problems, or at least converging to similar values of local minima.

Although the local search algorithms converge faster than the global optimization ones, they fail to converge to better solutions than their competitors, rendering them useless for this particular application. . The reason for such behaviour might be due to the non-smoothness and a probable non-convex nature of the multi-objective function of the supervisory predictive control.

Considering the results here presented, the optimization algorithm selected for implementing the supervisory predictive control is the Differential Evolution, since the differences between the winner PSO are most suitable for a computationally-intensive investigation as the one here presented. However, in a real case scenario, both algorithms could be implemented in cascade since the average time for converging is relatively low. DE accounts for 13.20 seconds, and 64.89 seconds for the PSO, summing a total time for optimization per time-step of 01:17 minutes on an i7-5600U CPU@ 2.60Ghz with 12GB of RAM, which could accommodate 46 optimization routines in one hour.

4.4.4 Supervisory Predictive Control optimization particularities

The multi-objective optimization process required for the supervisory predictive control is formulated by the meta-objective function proposed in the methodology chapter (Section 3.3). The optimization process aims at minimizing the meta-objective function which includes the objective functions for the occupants' comfort as well as the energy consumption of the HVAC system.

The objective functions topology depend on a set of parameters and assumptions which define the boundaries of the optimization problem and transform each of the objective functions to emphasize each of the goals required to be satisfied. For example, the energy consumption function depends on the energy tariffs for each time-step and each type of energy source if the objective is cost minimization, and the comfort objective function depends on the comfort limits defined to each of the building zones. Moreover, the meta-objective function depends on the weight assigned to each of the objective functions, and the optimization process depends on the *Status Quo* parameter to trigger the search for optimal set-points for the forecast window.

The subsequent sections present the selection of the parameters referred and the discussion of the assumptions made.

Energy tariffs

Usually, electric energy pricing follows either a fixed pricing contract where the price of the energy is invariable throughout a 24 hours day period, or it follows a dynamic pricing approach with varying tariffs depending on the time of use (TOU) of the day. The primary goal for varying pricing is to penalize certain periods of the day with a higher price than the rest of the day, so customers feel motivated to re-arrange their processes or energy usage schedules to minimize costs [163].

The advent of smart-grids expects an optimization of the tariffs for each time of day, giving to the demand side a real-time dynamic pricing depending on the measured demand by the smart-meters, the predicted demand for the next hours, and the predicted energy production injected in the network by intermittent and renewable sources. Literature shows that combining varying pricing tariffs with other demand reduction techniques significantly increases the energy security, lowering costs and GHG emissions of energy systems having a high share of renewable power [163].

The case-study presented here uses the concept of time of use tariff which penalizes certain periods of time with a higher price. Figure 4.28 shows the varying electricity tariff adapted from the electric energy pricing observed in Portugal, comprising a tri-hourly pricing scheme [164].

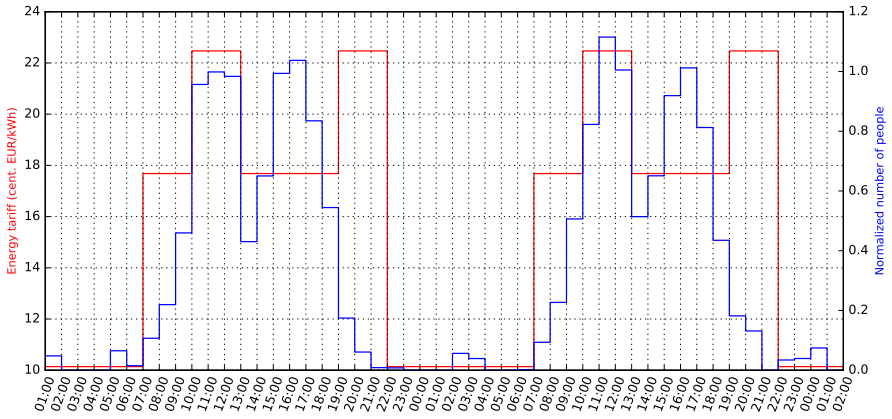

Figure 4.28: Example of the tri-hourly electric energy tariff used on the supervisory predictive control simulations.

This tariff scheme is associated with three different prices throughout the day, namely the on-peak (around noon and night), regular (morning and afternoon), off-peak (late-night and early morning). Table 4.17 summarizes the tariffs chosen for the supervisory predictive control simulations of the case-study presented in this thesis

Table 4.17: Electric energy tri-hourly tariff scheme used in the case-study of a small office building.

Type of demand	**Hours of day**	**Tariff** (cent. EUR/kWh)
Peak	[10,13[	22.47
	[19,22[	
Regular	[7,10[	17.68
	[13,19[	
Off-Peak	[0,7[	10.23
	[22,24[	

The presented tariffs present a case-scenario for varying energy prices. It only comprises electric energy prices since the HVAC system used on the case-study is only electric. However, the optimization formulation is prepared to adapt this tariff scheme to a smart-grid, or self-consumption scenario by defining a different price for each defined period of the day. The case where exists renewable sources of energy in the building, one can set the energy price to zero on the periods which the energy production guarantees the building energy demand. However, during this investigation such an scenario was out scope, but it will be suggested as future research work.

Comfort objective function and the penalty method

The comfort limits defined for the current investigation are based on Fanger's Predicted Mean Vote. The specified limit follows the extended range of acceptable PMV, ranging from -1 to 1, where -1 represents people feeling slightly cool and +1 with people feeling slightly warm .

For the convenience of the optimization formulation of the comfort related objective function (3.3.10), the statistical representation of PMV is considered, which is the Predicted Percentage of Dissatisfied (PPD), because it is expressed in percentage avoiding the need for normalization. Figure 4.29 shows the relationship between PMV and PPD. The plot also shows the acceptable limits chosen for this case-study. Hence, the PPD hard limit is 25%, which represents a PMV of$\pm$ 0.973, and the desired value is 10%, corresponding to the acceptable zone for PMV of approximately 1 (expanded), and 0.5 (neutral), respectively [65].

Figure 4.30 shows the objective function values considering the desired comfort goal in green, C^*, and the penalty, C^{pen}, in red. The value of the objective function for a given PPD is the maximum of both functions. It can be depicted that the cost does not vary for PPD values lower than 10% remaining at 0% till PPD reaches 10%. The objective values constantly increase until the penalty function is activated for PPD values over 25%. Afterwards, the objective function takes the values of the penalty function, starting at 50% and intersecting the comfort objective function at 100%.

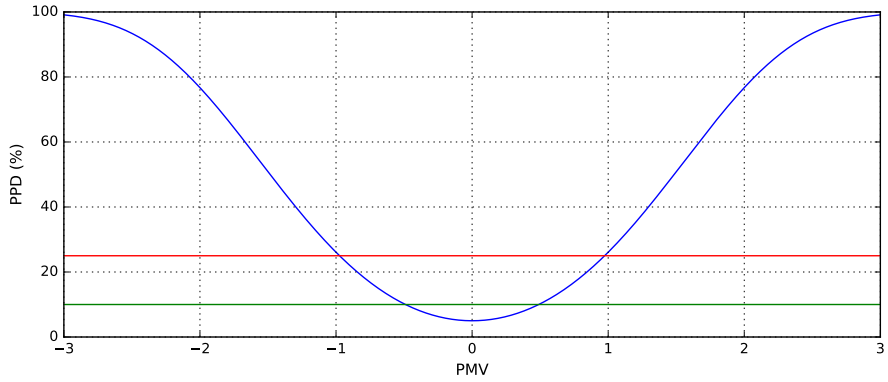

Figure 4.29: Fanger's Predicted Percentage of Dissatisfied (PPD) as a function of Predicted Mean Vote (PMV) [66]. The red line is equal to 25% and represents the comfort constraint for PPD, wheareas the green line represents the desired value of 10%.

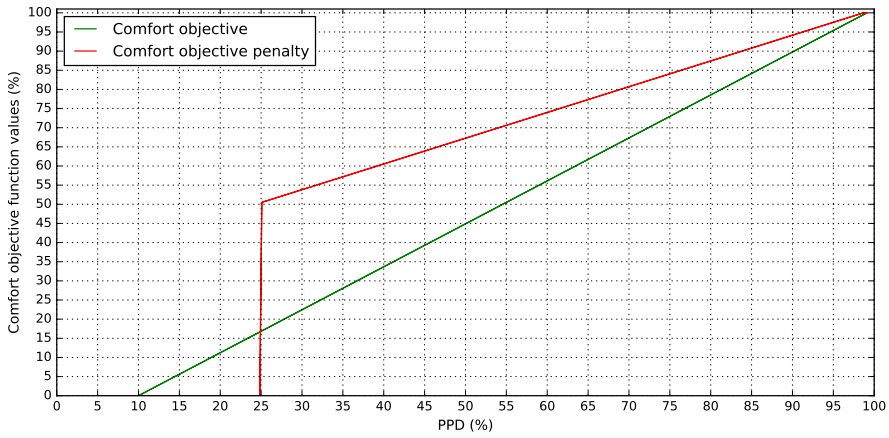

Figure 4.30: Comfort objective function values as a function of PPD.

The initial value for the penalization is arbitrary which in this case-study takes the value of 50%, meaning that a PPD of 25% would be as *bad* as a PPD of 55% if no penalization is imposed.

Besides the fact that both functions force the optimization algorithm to find control solutions which satisfy lower PPD values, the penalty method emphasizes the utility of values lower than 25 % which is the boundary of acceptable PPD considered for this case-study. Moreover, the monotonic behaviour of the objective function provides a good estimation of the relative utility between two consecutive values of the objective function, assisting the convergence of the optimization algorithm [129].

Status Quo threshold

The *Status Quo* parameter is a trigger which decides if an optimization routine should be initialized or not. Its main purpose is saving of computational time by eliminating the necessity to call the optimization process when one is not required.

Usually, a model predictive control implementation requires the optimization routines to start every simulated time-step to find the control set-points for the whole forecast window. However, only the results for the next time step, $t+1$, are used, discarding the remaining results for the time steps from $t+2$ to $t+k$, where k is the size of the forecast window. On the one hand, the disturbances predicted for the furthest time step of the forecast window, $t+k$, can be expected to be always new, affecting, therefore, the optimization problem, and leading the optimization algorithm to find different control set-points for the next time-step. On the other hand, these new disturbances entering in the optimization problem might not be considered as novelties to the problem, varying only slightly if they are compared with those from the previous forecast window. Therefore, the values of the objective function are being compared with the previous time step with the computation of the new objective function using the same set-points found before, repeating only the set-point of the furthest time set of the forecast window $t+k$.

For example, in long periods of non-occupation like weekends in office buildings, set-points should not be changed unless people is expected to occupy the building. Thus, there is no need to be continually optimizing every and each time-step, if the status of the building remains unchanged. Moreover, the *Status Quo* parameter can be interpreted as a novelty detector as well, triggering optimization only when optimization is necessary.

The definition of what to consider as novelty is inspired by the novelty detection methodology based on probabilistic analysis of time-series for outlier detection. Hence, a new building energy state will be considered as a novelty if the objective function variation exceeds the *Status Quo* threshold, SQ_τ, defining the outlier limit. The threshold definition follows a conservative employment of the *box-plot rule*, considering as novelties those values lying outside the 75^{th} percentile of the cumulative distribution function of the objective function values when comfort limits are satisfied, and the multi-objective function is different than zero. Thus, *Status Quo* threshold, SQ_τ, can be computed as the inverse of the cumulative function for an exponential distribution 4.4.3.

$$SQ_\tau = F^{-1}(0.75) = -\frac{ln(1-0.75)}{\lambda}, \tag{4.4.3}$$

where λ is the rate of the exponential and can be found fitting the exponential function to obtained data. Figure 4.31 shows the cumulative distribution function of the distribution of the objective function, highlighting the *Status Quo* threshold, SQ_τ, i.e. the 75^{th} percentile.

The 75^{th} percentile was found at the objective function value of 0.6%, for a $\lambda = 2.31$. This analysis was conducted using a population of 14655 values of the objective function

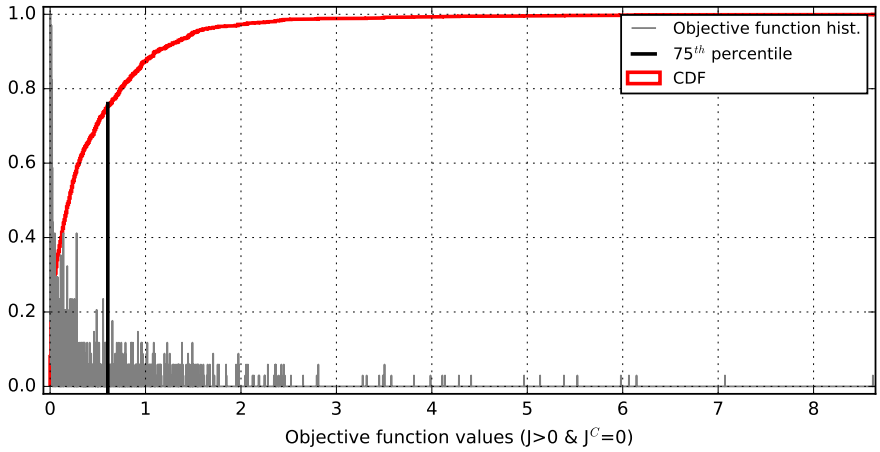

Figure 4.31: Identification of the *Status Quo* novelty detection threshold, SQ_τ, as the 75^{th} percentile of the cumulative distribution function of the objective function results.

evaluated during the simulations of the supervisory predictive control. Since the objective functions are normalized, this value can be interpreted as the allowable perceptual tolerance for the variation of the objective function for two consecutive time steps. That is to say, the status of the building regarding discomfort or energy consumption is only considered as a novelty if it increases more than 0.6% between two consecutive time steps. Note that values no greater than the 75^{th} percentile are being considered because outliers lower than the 25^{th} percentile of the data are considered as improvements to the objective function. Hence, optimization is not required.

Considering the optimization computational time described before, and the rate of one optimization per hour, the strategy presented here can save up to 66.6% of the computational if only working hours are subjected to optimization.

Comfort objective function weight - α

The formulation of the multi-objective optimization problem was conducted via a meta-objective function, combining the two objectives through a weighted sum, and transforming the multi-objective optimization problem in a single objective one. Hence, this case-study optimization problem tries to find suitable solutions for minimizing the two competitive objectives simultaneously, namely the energy consumption and the people thermal discomfort. The simplified version of the meta-objective function from Eq. 3.3.17 is formulated as equation 4.4.4:

$$\mathbf{J} = \alpha^{(C)} \cdot J^{(C)} + \alpha^{(E)} \cdot J^{(E)} \tag{4.4.4}$$

where $\mathbf{J}$ is the meta-objective function value, $\alpha^{(C)}$ is the weight associated with the

comfort objective $J^{(p)}$, and $\alpha^{(E)}$ is the weight associated with the energy consumption objective $J^{(E)}$. Since the individual objective functions values are normalized the sum of weights is expected to be unitary.The weight associated with the energy consumption, $\alpha^{(E)}$, can be described as a function of the weight for the comfort objective, $\alpha^{(C)}$, as:

$$\alpha^{(E)} = 1 - \alpha^{(C)} \tag{4.4.5}$$

This section focuses on the presentation of the weight $\alpha^{(C)}$ which depends on the occupancy rate and on the desired trade-off between objectives. The motivation for a weight parameter dependable on occupancy rates resides in the fact that the optimization problem is *unique* for each time frame and different importance should be given to the energy consumption minimization and comfort enhancement, whether or not zones are expected to be occupied. Hence, $\alpha^{(C)}$ is defined as equation 4.4.6:

$$\alpha^{(C)} = \begin{cases} 0 & \text{if } Occ < 0.1 \\ 0.5 & \text{if } Occ \geq 0.1, \end{cases} \qquad \text{with} \qquad Occ \in [0, 1]. \tag{4.4.6}$$

The presented piecewise function is expected to help the optimization process to ignore occupation rates under 10%, which in the present case-study is equivalent to one person in the Hall, since the it accommodates 14 occupants. Therefore, the minimization of the discomfort in the Hall will only be considered when there are at least two people in this zone, avoiding the HVAC system to spend energy to such low occupation rates. There might be cases where the minimum number of occupants might not be straightforward to set. For example, zones having either a very large, or a very low number of possible occupants, namely theatres, or building zones having a single person as maximum occupancy might benefit if the lower threshold for considering the minimization of discomfort is an absolute number of occupants rather than a fraction of occupancy rate.

Since no single optimal solution is observed for all the objective functions, multi-objective optimization problems look for trade-off between the competitive objectives, rather than finding a unique solution. Both objective functions presented in this case-study are commensurate and normalized between 0 and 100. It would be safe to admit that a trade-off of 0.5 would be a fair compromise between comfort and energy cost because it would favour solutions having the lowest Euclidean distance to the utopia point in a Pareto-front analysis (recall Fig. 2.12).

Literature is abundant in articles stating that a weighting parameter is required to combine competitive objectives such as comfort and energy consumption [25, 12, 150]. However, the values employed in such optimization problems are often left out for open interpretation. For example, the work from De Coninck and Helsen [28] states that when the weighting factor is thermal comfort, it will be guaranteed. However, the authors fail to mention the magnitude of how sufficiently large such weight should be.

When studying these trade-off closely, it seems that the compromise of 50/50 does not present the utility expected. Figure 4.32 shows the behaviour of the supervisory

predictive control with an α of 0.5, using as predictive models the surrogate models presented previously.

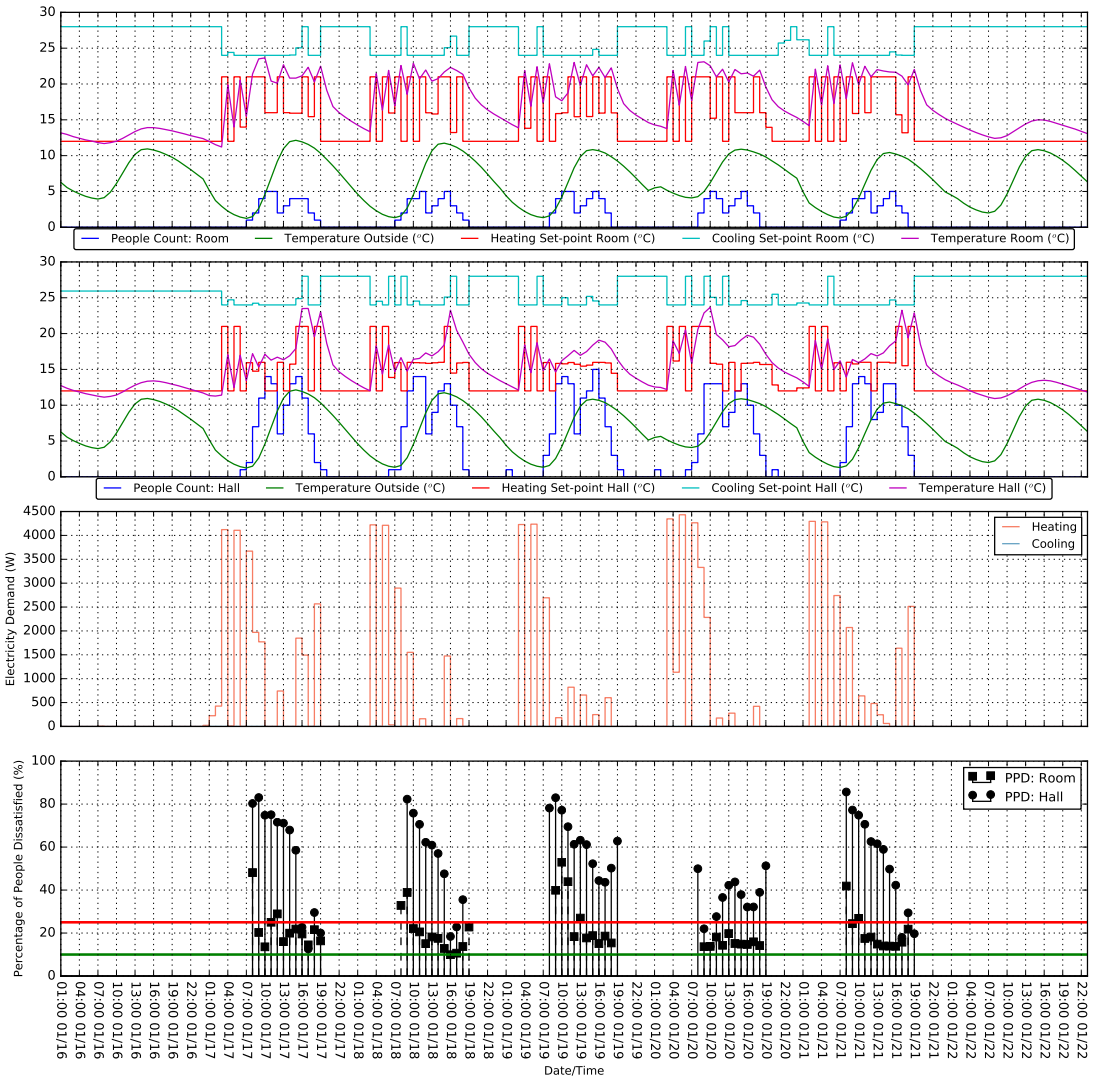

Figure 4.32: Winter's design week supervisory predictive control simulation using α equal to **0.5**, and surrogate models trained with reference control strategies database.

As it can be depicted, the supervisory predictive control is unable to guarantee the comfort of the occupants throughout the simulated Winter's week, suggesting a deviation of the trade-off from the comfort to the energy consumption. The optimization algorithm failed in choosing the temperature set-points which would provide thermal comfort to the occupants in the Hall, whereas in the case of the Room, that behaviour is not evident,

because the comfort levels in this zone seemed fairly satisfied throughout the week. Two phenomena might justify such a behaviour. Firstly, predictive models may be inducing errors in the optimization process, leading the algorithm to accept predicted PPD levels which are in fact higher than expected. The other possibility lies in the selection of the weighting parameter, α, which might not influence the optimization algorithm enough for searching control decisions capable of satisfying the comfort required. Unsurprisingly, the compromise in the thermal comfort was taken at the *expense* of the Hall because its volume would induce higher costs than the Room, to reach the same levels of comfort.

The predictive errors and control anomalies are expected in the initial phase of the supervisory predictive control. Its presentation of results, the error assessment of the surrogate models, and the training updates are reserved to the next section,

Table 4.18 summarizes the results of the search for the best compromise between objective functions. Hence, the weight parameter, α, has been varied between 0.5 and 0.9 and the overall results of simulated comfort and energy have been summarized and compared against the performance of the reference case-study Early-Off results refer to the coldest week of the weather file which comprise the period from 16-01 to 22-01.

Table 4.18: Comparison between Supervisory predictive Control and the Early-Off control strategy for coldest week of the year (16-01 to 22-01), varying comfort weight, α, and using surrogate models trained with reference control strategies database.

Metric	comfort weight: α			Reference
	0.5	0.7	0.9	EO
PPD violations	+25.75%	+32.82%	+11.59%	27.35%
$\overline{PPD}$	+11.53%	+11.85%	-0.12%	25.38%
Peak electricity demand	+0.36%	-4.53%	-0.75%	4415W
Energy Consumption	-19.18%	-16.21%	+6.64%	112.6kWh
Energy costs	-36.08%	-7.95%	-9.29%	20.89€

As it can be observed, all the possibilities are fairly poor regarding the capacity of the supervisory predictive control in guaranteeing the limits imposed for comfort (PPD$\leq$25%). Moreover, the results are not showing a monotonic trade-off. For example, the weight of 0.7 presented higher levels of PPD than the remaining cases. On the other hand, the same α registered the lowest peak of energy demand, but not the lowest energy consumption nor the lowest cost of energy.

The most relevant case is the α equal to 0.9. The simulation with this α is presented in Figure 4.33.

Even though privileging comfort on a 90 to 10 ratio, the PPD violations have increased 11.59%, when comparing with the Early-Off reference control strategy. Thermal comfort is violated 38.9% of the occupied time, but, at the same time, the control was capable of improving the overall PPD of the building during the simulated period by 0.12% while saving 9.29% of the energy costs with the HVAC system. Conversely, the

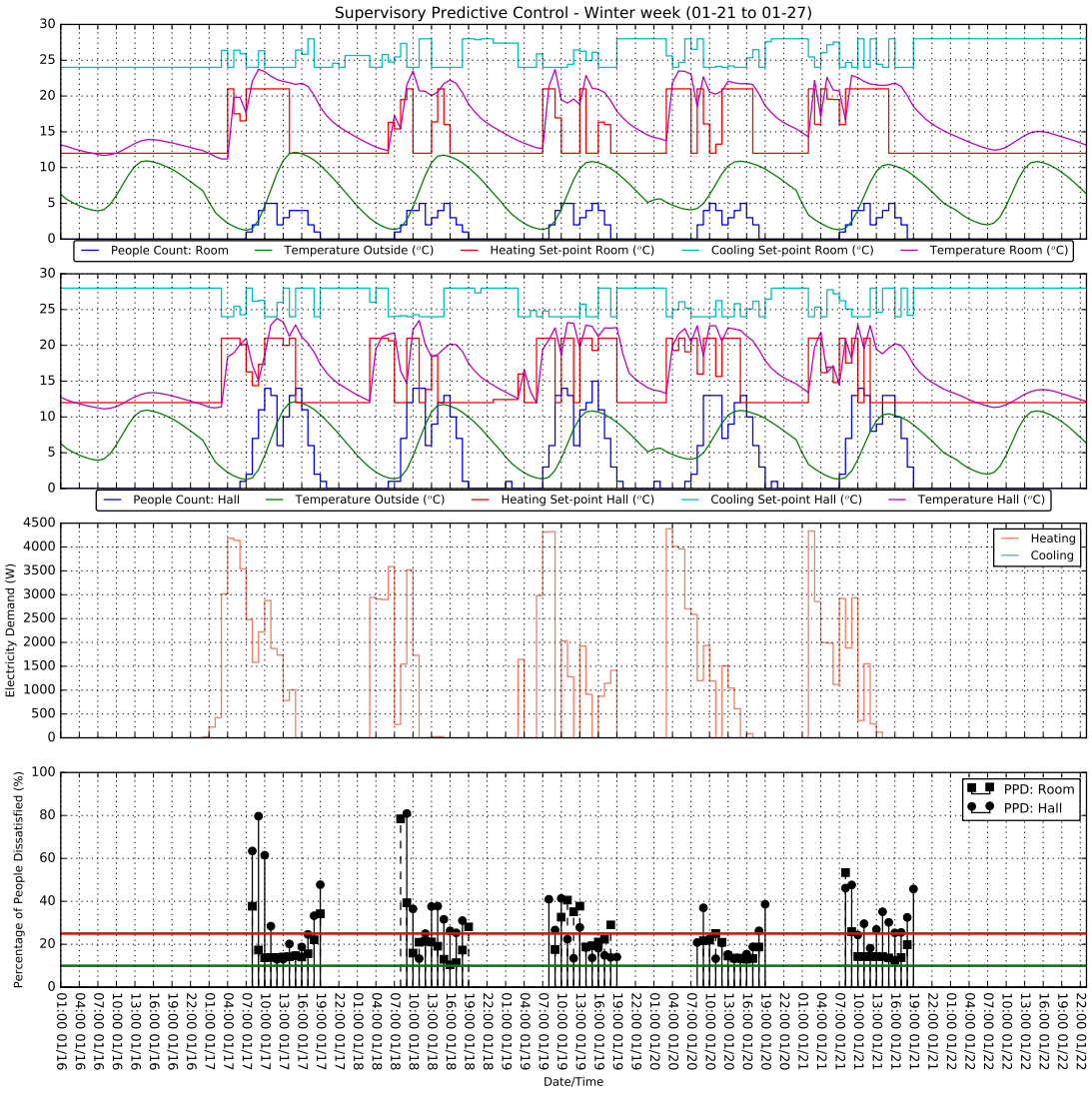

Figure 4.33: Winter's design week supervisory predictive control simulation using α equal to **0.9**, and surrogate models trained with reference control strategies database.

energy consumption increased 6.64%, meaning that the time of use of the energy was allocated to less costly periods than with the Early-Off control strategy.

In conclusion, results show that an α of 0.5 would lead to a considerable deprecation of the thermal comfort levels, even though the energy consumption and energy costs might be attractive. Such a behaviour of the SPC mirrors the results regarding the conventional control technique of Demand Reduction. If from the one hand it manages to reduce costs, it clearly fails if the purpose of an HVAC system is to provide comfort

to building's occupants. Hence, an acceptable α would be 0.9, considering the trade-off between comfort and energy consumption and ignoring the fact that the number of comfort violations is still unacceptable. Moreover, it corroborates the results obtained by De Coninck et al. [28] that stated that the weighting parameter to the comfort objectives should be considerably large. The same authors have stated the incapability of their model predictive control in reaching satisfactory levels of comfort, a behaviour possibly caused by the mismatch of the predictive models and the observed building state. Accordingly, the following section (Section 4.5) is dedicated to the error assessment of the surrogate models during supervisory predictive control simulations, and how to improve their predictive capabilities by presenting new data to the models.

4.5 Adaptive re-sampling and surrogate models update

The purpose of the re-sampling strategy proposed by this thesis is to improve the supervisory predictive control capabilities by enhancing surrogate models' predictive quality. Since data's optimal distribution for surrogate modelling is not known up front and populating an optimization domain represents a computational investment, it is often, if not always required re-sampling procedures for filling the domain of the optimization problems in the regions of interest [36, 127, 128]. Buildings are known for having a slow response to the typical loads of a thermodynamic system, hindering the modelling process for predictive control strategies based on data-driven methodologies [150]. Therefore, the selection of the appropriate data for surrogate modelling of buildings energy system should take into consideration the time-dependency between variables and building inertia. Conventional sampling methods such as Taguchi, Latin Hyper Cube, brute-force, might be impractical for the sampling of the problem presented in this case-study.

As presented in Section 4.3, the outputs of the building thermodynamic system exhibit not only autocorrelation, but also dependency to exogenous lagged variables, reflecting building's slow response to changes. Sampling the optimization domain of the six outputs presented on table 4.10 would turn out to be a very complex task if choosing any conventional sampling method referred above. See for example the case of modelling the Predicted Percentage of Dissatisfied people in the Room (**PPD_Z1** from table 4.10). Simultaneously, this output variable depends on its lagged version for the time-steps from $t-4$ to $t-1$, and on other output variables, namely Temperature in the Room and Hall (**Temp_in_Z1** and **Temp_in_Z2**) for the same time lags. These variables are outputs of EnergyPlus™ and not disturbances, drawing a design of experiment for populating the domain of those variables would require sending explicit commands to the simulator so it could populate the database in the desired region of interest. This interdependence between variables is observable for most the outputs subjected to modelling. Hence, a conventional sampling method would require simulations to be conducted by a predictive control solution so the points obtained by the simulator would

be useful to the surrogate modelling. Moreover, the sampling method proposed would also need to populate the transient domain, accounting for the derivative characteristic of each of the points sampled. To overcome this issue, this thesis proposes an adaptive sampling technique based on the optimization problems submitted by the supervisory predictive control and possible control anomalies.

4.5.1 Models mismatch investigation

The domain of the variables is inevitably biased towards the non-predictive controlling strategies used as reference case-studies, making the surrogate models naturally biased and, therefore, overfitted. Thus, the optimization routines conveyed by the base models are expected to converge to values different from those observed from the EnergyPlus™output results because the exploratory nature of the optimization algorithms forces the searching for feasible solutions to outside of the known regions of the model's domain (and data-driven models are not generally good at extrapolating). These mismatches may lead to unsatisfactory controllers behaviour as presented previously. The initial simulations using the surrogate models trained only with reference control data showed control mismatches similar to the ones pointed out by De Coninck, even though the strategy proposed for delivering the data-driven models has been designed for avoiding overfitting. Nevertheless, the occurrence of such anomalies is useful for the sampling methodology proposed, because those values contain information unknown to the data-driven models, contributing to increase their predictive qualities, hence improving the supervisory predictive control.

A co-simulation of 8760 hours has been used to investigate the models mismatch between the expected error analysis obtained during the modelling strategy and the observed error during the co-simulation. The chosen alpha for this simulation was 0.9, according to the results identified on the previous section.

As it can be seen on Table 4.19, the mismatch between models expectations and EnergyPlus™ results is considerable.

Table 4.19: Summary of the model selection error analysis for all the modelling algorithms under investigation.

Modelled Output variable	Modelling algorithm - Normalized Mean Error (NME)					
	NN		SVR		RF	
	Expected	Observed	Expected	Observed	Expected	Observed
Heating Power Demand	8.291%	49.914%	11.570%	77.121%	4.915%	53.485%
Cooling Power Demand	17.839%	84.177 %	21.973%	66.742 %	8.181%	63.878%
PPD Room	0.733%	7.324%	0.407%	6.716%	0.645%	4.144%
PPD Hall	0.750%	7.377%	0.508%	5.635%	0.588%	4.552%
Temperature in. Room	0.616%	7.151%	0.335%	4.653%	0.340%	3.902%
Temperature in. Hall	0.451%	8.149%	0.316%	5.055%	0.337%	4.971%

The expected and observed errors were calculated using the Normalized Mean Error

from Eq. 3.2.13 which normalizes the mean absolute error by the average of the observations. Since the co-simulation used only the surrogate models selected previously on the modelling selection section, the presented error estimation was conducted by predicting the results obtained by EnergyPlus™ output after the simulation process, rather than an on-line verification of models error. This approach allows for the comparison of the performance of all the modelling techniques previously presented.

Overall, the observed error has increased significantly in all the models and all the output variables, exhibiting, in most cases, an increment of one order of magnitude on the percent error. The mismatch observed in the predictions of PPD and temperature seem quite acceptable, where random forests performed better against overfitting relatively to the other modelling strategies. However, the results for energy demand predictions show considerably high error rates, exhibiting a clear model overfitting to the baseline reference case-study data. However, besides the magnitude of the presented errors, the supervisory predictive control is still providing acceptable results probably because the absolute values of the errors are still not prohibitive to the overall performance of the optimization algorithm. For instance, the mean absolute error for the observed predictions of the heating power demand by the Random Forest (the model used during simulation for predicting this output) is as high as 176.61 ± 3.39W, which only represents 3.5 of the maximum registered value. On the other hand, the mismatch observed on the predictions of PPD, although being smaller, have caused a more noticeable impact on the performance of the supervisory predictive control, especially the comfort measured in the Hall, as it can be seen in Fig. 4.33. The number of comfort violations in the Hall are substantial, reaching values of PPD around 80% which represent a PMV lower than -2 and an environment where most people would feel cold according to Fanger's scale for comfort.

This model mismatch investigation also suggests that the Random Forest algorithm seems to avoid overfitting better than the other algorithms presented. Such an observation is to be expected due to the ensemble nature of the algorithm [91]. The idea behind Random Forests is to train ensembles of CART models which are specialized to specific parts of the database and variables. Hence, while each of tree in the forest might be overfitted to the problem domain posed to it, the predictions of all trees considering the whole domain of inputs are averaged towards the more frequent result, leading the ensemble to provide more robust answers with lower variability.

Considering the hypothesis that the quality of the predictive models of a model predictive control do influence its performance, it seems mandatory to update the initial surrogate models to improve the reliability of the optimization processes inherent to supervisory predictive control [28, 59].

4.5.2 Surrogate models update

Even though the initial surrogate models were not leading the supervisory predictive control to make bad decisions all the time, the errors computed to the those models for

co-simulation were showing a considerable variance to the expected error rate. Hence, retraining the models became mandatory. The surrogate models presented in this thesis are based on machine learning algorithms capable of learning from experiences. Their heuristic nature should allow the algorithms for understanding the consequences of sending specific controls to the building HVAC system which are not desirable regarding the optimization process. Once the surrogate models provide accurate predictions to the controls proposed by the optimization algorithm, the latter naturally discards those set-points that do not represent an improvement to the problem given at a specific time step. The premise is that if they know the consequences of a specific *bad decision*, they will not consider it as a *good decision* afterwards.

The magnitude of the observed errors represents a beneficial quality of the generated data. In information theory, and re-sampling procedures for surrogate models, new data points inducing high entropy in the variable subject to modelling show the relevance of those points to the variable under investigation and the sensitivity of that variable to the changes made on the inputs [144, 59]. Therefore, it is safe to believe that the new data provided by the co-simulation process is useful to improve predictive capabilities of the surrogate models, and that the re-sampling strategy is capable of finding such points. Moreover, the risk of populating the database with irrelevant data to the optimization problems that require a solution is very low because the sampling was conducted by those optimization problems.

Surrogate models are updated simply by retraining the data-driven models by machine learning algorithms using the same methodology as the one presented in the surrogate modelling section (Section 3.2).

The major difference between the update of the surrogate models and the initial modelling is that the size of the training data set is now investigated to infer the relevance of the data to the predictive capabilities of the models. Figure 4.34 shows the evolution of the training and testing errors for different sizes of training data-sets and for the training of the model for predicting the PPD in the Hall.

The test and training data-sets are obtained by randomly dividing the whole database in two partitions of 80 and 20% of the size of the database, respectively. Green lines highlight a relative convergence of 0.01, suggesting smaller data-sets than the whole database without greatly compromising the predictive performance of the models trained.

As it can be depicted, the algorithm showing the best performance is the Support Vector Regression, corroborating the results observed in the modelling using baseline data (Chapter 4.3). A relevant aspect of this results is that it mirrors the nature of each algorithm. For example, the evolution of the error in the Neural Network shows higher variance than remaining ones, reflecting the instability of the model to the data presented for training, the high complexity inherent to the algorithm, and the stochastic dependence of the training process leading it to convergence to different results. However, since the observed difference between training and testing errors is relatively small, there is no evidence of overfitting.

Random Forests and Support Vector Regression show a more stable monotonic de-

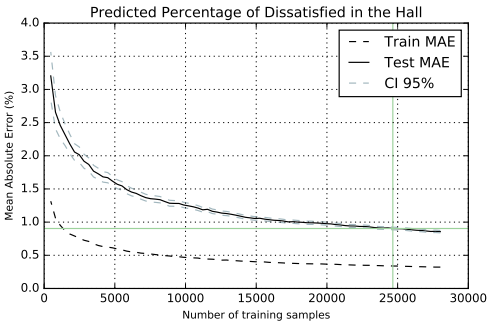

(a) Random Forests.

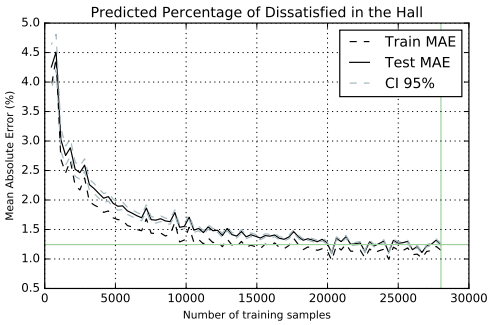

(b) Neural Networks.

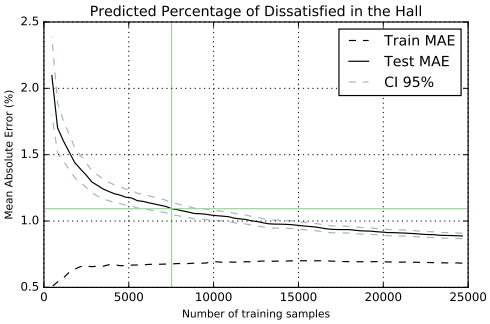

(c) Support Vector Regression.

Figure 4.34: Evolution of the training Mean Absolute Error (black dashed line) and testing Mean Absolute Error (full line and dashed limits of 95% confidence interval) for different training data-set sizes on the modelling of Predict Percentage of Dissatisfied in the Hall. a) Radom Forest algorithm results; b) Neural Networks results; c) Support Vector Regression

scent of the error rate for increasing sizes of randomly selected samples. Moreover, the characteristics of ensemble models to single models is also mirrored in the evolution of the error and the observed confidence interval for the testing error. While the Support Vector Regression model clearly overfits the initial data, reflecting a considerable amplitude between the training and testing errors, the Random Forests training error follows the monotonic behaviour of the testing error.

Besides the fact that the minimum observed testing error is produced by the SVR, the RF algorithm manages to generate predictive models of lower variance because the errors produced by each of the 90 trees are averaged, producing more stable predictions, and delivering a more accurate model.

The updated performance of the surrogate models, considering a 10-fold cross validation error assessment, as introduced in Section 4.3.8 is presented on Table 4.20. The

k-fold cross-validation method is a more reliable validation method than the 80-20 rule because it manages to investigate a model's capability of approximation across the whole database [92, 147].

Table 4.20: Summary of the surrogate models update for all the modelling algorithms under investigation.

Modelled Output variable	Modelling algorithm					
	NN		SVR		RF	
	NME	R^2	NME	R^2	NME	R^2
Heating Power Demand	11.676%	0.989	11.264 %	0.985	**10.970%**	**0.981**
Cooling Power Demand	31.556 %	0.858	95.86 %	0.452	**13.431%**	**0.972**
PPD Room	1.281%	0.995	2.014%	0.996	**0.822%**	**0.996**
PPD Hall	0.898%	0.996	1.301%	0.995	**0.879%**	**0.996**
Temperature in. Room	0.999%	0.991	0.645%	0.993	**0.527%**	**0.995**
Temperature in. Hall	0.646%	0.994	0.807%	0.995	**0.534%**	**0.996**

As it can be depicted, the SVR and NN did not not manage to get the same expected error as before. It is evident the superiority of the Random Forests in the modelling of the same output variables, given the new data. This algorithm has managed to outperform all its competitors. The major impact can be depicted on the modelling of the cooling energy demand, which the other algorithms failed to converge to a proper solution. This result shows the superiority of ensemble algorithms as the case of the random forests, corroborating the study performed by Fernandez-Delgado et al. [80].

4.5.3 Supervisory Predictive Control performance enhancement

This section aims at stressing the necessity of having robust predictive models to integrate a model predictive control strategy, or any other optimization process based on surrogate modelling, or response surface analysis.

Figure 4.35 shows the same simulation as the one presented in Fig. 4.32, but using the updated surrogate models instead of the ones trained using only reference data. The weighting parameter α has been set to 0.5 and the simulation was carried on the week from 16-01 to 22-01.

The comparison between Fig. 4.35 and Fig. 4.32 reflects a huge improvement in the capabilities of the supervisory predictive control with the updated surrogate models. The overall comfort has been improved in both zones, and the number of hours outside the comfort limits was reduced. As expected, the energy consumption and the related costs have increased, but they were considerably reduced if compared with the reference case-study of the Early-Off control strategy.

The re-sampled data to update the surrogate models was gathered through co-simulation of the supervisory predictive control using a α of 0.9. The question if such a large α makes sense given the improved quality of the surrogate models is answered

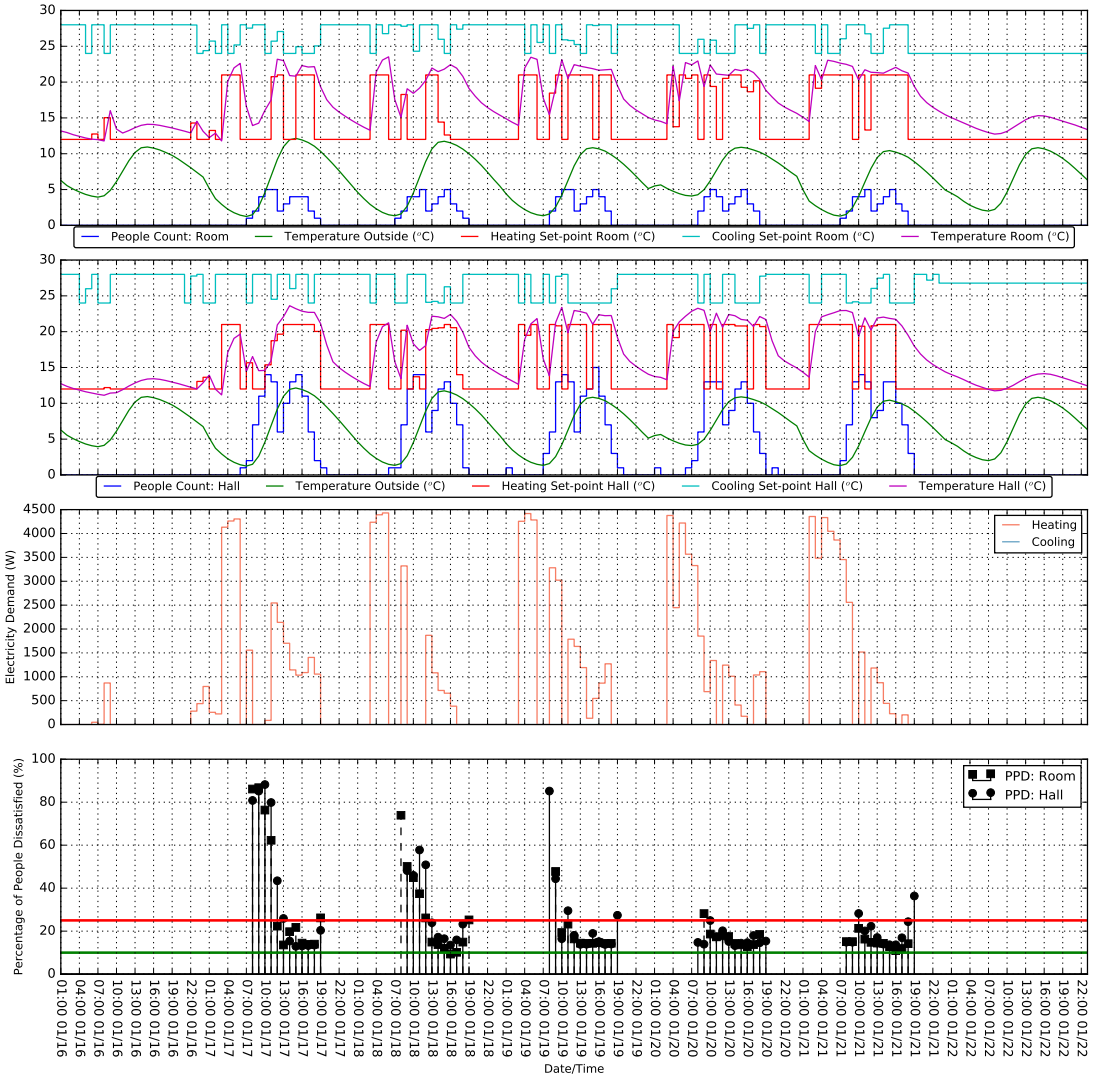

Figure 4.35: Winter's design week simulation of supervisory predictive control using α equal to **0.5**, and updated surrogate models trained with data from co-simulation process.

in the Figure 4.36 which shows a simulation using the α equal to 0.9 using the new predictive models.

Table 4.21 summarizes the performance metrics given the variation of α, and Figure 4.37 shows the plot of the normalized cost of energy and the normalized PPD, relative to the reference case-study of Early-Off.

The plot of the Pareto-front in Fig. 4.37 shows that the weight providing the highest

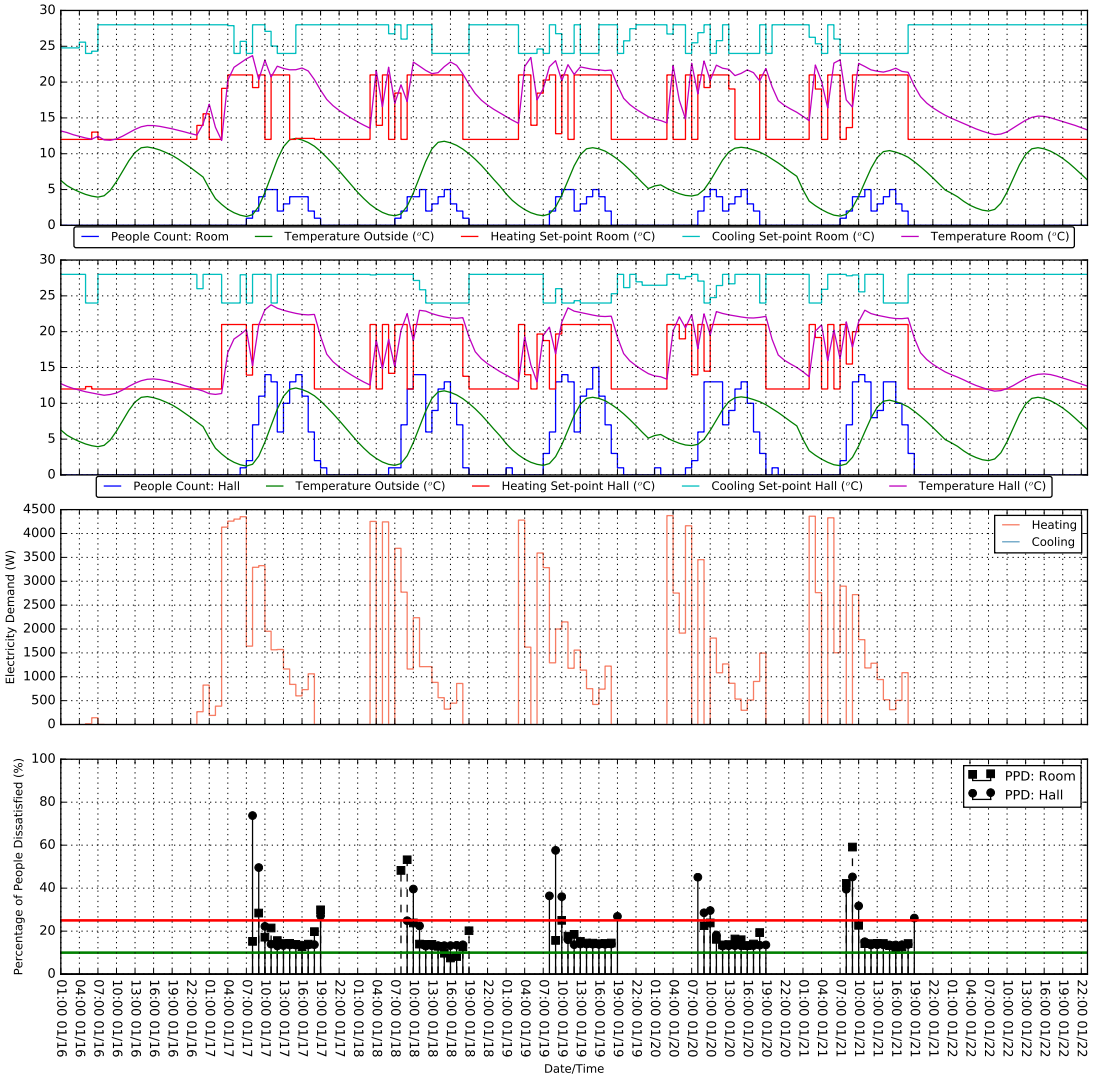

Figure 4.36: Winter's design week simulation of supervisory predictive control using α equal to **0.9**, and updated surrogate models trained with data from co-simulation process.

utility is 0.9, because it accounts for the minimum distance to the *utopia point*, which is the origin, when comparing it to the other values of α [129]. The minimum Euclidean distance to the origin is highlighted in green, and the boundaries in red refer to the PPD and energy cost observed in the simulation of the reference control strategy for the same period.

The selection of a weight of 0.9 will privilege more expensive control solutions than

Table 4.21: Comparison between Supervisory predictive Control against the reference control strategy Early-Off for coldest week of the year (16-01 to 22-01), varying comfort weight, α, and using updated surrogate models trained with data from co-simulation process.

Metric	**Reference**	SPC: α		
	EO	0.5	0.7	0.9
PPD violations	27.35%	25.66 %	24.78 %	19.47%
$\overline{PPD}$	25.38%	25.36%	24.20%	19.754%
Peak electricity demand	4415W	4430W	4376W	4259W
Energy Consumption	112.6kWh	126.49kWh	128.9kWh	137.3kWh
Energy costs	20.89€	19.21€	20.43€	21.84€

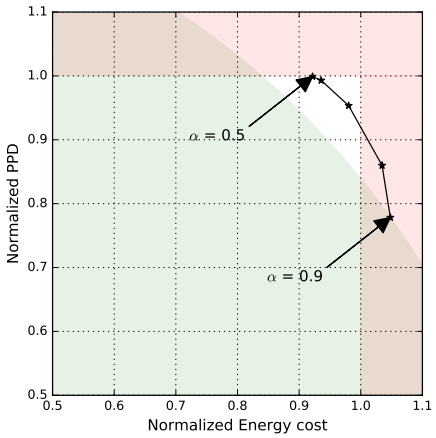

Figure 4.37: Pareto-front of PPD vs. energy cost relative to the reference control strategy Early-Off for the coldest week of the year (16-01 to 22-01), varying comfort weight, α, and using the updated surrogate models trained with data from co-simulation process.

the reference case-study used for this assessment. However, such a weight does represent the best compromise between comfort and energy cost, and that fact should be sufficient to motivate the choice of 0.9 to the α.

The selection of such a large weight corroborates again with the work of De Coninck [28]. However, this decision process is ultimately arbitrary. For example, if the priority is to reduce cost and a specified budget is defined, than the option of a lower α would be more convenient.

It was verified that re-sampling strategies with the goal of updating the predictive capabilities of surrogate models impact positively on the optimization process required for predictive control strategies. Moreover, the adaptive re-sampling strategy proposed in this section proved to be useful to accomplish such a goal. The adaptive data collection

strategy relied on the nature of machine learning algorithms to improve learning by experiencing samples outside the initial domain of knowledge. This learning principle can be compared with the capability of an intelligent individual of learning from its own mistakes, here called model mismatch. Surrogate models have learned from undesirable experiences and led the optimization process to better performing solutions than with the previous knowledge.

This adaptive data gathering approach can be related to sequential sampling techniques employed in surrogate-based engineering design optimization [127, 128]. Sequential sampling for design optimization emphasizes finding the global optimum by balancing a search for the optimal performance of a surrogate model and a search for unexplored regions to avoid missing promising areas due to the inaccuracy of the surrogate model [128]. In this approach, the unexplored regions are identified by the mismatch between optimization expectation and observed results during the co-simulation process between EnergyPlus™ and the supervisory predictive control. The implementation of this system in a real-world scenario is straightforward and recommended to guarantee good performance of the optimization routines.

4.6 Supervisory Predictive Control - Performance Benchmark

In this section, a benchmark is conducted to compare the performance of the Supervisory Predictive Control strategy being proposed in this thesis against the conventional rule-based control strategies presented earlier. The various key performance indicators are presented, and the co-simulation technical aspects and the assumptions are defined. Three major comparisons are held. The first assessment is the performance of the predictive controller during the heating season, followed by the cooling season, and the whole year analysis.

4.6.1 Reference cases and performance indicators

The first technique is based on a timer controller (TC). As referred previously the system is turned off after occupants leave the building and it is turned on 2h before expected people's arrival. In an office building, such as this case-study, the systems would be activated at 06:00, and deactivated at 18:00.

The second technique is called demand reduction by pre-heating, or pre-cooling (DR). Basically, it is intended to turn the systems off during peak hours of electricity consumption and prices. According to Garnier et al. [29], in a non-residential building it means switching on from 05:00 to 07:00, included, switching it off from 08:00 to 12:00, included, and finally turning HVAC on again at 13:00 till 18:00.

The third technique is called Early switch-Off (EO). It is the most similar to TC. However, this technique makes use of building's thermal inertia and turns off the HVAC

systems before the occupants leave the building. It starts at 6:00, like with TC, but it switches off at 16:00 two hours before people departure.

The comparisons are computed with an hourly resolution, for all days of the week, and are summed, or averaged for the given periods of assessment. The key performance indicators were introduced in Section 4.2 at the presentation of the mentioned baseline strategies. The eight performance indicators are listed below:

1. Mean Predicted Percentage of Dissatisfied – Average of the Predicted Percentage of Dissatisfied during occupied hours for the entire building.

2. Mean Predicted Percentage of Dissatisfied in the Room – Average of the Predicted Percentage of Dissatisfied during occupied hours of the Room (Zone 1).

3. Mean Predicted Percentage of Dissatisfied in the Hall – Average of the Predicted Percentage of Dissatisfied during occupied hours of the Hall (Zone 2).

4. Percentage of PPD violations – Number of hours outside the boundaries of acceptable Predicted Percentage of Dissatisfied for the entire building.

5. Accumulated people dissatisfied – Sum of the number of people in the building multiplied by the Predicted Percentage of Dissatisfied.

6. Peak electricity demand – Peak value for the electricity power demand by the VRF system.

7. Specific energy consumption – Average of Energy consumption per unit area.

8. Energy consumption costs – Sum of the costs related to energy consumption by the VRF air-conditioning system.

The percentage variation of each of the parameters referred will be computed against each of the reference case-studies using conventional control techniques,

4.6.2 Building energy performance co-simulation

The co-simulation process used the supervisory predictive control presented in the previous sections, and its parameters and assumptions may be summarized as follows:

- The simulation is carried out by EnergyPlus™ using six time-steps per hour, from the 2^{nd} of January to the 30^{th} of December.

- The weather file is provided by LNEG and it refers to Oliveira de Azémeis, Portugal.

- The controllable variables are the dual-temperature set-points of both zones, controlled independently. The heating temperature limits are 21^oC with a set-back of 12^oC, and the cooling temperature limits are 24^oC with a set-back temperature equal to 28^oC.
- The disturbances forecast assumes a standard deviation weight, λ, equal to zero, meaning that the forecast is always correct, as presented in section 4.4.2. The investigation of the effects of forecast uncertainty are presented further ahead, in section 4.6.7.
- The surrogate models used have been trained with data from the three control strategies and 8760 hours of re-sampled data, as pointed out in section 4.5.
- The optimization algorithm used is the Differential Evolution.
- The forecast window considered is six hours.
- The energy tariffs employed are subjected to Time Of Use pricing scheme of tri-hourly prices, as presented in section 4.4.4.
- The comfort objectives are PPD equal to 10%, idealistically with penalty to values over 25%.
- The *Status Quo* threshold is equal to 0.6, as presented in section 4.4.4.
- The comfort objective weight, α, is equal to 0.9, as presented in section 4.4.4.

The benchmark is divided into three periods of the simulation. First, the performance of the supervisory predictive control is compared against the reference case-studies for the heating season, then the results for the cooling season are compared, and, at last, the results of the year benchmark are presented.

4.6.3 Heating season analysis

The heating season considered for this benchmark starts on November the 1^{st}, ending on March the 31^{st} in agreement with the work of Garnier et al. [29]. The heating design day is 17^{th} of January, representing the coldest day observed in the provided weather database from LNEG (1.6^oC at 7:00).

Fig. 4.38 presents the overall performance benchmark of the supervisory predictive control against the conventional control strategies for the heating season simulation. The costs regarding the energy consumption of the VRF system are shown in the graphic at the top, followed by the system energy consumption. The cumulative violations of the comfort limit (PPD>25%), and building's average Predicted Percentage of Dissatisfied (PPD) across all air-conditioned zones are presented afterwards. The most economical control strategy is the Demand Reduction (DR), presenting less 18.82% of related costs

when comparing with the 218.99€ *expended* by the Supervisory Predictive Control. Whereas the most expensive control solution is the Timer Controller which accounted for more 14% of energy costs comparing to SPC, followed by the Early-Off strategy with 7.42% more costs. The closest strategy to the SPC regarding costs is the Early-Off strategy.

The ranking of the energy consumption puts SPC at the most energy-demanding solution, summing up the highest energy consumption for the simulated period, for all techniques tested. The contradiction between energy costs and energy consumption rankings identifies the effort of the supervisory predictive control on shifting the energy demand to more economical hours than the remaining strategies, at the expense of requiring more energy in total due to energy losses during peak tariffs periods where the temperature set-points tend to be reduced as shown in the Fig 4.39. This evidence shows the benefit of having an *intelligent* system such as the one proposed, to allow for load scheduling to more economical or less carbon-intensive periods of the day, as well as periods of high availability of energy, depending on the distributed generation from renewable energy sources [163, 47].

The comparative performance of Demand Reduction regarding comfort is very poor, accounting for more than 500% of hours outside comfort boundaries when comparing to SPC, as well as an increase of 57.04% on the average PPD. The best performing strategy on the PPD violations indicator is the Timer Control, summing up less 21% of comfort violations than the SPC. However, in what concerns the average PPD, the SPC has managed to achieve 13.69%, resulting on the best comfort of all control techniques during occupied hours. This comfort level allows for this strategy to be the only one achieving the category III regarding comfort standard EN 15251:2007 which states that a PPD lower than 15 % (-0.7 < PMV < 0.7) provides an acceptable and moderate level of thermal comfort and may be used for existing buildings [63]. Table 4.22 summarizes the performance of the presented strategies based on the key indicators shown in Fig. 4.38, and on the metrics introduced previously on Section 4.6.1.

The APD metric is the Accumulated People Dissatisfied, representing a weighted version of the PPD by multiplying it by the number of occupants observed in that zone for a given time of the day. Peak power demand is the maximum value of electricity power required by the VRF system during the simulation period which in this analysis spans five months between November 1^{st} and March 31^{st}. The specific energy consumption represents the energy intensity for a given season, and the energy costs are the expected costs allocated to the VRF system.

The categories where the supervisory predictive control performs better than the other techniques are those related to the occupants' Predicted Percentage of Dissatisfied, both the average of the entire building and each zone individually. The Room is the best zone in what concerns comfort, with PPD values falling under the 15% for most of the strategies, except for DR, managing to supply the requirements for reaching a category of III regarding EN 15251:2007 comfort standards [63]. The PPD value of the Room shows an increment of 1.97 percent points over the objective value defined for PPD on the

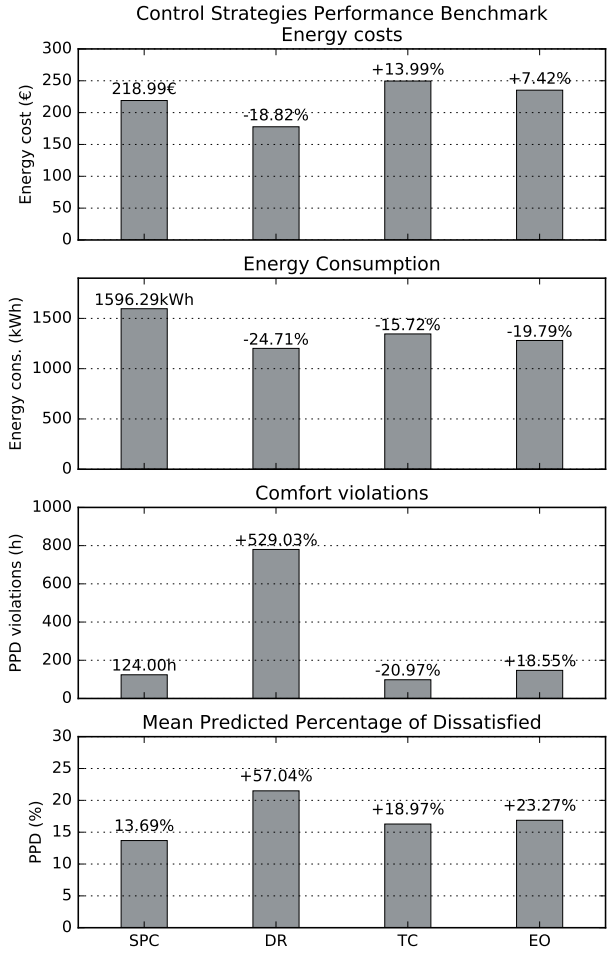

Figure 4.38: Control strategies performance benchmark for the heating season simulation. SPC: Supervisory Predictive Control; DR: Demand Reduction; TC: Timer Controller; EO: Early-Off. From the top: the costs regarding the energy consumption of the VRF system; the energy consumption of VRF system; The cumulative violations of the comfort limit (PPD>25%); Building's average Predicted Percentage of Dissatisfied (PPD) across all air-conditioned zones

optimization problem constraints. Thus, air-conditioning the Room can be considered as a less demanding challenge as compared to the Hall. The differences between the areas of

the Room and the Hall, adding a lower fenestration density and a higher solar exposure (i.e. it faces south and east) due to being facing south and east, might be responsible for this discrepancy in comfort between zones. Moreover, the higher solar gains due to the solar orientation should help the envelope to remain at higher temperatures, by increasing the surface temperature of the inside walls. This characteristic, plus the lower infiltration rate due to a reduced number of windows, should increase the heating loads required to satisfy the temperature set-point in a colder environment, especially in the mornings, reducing the effort to reach the desired PPD values during the heating season.

Table 4.22: Performance benchmark of the control strategies Supervisory Predictive Control (SPC), Demand Reduction (DR), Timer Control (TC), and Early-Off (EO). The simulation period is the heating season starting on November 1^{st} and finishing on March 31^{th}.

	$\overline{PPD}$ (%)	PPD Room (%)	PPD Hall (%)	PPD_{viol} (%)	APD	Peak Power Demand (W)	Specific Energy Cons. (kWh/m^2)	Energy Costs (€)
SPC	13.69	11.97	15.40	4.91	2220	4363.9	7.68	218.99
DR	21.49	16.77	26.21	30.86	3812	5833.9	5.78	177.76
TC	16.28	13.85	18.71	3.87	2686	4329.9	6.48	249.61
EO	16.87	14.17	19.58	5.81	2733	4415.9	6.16	235.23

The Hall presents higher levels of dissatisfaction with thermal comfort than the Room. Moreover in what concerns the Hall, for all strategies analysed, the values lie outside the limits imposed by the standard EN 15251:2007 to be considered category III of comfort [63]. The closest strategy to that limit was the SPC with as little as 0.4 percent points above the PPD imposed by the standard.

Supervisory Predictive Control accounted for 4.91% of occupied time, with PPD outside the imposed limits defined in the penalty function (i.e. PPD> 25%). During the heating season, Room's total occupied time was 1247 hours, while the Hall had 1272 hours with people present. De Coninck et al. [28] have set an acceptable comfort violation limit equal to 5% of the working hours outside the imposed comfort (category I of the EN 15251:2007 standard in their case-study) on their model predictive control. If that same limit was here to be considered, then the supervisory predictive control along with the Timer Control strategy would be the only techniques capable of guaranteeing no violations of thermal comfort. This 5% of acceptable threshold would result in a maximum of 12h in the course of the five months of the heating season.

The accumulated number of people dissatisfied (APD) shows a higher discrepancy between the predictive control solution and the traditional strategies. The difference between the number of people dissatisfied has increased to 247% in the case of Early-Off and 220% for TC, whereas the percent variation of PPD between SPC and TC, and SPC and EO ranged towards values closer to 20%. This observation shows the effectiveness of the supervisory predictive control in providing better overall comfort levels than its competitors.

Overall, it can be said that the proposed supervisory predictive control has managed to fulfil both objectives regarding the multi-objective problem of reducing energy costs while improving the occupants comfort during the heating season.

Heating season – Set-point investigation

This section focuses on the exploration of the temperature set-points distribution for each hour of the day across the whole period of simulation for each of the air-conditioned zones. The objective is to identify what kind of decisions have been taken by the supervisory predictive control to achieve the results benchmarked previously.

Figure 4.39 compares the hourly distributions of the lower side of the dual-band temperature set-points for the Room, whereas Figure 4.40 presents the same results for the Hall.

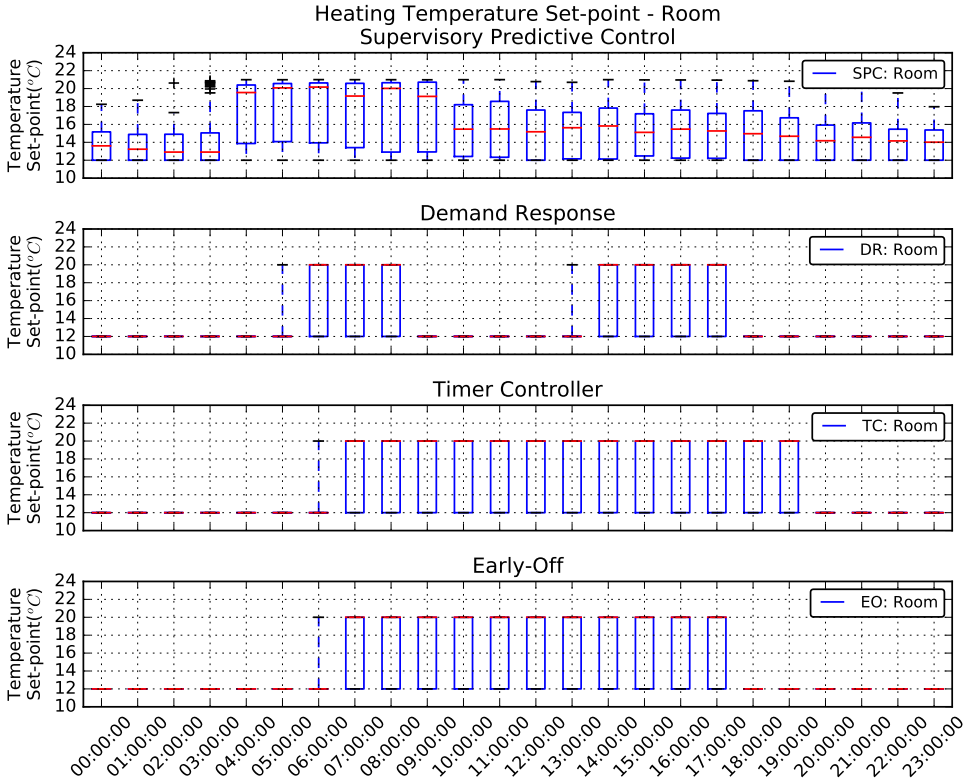

Figure 4.39: Comparison between control strategies of hourly distributions of the heating temperature set-points for the heating season applied to the Room.

The Box-plots presented enable to depict groups of numerical data using five quantities: the smallest observation (presented as the bottom end of the whisker), the lower

quartile (bottom end of the blue box), median (the red line), upper quartile (the top end of the blue box), and largest observation (the top end of the whisker). The outliers are not represented in those quantities and are plotted separately. The box (Inter Quartile Range) accommodates 50% of the whole data for that hour, whereas the minimum and maximum limits were set as $1.5 \times IQR$. Therefore, the outliers are shown only if they *fall* outside the 99.3% of the distribution of values [165].

It can clearly be seen (Fig. 4.42)that the supervisory predictive control has decided to define the heating temperature set-points, before the other techniques, to guarantee the comfort levels at the time corresponding to people entering the building. Moreover, this decision also implies an increase in the energy storage in terms of building mass which allows the HVAC system to reduce its consumption during the peak energy cost period, the initial hours of the day.

The temperature set-point shows a distribution around the median value of 16^oC after being reduced at 10:00, due to the rise of the energy costs at that time. Besides the fact that these values are lower than the other techniques, the distribution of these values is more centred, meaning that 50% of the values are usually over that median value. Nevertheless, these set-points tend to converge towards the set-back temperature along the day. This conclusion is supported by a descent value of the median, as the kurtosis of the hourly distributions rises.

The temperature set-back points during unoccupied periods have a median value over 12^oC , which is the value set for the reference case-studies, translated in an increase of the energy consumption during unoccupied periods as presented in Fig. 4.41, while its decreases the peak power demand required for setting the required temperature in the building, as exposed on Table 4.22. However, the Timer Controller has managed to diminish that peak power demand by increasing the temperature at the end of the occupied time.

Figure 4.40presents the temperature set-points distribution for the Hall. The results are similar to those of the Room. However, the box-plots show a higher skewness of the set-points distribution towards higher values of temperature after 4:00, indicating the increased heating loads necessity for the Hall when comparing it to the Room. These findings corroborate the conclusions withdrawn on Table 4.22 regarding the PPD observed in the Hall, when comparing it to the Room. By giving a high emphasizes to the heating set-points in the Hall, the SPC strategy has managed to produce the lower difference of average PPD between zones. SPC accounted for more 3.45% of PPD in the Hall than in the Room, whereas with the TC and EO strategies have summed up a difference of 4.86% and 5.41% for the same zones, respectively.

Another fact highlighting the difficulty on guaranteeing the comfort levels in the Hall is the distribution of the hourly temperature set-points defined by the SPC during the peak values of the tariff, especially at 11:00. As it can be depicted by comparing figures 4.39 and 4.40, 6.3, the Halls temperature set-points at the peak time reached the 75^{th} percentile at 20^oC, showing that during 25% of the time the temperature set-point is ranging between 16^oC and 20^oC, whereas in the Room the percentile is limited at 18^oC.

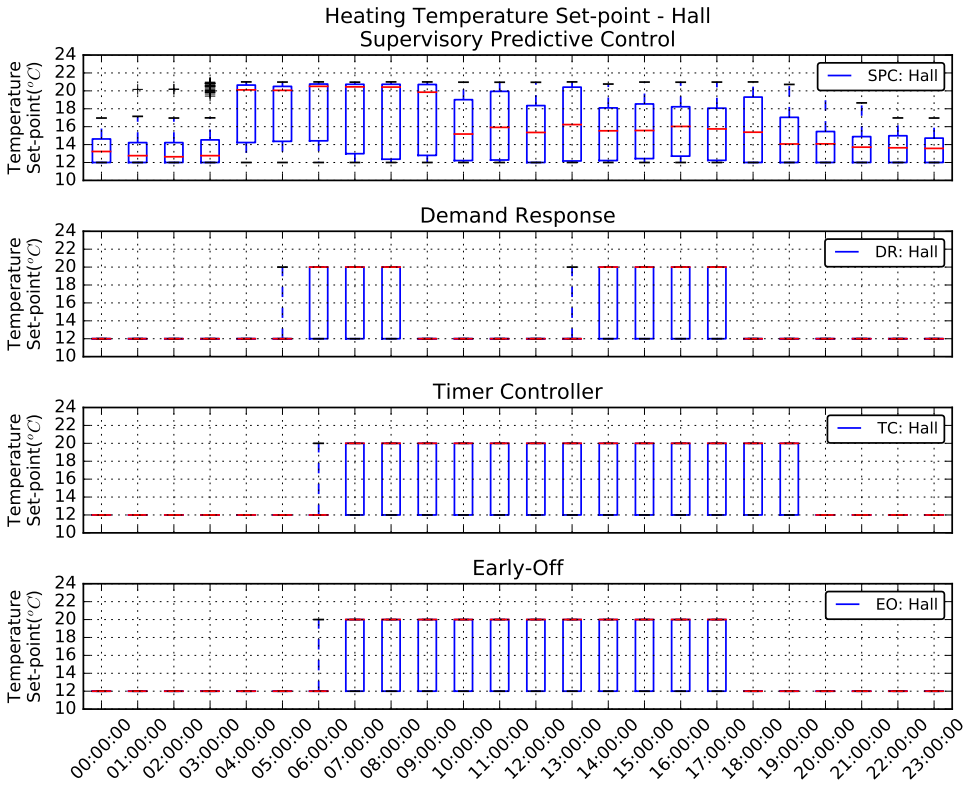

Figure 4.40: Comparison between control strategies of hourly distributions of the heating temperature set-points for the heating season applied to the Hall.

Heating season – Energy demand investigation

Figure 4.41 6.4 presents at the top the distribution of electricity power demand by the VRF systems observed by the simulation of the supervisory predictive control, followed by the differences from the conventional control techniques, to highlight the discrepancy between strategies.

Besides the fact that the median value of the power demand is monotonically decreasing through the day, the peak power demand required on the SPC simulation is observed at 5:00 on 01-24 accounting for 4363.9W, one hour after the usual start of the HVAC system. Conversely, the other techniques presented their peak value on the coldest day of the year which is the 17^{th} of January at the time of starting the HVAC system.

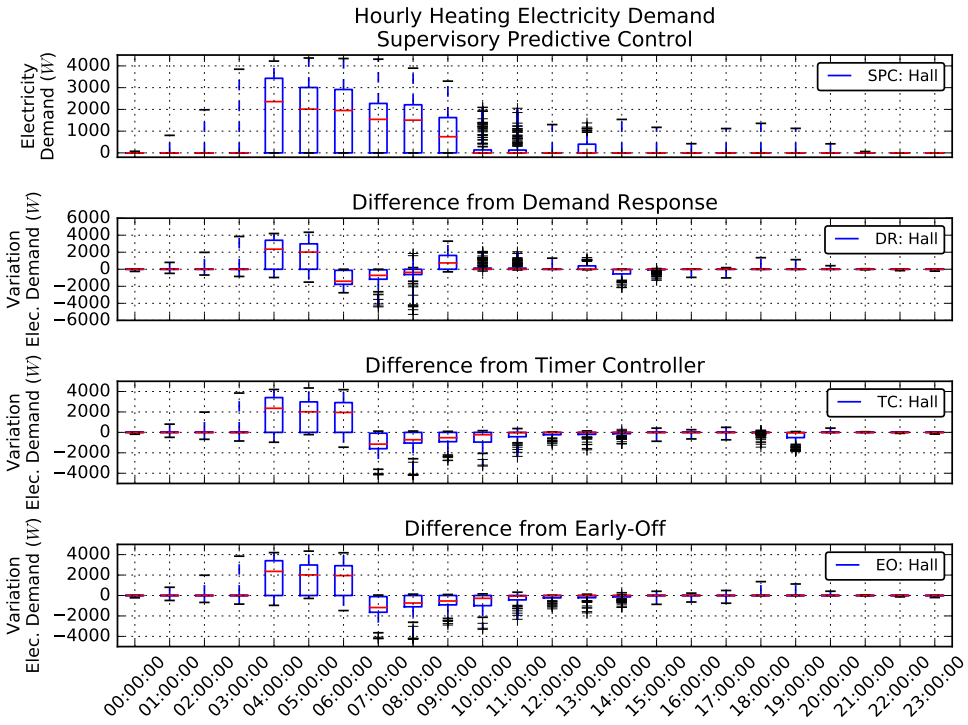

Figure 4.41: Hourly distributions of differences between conventional strategies and supervisory predictive control regarding electricity power demand.

The difference of the costs of energy observed in the whole heating season results is also seen in Fig. 4.41.. The energy consumption at the first two hours of the highest tariff, 10:00 and 11:00, presents a distribution highly skewed towards zero, presenting several outliers which reach power demands of 2000W. Therefore, 99.3% of the time, the energy consumption and related costs are close to zero between 10:00 and 12:00, reflecting the capability of the optimization process to avoid prohibitive periods of consumption. The energy demand then slightly increases again at 12:00, and more evidently at 13:00 when the energy costs decrease. This behaviour is of utmost importance regarding the paradigm of smart-grids, and demand side energy management where the energy consumption should be allocated to periods of high availability, low costs and carbon footprint [163].

Most of the conventional techniques presented in this benchmark start the HVAC system at 7:00 when the tariff changes from off-peak to regular, except for the Demand Reduction strategy that rises the temperature set-point one hour before. The supervisory predictive control managed to save energy even on that periods of regular tariff compared to the reference case-studies, leading the SPC to save energy and its related costs during all periods of costs over the off-peak tariff schedule and reinforcing its utility as demand

shift solution.

Heating season – Comfort investigation

This section focuses on the investigation of the effects on the comfort levels due to the decisions made by the supervisory predictive control during the heating season. Fig. 4.42 presents the results regarding the Predicted Percentage of Dissatisfied people in the Room for occupied hours. The comfort levels distributions observed for the SPC strategy are shown at the top of the figure, followed by DR, TC, and EO.

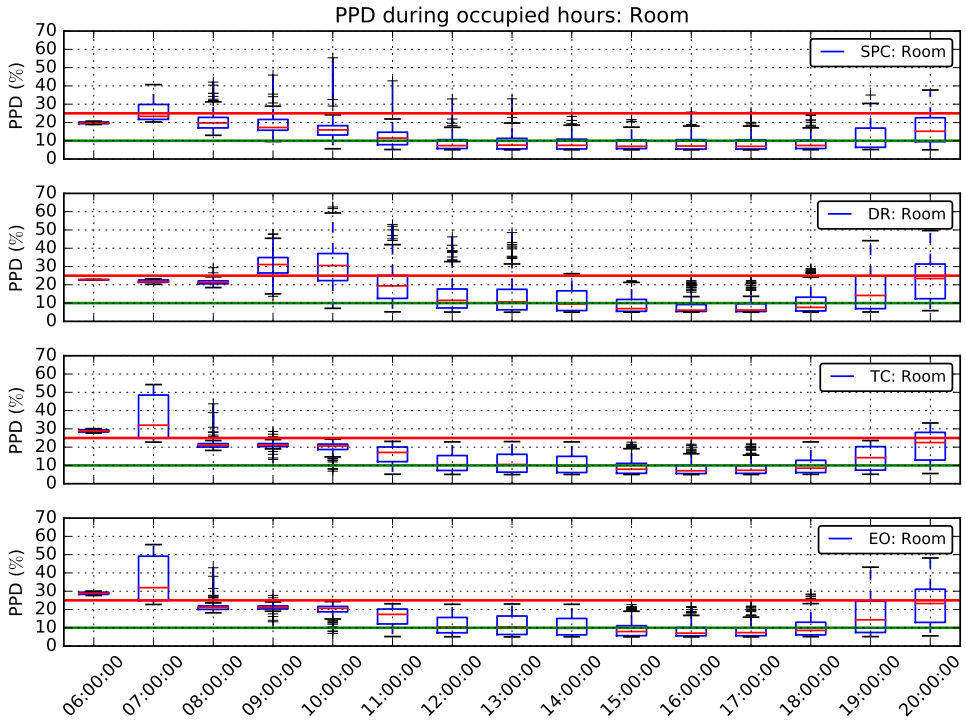

Figure 4.42: Comparison of hourly distributions of Predicted Percentage of Dissatisfied (PPD) in the Room during occupied hours only.

As it can be seen, the comfort levels provided by the supervisory predictive control in the Room satisfy the imposed limits for most of the occupied hours with the only exception at 7:00, where the distribution of the PPD shows that almost 50% of the values fall outside the imposed limit of 25%. Until 8:00, DR has managed to provide similar comfort levels as the SPC, since the latter has decided to heat the building at similar hours as DR. As expected, both techniques show lower values of PPD than the conventional techniques of TC and EO at the first occupied hours of the day.

After 9:00, the number of outliers over the PPD threshold on the SPC simulation is considerably high, when comparing it to the conventional techniques of TC and EO. The presence of such outliers might be originated by either model mismatches for the given hours, leading the optimization algorithm to converge to an unexpected result, or due to the investigation of the trade-off between the level of comfort and the energy costs at the given time of the day. Since the increasing of outliers is more evident after 10:00, and higher than TC and EO for the same time, it can be concluded that the main reason for such outliers might reside on the efforts for saving energy costs.

The inter quartile range (IQR) of the distributions presented shows a reduction of the variance of the PPD values throughout the day, concentrating these values closer to the median values (red line) which present a tendency to reach the optimization objective. The desired value of 10% PPD is mostly reached at 12:00, three hours before the other techniques, reflecting both the effort of the SPC in reaching the desired PPD defined on the optimization formulation, as well as the effects of increasing the temperature set-points earlier than the other techniques.

Figure 4.43 presents the cumulative distribution function for the PPD observed in the Room during the present simulation period, showing the estimated probabilities for each control strategy simultaneously. The red line represents the maximum comfort allowed.

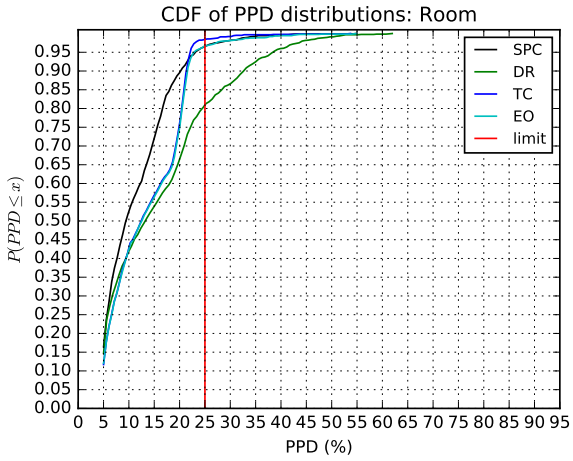

Figure 4.43: Heating season comparative analysis of Cumulative Distribution Functions of Predicted Percentage of Dissatisfied (PPD) for the Room.

As it can be depicted, TC and EO present almost the same values except after the 95th percentile where they diverge. These separation of EO follows the same pattern as the SPC after crossing the comfort limit of 25% PPD above the referred percentile. Thus, the remainder observations sum, which are violations of the PPD, accounting for less than the acceptable limit of 5% - the value proposed by De Coninck et al. [28].

The Demand Reduction presents the least steep slope of CDF, crossing the comfort constraint at a probability of 0.8. Hence, 20% of the whole period of the heating season simulation this zone is outside the acceptable comfort range when supervised by the Demand Reduction strategy.

If the comfort set was defined as 20% instead of 25% as it was, the SPC would perform better than the other techniques because the sums of observations lower than 25% are always higher on SPC than on the other techniques. As shown in Fig.4.43, the concentration of PPD values close to 20% is high for both TC and EO, representing that the given techniques favour PPD values of that magnitude.

Figure 4.44 shows the PPD distributions for each hour of the day in the Hall. The following exposition of results is similar to the discussion held for the case of the Room, since the results are rather similar. Besides the fact that the monotonicity of the hourly distributions of PPD in the Hall is similar to the Room, the observed values reflect a higher effort in achieving the desired comfort boundaries for all the techniques.

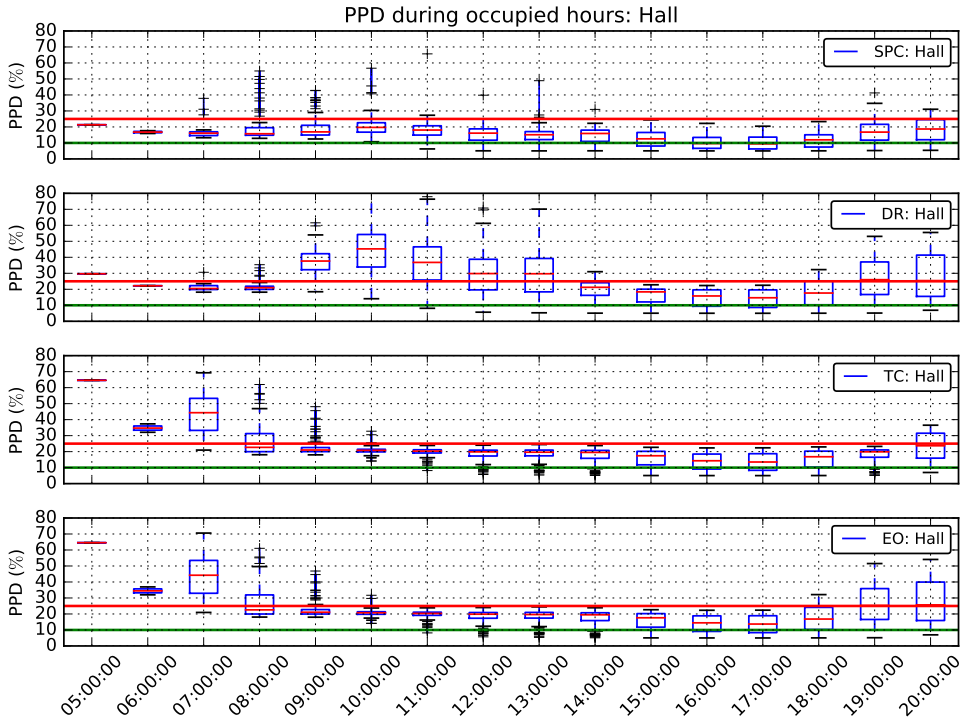

Figure 4.44: Comparison of hourly distributions of Predicted Percentage of Dissatisfied (PPD) in the Hall during occupied hours only.

The values observed show a clear superiority of the SPC, because the violations of the comfort limit are mostly found as outliers of the hourly distributions, except for the

9:00 and 10:00, as well as the end of the working day at 19:00 and 20:00. At these periods of the day, the violations of the comfort are representative of no more than 12.5% of all observations for each of the hours selected due to being at the whiskers of the respective box-plots.

Figure 4.45 presents the cumulative distribution function for the PPD observed in the Hall. The major difference observed in respect to the Room is the convergence of the lines of SPC and TC. In the case of the Room the cumulative distribution on the SPC control followed the probability of the EO after converging above the percentile 90^{th},whereas in this case, the probability follows the TC which provides better comfort levels. This behaviour mirrors the effort taken by the SPC to achieve the desired comfort levels.

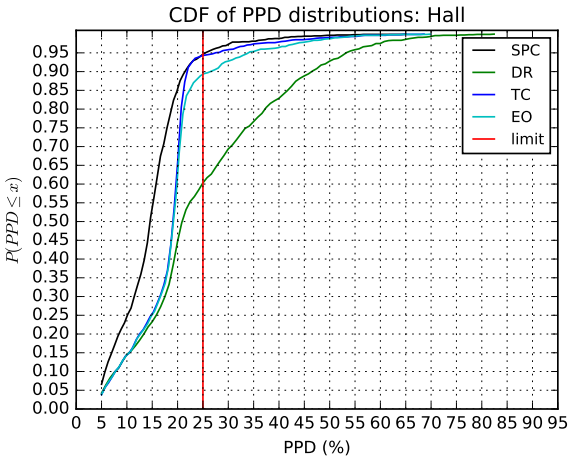

Figure 4.45: Heating season comparative analysis of Cumulative Distribution Functions of Predicted Percentage of Dissatisfied (PPD) for the Hall.

As it can be observed, the closest technique to the SPC regarding the occupants' comfort in the Hall is the TC which manages to reach the 95^{th} percentile at the same value of SPC close to a Predicted Percentage of Dissatisfied of 25%. The EO diverges from the best performing techniques reaching the 95^{th} percentile only at a PPD of 35% which lies out of the acceptable limits. Its probability of having values lower or equal to 25% is 0.9, meaning that 10% of the time EO presents comfort levels outside the acceptable threshold.

The worst performing technique is DR, presenting a probability as low as 0.6 for showing values within the acceptable range of PPD. Given the presented results, the SPC strategy is more likely to generate lower PPD values than the other technique presented, since it shows higher probabilities for any given PPD in both zones. i.e. the level of comfort in the Room and Hall with SPC during the heating season is expected to be always higher, or equal, comparing to the conventional control techniques.

4.6.4 Cooling season analysis

This section presents the performance benchmark during cooling season of supervisory predictive control against the conventional control techniques, namely the Timer Controller, Early-Off and Demand Reduction. The results presented here span the period of four months, from June 1^{st} to September 30^{th}.

Fig. 4.46 presents the performance benchmark for the whole cooling season. The overall costs regarding HVAC energy consumption show a higher discrepancy between techniques comparing to the heating season analysis performed previously. Moreover, the total costs and energy consumption using the SPC technique were accounted to be the lowest of all techniques tested. Thus, the most economical control strategy is the Supervisory Predictive Control with the other strategies presenting variations above 60% of the costs and energy consumption when comparing to 109.57€ and 616.23kWh observed using SPC, respectively. The most expensive control solution is the Timer Controller, accounting for more 105.90% of energy costs when comparing to SPC.

The best performing strategy regarding the PPD violations indicator is the SPC, summing up less 41.30% of comfort violations comparing to EO strategy which is the best performing strategy of the conventional solutions in this matter. Moreover, the average PPD on SPC achieved 14.18%, resulting on the best average comfort of all control techniques during occupied hours. Therefore, SPC strategy is the only one capable of achieving the category III for both air-conditioned zones, regarding the comfort standard EN 15251:2007 [63]. The fact that the Early switch-Off technique has managed to convey a more comfortable environment than the Timer Controller method expresses the counter-productive aspect of TC regarding the setting of temperature set-points two extra hours than EO. The following sections focus on the evidences of this response.

Table 4.23 summarizes the performance of the presented strategies based on the key indicators presented in Fig. 4.46, and on the metrics introduced previously in section 4.6.1. The APD metric represents the Accumulated People Dissatisfied which can be interpreted as a weighted version of the PPD by multiplying it by the number of occupants observed in each zone for a given time of the day.

Peak power demand is the maximum value of electricity power required by the VRF system during the simulation period, which in this analysis ranges from June 1^{st} to September 30^{th}. The specific energy consumption represents the energy intensity for the given season, and the energy costs are the expected costs allocated to the VRF system.

As it can be observed on the Table 4.23, the supervisory predictive control is the best performing strategy across all key performance indicators. The proposed strategy has managed to save energy consumption and the related energy costs while improving occupants comfort. Thus, is can be concluded that the conventional strategies presented in this case-study are neither fit to suit the comfort demand, or energy conservation during the cooling season for this climate region, considering the rules imposed to the system supervisor, namely the temperature set-points and its schedules.

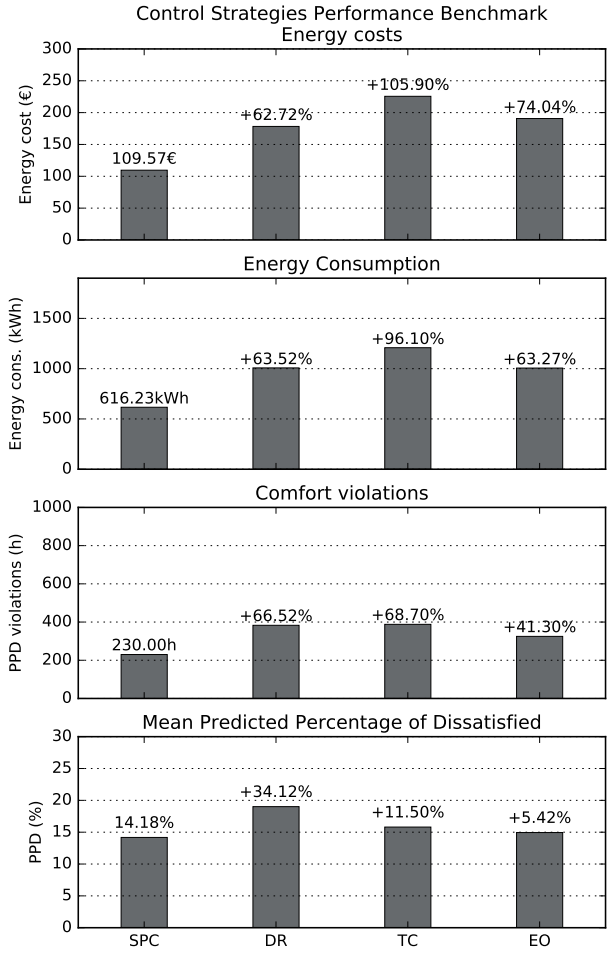

Figure 4.46: Control strategies performance benchmark for the cooling season simulation. SPC: Supervisory Predictive Control; DR: Demand Reduction; TC: Timer Controller; EO: Early-Off. From the top: the costs regarding the energy consumption of the VRF system; the energy consumption of VRF system; The cumulative violations of the comfort limit (PPD>25%); Building's average Predicted Percentage of Dissatisfied (PPD) across all air-conditioned zones.

Cooling season – Set-point investigation

This section focuses on the understanding of the reasons behind the behaviour of the Supervisory Predictive Control in performing better than the conventional techniques.

Table 4.23: Performance benchmark of the control strategies Supervisory Predictive Control (SPC), Demand Reduction (DR), Timer Control (TC), and Early-Off (EO). The simulation period is the **cooling season** starting on June 1^{st} ending on September 30^{th}.

	$\overline{PPD}$ (%)	PPD Room (%)	PPD Hall (%)	PPD_{viol} (%)	APD	Peak Power Demand (W)	Specific Energy Cons. (kWh/m^2)	Energy Costs (€)
SPC	14.18	13.46	14.90	11.19	1762	4226	2.97	109.57
DR	19.01	18.25	19.78	18.66	2447	4385	4.85	178.29
TC	15.81	14.80	16.81	18.90	1979	4263	5.82	225.60
EO	14.95	13.93	15.97	15.84	1885	6017	4.84	190.69

Figures 4.47, and 4.48 present the distributions of upper limits of the temperature set-points during the cooling season for all strategies involved in the benchmark.

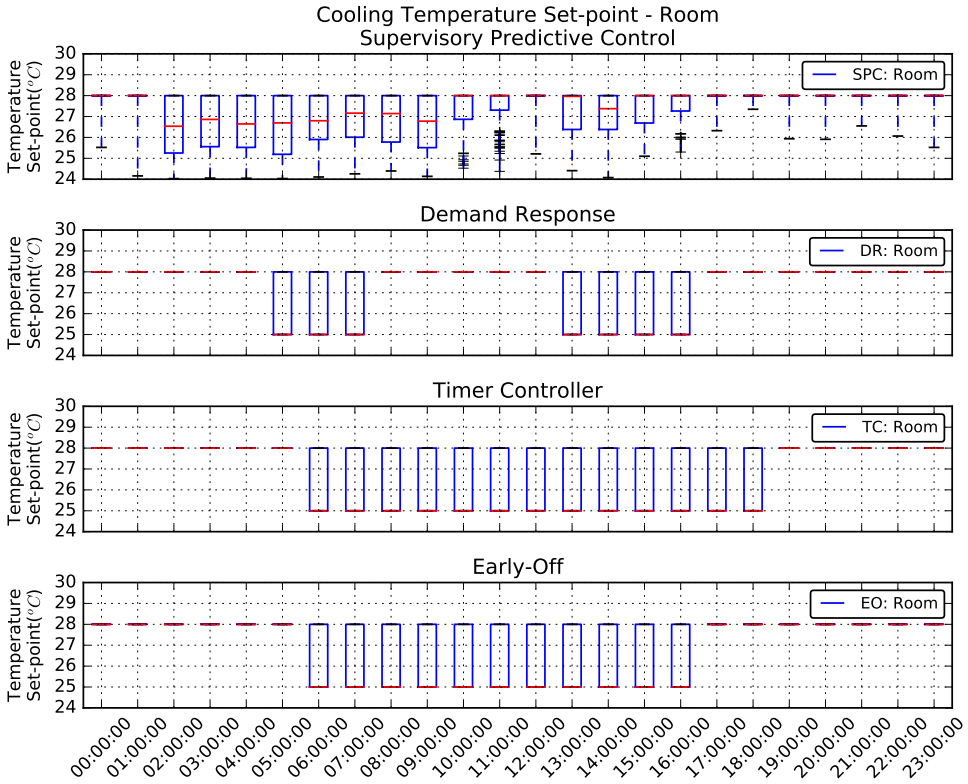

Figure 4.47: Comparison between control strategies of hourly distributions of the cooling temperature set-points for the cooling season applied to the Room.

As it can be depicted from Fig.4.47, the temperature set-points defined by the SPC

are mostly centred between 26^oC and 27^oC for the initial part of the day until 10:00. Afterwards, the set-points distributions become considerably skewed towards the set-back temperature of 28^oC, highlighting its attempt in reducing power demand at the peak tariff periods. The set-points are reduced again from 13:00 to 16:00, included. However, as exposed by energy consumption distributions in Fig. 4.49, the setting of temperature to such values at the beginning of the day does not induce cooling thermal loads in the building because there is no substantial energy consumption until 09:00, regarding the VRF system demands.

Figure 4.48 shows a similar response to the Room regarding the set-points imposition in the Hall for the cooling season. It is evident, however, a pre-cooling attempt in the early mornings, followed by a rise on the temperature set-points at the peak tariff time of the day, from 10:00 to 13:00, included. Afterwards, the set-point suffers a decrease until 16:00, when returning to the temperature set-back from 17:00 until the next day.

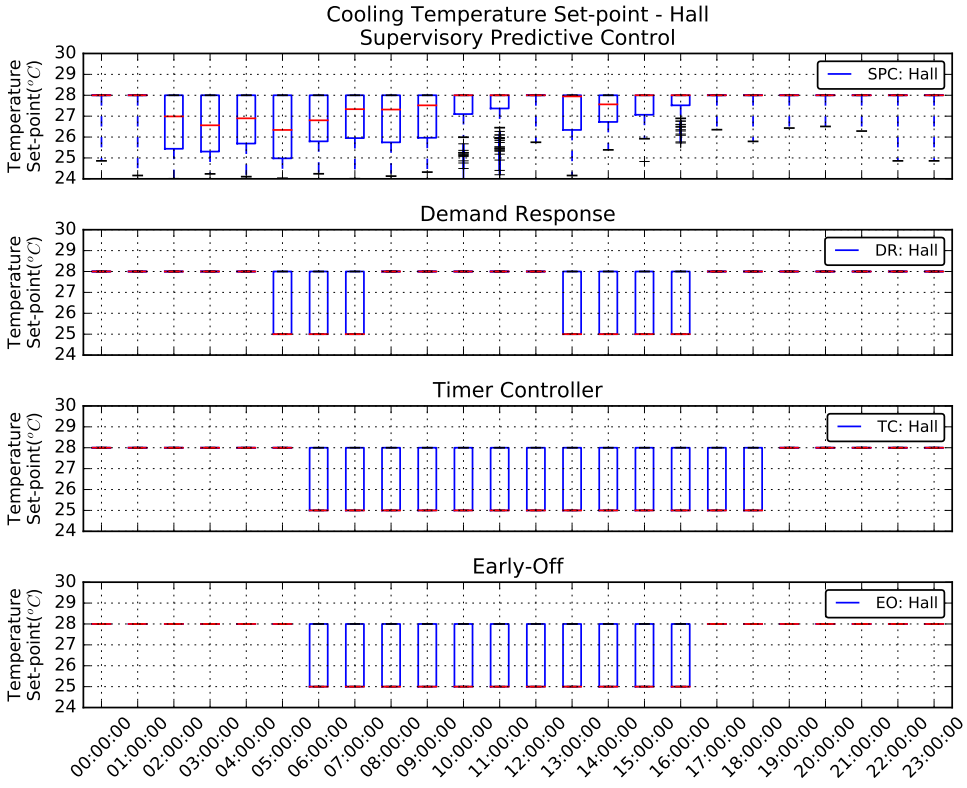

Figure 4.48: Comparison between control strategies of hourly distributions of the cooling temperature set-points for the cooling season applied to the Hall.

Cooling season – Energy demand investigation

The energy consumption observed in this simulation, Fig. 4.49, shows that the effort in the temperature set-points imposed by the Supervisory Predictive Control do not induce a significant energy consumption in the early mornings.

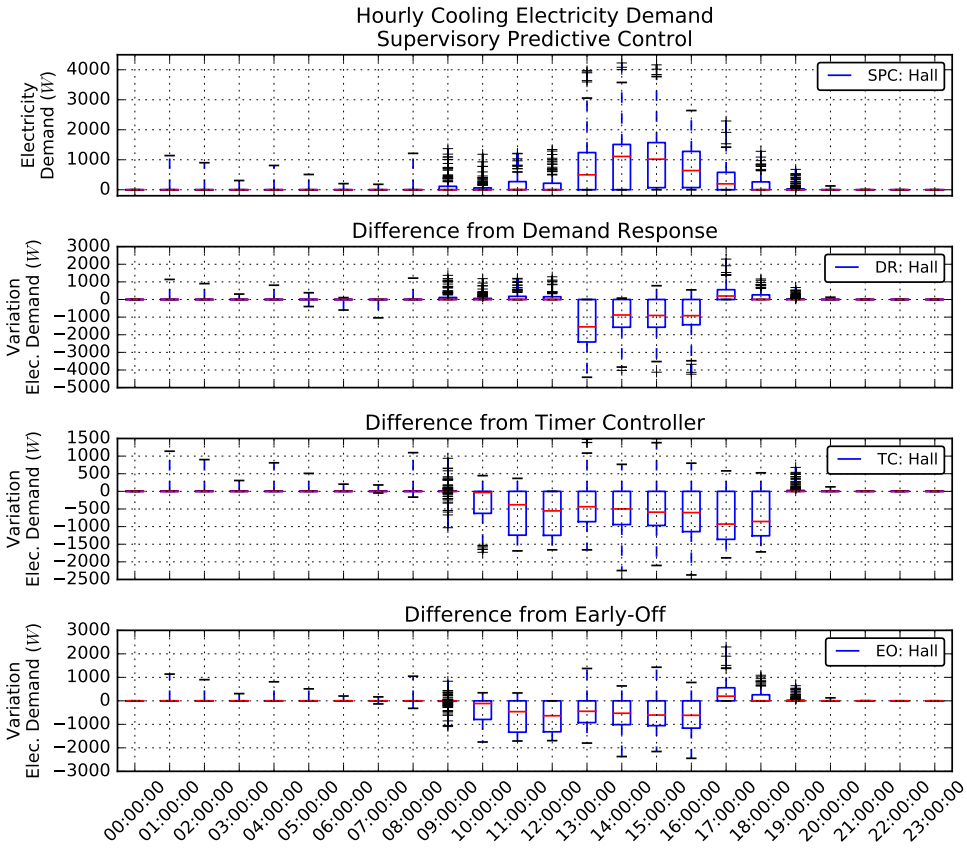

Figure 4.49: Hourly distributions of differences between conventional strategies and supervisory predictive control regarding electricity power demand for cooling loads.

When comparing the temperature set-points distributions in Figures 4.47 and 4.48 with the observed temperatures between 02:00 and 08:00, it can be concluded that pre-cooling can only be performed by the ventilation system and infiltrations because there is no relevant energy consumption between 02.00 to 08:00, and temperatures do not exceed the minimum cooling temperature set-point available (24^oC), as shown on table 4.24.

The maximum average temperatures observed in either rooms between 02:00 and 08:00 exclude the hypothesis of the set-points imposed by the SPC in being capable of

Table 4.24: Maximum observed values of averaged hourly dry-bulb temperatures for both air-conditioned zones and outside. Period of analysis ranges from 02:00 to 08:00, included, for the cooling season.

	Outside	Room	Hall
Max. $\overline{T_{out}}$ d.b. (^oC)	17.32±0.32 (02:00)	23.46±0.22 (08:00)	23.28±0.19 (02:00)

inducing any effect in the building thermodynamic state. The maximum average temperature within that period was observed in the Room at 08:00 equal to 23.46 ± 0.22^oC. Considering the 95% confidence interval imposed, it is unlikely that the VRF system is activated to cool the air-conditioned zoned during that period of the day.

Overall, the energy consumption induced by the SPC strategy is comparatively lower than the other techniques at the peak tariff hours, representing the effort in saving costs and the inefficiency of the conventional methods. The period of the day where the energy consumption registered by the SPC is higher than those of EO and DR is at the last two hours of the occupied time.

Cooling season – Comfort investigation

The hourly distributions of the PPD for the Room and the Hall are shown in Figures 4.50, and 4.51. The overall comfort is reduced at the beginning of the occupied hours. The fact that people are arriving in colder hours of the day, and the clothing insulation is being set to the cooling season (0.5 clo) might originate such rise on the PPD, and related comfort violations.

The minimum observed average PMV values between 05:00 and 09:00 were 0.93±0.07, and -1.06±0.07, for the Room and Hall, respectively. Therefore, the reason for the thermal dissatisfaction was due to the environment being slightly cool (According to the Fanger's PMV classification).

The incapability of the control techniques on working towards a better comfort level during those referred periods can be explained by a similar argument as the one exposed in the previous section regarding pre-cooling. The average temperatures of both zones are Gaussian distributed and present a mean and confidence interval boundary higher than the available temperature set-point limit for heating (21^oC), preventing the VRF to heat the interior environment. Table 4.24 exposes the maximum hourly averaged drybulb temperatures for both zones and exterior for the periods between 02:00 and 08:00, included.

After 10:00 all strategies have presented no violations of the PPD maximum limit. In fact, both EO and TC have managed to perform considerably better than the other techniques, exhibiting a virtually non-existent variance bellow the desired limit of 10% PPD in the Room and Hall zones, Figs. 4.50, and 4.51. However, it can be noticed that those strategies offering higher values of PPD at the end of the day (18:00), especially

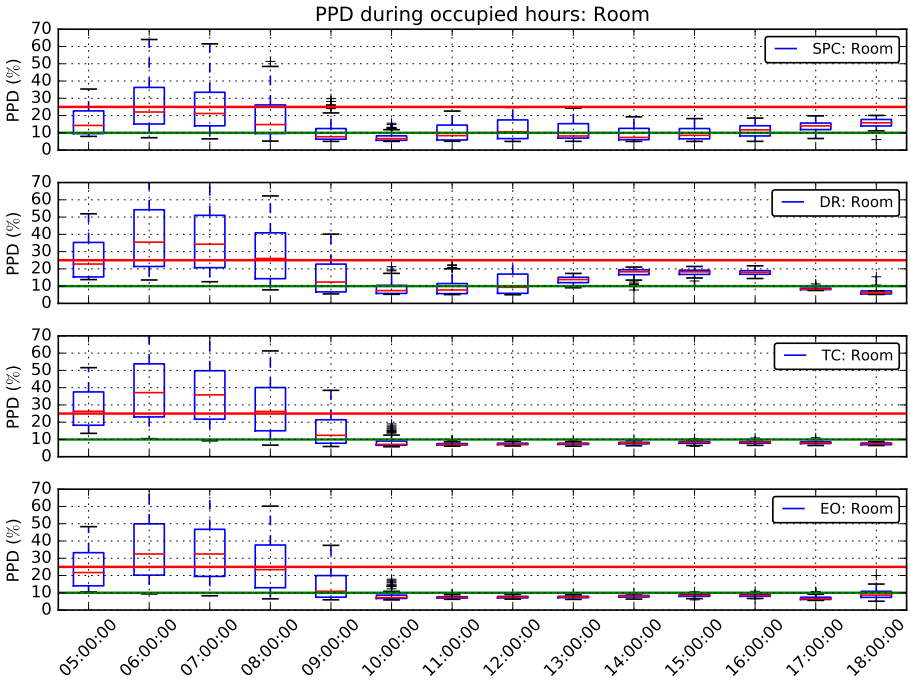

Figure 4.50: Comparison of hourly distributions of Predicted Percentage of Dissatisfied (PPD) in the Room during occupied hours only – Cooling season.

SPC and EO, that have managed to improve the comfort levels during the first hour of the occupied period (05:00), when comparing to TC.

Building's inertia might be the reason for such response. That is to say, when using TC strategy, the temperature at the end of the occupied period for the overall building is lower than when using the other strategies and manages to remain lower until the arrival of the occupants in the building because no internal loads are added during the unoccupied periods. Therefore, the occupants thermal perception is colder than when using the other techniques, especially in the case of supervisory predictive control. A note worth mentioning is that this observation is not directly inferable from a decision taken by the SPC, since from the end of the occupied period till the beginning of the occupation there is a period of ten hours, whereas the forecast window considered for this case study was six hours.

Overall, the Supervisory Predictive Control has managed to induce lower PPD levels than the other strategies, while reducing the energy consumption taking advantage of the acceptable range of comfort levels, as shown by the variance of the PPD throughout the last hours of occupied time (Figs.4.50, and 4.51), as well as the results of the probabilities of the cumulative distribution functions (CDF) of all strategies for a PPD of 25%, as presented in Fig. 4.52.

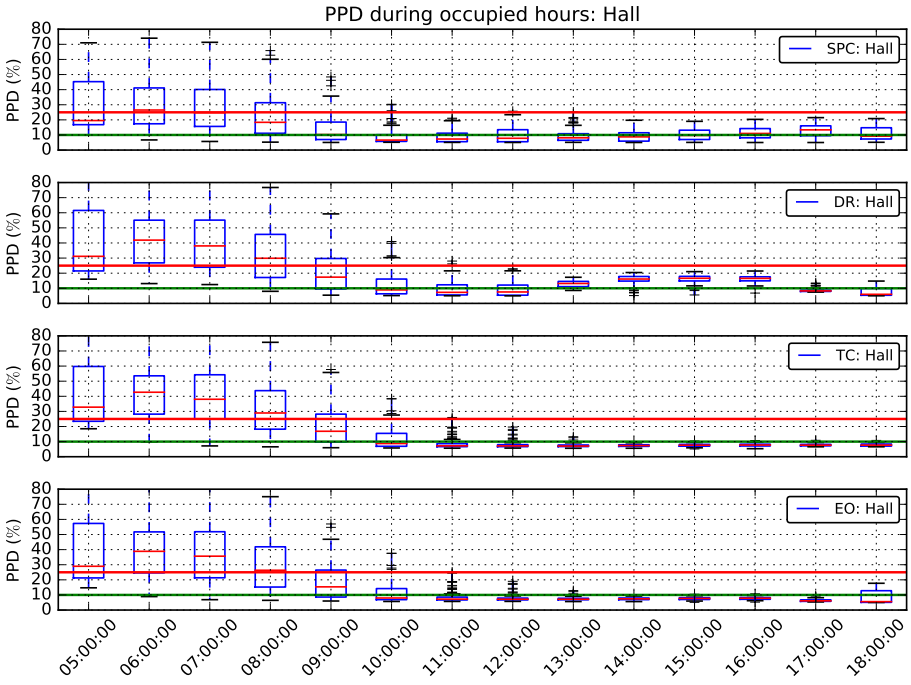

Figure 4.51: Comparison of hourly distributions of Predicted Percentage of Dissatisfied (PPD) in the Hall during occupied hours only – Cooling Season.

From this analysis it is quite clear the superiority of the SPC regarding comfort levels. The probability of finding PPD values lower or equal to 25% is clearly higher in the SPC, when comparing to the other techniques. The SPC managed to reach the percentile 90 before the PPD reached 25% in the Room, whereas in the Hall it reached the 25% above percentile 85.

The purpose of multi-objective optimization routines is to find solutions where competitive objectives are minimised simultaneously. The proposed supervisory predictive control has proved to achieve that demand by minimising both the expected dissatisfaction with the thermal comfort, while minimizing the energy-related costs for the heating and cooling seasons. Moreover, the optimization process conducted in this case-study has highlighted the inefficiencies induced by the conventional strategies during the cooling season by improving all key performance indicators simultaneously.

4.6.5 Whole year analysis

The whole year co-simulation process was held considering the period of simulation from the 2^{nd} of January to the 30^{th} of December, included. Fig. 4.38 presents the overall performance benchmark of the supervisory predictive control against the conventional

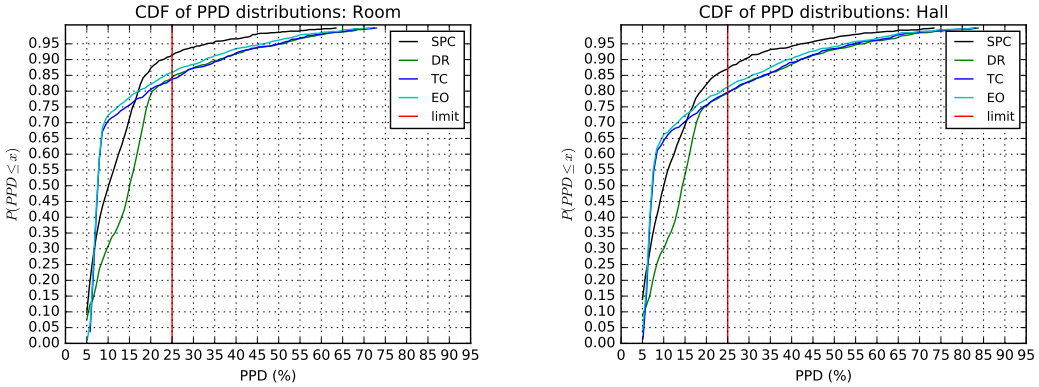

(a) Room.

(b) Hall.

Figure 4.52: Cooling season comparative analysis of Cumulative Distribution Functions of Predicted Percentage of Dissatisfied (PPD) for both zones. a) Room; b) Hall.

control strategies for the whole year co-simulation process.

The overall results favour supervisory predictive control. Regarding costs with electricity consumption it has managed to save 27.63%, when comparing it to the Early switch-Off strategy, which proved to be the most suitable of the conventional techniques concerning comfort related key performance indicators.

As expected, the overall energy consumption shows the least variability among solutions, since during cooling season the SPC has compensated the extra energy spent during heating season. Nevertheless, the overall difference between seasons has favoured SPC, designating it as the most conservative solution regarding energy consumption of

The comparison between the comfort results of all strategies has identified the SPC as the most interesting strategy, followed by EO and TC, concerning both the accumulated number of comfort violations and the average PPD observed in the building. SPC has violated the comfort limits 1021 hours in a total of 6071 occupied hours (sum of both zones), representing a percentage of violations equal to 16.78%.

The PPD levels show similar results to the comfort violations, when comparing SPC to EO. DR has managed to improve the difference to SPC, with an yearly average PPD considerably high, falling outside the acceptable limit. TC has managed to improve its variation, presenting a value identical to the EO strategy.

Table 4.25 summarizes the results for the key performance indicators for the whole year simulation.

Fig. 4.54 shows the monthly benchmark of SPC against EO concerning the energy cost at the top, followed by the energy consumption for cooling and heating, and the accumulated number of comfort violated hours. The choice for the monthly comparison between these two strategies lies in the fact that EO was the closest strategy to SPC

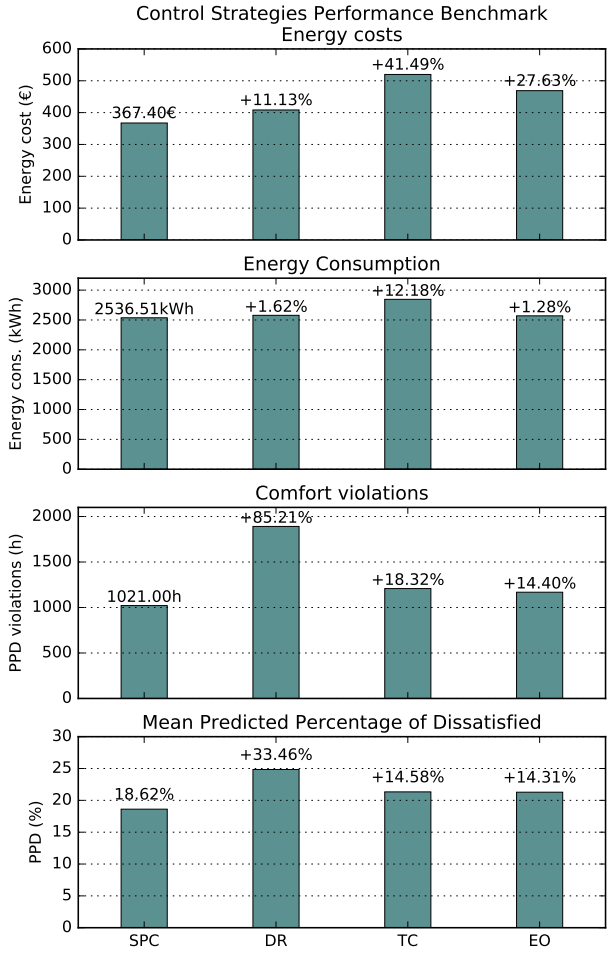

Figure 4.53: Control strategies performance benchmark for the whole year simulation. SPC: Supervisory Predictive Control; DR: Demand Reduction; TC: Timer Controller; EO: Early-Off. From the top: the costs regarding the energy consumption of the VRF system; the energy consumption of VRF system; The cumulative violations of the comfort limit (PPD>25%); Building's average Predicted Percentage of Dissatisfied (PPD) across all air-conditioned zones.

regarding their overall performance.

As depicted in Fig. 4.54, the source for the accumulated hours of comfort violations

Table 4.25: Performance benchmark of the control strategies Supervisory Predictive Control (SPC), Demand Reduction (DR), Timer Control (TC), and Early-Off (EO). The simulation period is the whole year starting on January 2^{nd} and finishing on December 30^{th}.

	$\overline{PPD}$ (%)	PPD Room (%)	PPD Hall (%)	PPD_{viol} (%)	APD	Specific Energy Cons. (kWh/m^2)	Energy Costs (€)
SPC	18.60	16.85	20.35	16.78	7236	12.21	367.39
DR	24.81	21.51	28.11	31.07	10070	12.41	408.27
TC	21.33	18.83	23.83	19.86	8329	13.70	519.82
EO	21.27	18.65	23.88	19.21	8273	12.37	468.92

resides especially in the months of April, May, June and September. This result is associated with the insulation clothing set for the cooling and heating seasons, being 1 and 0.5 clo, respectively. Two solutions could overcome this issue, either allowing the heating set-point to increase the temperatures observed in both zones in early morning or colder days, or varying clothing of occupants dynamically regarding the outdoor temperature observed in the morning of each day. The former hypothesis is more energy efficient since it would generate no additional energy consumption and people's comfort would be guaranteed. Accordingly, Garnier et al. have used an heuristic model to accommodate such a dynamic clothing simulation. The clothing was set every morning at 6:00 regarding the temperature *measured* outside the building [29]. Future works should take into account such an approach.

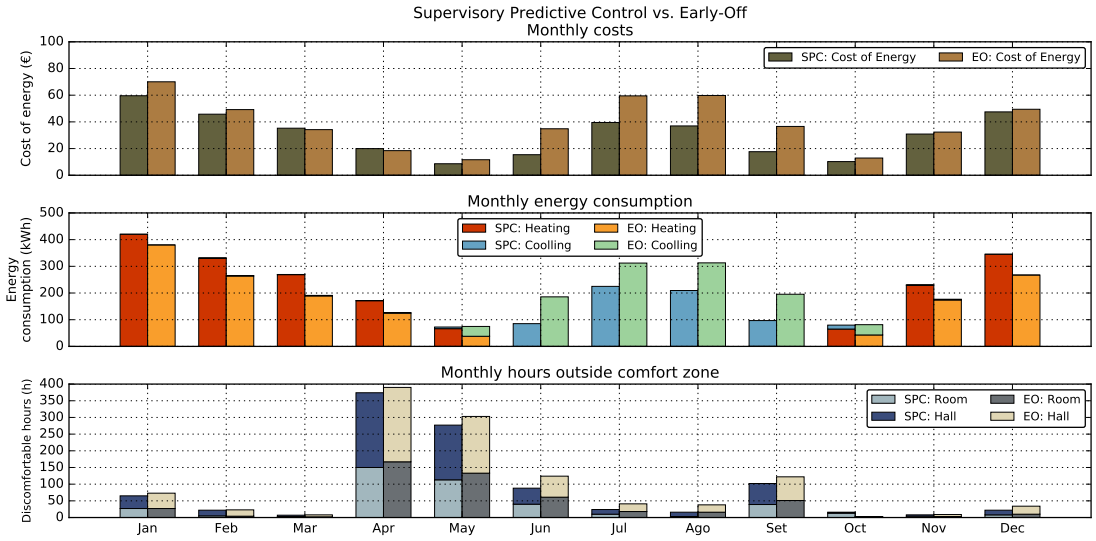

Figure 4.54: Monthly analysis of Supervisory Predictive Control vs. Early-Off control strategy.

May and October are the transition season since both account for heating and cooling energy demands. However, especially in May, the discrepancy between heating demand and cooling demand is notorious. Whereas EO spends roughly the same amount of energy for both types of loads, the SPC related energy consumption is mostly due to heating. Since comfort is improved in the SPC strategy for that month, it can be considered that this strategy has managed to suit thermal demand more accordingly. March and April are accounted for spending more energy when using SPC, rather than EO. Nevertheless, the energy consumption variation only favours SPC during cooling periods.

4.6.6 Computational cost of *eppyco*

The results presented in this section were conducted as a co-simulation process implemented in eppyco. A year analysis took 28h57min to conclude, operated on a laptop characterized by a processor i7-5600U CPU@ 2.60Ghz and 12GB of RAM. The mean time for convergence using the Differential Evolution algorithm was 20.40 seconds for a total of 5105 optimization routines. However, the Status Quo has managed to save approximately 41.8% of the time because rather than solving 8712 optimization problems (363d*24h) it has solved only 5105.

The time the algorithm took to converge shows a high variance, as presented in Fig. 4.55, displays a standard deviation of 19.98 seconds.

The implementation of such an approach during the design phase of a project might be prohibitive since a considerable amount of simulations are to be conducted. Future

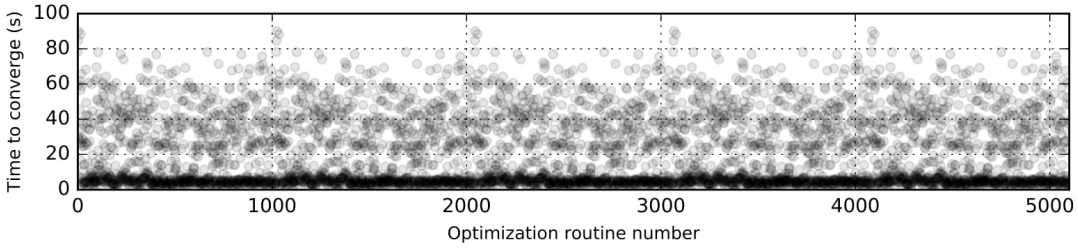

Figure 4.55: Converging times for the whole year co-simulation process using Differential Evolution Algotithm.

works should focus on improving the computational performance of *eppyco*. A possible direction of actuation could be to implement multi-thread computation on the optimization process, as well as using memory to store feasible solutions of the optimization processes conducted previously so it could enhance time for converging. As pointed out by Branke [166], "If the optimum repeatedly returns to exact previous locations, that's perfect for memory-based Evolutionary Algorithms". The optimization problems conducted in this thesis did show a tendency towards specific values of temperature set-points in the set-point analysis presented in Figs. 4.39,4.40,4.47, and 4.48.

The maximum observed computational time was 90 seconds. In a real world implementation of the supervisory predictive control presented in this case study, this elapsed time would be computationally affordable since it would take only 2.5% of the decision time-step available (1 hour). The optimization process could be started only 90 seconds before the end of the hour to maximize the information available before sending the decision. In the event of remaining sufficient time for repeating the process, the optimization convergence presenting better objective function value would be taken as the control solution for the next time-step.

4.6.7 Supervisory Predictive Control robustness investigation

This section presents a series of co-simulation processes in order to infer the robustness of the presented supervisory predictive control. The first test focuses on the investigation of inducing noise to the disturbances forecast as presented in section 4.4.2. The second studies the effects of varying the forecast window in the supervisory predictive control process, from 6h to 12h. The third tests the SPC using a constant energy tariff, i.e. minimizing energy consumption rather than costs. At last, the test will deal with two particular cases of occupancy abnormally. The simulation period is the same for all analysis, starting on 16^{th} of January, ending on 22^{nd} of January, included.

According to the previous simulations, the simulation conducted considered a forecast window of six hours. The weighting parameter of the multi-optimization problem formulation, α, was set to 0.9, the objective for PPD was set to 10%, and the penalty

at 25%.

Inducing uncertainty in disturbances forecast

Section 4.4.2 presented the uncertainty induction procedure in order to provide realistic scenarios of disturbances forecast.

The chosen standard deviation multiplier, λ_i, follows a linear function from 0 to 0.05, for a maximum forecast window of 24h to accommodate the forecast error expected for predicting outdoor temperature with 24h of window. The error induction to all disturbances varibles was presented on Table 4.14 of section 4.4.2.

The addition of the presented error to the disturbances forecast expects an increasing of surrogate models mismatches because the inputs will no longer represent the forecast window accordingly. The error propagation from the disturbances forecast to the prediction of the energy consumption is highlighted in Fig. 4.56. As it can be depicted in the example figure, the induction of noise in the inputs has led the random forest error to diverge to the triple of the expected error without considering the induced error at the end of the forecast window, i.e. 24h. The error estimation without considering forecast uncertainty saturates around 27W and encounters its maximum at $t + 14$ hours with an error equal to 27.71W. However, the estimated error deviates substantially when noise is added to the disturbances forecast. The maximum estimated error when noise is added to the forecast increases to 92.78W at t + 20 h.

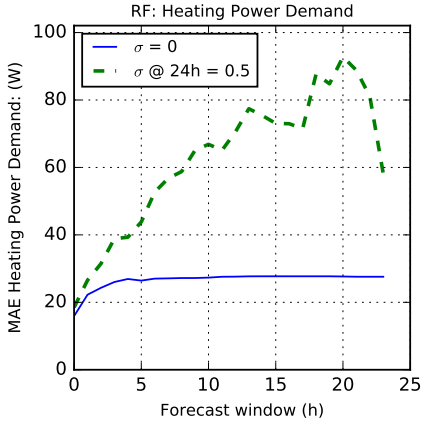

Figure 4.56: Uncertainty propagation on the predictions of Heating Power Demand by Random Forest model over a forecast window of 24h subjected to disturbances forecast noise. The noise generation used a λ_i of 0.5 for i equal to 24h.

Figure 4.57 shows the building response to the supervisory predictive control decisions, considering the imposed uncertainty. As shown, the SPC has managed to avoid major control pitfalls. Since the error is gradually increasing throughout the window

forecast, the SPC can adapt to the new scenarios if the expectations gradually become more accurate in the approximation of the time of decision $(t+1)$.

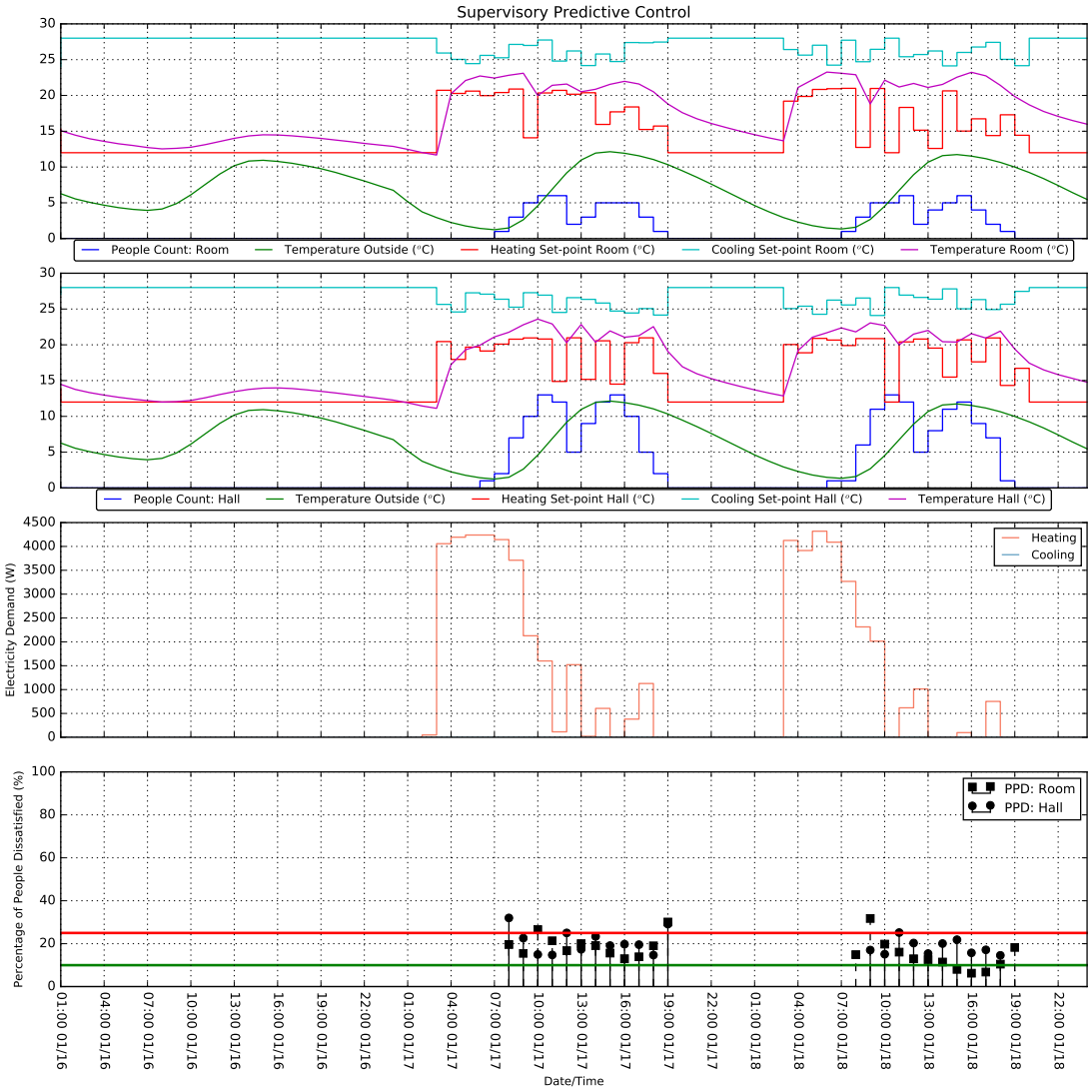

Figure 4.57: Winter's design week simulation of supervisory predictive control inducing disturbances forecast uncertainty with λ_i equal to 0.5 for i equal to 24h.

The behaviour of the SPC presents no relevant differences to the set-points investigation on the heating season in section 4.6.3:

- The heating set-points are increased four hours before building occupants arrival at 8:00;

- The energy consumption was 58652Wh, and the energy related costs summed up 8.75€.
- The SPC has managed to reduce costs by minimizing consumption at peak hours to zero, especially at 12:00 on the 17^{th} and at 11:00 on the 18^{th};
- The percentage of comfort violations is 15.2%;
- The average PPD for both zones is 18.14%, with Room and Hall equal to 16.66% and 19.77%, respectively.

In conclusion, this analysis refers to the effectiveness of the SPC in accommodating the uncertainty of disturbances forecast. The Summer version of this simulation is presented in Appendix A.

Varying forecast window size

The following study investigates the influence of increasing the forecast window to 12h instead of the previously used six hours. Figure 4.58 shows the building's response to such a configuration of Supervisory Predictive Control.

The major difference encountered lies in the computational time it takes to solve each optimization problem. The total simulation time accounted for 2h44min, representing a convergence time of 4min34s. Therefore, the computational time has increased 13 times comparing to the SPC using a forecast window equal to six hours. Moreover, the optimization space domain has changed from 24 dimensions to 48, increasing the complexity of the optimization problem.

The list bellow summarizes the performance of the current robustness test:

- The heating set-points are increased five hours before the building's occupants arrival at 8:00;
- The SPC has managed to reduce costs by minimizing consumption at peak hours to zero, especially at 10:00 on the 17^{th} and at 11:00 on the 18^{th};
- The energy consumption was 60429Wh, and the energy related costs summed 8.80€.
- The percentage of comfort violations is 13.04%;
- The average PPD for both zones is 19.15%, with Room and Hall equal to 17.52% and 20.93%, respectively.

The time considered by the SPC to start the heating process was at 03:00, an hour before the time defined using six hours of forecast window. Accordingly, the energy consumption has increased to 60429Wh, when comparing to the 58652Wh observed

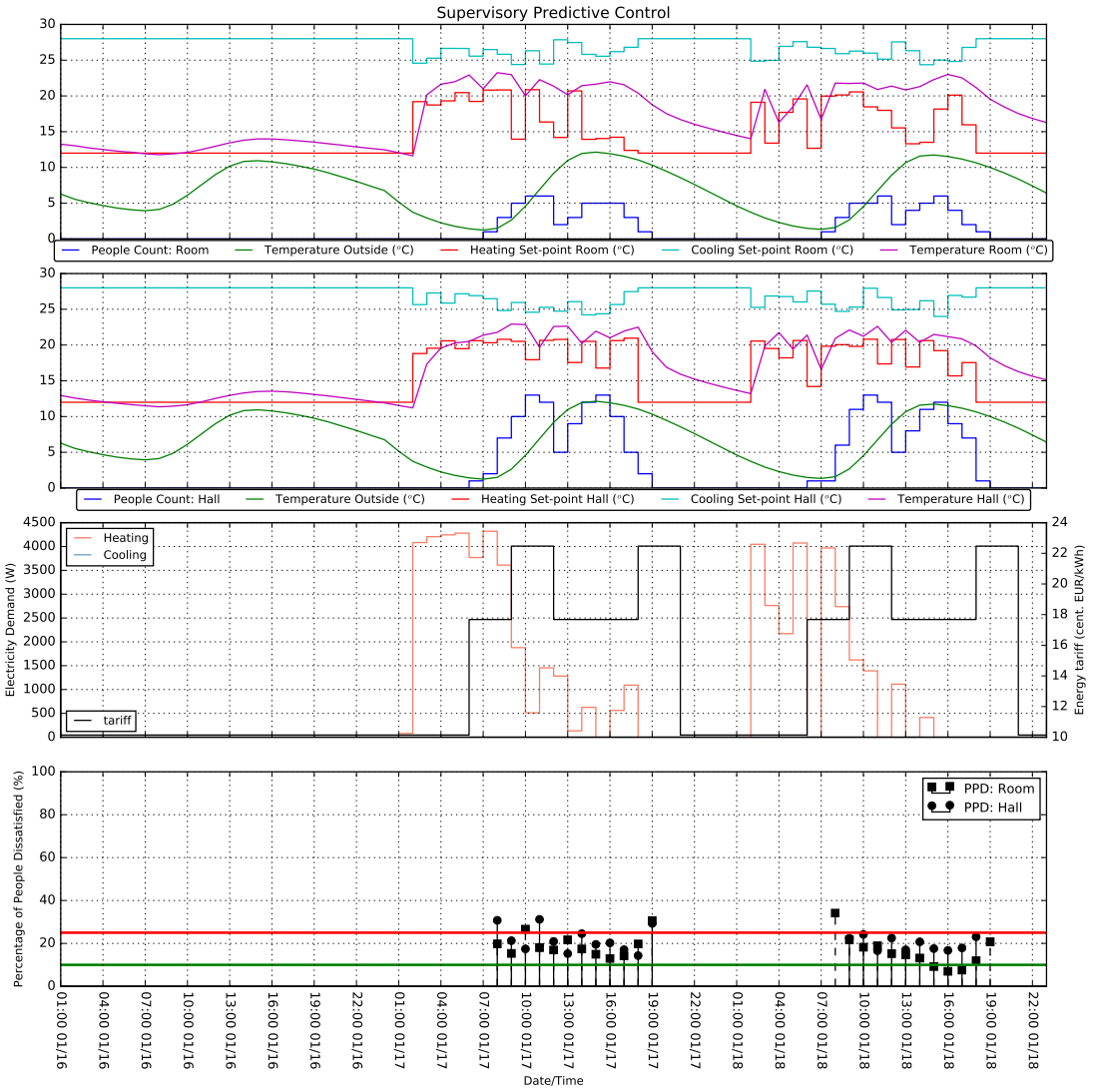

Figure 4.58: Winter's design day simulation of supervisory predictive control considering a forecast window equal to 12h.

in the previous example of section 6.7.1, representing an increase of 3.02%. However, regarding costs, the current strategy was capable of saving 0.5%, from 8.80€ of the previous example to the 8.75€ of this one. Regarding occupants comfort, violations of PPD have decreased to 13.04%, besides the fact that the overall PPD has increased, when comparing it to the previous example.

In conclusion, this test highlights the utility in increasing the forecast window to 12h. Besides the fact that the energy consumption has increased, the costs were improved

along with the number of violations to comfort. Such a window would provide the SPC with more information, which could help it to take better decisions regarding events further in the future. For example, given a situation similar to the one observed during the cooling season, the SPC could infer what would be the decision to take at the end of one day considering the information of the next morning. The drawbacks in using such a forecast window could be the computational time, and the available forecast. In fact, the computational time presents itself as a limitation, only in a design phase where several simulations might be required, because in a real world application, the time to converge is still acceptable for solving an optimization in the last 10 minutes of each hour. The Summer version of this simulation is presented in Appendix A.

Energy minimization objective function formulation

The section focuses on analysing the performance of the supervisory predictive control considering a constant tariff and equal to 1. Hence, the optimization problem which previously was set to minimize the energy costs while guaranteeing the desired comfort, has been converted to an energy conservation problem, bypassing the energy tariff expected in the optimization formulation.

Figure 4.59 presents the building's thermal behaviour considering a SPC focused on minimizing the energy consumption. It can be observed that besides the energy reduction due to inertia, the predictive controller has made no evident decision in saving energy during the peak tariff time. For example, the heating temperature set-point in the Hall has only been reduced at 14:00, and two hours later in the Room on the 17-01. Accordingly, the cost related to energy has been increased compared to the previous examples, accounting for 9.07€ which represents an increasing of 3.66% when comparing it to the SPC using 12h of forecast window. However, the energy consumption has been reduced successfully comparing to both cases presented previously, accounting for a reduction of 9.51% if compared to SPC using a 12h forecast window.

The following list summarizes the performance of the robustness test using a SPC targeted to energy consumption reduction:

- The heating set-points are increased three hours before the building's occupants arrival at 8:00;
- The SPC has managed to reduce the energy consumption overall to 54681Wh, and the energy related costs summed 9.07€.
- The percentage of comfort violations is 17.4%;
- The average PPD for both zones is 19.15%, with Room and Hall equal to 19.62% and 19.67%, respectively.

This result attests the versatility inherent to the SPC proposed by this thesis. As it was observed, the SPC has accomplished the task of saving energy consumption. Such a

formulation might be useful in conditions when the energy prices, or the energy supply are constant. This approach seems to fit the requirements for problems regarding energy conservation.

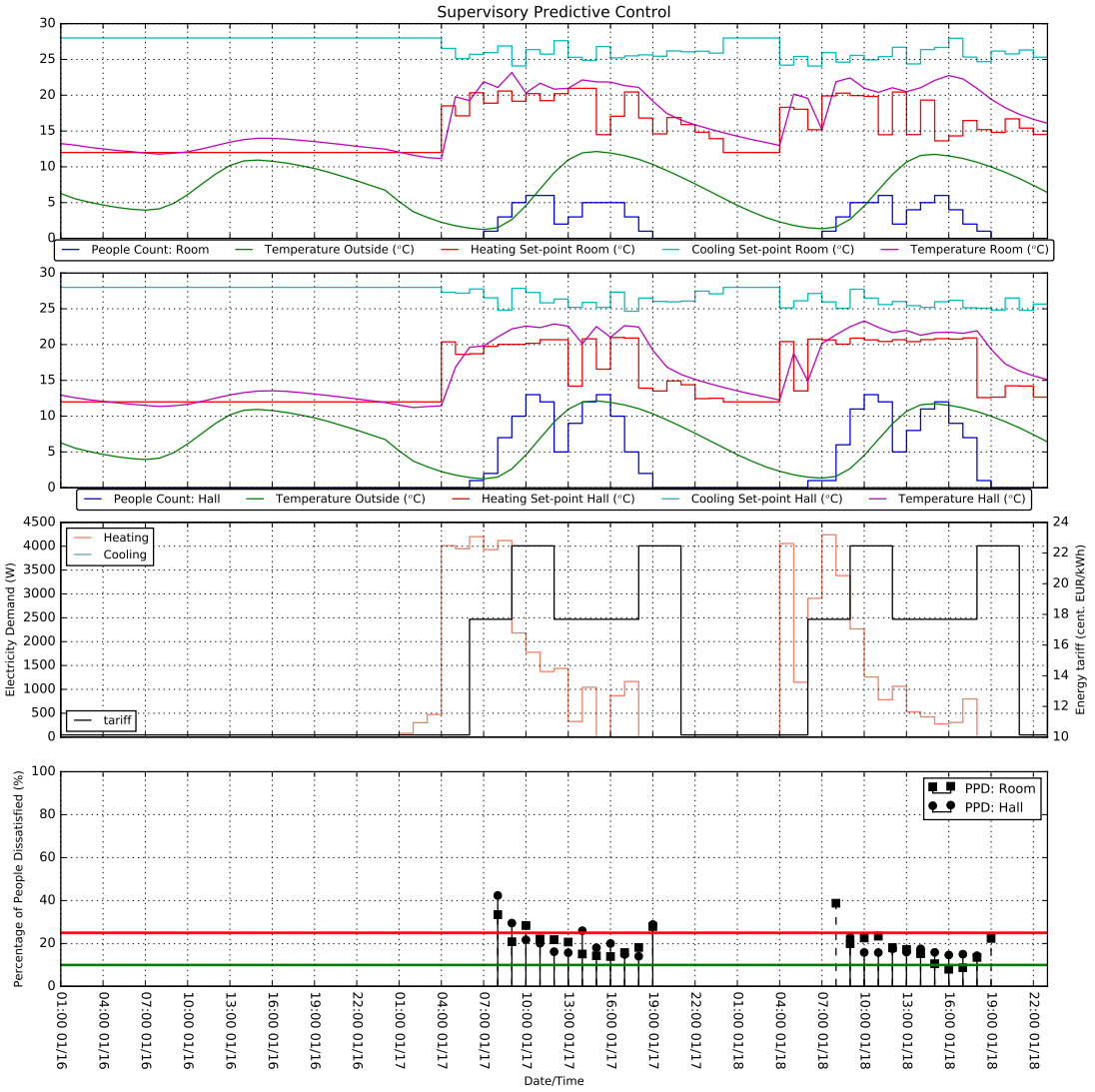

Figure 4.59: Supervisory Predictive Control performance considering energy tariffs constant. Simulation period from 16-01 to 18-01, including coldest day of the year – 17-01.

Table 4.26 summarizes the simulation for both the Winter day referred previously and the Summer day to allow for a comparison with reference control techniques presented in Section 4.2 which considered only the energy consumption and comfort results for the

period of a day.

The results regarding the supervisory predictive control performance on the Summer day, considering the optimization of the energy consumption rather than the cost of energy are presented in Fig. 4.61

Table 4.26: Energy and comfort performance of the reference case-study using Supervisory Predictive Control strategy, minimizing the energy consumption and discomfort.

Metric	**Winter day**	**Summer day**
Accumulated people dissatisfied	43	19
Percentage of PPD >25%	29.17%	0 %
$\overline{PPD}$	21.65 %	11.79 %
$\overline{PPD}$ @ Room	21.02 %	10.14 %
$\overline{PPD}$ @ Hall	22.27 %	13.43 %
Peak electricity demand	4200 W	2763 W
Energy Consumption	31234 Wh	14031 Wh
Specific energy consumption per m^2	150 Wh/m^2	67 Wh/m^2

The benchmark of these values against the baseline case-studies show that the Supervisory Predictive Control manages to provide better comfort in the Winter at the expense of spending more energy. When comparing it to EO, which is the reference case-study presenting lower energy consumption than SPC, being still relevant regarding comfort. However, when analysing the Pareto fronts for both Winter and Summer days, Fig. 4.60, provided by the performance results of the control techniques under investigation, it is clear that the SPC conveys more utility than the other techniques for both seasons. Therefore, regarding the trade-off between energy consumption and comfort, SPC is the most interesting solution.

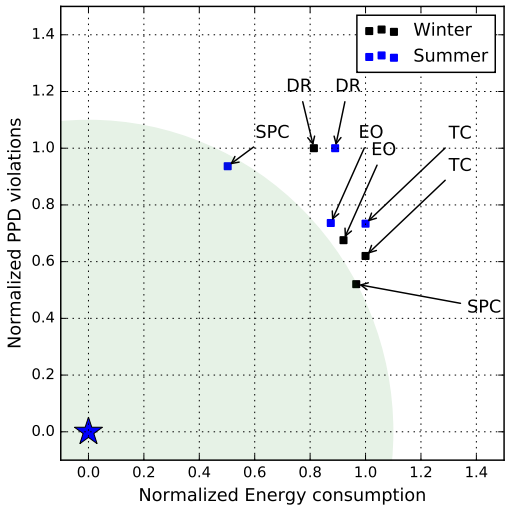

Figure 4.60: Winter and Summer analyses of Pareto fronts of the control techniques under investigation. SPC problem formulation focused on energy minimization.

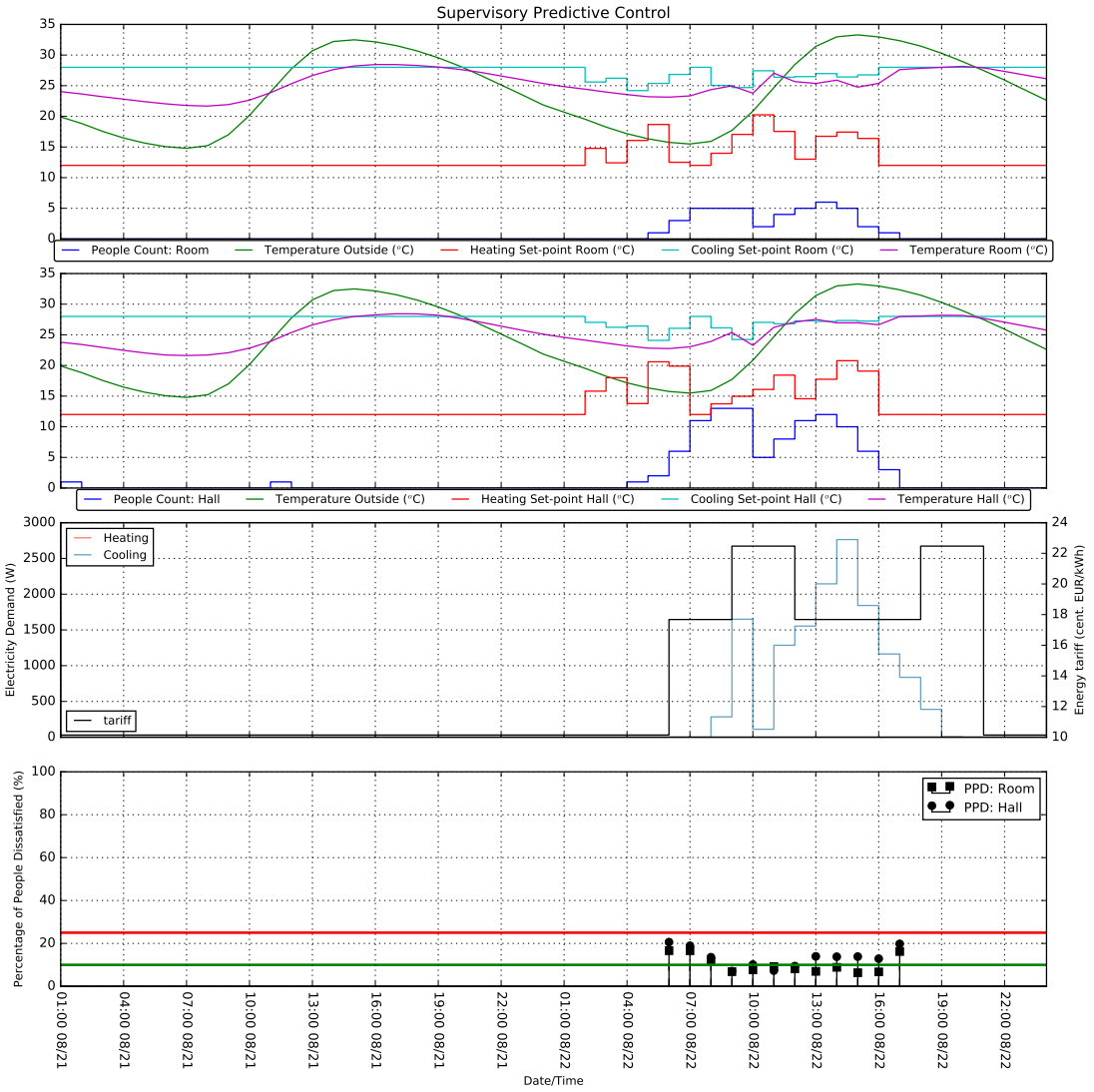

Figure 4.61: Supervisory Predictive Control performance considering energy tariffs constant. Simulation period from 16-01 to 18-01, including warmest day of the year – 22-08.

Dealing with abnormal occupation patterns

The final case-study to infer the robustness of the proposed SPC focuses on the scenario of abnormal occupation. For that purpose, an anomaly was introduced in the simulation files and forecast data to simulate an event when the building is occupied in abnormal periods of functioning.

It can be depicted in Fig. 4.62, a total of 25 people occupied the Hall of the building

from 18:00 till 02:00 on a Sunday evening. Moreover, six people occupied it for two additional hours, one at 17:00 and again at 03:00.

Overall, the SPC has managed to prepare a thermally comfortable environment to the occupants. Four PPD violations were observed during the special scenario of occupation which lasted for 11 hours, representing 36.4% of the occupied time.

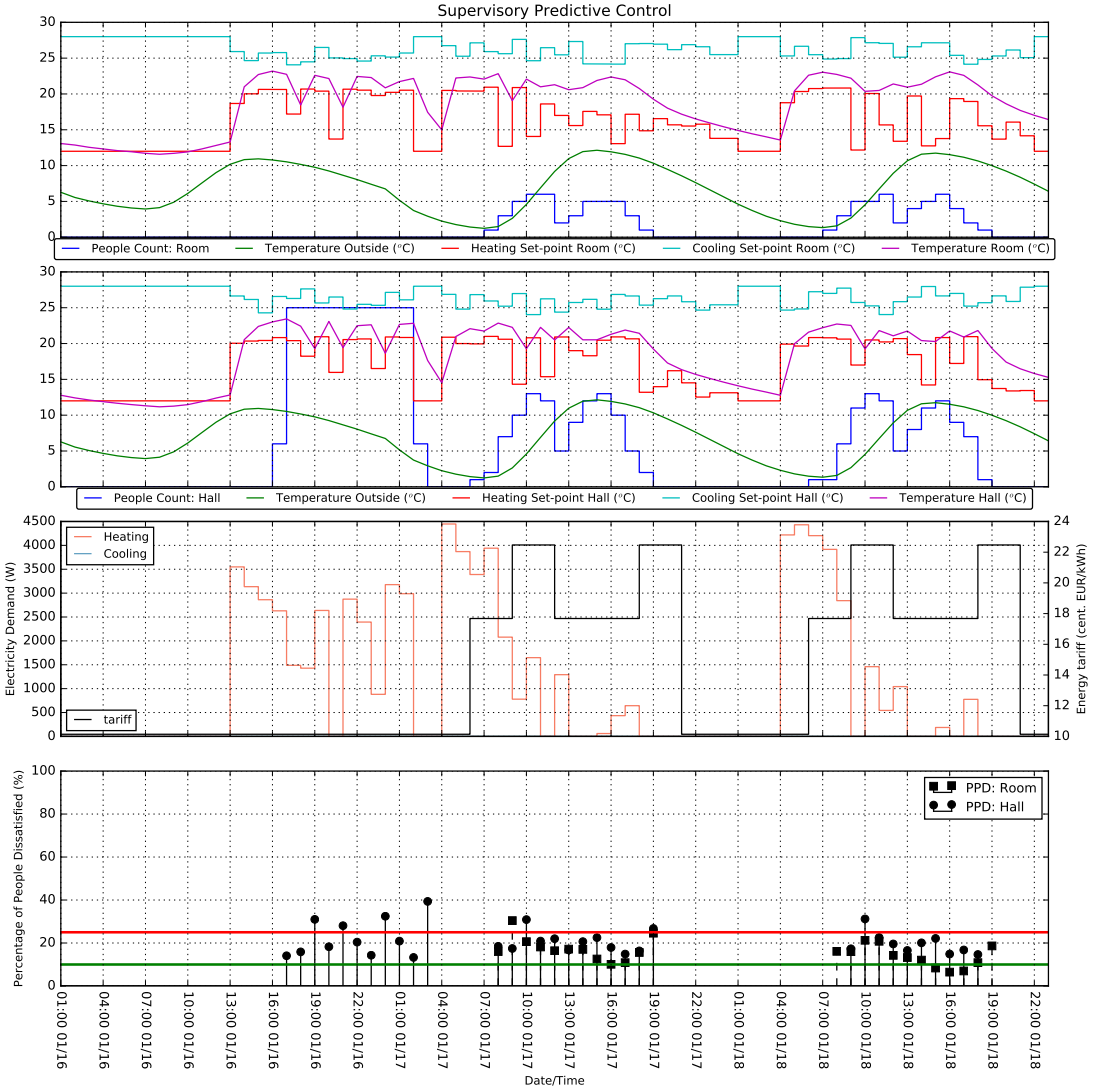

Figure 4.62: Winter's design day simulation of supervisory predictive control considering abnormal occupation pattern.

The procedure was similar to the results presented so far, where the temperature set-

point was set three hours before the arrival of the six people. However, not only the set-points of the Hall were changed, but also the Room temperature set-points, suggesting a possible interdependence induced by the predictive models in relation to the controllable variables, i.e. so far, all the training data has contained data samples with occupancy between zones correlated (see Fig. 4.12). This effect can influence the models to divide the importance of variables equally when no guaranteed influence exists. For example, the predictive model of the PPD of the Hall has assigned the same importance to the PPD of the Room (Table 4.10). Besides the fact that there is heat transfer between adjacent zones, it can be an over estimation by the SPC as well, deciding upon heating an adjacent zone to help heating the zone requiring to be heated. The problem regarding such a behaviour resides in the energy required for accomplishing the desired objective, which might not be optimal.

Future works should focus on the investigation of the decision making taken by the SPC to infer the true nature of decisions and help understanding when a decision is being biased due to model characteristics. The Summer version of this simulation is presented in Appendix A.

4.6.8 Energy Management Systems towards sustainability

It does not matter how energy efficient a building architecture, an HVAC system, a boiler or a fan unit might be if they operate in an inefficient way. The results presented throughout this chapter highlighted the capability of the proposed supervisory predictive control in finding acceptable compromises between comfort and energy consumption. In particular, the efficacy of the proposed strategy in reducing costs related to energy by naturally applying demand shifting seems well aligned with the current and future energy framework.

The standard BS EN 15232 has estimated that the retrofitting of the control systems of buildings HVAC systems have an energy saving potential factor of 0.87 of the energy consumption when conventional control solutions are retrofitted to advanced controls contemplating optimization [167]. The estimation of the yearly energy consumption of the co-simulation process regarding the energy consumption minimization can be computed by a weighted sum of energy consumption for the Winter and Summer design days (5*Energy Winter day + 4*Energy Summer day) from Tables 4.27, and 4.4, for the estimation of SPC, and EO, respectively. The accomplished saving potential factor equals 0.88, which is 1% higher than the value proposed by the BS EN 15232. The comparison of the energy consumption of SPC with the TC control solution, from Table 4.3, shows an energy saving factor of 0.80 in favour to SPC (20% of savings). This value is quite above the proposed by the referred standard but more aligned with the 30% expectation of energy saving potential due to the implementation of an advanced control [23].

The building used as case-study can be considered a modern office building with a construction appropriate for energy conservation, namely insulation, fenestration, and

HVAC system. However, without the inclusion of intelligent energy management, the advantage of energy efficient construction elements and system is not fully exploited as verified by the presented results. Therefore, the retrofitting of the construction elements and systems cannot be expected to capitalize the improvement of the energy efficiency alone. However, retrofitting assessments that consider the implementation of an energy management system capable of adapting to the conditions of the building energy state, would provide an additional possibility for reducing the carbon intensity, energy costs.

The advent of the smart grids, energy self-production and the ever increasing injection of renewable and unstable energy sources in the grid, only escalates the relevance of adaptive strategies similar to the one here proposed. The possibility of consuming energy especially when its carbon intensity is lower would impact the global energy efficiency of buildings positively. Moreover, the possibility of reducing the carbon intensity of buildings would assist in achieving the goals of 2020 for Europe regarding the reduction of greenhouse gases and primary sources of energy consumption [14, 9].

In conclusion, the implementation of a supervisor management system should be considered as a valuable retrofitting solution, especially due to its impact on the reduction of costs, and energy consumption, as well as the lower impact of implementation, compared to retrofitting solutions focused on the architectural features of buildings as well as HVAC systems. Moreover, such an implementation is less invasive to the buildings, generating less entropy to its normal operation.

Chapter 5

Conclusion

The scope of this research was building' energy management. The survey on open literature highlighted the pertinence of retrofitting of existing buildings' energy efficiency because their long lifespan leads to make architecture and systems performance to degrade or to become obsolete. Two major approaches were identified regarding retrofitting. The most common approach is the retrofit of buildings' architecture and systems, while an alternative becoming more popular in buildings with existing HVAC systems is to retrofit these systems' controls into advanced control solutions.

The retrofitting of buildings' architecture elements and systems has shown promising results regarding the energy efficiency improvement with savings ranging 20% comparing to pre-retrofit data. However, the variability of economy, climate, energy, and society frameworks increases the uncertainty on deciding which features should be renovated and to what extent to maximize the return of investment. For example, the upgrade of an architectural feature such as a building's envelope is usually cost intensive and involves a considerable amount of civil work, demanding for the setting of sustained assumptions during the decision making process to lower the risk of the investment.

On the other hand, the upgrade of HVAC control to advanced control solutions should be adaptable to variable energy pricing paradigms, change of climate and priorities because its major contribution is due to a software integration with the existing HVAC system, and software should be more straightforward to update. According to the British Standard BS EN 15232, the upgrade of the HVAC control from conventional to advanced controls is expected to always improve the energy performance of the building, being the estimation of energy savings around 0.87 multiplying by the energy consumption before retrofit [167]. The reviewed literature has highlighted the state-of-the-art regarding advanced control solutions as being the Model Predictive Control divided as a local approach at machine level, and a supervisory approach at zone, or building level, characterized by being more flexible and adaptable to different types of problems. Nevertheless, the solutions presented in the literature showed limited flexibility regarding the type of HVAC system and control, leading the replication to other buildings and

HVAC systems quite cumbersome. This limitation was identified as an opportunity to develop a methodology for implementing flexible and adaptable supervisory predictive control solutions capable of improving the energy efficiency of existing HVAC systems.

The methodology for implementing a supervisory predictive control encompassed two critical steps: the development of models capable of predicting future states of building energy demand and comfort related metrics; and the formulation of an optimization problem capable of searching for the most suitable set-points for each time-step, considering simultaneously past, current, and future states.

The methodology for modelling has followed a hybrid approach based on surrogate modelling which employed machine learning algorithms (Neural Networks, Support Vector Machines, and Random Forests) to model the responses of the physics-based model developed in EnergyPlus. The selection of the inputs to the data-driven models was crucial to guarantee the generality and flexibility of the methodology. The key requirement was that the input variables selected for control should be accessible to human interface to emulate the decision making process conducted by humans when adjusting the thermal conditions of the inner environment. For example, in the case-study provided, the control variables available were the dual-band temperature set-points for each zone for both heating and cooling modes of the air conditioning system (Variable Refrigerant Flow system). Along with these control variables, endogenous and exogenous variables related to weather (temperature, humidity, and solar irradiation), inner environment (temperature) and the number of occupants were selected as well. The data generated by the simulation of conventional control techniques in the building energy simulation software (EnergyPlus) fed the data-driven models with sufficient samples for conducting the modelling process explained in Section 3.2. The trained data-driven models were capable of emulating the EnergyPlus responses for the dry-bulb temperature and the Predicted Percentage of Dissatisfied (PPD) in each zone, and the electrical energy demand for heating and cooling modes, considering the building design and HVAC system of the case-study presented in Chapter 4.

The initial data provided to the models was intentionally biased towards the conventional control solutions so that the models' capability to adapt to new data could be assessed, as well as to conduct an adaptive sampling of new data points from the responses of the optimization process inherent to the supervisory predictive control. The small variance of the conventional control solutions led the models to over-fit the data and perform poorly when applied in the optimization process. In fact, the observed mean relative error showed an increment of an order of magnitude in all predicted variables of the best models. This models' mismatch highlights the necessity of significant variance on the training data, especially in the controllable variables so that the data-driven models can capture the influence of changing a set-point on the output variables.

The data gathered was used to train the models, allowing for them to adapt to the previously unknown data samples. The most robust machine learning algorithm implemented was the Random Forests algorithm, achieving the best validation error on all the six models developed on the final data set. The mean percentage error for

predicting PPD and zone temperature for both zones has stayed below 0.8%, whereas the predictions of electricity demand for heating and cooling accounted for an error of 10.97% and 13.43%, respectively. These models were considered robust enough to incorporate the optimization process of the supervisory predictive control.

The multi-objective optimization strategy formulated in Section 3.3 focused on minimizing simultaneously the energy related costs on a variable pricing framework, and the Predicted Percentage of Dissatisfied. Since both objectives are competitors, the methodology proposes a formulation of the meta-objective by a weighted sum of both while handling the constraint of minimum acceptable comfort via the penalty method. The comfort objective weight was fine-tuned during early runs of the supervisory predictive control, achieving the best utility at 0.9 when all the tested weights were plotted in a Pareto-front graph of PPD vs. energy cost. It can be concluded that for the optimization problem formulation of this thesis and the case-study presented, a variation of the energy cost leads to higher variations on occupants' comfort, leading higher values of comfort weight to present a better compromise between both objectives. Such a large value of weight can be corroborated by recent literature on model predictive control applied to office buildings [28].

A comparative study was conducted in Section 4.4 to identify which of the optimization algorithms would be more suitable for the task. The Differential Evolution algorithm was found as the most suitable when comparing to the Particle Swarm Optimization (PSO), the Nelder-Mead, and the conjugate gradient method, besides the fact that the PSO achieved the lowest objective function value more often, accounting for 68.35% of the simulations. The Differential Evolution algorithm was selected because it took on average 13.20 seconds to converge comparing to the 64.89 seconds of PSO (on a i7-5600U CPU 2.60Ghz with 12GB of RAM), and the average objective function values after convergence were the lowest of all algorithms. It can be concluded, that for the formulation of the optimization problem and the implementations of the optimization algorithms conducted in this thesis, the Differential Evolution algorithm is more robust and faster than the Particle Swarm Optimization algorithm if comparing the algorithms with similar nature. Thus, the supervisory predictive control implementation integrated the Differential Evolution algorithm to solve the optimization process for each required time-step. The computational cost of the proposed solution has proved to be suitable for a real-world implementation because the time taken by the optimization process to be concluded was lower than the time-step which was set as hourly.

The supervisory predictive control presented in this thesis was implemented in a simulation environment where the EnergyPlus played the part of the real building. The time taken for completing a whole year simulation has taken 28h27min which is approximately less 41.8% of the time expected because rather than calling the optimization process 8712 time-step (363d*24h) it was only called 5105 times due to the Status Quo parameter. The purpose of this parameter was to serve as a trigger to the optimization process, leaving decisions encountered in previous time-steps to prevail to the following if the change of building thermal state, or disturbances such as weather or occupation

were not significant.

The performance of the proposed supervisory predictive control was benchmarked against conventional control solutions for HVAC systems. The detailed results are presented in Section 4.6.2. Overall, the supervisory predictive control has managed to save energy costs throughout the year, achieving 29.3% lower costs related to heating and cooling comparing to the Timer Control solution, ignoring potential savings from abnormal energy consumption derived from faulty control which alone can be accounted for 20% of the total energy consumption [8]. Regarding the energy consumption, the advanced control proposed was the best performing technique as well, but only by the slight margin of less 1.26% than the Early Switch-Off, whereas it saved 10.86% compared to Timer Control strategy. This results might be interpreted as the intent of the optimization algorithm in finding lower cost hours of energy pricing rather than minimizing the energy consumption itself. In fact, the optimization formulation focused on an approach capable of minimizing variable pricing energy. In what concerns occupants comfort, the proposed solution was also paramount, achieving an average PPD equal to 18.62% which is significantly lower than the limit of 25%.

Overall, the methodology presented in this thesis seems to be a promising start for the development of a supervisory predictive control which is agnostic to the type of HVAC system and type of building. This methodology may also be viewed as an acceptable approach to solve the "cold-start" problem of using data driven methods to control HVAC systems of new buildings, or building with insufficient data. The surrogate method could be key for performing data fusion by mixing sensor data with simulators data to deliver more robust models and consequently a better performing supervisory predictive control.

This thesis aimed at answering three research questions which are addressed in the list that follows:

- **How to design a HVAC supervisory advanced control system independent of the HVAC itself?** – The review of the state of the art highlighted that an approach related to model predictive control could provide satisfactory results regarding the need for optimized decisions based on past, current, and future states of the building. The review allowed for identifying the major aspects of designing such a solution. First, a model sensitive to past and current events is required to predict the future state of a building, namely the energy consumption and occupants comfort. The approach used to satisfy this necessity was to develop a surrogate model of the building physics-based model by employing machine learning algorithms, namely Random Forests, Neural Networks, and Support Vector Machines, to deliver predictive models of the electrical energy demand required for heating and cooling, as well as the occupants' thermal comfort (PPD) in each zone of the building. The input variables selected for constructing these data-driven models are key for allowing the predictive control to be supervisory and agnostic to the HVAC system and building types, simultaneously. Hence, the only inputs

depending on the HVAC system are the dual-band temperature set-points which are the control of the system itself and accessible from the supervision level (human interface), and the inner environment related variables are zone temperature, and the number of occupants per zone. The named data-driven models have managed to approximate the behavior of the physics simulator sufficiently (EnergyPlus), allowing for the incorporation of their predictions in the optimization process required for selecting suitable set-points based on the estimation of the future states. The best performing models were those from the Random Forests, achieving a mean relative error of 0.82% and 0.88% for the thermal comfort (PPD) in both zones of the building, 10.98% and 13.43% for the electrical energy demand for heating and cooling, respectively. These models were incorporated in the optimization process which is formulated to maximize the occupants' comfort while minimizing the energy consumption costs. The optimization formulation constraint must also be generic for achieving the desired flexibility of approach. In the case of the presented case-study, it was imposed a maximum limit to the PPD. The optimization algorithm selected for the task was the Differential Evolution due to its best trade-off regarding the computational cost and the quality of solutions. The optimization process took on average 20.40 seconds to converge to suitable set-points for both zones for the subsequent hour, considering that the forecast window is 6h. Hence, the time taken for finding the solution is lower than the time required, leaving room for increasing the complexity of the building (number of zones and window forecast size), or accelerating the decision time-steps to sub-hourly rather than hourly. Overall, the methodology presented to develop adaptive surrogate models and the formulation of the optimization process convey the necessary flexibility to the supervisory predictive control to be agnostic to the HVAC system and building type.

- **How does a HVAC supervisory predictive control solution compare with architecture and systems retrofitting approaches?** – Regarding the implementation of each approach, the supervisory predictive control seems to be more straightforward than an architecture or system retrofitting. The retrofit of building architecture features requires a significant amount of civil work to be done while the implementation of a supervisory predictive control requires mostly the installation simple hardware such as energy meters, temperature and occupation sensors if following a similar approach as the one proposed by this thesis. The data required for the implementation of both retrofits is similar if referring to the building architectural features since both need a representation of building's thermodynamic behaviour. However, the supervisory predictive control is more data intensive because it expects near real-time data from sensors and meters, as well as weather and occupation forecast services for the optimization of the set-points for each time step. Although both types of retrofits suggest that an optimization problem is required, the decision making process for selecting the most appropri-

ate set of features required to be changed in an architecture retrofit involves more uncertainties than the decision of investing in a supervisory predictive control. Since the supervisory predictive control is mostly software-based, the models, the optimization process, or even the whole concept should be able to be altered if the performance is not satisfactory enough due to an alteration of economic or environmental paradigm, or if any breakthrough has occurred after the implementation of the supervisory predictive control. On the other hand, the retrofitting of architecture features are commitments for the long term because the amount of work and investment is substantially higher, increasing the uncertainty regarding future economic, environmental, and societal paradigms. Moreover, the retrofit of architecture and systems are passive solutions preventing the opportunity to manage costs and environmental impacts inherent to a dynamic energy pricing context. Regarding energy performance improvement, the work conducted in this thesis has demonstrated that there is room for improvement in the way energy is spent even in buildings with energy efficient construction and HVAC system. The factor for energy savings was 0.80 comparing to the system with a conventional control system (Timer Control 9:00 - 18:00) without considering savings from abnormal energy consumption derived from faulty control which alone can be accounted for 20% of energy consumption. Nevertheless, the major advantage of a retrofitting solution based on advanced controls is the energy cost savings due to shifting the consumption peaks to lower priced time of the day as presented in Section 4.6.2. The energy cost savings of the supervisory predictive control comparing to the Timer Control solution were 12.3% for the heating season, 51.7% for the cooling season, and 29.3% for the yearly total savings. Retrofit solutions based on passive elements cannot easily adapt to different pricing, hindering saving potentials related to optimal pricing, as well as demand shifting towards less carbon intensive times of the day.

- **How to implement a real-time supervision system for a large commercial and services building, capable to establishing optimal operating conditions within an acceptable computational cost?** – The literature review pinpointed the key aspects hindering the development of model predictive control solutions, namely the building response model, the simulation time-step and forecast horizon, the forecast resolution, and the optimization algorithm. This research focused mainly on the building response model and the optimization algorithm. The presented case-study, a small office building, has achieved an acceptable performance regarding the building response model with all relevant prediction errors spanning from 0.54% to 13.43%. The implementation software called ***eppyco*** and developed in Python™for this thesis, has managed to integrate the predictive models in the optimization problem formulation and optimization algorithms and achieve a computational cost for finding the set-points for two zones for the following time-step in 20.40 seconds, leaving room for accelerating the rate of

optimizations per hour without compromising the solutions provided. The overall methodology allows for its implementation to different buildings and different HVAC systems. Thus, to implement the real-time supervision system for a large commercial building it would be necessary to develop a simplified model of the building in EnergyPlus™and perform simulations considering a control strategy similar to the one being used. Then, employing the methodology for surrogate modelling proposed on the Section 3.2 it would be possible to develop the necessary predictive models. Having validated the models, it is necessary to define the constraints to the optimization problem, namely the minimum required comfort to the occupants. After that, the models are ready to integrate the optimization process and connect it to the building HVAC supervision controls. The work conducted in this thesis cannot answer if the computational cost will be acceptable to a large scale building because no study was conducted regarding scalability. However, since the optimization algorithms selected are population based, they allow for parallel computation during the calculations of objective function values, opening the possibility for scaling the computational process horizontally.

5.1 Challenges and Future works

The conducted research enabled to successfully contribute to the scientific knowledge regarding the field of building energy management. However, the work conducted here is still embryonic and lacks for validation in some aspects, especially in its ability to scale and real world validity. For future work it is of the utmost importance to simulated more case studies with different optimization time-steps, different climates and building types, different architecture and systems, more air-conditioned zones, and longer forecast horizons, to stress the methodology here presented and search for loopholes so the final methodology can be more robust. Moreover, it can be useful, especially in the simulations of several air-conditioned zones, to implement a parallel computing solution in the optimization algorithms to attempt lowering the computational cost. It is necessary to implement the methodology proposed by this thesis in a real office building to compare results and fine-tune the solution.

Throughout the development of this thesis, additional questions arise and research ideas were revealed as a natural result of the developed work. Hence, bellow is listed a few items which the authors find as interesting challenges for the future of the field:

- **Multi-objective optimization formulation** – The approach to the formulation of the objective function has considered the minimization of a weighted sum of the single objectives (Discomfort and Energy/Energy-costs). However, as it was shown, the solutions found via this method are forced to form a convex Pareto front, leaving out the possibility of finding non-dominated solutions closer to utopia point. Therefore, it could be interesting to adapt the optimization process to minimize a distance metric independent of a weight factor, such as minimizing

directly the Chebyshev, Manhattan, or Euclidean distance from each solution to the utopia point and address which could offer a more reliable implementation of the Supervisory Predictive Control.

- **Double retrofit optimization** – The code for conducting the co-simulation process is still taking a considerable computational burden. Future works should improve the code for the reduction of computational cost, as an attempt to perform double optimization of retrofit. i.e. performing a co-simulation capable of answering which would be the best architectural and systems retrofitting when considering the advanced control solution proposed. To answer that it is necessary to wrap up the case-study presented in this thesis and turn it into an optimization iteration of the larger optimization problem which is focused on the architecture and systems characteristics.

- **Deep-learning** – We are in the era of artificial intelligence, and while information was never as abundant as it is today, neither was the computational power of machines. Deep-learning is basically big artificial neural networks capable of high abstraction due to the inclusion of more complex processing units (neurons), and its current trend of results are astonishing, namely in complex areas such as artificial vision, natural language interpretation, and self-learning. The latter seems to be the most relevant to the context of this thesis. There is an algorithm based on deep reinforcement learning which has managed to learn how to play several computer games (arcade) and beat humans easily at it [168]. The idea of employing it in building autonomous control of the HVAC system seems to be very promising and could bring interesting results regarding energy efficiency measures proposed by the algorithm, especially at large and complex commercial and services buildings.

Bibliography

[1] UN. Concise Report on the World Population Situation in 2014. New York, NY, USA; 2014.

[2] Dounis aI, Tiropanis P, Argiriou a, Diamantis a. Intelligent control system for reconciliation of the energy savings with comfort in buildings using soft computing techniques. Energy and Buildings. 2011;43(1):66–74.

[3] United Nations. UNITED NATIONS FRAMEWORK CONVENTION ON CLIMATE CHANGE; 1992.

[4] OECD/IEA. CO2 EMISSIONS FROM FUEL COMBUSTION; 2012.

[5] U S Energy Information Administration. Energy Consumption by Sector - Monthly Energy Review November 2015; 2015. November.

[6] European Commission. EU energy in figures, Statistical Pocketbook 2015; 2015.

[7] Costa A, Keane MM, Torrens JI, Corry E. Building operation and energy performance: Monitoring, analysis and optimisation toolkit. Applied Energy. 2013 jan;101:310–316.

[8] Roth KW, Westphalen D, Feng MY, Llana P, Quartararo L. Energy Impact of Commercial Building Controls and Performance Diagnostics: Market Characterization, Energy Impact of Building Faults and Energy Savings Potential. US Department of Energy. 2005;.

[9] EU. Directives on enegy efficiency. Official Journal of the European Union. 2012;L 315(November):1–56.

[10] OECD/IEA. CO2 EMISSIONS FROM FUEL COMBUSTION; 2012.

[11] Meijer F, Itard L, Sunikka-Blank M. Comparing European residential building stocks: performance, renovation and policy opportunities. Building Research & Information. 2009;37(5-6):533–551.

[12] Shaikh PH, Nor NBM, Nallagownden P, Elamvazuthi I, Ibrahim T. A review on optimized control systems for building energy and comfort management of smart sustainable buildings. Renewable and Sustainable Energy Reviews. 2014;34:409–429.

[13] Rysanek AM, Choudhary R. Optimum building energy retrofits under technical and economic uncertainty. Energy and Buildings. 2013 feb;57:324–337.

[14] Treado S, Chen Y. Saving Building Energy through Advanced Control Strategies. Energies. 2013;6(9):4769–4785.

[15] Pombo O, Allacker K, Rivela B, Neila J. Sustainability assessment of energy saving measures: a multi-criteria approach for residential buildings retrofittingA case study of the Spanish housing stock. Energy and Buildings. 2016;116:384–394.

[16] Hong T, Koo C, Kim J, Lee M, Jeong K. A review on sustainable construction management strategies for monitoring, diagnosing, and retrofitting the building's dynamic energy performance: Focused on the operation and maintenance phase. Applied Energy. 2015;155:671–707.

[17] Shao Y, Geyer P, Lang W. Integrating requirement analysis and multi-objective optimization for office building energy retrofit strategies. Energy and Buildings. 2014;82:356–368.

[18] Asadi E, Silva MGD, Antunes CH, Dias L, Glicksman L. Multi-objective optimization for building retrofit: A model using genetic algorithm and artificial neural network and an application. Energy and Buildings. 2014;81:444–456.

[19] Evins R, Pointer P, Vaidyanathan R. Configuration of a genetic algorithm for multi-objective optimisation of solar gain to buildings. Proceedings of the 12th annual conference on Genetic and evolutionary computation - GECCO '10. 2010;p. 1327.

[20] Pombo O, Rivela B, Neila J. The challenge of sustainable building renovation: Assessment of current criteria and future outlook. Journal of Cleaner Production. 2016;123:88–100.

[21] Mauser I, Müller J, Allerding F, Schmeck H. Adaptive building energy management with multiple commodities and flexible evolutionary optimization. Renewable Energy. 2015;p. 1–11.

[22] Missaoui R, Joumaa H, Ploix S, Bacha S. Managing energy Smart Homes according to energy prices: Analysis of a Building Energy Management System. Energy and Buildings. 2014;71:155–167.

[23] US Department of Energy. An Assessment of Energy Technologies and Research Opportunities; 2015. September.

[24] Moroan PD, Bourdais R, Dumur D, Buisson J. Building temperature regulation using a distributed model predictive control. Energy and Buildings. 2010;42(9):1445–1452.

[25] Afram A, Janabi-Sharifi F. Theory and applications of HVAC control systems - A review of model predictive control (MPC). Building and Environment. 2013;72:343–355.

[26] Wang S, Ma Z. Supervisory and Optimal Control of Building HVAC Systems: A Review. HVAC&R Research. 2007;14(1):3–32.

[27] Bengea SC, Kelman AD, Borrelli F, Taylor R, Narayanan S. Implementation of model predictive control for an HVAC system in a mid-size commercial building. HVAC&R Research. 2014;20(February 2014):121–135.

[28] De Coninck R, Helsen L. Practical implementation and evaluation of model predictive control for an office building in Brussels. Energy and Buildings. 2016;111:290–298.

[29] Garnier A, Eynard J, Caussanel M, Grieu S. Predictive control of multizone heating, ventilation and air-conditioning systems in non-residential buildings. Applied Soft Computing. 2015;37:847–862.

[30] Anderson JE, Wulfhorst G, Lang W. Energy analysis of the built environmentA review and outlook. Renewable and Sustainable Energy Reviews. 2015;44:149–158.

[31] Pérez-Lombard L, Ortiz J, Pout C. A review on buildings energy consumption information. Energy and Buildings. 2008;40(3):394–398.

[32] Boyd S, Vandenberghe L. Convex Optimization. vol. 25; 2010.

[33] Asadi E, Da Silva MG, Antunes CH, Dias L. Multi-objective optimization for building retrofit strategies: A model and an application. Energy and Buildings. 2012;44(1):81–87.

[34] Magnier L, Haghighat F. Multiobjective optimization of building design using TRNSYS simulations, genetic algorithm, and Artificial Neural Network. Building and Environment. 2010;45(3):739–746.

[35] Deb K, Pratap A, Agarwal S, Meyarivan T. A fast and elitist multiobjective genetic algorithm: NSGA-II. IEEE Transactions on Evolutionary Computation. 2002;6(2):182–197.

[36] Eisenhower B, O'Neill Z, Narayanan S, Fonoberov Va, Mezić I, O'Neill Z, et al. A methodology for meta-model based optimization in building energy models. Energy and Buildings. 2012 apr;47:292–301.

[37] Chantrelle FP, Lahmidi H, Keilholz W, Mankibi ME, Michel P. Development of a multicriteria tool for optimizing the renovation of buildings. Applied Energy. 2011 apr;88(4):1386–1394.

[38] Fanger PO. Thermal comfort. Analysis and applications in environmental engineering. ... comfort Analysis and applications in environmental .... 1970;.

[39] Ascione F, Bianco N, De Stasio C, Mauro GM, Vanoli GP. A new methodology for cost-optimal analysis by means of the multi-objective optimization of building energy performance. Energy and Buildings. 2015;88:78–90.

[40] Ascione F, Bianco N, De Stasio C, Mauro GM, Vanoli GP. Multi-stage and multi-objective optimization for energy retrofitting a developed hospital reference building: A new approach to assess cost-optimality. Applied Energy. 2016;174:37–68.

[41] Penna P, Prada A, Cappelletti F, Gasparella A. Multi-objectives optimization of Energy Efficiency Measures in existing buildings. Energy and Buildings. 2015;95:57–69.

[42] Malatji EM, Zhang J, Xia X. A multiple objective optimisation model for building energy efficiency investment decision. Energy and Buildings. 2013;61:81–87.

[43] Wang B, Xia X, Zhang J. A multi-objective optimization model for the life-cycle cost analysis and retrofitting planning of buildings. Energy and Buildings. 2014 jul;77:227–235.

[44] De Boeck L, Verbeke S, Audenaert A, De Mesmaeker L. Improving the energy performance of residential buildings: A literature review. Renewable and Sustainable Energy Reviews. 2015;52:960–975.

[45] Ma Z, Cooper P, Daly D, Ledo L. Existing building retrofits: Methodology and state-of-the-art. Energy and Buildings. 2012;55:889–902.

[46] Magnier L, Haghighat F. Multiobjective optimization of building design using TRNSYS simulations, genetic algorithm, and Artificial Neural Network. Building and Environment. 2010 mar;45(3):739–746.

[47] Lazos D, Sproul AB, Kay M. Optimisation of energy management in commercial buildings with weather forecasting inputs: A review. Renewable and Sustainable Energy Reviews. 2014;39:587–603.

[48] Hilliard T, Kavgic M, Swan L. Model predictive control for commercial buildings: trends and opportunities. Advances in Building Energy Research. 2015 sep;p. 1–19.

[49] Coffey B, Haghighat F, Morofsky E, Kutrowski E. A software framework for model predictive control with GenOpt. Energy and Buildings. 2010;42(7):1084–1092.

[50] Prívara S, Široký J, Ferkl L, Cigler J. Model predictive control of a building heating system: The first experience. Energy and Buildings. 2011 feb;43(2-3):564–572.

[51] Široký J, Oldewurtel F, Cigler J, Prívara S. Experimental analysis of model predictive control for an energy efficient building heating system. Applied Energy. 2011;88(9):3079–3087.

[52] Li GC, Huang GH, Sun W, Ding XW. An inexact optimization model for energy-environment systems management in the mixed fuzzy, dual-interval and stochastic environment. Renewable Energy. 2014;64:153–163.

[53] He X, Zhang Z, Kusiak A. Performance optimization of HVAC systems with computational intelligence algorithms. Energy and Buildings. 2014;81:371–380.

[54] Kusiak A, Li M, Tang F. Modeling and optimization of HVAC energy consumption. Applied Energy. 2010;87(10):3092–3102.

[55] Shaikh PH, Nor NM, Nallagownden P, Elamvazuthi I. Intelligent Optimized Control System for Energy and Comfort Management in Efficient and Sustainable Buildings. Procedia Technology. 2013;11(Iceei):99–106.

[56] Yang R, Wang L. Multi-zone building energy management using intelligent control and optimization. Sustainable Cities and Society. 2013;6:16–21.

[57] Kusiak A, Li M, Zhang Z. A data-driven approach for steam load prediction in buildings. Applied Energy. 2010;87(3):925–933.

[58] Foucquier A, Robert S, Suard F, Stéphan L, Jay A. State of the art in building modelling and energy performances prediction: A review. Renewable and Sustainable Energy Reviews. 2013;23:272–288.

[59] Forrester AIJ, Sóbester A, Keane AJ. Engineering Design via Surrogate Modelling - A Practical Guide. Wiley Subscription Services, Inc., A Wiley Company; 2008.

[60] Hunn BD. Fundamentals of building energy dynamics. vol. 4; 1996.

[61] Fadzli Haniff M, Selamat H, Yusof R, Buyamin S, Sham Ismail F. Review of HVAC scheduling techniques for buildings towards energy-efficient and cost-effective operations. Renewable and Sustainable Energy Reviews. 2013;27:94–103.

[62] ASHRAE. 2009 Ashrae Handbook Fundamentals. vol. 30329; 2009.

[63] CEN. EN 15251:2007. Indoor environmental input parameters for design and assessment of energy performance of buildings- addressing indoor air quality , thermal environment , lighting and acoustics; 2006.

[64] LAWRENCE BERKELEY NATIONAL LABORATORY. EnergyPlus Documentation - Engineering Reference - The Reference to EnergyPlus Calculations; 2015.

[65] Pitts A. Thermal Comfort in Transition Spaces. Buildings. 2013;3(1):122–142.

[66] ASHRAE. THERMAL COMFORT. In: ASHRAE Fundamentals Handbook (SI). ASHRAE; 1997. .

[67] Chantrelle FP, Lahmidi H, Keilholz W, Mankibi ME, Michel P. Development of a multicriteria tool for optimizing the renovation of buildings. Applied Energy. 2011 apr;88(4):1386–1394.

[68] Fumo N. A review on the basics of building energy estimation. Renewable and Sustainable Energy Reviews. 2014;31:53–60.

[69] Harish VSKV, Kumar A. Techniques used to construct an energy model for attaining energy efficiency in buildings: A Review. International Conference in Control, Instrumentation, Energy & Communication. 2014;p. 366–370.

[70] Zhao Hx, Magoulès F. A review on the prediction of building energy consumption. Renewable and Sustainable Energy Reviews. 2012 aug;16(6):3586–3592.

[71] Ohlsson MBO, Rognvaldsson TS, Peterson CO, Soderberg BPW, Pi H. Predicting system loads with artificial neural networks - methods and results from 'the great energy predictor shootout'. ASHRAE Transactions. 1994;100(2):1063–1074.

[72] Paudel S, Elmtiri M, Kling WL, Corre OL, Lacarrière B. Pseudo dynamic transitional modeling of building heating energy demand using artificial neural network. Energy and Buildings. 2014 feb;70:81–93.

[73] Li K, Su H, Chu J. Forecasting building energy consumption using neural networks and hybrid neuro-fuzzy system: A comparative study. Energy and Buildings. 2011;43(10):2893–2899.

[74] Li K, Su H. Forecasting building energy consumption with hybrid genetic algorithm-hierarchical adaptive network-based fuzzy inference system. Energy and Buildings. 2010;42(11):2070–2076.

[75] Kumar S, Chaturvedi DK. Optimal power flow solution using fuzzy evolutionary and swarm optimization. International Journal of Electrical Power & Energy Systems. 2013;47:416–423.

[76] Mohanraj M, Jayaraj S, Muraleedharan C. Applications of artificial neural networks for refrigeration, air-conditioning and heat pump systemsA review. Renewable and Sustainable Energy Reviews. 2012 feb;16(2):1340–1358.

[77] a S Ahmad, Hassan MY, Abdullah MP, Rahman Ha, Hussin F, Abdullah H, et al. A review on applications of ANN and SVM for building electrical energy consumption forecasting. Renewable and Sustainable Energy Reviews. 2014;33:102–109.

[78] Dietterich TG. Ensemble Methods in Machine Learning. In: Proceedings of the First International Workshop on Multiple Classifier Systems. London, UK, UK: Springer-Verlag; 2000. p. 1–15.

[79] Fan C, Xiao F, Wang S. Development of prediction models for next-day building energy consumption and peak power demand using data mining techniques. Applied Energy. 2014 aug;127:1–10.

[80] Fernández-Delgado M, Cernadas E, Barro S, Amorim D. Do we Need Hundreds of Classifiers to Solve Real World Classification Problems? Journal of Machine Learning Research. 2014;15:3133–3181.

[81] Hopfield JJ. Neural networks and physical systems with emergent collective computational abilities Biophysics : Hopfield I T ., V . 1982;79(April):2554–2558.

[82] Shawe-Taylor J. Neural Network Learning: Theoretical Foundations. AI Magazine. 2001;22(2):99.

[83] Mitchell TM. Machine Learning. 1st ed. New York, NY, USA: McGraw-Hill, Inc.; 1997.

[84] Hagan MT, Demuth HB, Beale M. Neural Network Design. Boston, MA, USA: PWS Publishing Co.; 1996.

[85] Fine TL. Feedforward neural network methodology. Springer Verlag; 1999.

[86] Hecht-Nielsen R. Theory of the Backpropagation Neural Network. In: Neural Networks, 1989. IJCNN., International Joint Conference on. vol. 1. IEEE; 1989. p. 593–605.

[87] Cortes C, Vapnik V. Support-vector networks. Machine learning. 1995;20(3):273–297.

[88] Scholkopf B, Smola AJ, Williamson RC, Bartlett PL. New Support Vector Algorithms. Neural computation. 2000;12(5):1207–1245.

[89] Smola A, Schölkopf B. A tutorial on support vector regression. Statistics and Computing. 2004;14(3):199–222.

[90] Biau G, Devroye L, Lugosi G. Consistency of random forests and other averaging classifiers. The Journal of Machine Learning Research. 2008;9(2008):2015–2033.

[91] Breiman L. Random Forests. Machine learning. 2001;45.1:5–32.

[92] Berk RA. Statistical Learning from a Regression Perspective. NY, USA: Springer; 2001.

[93] Abdulsalam H, Skillicorn DB, Martin P. Streaming Random Forests. Proceedings of the International Database Engineering and Applications Symposium, IDEAS. 2007;p. 225–232.

[94] Crawley DB, Hand JW, Kummert M, Griffith BT. Contrasting the capabilities of building energy performance simulation programs. Building and Environment. 2008;43(4):661–673.

[95] Henninger RH, Witte MJ. EnergyPlus testing with ANSI/ASHRAE standard 140-2001 (BESTEST); 2004. June.

[96] Wetter M. Building Controls Virtual Test Bed User Manual Version 0.8.0. Lawrence Berkeley National Laboratory. 2010;(c):1–69.

[97] Bernal W, Behl M, Nghiem T, Mangharam R. MLE+: design and deployment integration for energy-efficient building controls. 4th Workshop on Embedded Sensing Systems for Energy-Efficiency in Buildings (BuildSys). 2012;p. 215–216.

[98] Gorissen D, Couckuyt I, Demeester P, Dhaene T, Crombecq K. A Surrogate Modeling and Adaptive Sampling Toolbox for Computer Based Design. Journal of Machine Learning Research. 2010;11:2051–2055.

[99] Yi H, Srinivasan RS, Braham WW. An integrated energyemergy approach to building form optimization: Use of EnergyPlus, emergy analysis and Taguchi-regression method. Building and Environment. 2015 jan;84:89–104.

[100] Gong X, Akashi Y, Sumiyoshi D. Optimization of passive design measures for residential buildings in different Chinese areas. Building and Environment. 2012 dec;58:46–57.

[101] Filfli S, Marchio D. Parametric models of energy consumption based on experimental designs and applied to building-system dynamic simulation. Journal of Building Performance Simulation. 2012;5(5):277–299.

[102] Lee B, Hensen JLM. Towards zero energy industrial halls - Simulation and optimization with integrated design approach. Proceedings of BS 2013: 13th Conference of the International Building Performance Simulation Association. 2013;p. 1339–1346.

[103] Heo Y, Choudhary R, Augenbroe Ga. Calibration of building energy models for retrofit analysis under uncertainty. Energy and Buildings. 2012 apr;47:550–560.

[104] Shen H, Tzempelikos A. Sensitivity analysis on daylighting and energy performance of perimeter offices with automated shading. Building and Environment. 2013 jan;59:303–314.

[105] Trcka M, Wetter M, Hensen J. COMPARISON OF CO-SIMULATION APPROACHES FOR BUILDING AND HVAC / R SYSTEM SIMULATION. Proceedings of the Building Simulation. 2007;p. 3–5.

[106] Kasprzak EM. Pareto Analysis in Multiobjective Optimization Using the Colinearity Theorem and Scaling Method. 2001;22(3):208–218.

[107] Zitzler E, Thiele L. Multiobjective evolutionary algorithms: a comparative case study and the strength Pareto approach. IEEE Transactions on Evolutionary Computation. 1999;3(4):257–271.

[108] Wetter M, Polak E. A convergent optimization method using pattern search algorithms with adaptive precision simulation. Building Services Engineering Research and Technology. 2004;25(4):327.

[109] Wetter M, Wright J. A comparison of deterministic and probabilistic optimization algorithms for nonsmooth simulation-based optimization. Building and Environment. 2004;39(8 SPEC. ISS.):989–999.

[110] Kennedy J, Eberhart R. Swarm Intelligence; 2001.

[111] Eberhart R, Kennedy J. A new optimizer using particle swarm theory. MHS'95 Proceedings of the Sixth International Symposium on Micro Machine and Human Science. 1995;p. 39–43.

[112] Parsopoulos KE, Vrahatis MN. Recent approaches to global optimization problems through Particle Swarm Optimization. Natural Computing. 2002;(1):235–306.

[113] Blum C, Li X. Swarm Intelligence in Optimization. Springer Berlin Heidelberg; 2008. p. 43–85.

[114] Poli R, Kennedy J, Blackwell T. Particle swarm optimization. Swarm Intelligence. 2007;1(1):33–57.

[115] Kennedy J. The behavior of particles. In: Evolutionary Programming VII; 1998. .

[116] Carlisle A, Dozier G. An Off-The-Shelf PSO. In: Proceedings of the Workshop on Particle Swarm Optimization; 2001. .

[117] Storn R, Price K. Differential evolutiona simple and efficient heuristic for global optimization over continuous spaces. Journal of global optimization. 1997;p. 341–359.

[118] Coelho BC. Energy efficiency of water supply systems using optimisation techniques and micro-hydroturbines. Universidade de Aveiro; 2016.

[119] Cunha AG, Takahashi R, Antunes CH. Manual de computação evolutiva e metaheurística. Coimbra: Imprensa da Universidade de Coimbra; 2012.

[120] Das S, Nagaratnam Suganthan P, Member S. Differential Evolution : A Survey of the State - of - the - Art. Ieee Transactions on Evolutionary Computation. 2011;15(1):4–31.

[121] Lamoudi MY, Alamir M, Béguery P. Distributed constrained Model Predictive Control based on bundle method for building energy management. Proceedings of the IEEE Conference on Decision and Control. 2011;p. 8118–8124.

[122] Shmueli G. To Explain or to Predict ? Statistical Science. 2010;25(3):289–310.

[123] Montgomery DC, Jennings CL, Kulahci M. Introduction to Time Series Analysis and Forecasting. Wiley; 2008.

[124] Fumo N. A review on the basics of building energy estimation. Renewable and Sustainable Energy Reviews. 2014;31:53–60.

[125] Ha DL, Joumaa H, Ploix S, Jacomino M. An optimal approach for electrical management problem in dwellings. Energy and Buildings. 2012 feb;45:1–14.

[126] Hoens TR, Polikar R, Chawla NV. Learning from streaming data with concept drift and imbalance: an overview. Progress in Artificial Intelligence. 2012;1(1):89–101.

[127] Sasena M, Papalambros P, Goovaerts P. Metamodeling sampling criteria in a global optimization framework. In: 8th AIAA/USAF/NASA/ISSMO Symposium on Multidisciplinary Analysis and Optimization. Long Beach, CA: American Institute of Aeronautics and Astronautics; 2000. .

[128] Jin R, Chen W, Sudjianto A. On sequential sampling for global metamodeling in engineering design. ... Engineering .... 2002;p. 1–10.

[129] Branke J, Deb K, Miettinen K, Slowinskyi R. Multiobjective Optimization - Interactive and Evolutionary Approaches. vol. 5252 LNCS; 2008.

[130] Xiao F, Fan C. Data mining in building automation system for improving building operational performance. Energy and Buildings. 2014;75:109–118.

[131] Fang TY, Chen J, Fang MX, Wang J. Research of the Building Energy Efficiency Data Analysis Based on Time Series Algorithm in Anhui Province, China. Applied Mechanics and Materials. 2012 oct;209-211:1836–1842.

[132] Guyon I. An Introduction to Variable and Feature Selection. 2003;3:1157–1182.

[133] Kohavi R, John GH. Wrappers for feature subset selection. Artificial Intelligence. 1997;97(1-2):273–324.

[134] Mo Jang S, Park YJ. The Internet, selective learning, and the rise of issue specialists. First Monday. 2012;17(5).

[135] Wang W, Jones P, Partridge D. A comparative study of feature-salience ranking techniques. Neural computation. 2001 jul;13(7):1603–1623.

[136] Frénay B, Doquire G, Verleysen M. Is mutual information adequate for feature selection in regression? Neural Networks. 2013;48:1–7.

[137] Gregorutti B, Michel B, Saint-Pierre P. Correlation and variable importance in random forests. Statistics and Computing. 2016;(March 2014):1–20.

[138] Liu H, Motoda H. Feature Extraction, Construction and Selection: A Data Mining Perspective. New York, New York, USA: Springer; 1998.

[139] Langley P. Selection of Relevant Features in Machine Learning. In: In Proceedings of the AAAI Fall Symposium on Relevance. AAAI; 1994. p. 140–144.

[140] Leray P, Gallinari P, Ia LIPP. Feature Selection with Neural Networks;.

[141] Blachnik M. Comparison of Various Feature Selection Methods in Application to Prototype Best. Computer Recognition Systems 3. 2009;p. 257–264.

[142] Guyon I, Elisseeff A. An Introduction to Feature Extraction. vol. 207; 2006.

[143] Saeys Y, Inza I, Larrañaga P. A review of feature selection techniques in bioinformatics. Bioinformatics (Oxford, England). 2007 oct;23(19):2507–17.

[144] Altmann A, Tolosi L, Sander O, Lengauer T. Permutation importance: A corrected feature importance measure. Bioinformatics. 2010;26(10):1340–1347.

[145] Yang JB, Shen KQ, Ong CJ, Li XP. Feature selection for MLP neural network: The use of random permutation of probabilistic outputs. IEEE Transactions on Neural Networks. 2009;20(12):1911–1922.

[146] Sung AH. Ranking importance of input parameters of neural networks. 1998;15:405–411.

[147] Hastie T, Tibshirani R, Friedman J. The Elements of Statistical Learning. vol. 1. 2nd ed. Berlin: Springer; 2009.

[148] Moreno MV, Dufour L, Skarmeta AF, Jara AJ, Genoud D, Ladevie B, et al. Big data: the key to energy efficiency in smart buildings. Soft Computing. 2015;.

[149] Oldewurtel F, Parisio A, Jones CN, Gyalistras D, Gwerder M, Stauch V, et al. Use of model predictive control and weather forecasts for energy efficient building climate control. Energy and Buildings. 2012;45:15–27.

[150] Hilliard T, Kavgic M, Swan L. Model predictive control for commercial buildings: trends and opportunities. Advances in Building Energy Research. 2015;2549(November):1–19.

[151] EnergyPlus. External Interface(s) Application Guide Guide for using EnergyPlus with External Interface(s). LAWRENCE BERKELEY NATIONAL LABORATORY; 2013.

[152] Kottek M, Grieser J, Beck C, Rudolf B, Rubel F. World map of the Köppen-Geiger climate classification updated. Meteorologische Zeitschrift. 2006;15(3):259–263.

[153] Ministério Da Economia E Do Emprego. Despacho n.º 15793-F/2013, de 3 de dezembro. Diário da Répuplica. 2013;2.ª série(234):26–31.

[154] Aguiar R. Climatologia e Anos Meteorológicos de Referência para o Sistema Nacional de Certificação de Edifícios. 2013;(versão):1–55.

[155] Ministério Da Economia E Do Emprego. Portaria n.º 349-D/2013. Diário da Répuplica. 2013;(40):40–73.

[156] He H, Garcia EA. Learning from imbalanced data. IEEE Transactions on Knowledge and Data Engineering. 2009;21(9):1263–1284.

[157] Azadeh a, Tarverdian S. Integration of genetic algorithm, computer simulation and design of experiments for forecasting electrical energy consumption. Energy Policy. 2007;35(10):5229–5241.

[158] Lai F, Magoulès F, Lherminier F. Vapnik's learning theory applied to energy consumption forecasts in residential buildings. International Journal of Computer Mathematics. 2008;85(10):1563–1588.

[159] Chou JS, Bui DK. Modeling heating and cooling loads by artificial intelligence for energy-efficient building design. Energy and Buildings. 2014;82:437–446.

[160] Krawczyk B. Learning from imbalanced data : open challenges and future directions. Progress in Artificial Intelligence. 2016;5(4):221–232.

[161] Zhang Y, Hanby VI. Short-Term Prediction of Weather Parameters Using Online Weather Forecasts. Building Simulation. 2007;p. 1411–1416.

[162] BIPM. Evaluation of measurement data Guide to the expression of uncertainty in measurement. 2008;(September).

[163] Palensky P, Member S, Dietrich D. Demand Side Management : Demand Response , Intelligent Energy Systems , and Smart Loads. 2011;7(3):381–388.

[164] Entidade Reguladora dos Serviços Energéticos. Diretiva n.º 1/2017; 2017.

[165] Cox NJ. Speaking Stata: Creating and varying box plots. The Stata Journal. 2009;9(3):478–496.

[166] Branke J. Memory enhanced evolutionary algorithms for changing optimization problems. Proceedings of the 1999 Congress on Evolutionary Computation, CEC 1999. 1999;3(721):1875–1882.

[167] Mitsubishi Electric. The Impact of Control Strategies on Building Energy Performance Using BS EN 15232; 2014.

[168] Rusu AA, Colmenarejo SG, Gulcehre C, Desjardins G, Kirkpatrick J, Pascanu R, et al. Human-level control through deep reinforcement learning. Nature. 2015;518(7540):529–533.

Appendices

Appendix A

Supervisory Predictive Control robustness investigation – Summer

A.1 Inducing uncertainty in disturbances forecast - Summer

Figure A.1 shows the building response to the supervisory predictive control decisions, considering the imposed uncertainty of 0.5σ at $t+24$, as presented in section 4.6.7. The optimization problem focused on minimizing the energy costs while maximizing the occupants comfort, according to section 4.6.2. As depicted, the SPC did not evidenced major control pitfalls. This observation follows results presented in the heating season version presented in section 4.6.7.

The predictive error is gradually increasing throughout the window forecast, giving the SPC opportunity to adapt to the new scenarios when the expectations gradually become more accurate in the approximation of the time-step of decision $(t+1)$.

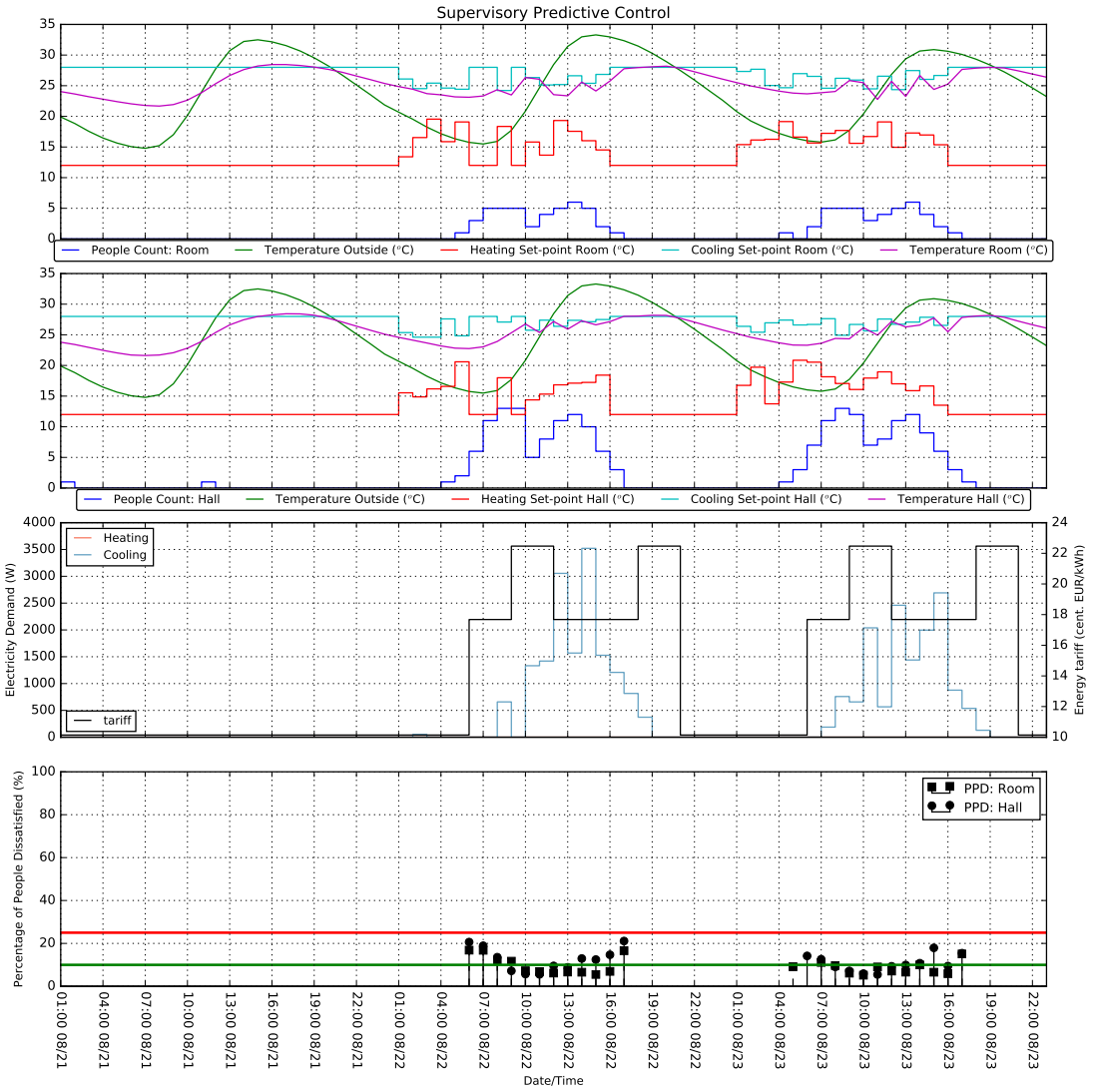

Figure A.1: Summer's design week simulation of supervisory predictive control inducing disturbances forecast uncertainty with λ_i equal to 0.5 for i equal to 24h.

The behaviour of the SPC for the co-simulation considering the addition of uncertainty in the disturbances forecast can be listed as follows:

- The cooling set-points are decreased from set-back four hours before building occupants arrival at 6:00;
- The energy consumption was 29870Wh, and the energy related costs summed up 5.59€.

- The SPC has managed to reduce costs by attempting to minimize consumption at peak hours, especially on the 22^{th} of August;

- The percentage of comfort violations is 0%;

- The average PPD for both zones is 10.41%, with Room and Hall equal to 11.60% and 9.22%, respectively.

In conclusion, this analysis refers to the effectiveness of the SPC in accommodating the uncertainty of disturbances forecast during cooling season.

A.2 Varying forecast window size – Summer

The following study investigates the influence of increasing the forecast window to 12h. Figure A.2 shows the building's response to such a configuration of Supervisory Predictive Control for the co-simulation of the Summer Design day (22-08).

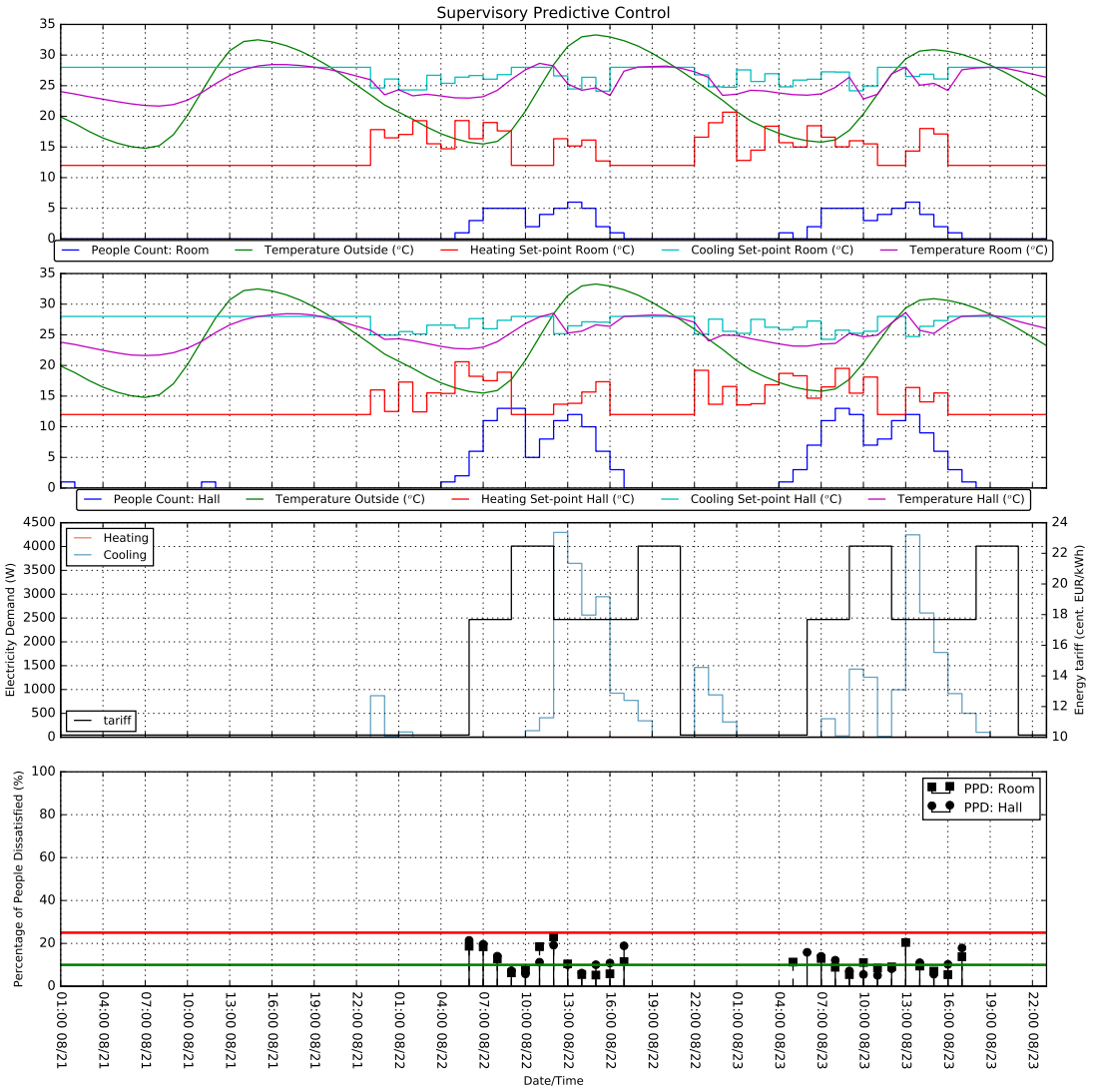

Figure A.2: Summer's design day simulation of supervisory predictive control considering a forecast window equal to 12h.

The list bellow summarizes the performance of the current robustness test:

- The heating set-points are increased five hours before the building's occupants arrival at 6:00;
- The SPC has managed to reduce costs by minimizing consumption at peak hours, especially on the 22^{th} of August;

- The energy consumption was 33954Wh, and the energy related costs summed 5.90€.

- The percentage of comfort violations is 0%;

- The average PPD for both zones is 11.56%, with Room and Hall equal to 11.13% and 11.99%, respectively.

Between the simulated days, the set-points chosen at the end of the occupied hours show that the supervisory predictive control has a tendency to increase the cooling set-points to the set-back temperature, rising the building's temperature when there are no occupants present. This behaviour can play an important role on the colder days of the cooling season, since the temperature would be more comfortable once the occupants arrive at the following day.

A.3 Dealing with abnormal occupation patterns –Summer

This appendix presents the building response to an abnormal occupation pattern for the simulation of two days of the cooling season. It can be depicted in Fig. A.3, a total of 25 people occupied the Hall of the building from 17:00 till 01:00 on a Sunday evening. Six people occupied it for two additional hours, one at 16:00 and again at 02:00, and there was no occupation between 23:00 and 00:00. Moreover, there was observed an occupation of 25 people for one hour on the Monday (22-08) evening at 23:00.

Overall, the SPC has managed to prepare a thermally comfortable environment to the occupants. One PPD violations was observed during the whole simulation period, representing 1.7% of the time occupied period.

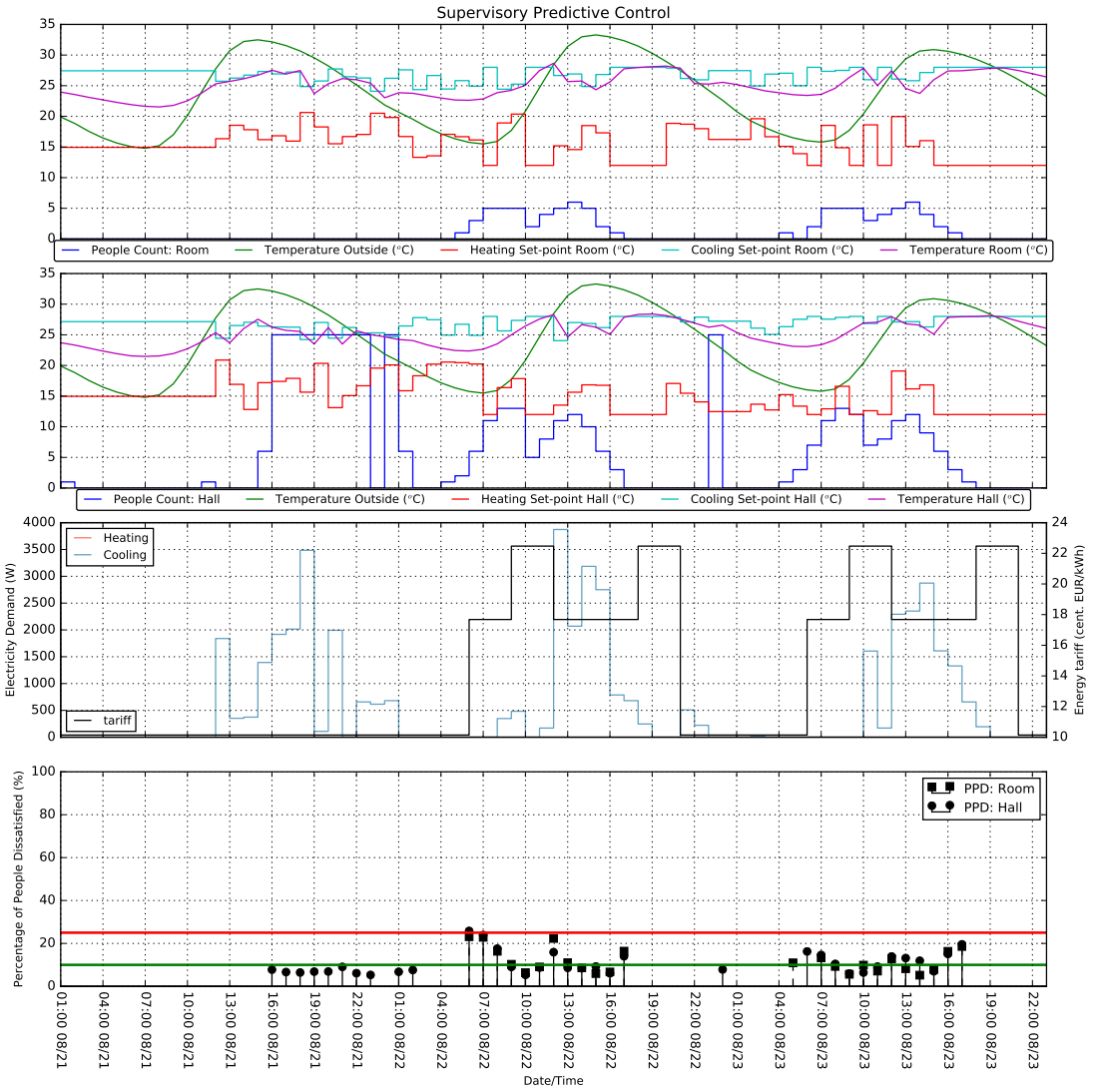

Figure A.3: Summer's design day simulation of supervisory predictive control considering abnormal occupation pattern.

The temperature set-point was set three hours before the arrival of the six people, corroborating the decision taken for the same simulation on the heating season. Moreover, the same control behaviour regarding the parity of decisions across air-conditioned zones is observed, suggesting a possible interdependence induced by the predictive models in relation to the controllable variables, i.e. so far, all the training data has contained data samples with occupancy between zones correlated (see Fig. 4.12). This effect can influence the models to divide the importance of variables equally when no guaranteed

influence exists. For example, the predictive model of the PPD of the Hall has assigned the same importance to the PPD of the Room (Table 4.10).

This simulation presented a novelty when comparing to the other simulations of the cooling season using the SPC strategy. It was observed a comfort penalty at 06:00 of the 22^{th} of August with a PPD equal to 25.82%. The temperature observed was $22.36^{o}C$, a slightly cooler temperature promoted by the cooling of the zone on the previous evening. This result corroborated the hypothesis of promoting higher temperatures during the evening to allow for better comfort levels in the arrival of the occupants in the zone.